On the Dynamics of Rock Glaciers

Dissertation

zur

Erlangung der naturwissenschaftlichen Doktorwürde

(Dr. sc. nat.)

vorgelegt der

Mathematisch-naturwissenschaftlichen Fakultät

der

Universität Zürich

von

Alessandro Cicoira

aus

Italien

Promotionskommission

Prof. Dr. Andreas Vieli (Vorsitz und Leitung)

Dr. Isabelle Gärner-Roer

Dr. Jérome Faillettaz

Prof. Dr. Ross Purves

Zürich, 2020

Summary

Mountain permafrost is currently enduring substantial modifications due to climate change. A drastic increase in the creep rates of rock glaciers and the onset of rock glacier destabilization have been observed at the regional scale since the 1990s, concurrent with ground temperatures warming and widespread ice loss. These observations rise several questions on the fundamental mechanisms controlling rock glacier dynamics and its coupling to the climate, with implications in the fields of paleo-climatology, natural hazard management and planetary sciences. As a result, large research efforts have been undertaken in order to answer these questions. The statistical analysis of kinematic time series highlighted a strong correlation between creep rates and air temperature at seasonal-, inter-annual, and decennial temporal scales. Detailed field investigations have demonstrated the importance of rock glacier hydrology (through pore water pressures) in determining the short-term velocity variations. At the state of the art however, an accurate and coherent description of the evolution of rock glacier dynamics at the regional scale is hampered by its multi-disciplinary nature and by the scarcity and the limitations of the available database. In fact, on the one hand the current dynamical and geomorphological state of rock glaciers is at present largely unknown at a regional scale, and on the other hand our understanding of rock glacier dynamics and its complex interactions with thermal and hydrological processes at the local scale remains limited and primarily qualitative. With the aim of contributing to fill these knowledge gaps, this thesis investigates the processes controlling the evolution of rock glacier dynamics at multi spatio-temporal scales by means of process-based numerical modelling, data collection and analysis, and remote sensing techniques.

At a local scale, I investigated the dynamic response of rock glacier dynamics to variations in external temperature and water input at seasonal and inter-annual temporal scales by designing a novel process-based modelling approach. The modelling accounts for heat transfer into the ground, the catchment hydrology, the hydro-mechanics of the rock glacier and its rheology. By these means, I critically discussed the hypotheses that (i) external temperature forcing through heat conduction and (ii) water input through pore water pressure at the shear horizon can explain seasonal and inter-annual variations in rock glacier dynamics. For five well documented study cases in the Swiss Alps, I showed that the direct influence of external temperature forcing on rock glacier rheology can explain only up to 25% of the observed seasonal and inter-annual variations in surface velocities so that the magnitude of the variations is underestimated at least by one order of magnitude and the phase of the seasonal peaks is delayed by 2-3 months. On the contrary, when including the

influence of pore water pressure at the shear horizon depth, our model could reproduce the velocity variations both in magnitude and phase at seasonal and inter-annual time scales and could be used to derive indirect information on the hydro-mechanical regime of rock glaciers. The results corroborated the hypothesis that the rhythm of rock glacier dynamics can be explained by water and external temperature, with a preponderant influence of water at the shear horizon depth, also indirectly controlled by temperature. Temperature changes over the entire thickness of the rock glacier can cause substantial variations in creep rates, but require changes in climate over decades or centuries.

In order to extend the investigation at a regional scale, I investigated a large database comprising information about rock glacier geometry (thickness and slope angle), geomorphological and permafrost conditions, and surface velocities. The analysis of a restricted dataset, for which detailed information about the thickness of the rock glaciers is available, showed that the typical driving stress is 92 ± 13 kPa, similar to ice glaciers and therefore, rock glacier thickness can be efficiently estimated with the inversion of simple models (e.g. perfectly plastic model). Thus, I developed a general theory of rock glacier creep by coupling the thickness model with a creep model for ice-rich permafrost. I introduced the Bulk Creep Factor BCF, a dimensionless parameter which allows the disentanglement of the two contributions to the surface velocity from (i) material properties and (ii) geometry. The proposed approach only requires remote sensing observations on creep velocities and surface slope angle, hence can be applied operationally over large areas. The application at a regional scale showed that most alpine rock glaciers are characterized by low values $BCF < 5$, whereas only rock glaciers currently experiencing destabilization or set in conditions unfavourable to permafrost occurrence show larger values $BCF < 20$. At a local scale, I found that for dynamically stable rock glaciers the geometry can explain the spatial variability in creep rates with almost constant rheological properties (BCF), while destabilized rock glaciers show contrasting and discontinuous values. Thus, the evaluation of the dynamical state of a rock glacier should account for its geometry, material properties and the processes controlling its movement rather than solely on geomorphological and kinematical observations.

The synthesis of the regional- and local scale investigations, based on in-situ and remote sensing observations analysed through the lens of process-based modelling, advanced our understanding of the processes controlling rock glacier dynamics at different spatio-temporal scales. Air and ground temperatures appear to be the major drivers of rock glacier dynamics, determining the rheological properties of the rock glacier material, but also controlling mass and energy fluxes through multiple non-linear processes. Eventually, approaching isotherm conditions at 0°C, the onset of permafrost degradation leads to important changes in the structure of the rock glacier itself. Hence, thermal mechanisms become less important and hydro-mechanical processes (also through the onset of rock glacier destabilization) take over the control of the short-term dynamic variations of the rock glacier.

In a nutshell, this dissertation provides the first quantitative framework for the assessment of the influence of climatic forcing on rock glacier dynamics and, with the development of a new theory, discloses great potential for long-term regional-scale analysis of rock glacier evolution.

Acknowledgements

This dissertation is the result of plentiful days in the field in the mountains of Engadine and Vallis, countless hours of reading, as many of writing and overall of abundant lively discussions at the University and at the ETH of Zurich. This thesis is not a monograph, but rather a colourful mosaic, whose theme was designed and whose tiles have been put with the help of different people, who deserve my sincere acknowledgments. A tutti loro vanno i miei ringraziamenti.

Grazie Andreas, in the first place for your trust and for the opportunity to work with the 3Gs. You have supported me at all stages of the PhD and you granted everything I needed to freely develop my own research. Thank you for your curiosity and your modesty: I found much inspiration in your approach to science and teaching.

Un grande grazie to the 3Gs. The profile of the Matterhorn with the PhD on the summit, drawn on the board of Caffi Hasler, very well speaks for the atmosphere in our group. The coffee breaks, the readings, the field- (and the safety) courses, the SOLA races, and the camp fires are exuberant evidence of a flourishing environment. All the discussions we had on how to further improve are the best proof that you are doing great. Although I am grateful to all the 3Gs, some special mentions are worth. Grazie to Nico and Philip: working with you was like an adventure in the jungle. We shared endless hours sitting in the office while thinking about the mountains; and we spent long hours climbing a mountain whilst discussing about work: that is commitment. As for now, we have to talk about different jobs but maybe one day we will sit again in the same office. Grazie Samuel for your support with the difficulties of the PhD life. It was a pleasure to scramble this mountain together. Grazie Andrea, for your friendship and for being such a solid pillar for the 3Gs. Our swim in the (frozen) lake in front of the Rotondo Hut is one of my favourite memories of the PhD. Finally, grazie ai tanti who joined me in the field, or whom I joined. These were joyful days!

Un ringraziamento to all the committee members and the others who guided me through the PhD, for keeping me on track with your supervision, critical questions and constructive comments. In particular grazie Jan, we have learned to know each other during almost four years of common work, in the mountains and in the office. I have always enjoyed working with you and, most importantly, I have found a good friend. Also grazie Isabelle for our long discussions at the University of Zurich and for those in Turtmanntal. I could always count on you. Thank you and Ross for all the effort you put in the indispensable and very much appreciated activities of the graduate school.

Un ringraziamento speciale to the two Kollege, for hosting me during an intense period of writing. The flat in Hammerstrasse was a peaceful shelter where I could finish writing my thesis during the corona outbreak. This is how you make the best out of a difficult situation.

Grazie ai miei genitori, a mio fratello, mia sorella ed ai miei nipoti, da voi ho tratto gli insegnamenti più importanti. Infine, grazie Muriel! For your presence, your generous support, for the encouragement, and for your endless patience.

Structure and contents

Structure

This thesis is a cross-disciplinary collaboration between Geography and Engineering and was developed within the PERMOS (Swiss Permafrost Monitoring Network) and the X-Sense2 project. The overarching aim of this thesis is to achieve a deeper understanding of the processes governing rock glacier dynamics and their connection to the climate. This aim was achieved by combining field observations, remote sensing techniques, data analysis and process-based numerical modelling. This thesis is characterized by a strong interdisciplinary spirit, which pervades all of its parts and is well manifest in the research publications that stem from it.

The present dissertation consists of three complementary parts:

Part I **Synopsis**
This part provides a compendium of the research conducted in the scope of this thesis. Firstly, the relevance and the motivation of the dissertation are introduced and followed by a review of the state of the art in the research field. Then, the methods used in the thesis and the main results are summarized and discussed within a wider context in relation to the three research publications.

Part II **Research publications**
Three peer-reviewed publications stem from the research conducted during this thesis. They constitute the main body of this dissertation:
① Cicoira et al. (2019), *The Cryosphere*
② Cicoira et al. (2019), *Earth and Planetary Science Letters*
③ Cicoira et al. (submitted), *Permafrost and Periglacial Processes*

Each publication is anticipated by a short summary in plain language, a list of the main findings, a statement about author contributions, data availability and the publishing journal.

Part III **Appendix**
Personal bibliography of the author.

Contents

Abbreviations

a.s.l.	above sea level
BCF	Bulk Creep Factor
BH	Borehole
DEM	Digital Elevation Model
DGPS	Differential Global Positioning System
ECV	Environmental Climate Variable
EPSL	Earth and Planetary Science Letters (Journal)
ERT	Electrical Resistivity Tomography
ETH	Eidgenössische Technische Hochschule
GIS	Geographical Information System
GPR	Ground Penetrating Radar
GST	Ground Surface Temperature
InSAR	Synthetic Aperture Radar Interferometry
IPA	International Permafrost Association
MAAT	Mean Annual Air Temperature
MAGST	Mean Annual Ground Surface Temperature
PERMOS	Swiss Permafrost Monitoring Network
PPP	Permafrost and Periglacial Processes (Journal)
PZI	Permafrost Zonation Index
RG	Rock Glacier
RMSE	Root Mean Squared Error
SIA	Shallow Ice Approximation
SfM	Structure from Motion
TC	The Cryosphere (Journal)
TGS	Terrestrial Geodetic Survey
UAV	Unmanned Aerial Vehicle
UZH	Unversity of Zurich

Part I

Synopsis

1 Introduction

Rock glaciers are the visible expression of the creep of mountain permafrost. During a century of scientific research, due to their significance in the fields of geomorphology, paleo-climatology, engineering, hydrology and natural hazard management they have become iconic landforms of the periglacial environment. This chapter expresses the motivation and relevance and formulates the research questions of this thesis.

"For the mind is not a vessel to be filled,
but rather a fire to be kindled."

PLUTARCH

1.1 Motivation and relevance

Rock glaciers are iconic landforms shaping the periglacial environment, arousing interest in the fields of geomorphology, climatology, geotechnical engineering, and hydrology (e.g. Barsch, 1992, Humlum, 2000, Haeberli et al., 2006, Arenson et al., 2007, Jones et al., 2018, Bolch et al., 2019). Despite the relevance and the increasing number of studies in the copious facets of rock glacier research, our knowledge of both the fundamental mechanisms linking climatic forcing to permafrost creep, the patterns and temporal evolution of rock glacier dynamics at the regional scale remain rather limited. Therefore, further research in rock glacier dynamics can lead to important progresses in several research fields, such as glaciology, geophysics, (paleo) climatology, geomorphology and natural hazard management. Three main research fields would largely benefit from advances in our understanding of the processes controlling rock glacier dynamics as described in the following three paragraphs.

The observed recent acceleration concurrent with increasing air temperature anomalies, and the onset of rock glacier destabilization at many sites worldwide have reinforced the interest in rock glacier dynamics and in its coupling to the climate system (Gärtner-Roer et al., 2005, Delaloye et al., 2010, Wirz et al., 2016b, Hartl et al., 2016, Eriksen et al., 2018). The Global Climate Observing System (GCOS) has introduced permafrost amongst its Essential Climate Variables (ECV) and the International Permafrost Association has recently proposed rock glacier kinematics as an associated parameter. A physically based interpretation of such a product relies on a deep understanding of the processes controlling rock glacier creep and

their dynamics at seasonal and inter-annual time scales (Ikeda et al., 2008, Delaloye et al., 2013, Arenson et al., 2016, Müller et al., 2016, Monnier and Kinnard, 2016, Cicoira et al., submitted). Therefore, the present thesis not only represents an important step forward for fundamental research but it is also beneficial for operational monitoring activities at the global scale.

Due to their thermal inertia rock glaciers can develop over millennial time scales, thus preserve significant climate archives (Clark et al., 1996, Humlum, 1998, Haeberli et al., 1999). Therefore, the long lasting creep in combination with absolute and relative age dating techniques offer valuable insights in the paleo-climatic history and landscape evolution during the late-glacial and the Holocene (Haeberli et al., 2003, Avian et al., 2005, Böhlert et al., 2011, Krainer et al., 2015). In a contemporary perspective, although the current distribution and state of mountain permafrost is of scientific and practical interest for many countries worldwide, its evaluation is often based on scarce evidence, in large part represented by rock glacier inventories (Cremonese et al., 2011, Boeckli et al., 2012). Moreover, rock glaciers have been observed on other planetary bodies in the solar system, where they provide evidence of ground ice occurrence and can be used to derive information about extra-terrestrial atmospheric composition and geologic history (Carr, 1987, Baker, 2001, Whalley and Azizi, 2003). Thus, a deeper understanding of rock glacier dynamics and their surficial and internal deformation processes can further their potential as indicators for the present state and the future development of alpine permafrost, for the estimation of erosion rates and sediment fluxes under different climate conditions and for paleo-climatic interpretation of former mountain environments on Earth and on other planetary bodies.

In the field of engineering, although it is generally recognized that structure building should be avoided on active rock glaciers, increasing pressure on the periglacial environment from human activities and the ongoing degradation of mountain permafrost pose a hazard on infrastructure stability and safety (Giardino and Steven, 1985, Haeberli et al., 1997, Bommer et al., 2010, Duvillard et al., 2019). Moreover, the sediment supply to torrential catchments through rock falls, erosion processes and active layer detachments influences the frequency and magnitude of debris flows, which in turn pose a hazard on buildings and infrastructures (Haeberli, 2008, Lugon and Stoffel, 2010, Gärtner-Roer, 2012, Kummert et al., 2017). Understanding the interaction between rock glacier creep, structure building and natural hazards is fundamental for the assessment and management of activities on and below rock glaciers (Springman et al., 2013, Arenson and Jakob, 2014, Schoeneich et al., 2015).

1.2 Scope and research questions

The overarching scope of this thesis is to investigate the processes governing rock glacier dynamics and its variations across temporal and spatial scales. The thesis is set into the wide and inter-disciplinary context of mass movement monitoring. This dissertation is framed by three fundamental research questions:

Research Question I:

What is the influence of external temperature forcing on rock glacier creep?
Rock glaciers show strong seasonal and inter-annual variability in creep rates. In the literature, it is commonly accepted that the observed variations can be explained through the dependency of rock glacier rheology on temperature, but quantitative evidence is missing. This hypothesis is tested in *Publication I*.

Research Question II:

How does unfrozen water influence the dynamics of rock glaciers?
Liquid precipitation and snow melt are thought to influence rock glacier dynamics through increased pore water pressure at the rock glacier shear horizon. Although substantial evidence from in-situ and remote sensing observations confirm this hypothesis, our understanding of this process remains mostly qualitative and conjectural. This hypothesis is tested in *Publication II*.

Research Question III:

How to mathematically describe rock glacier dynamics at a regional scale?
Geophysical investigations, in-situ surveys and remote sensing observations substantially contribute to our understanding of rock glacier dynamics. However, the regional-scale long-term evolution of rock glacier dynamics remains at present mostly unknown or only qualitatively investigated. A novel methodology to approach this research gap is proposed in *Publication III*.

2 State of the art in the research field

More than a century ago, Spencer (1900) published the first scientific article on rock glaciers, which he addressed as "a peculiar form of talus", already identifying them as gravity driven mass movements and describing some of their characteristic features. Although his intuition remains fascinating and inspiring, the scientific advances reached through the scientific process have greatly expanded our knowledge on rock glaciers and their creep and partly contradicting his (and others') theories. This chapter provides a brief overview of the current knowledge on the physics of permafrost creep and rock glacier dynamics.

"If I have seen further it is by standing on the shoulders of giants."

ISAAC NEWTON

2.1 Permafrost and rock glaciers

Permafrost is thermally defined as ground material (i.e. soil and rock) which temperature remains below 0° C for more than two consecutive years (Muller, 1945, Harris et al., 1988). Permafrost occurs in regions were the mean annual air temperature (MAAT) is below freezing and affects nearly all of the Artic and a great portion of the Subartic, covering about one-fifth of the entire land surface of the world (Nikiforoff, 1928, Muller, 1945, Frost and Mintzer, 1950, Gruber, 2012). The thermal regime of permafrost enables the formation and preservation of ground ice and determines the spatio-temporal scales of its creep (Taber, 1930, Murton and French, 1994, Haeberli et al., 2006). Until the second half of the XIX century, the study of permafrost was limited to a few miners, explorers, some natural scientists and a limited number of engineers, mostly interested in high altitude regions. Increasing economic activities in the 1970s, largely associated with the exploitation of natural resources in the North, increased the interest in research on frozen soils due to the destructive action of frozen ground and the related engineering problems (Muller, 1945, Frost and Mintzer, 1950, French, 2003, Arenson et al., 2007).

In more recent years, many aspects of periglacial research have become important in the context of climate change. In fact, permafrost is one of the Earth's components most sensi-

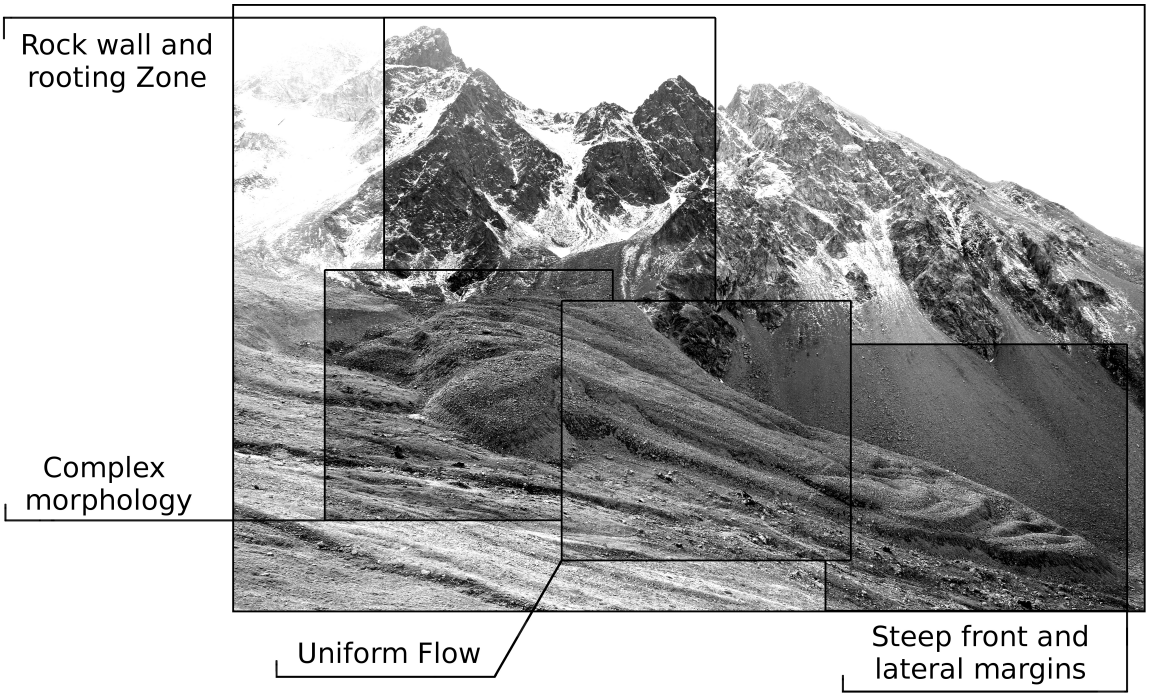

Figure 2.1: Illustration of the typical components and visual features of an alpine rock glacier. From the top to the bottom, the rock walls, the talus slope, then the elegant (Muragl) Rock Glacier. Evident areas characterized by complex morphology, uniform flow patterns, steep front and lateral margins distinguish the rock glacier in the landscape.

tive to increasing air temperatures and is currently experiencing strong warming and thawing, posing hazards to nature and human activities (Romanovsky et al., 2002, Harris et al., 2003, Chadburn et al., 2017, Karjalainen et al., 2019, Biskaborn et al., 2019). From a global standpoint, a warming climate can induce an acceleration in the release of large quantities of organic carbon that are currently stored in high-latitude regions of the Earth, thus accelerating climate change (Schuur et al., 2015). At lower latitudes, growing evidence indicates that the rate of atmospheric warming is amplified with elevation and that this effect will be accompanied by striking changes in the extent and the dynamics of mountain permafrost (Haeberli and Beniston, 1998, Pepin et al., 2015). Therefore at a local scale, permafrost represents an important subject for local communities living in mountain ranges all over the world, from the Arctic, to the European Alps, to the dry Andes of Argentina and Chile. In Switzerland, approximately 5% of the land surface (generally above 2600 m a.s.l.) is characterized by mountain permafrost (Keller et al., 1998, Cremonese et al., 2011, Boeckli et al., 2012). The evaluation of future effects of climate change on and from the periglacial environment and the consequent development and implementation of adaptation measures to reduce these impacts necessitates understanding of deformation processes (Romanovsky et al., 2002, Arenson et al., 2016).

Permafrost is usually invisible from the surface and the application of various indirect methods, such as interpretative analysis of aerial imagery, has been required for its detection

and characterization since the first studies on the topic (Frost and Mintzer, 1950, Beniston et al., 2018). After almost a century of technological advances, state-of-the-art contemporary remote sensing techniques allow the multi-temporal quantification of surface deformations over large areas (Arenson et al., 2016, Strozzi et al., 2020). Amongst the evidence of past- and present permafrost occurrence, the most discernible and spectacular are unequivocally rock glaciers (Fig. 2.1).

According to Barsch (1992):

Active rock glaciers are lobate or tongue-shaped bodies of perennially frozen debris supersaturated with interstitial ice and ice lenses or even with bodies of massive ice, which move downslope by creep as a consequence of the deformation of the ice contained in them and which are, thus, features of choesive flow.

Rock glaciers have received increasing attention from the international scientific community due to their distinct appearance, their scientific and social relevance and due to their intrinsic beauty and allure (Wahrhaftig and Cox, 1959, White, 1976, Humlum, 1998, Haeberli et al., 2006). Over time, the origin and the classification of rock glaciers has been a matter of dispute. In this thesis, the term "rock glacier" will be used without discriminating between different classifications systems. The establishment of a consensus and the formulation of a broadly accepted definition of rock glaciers and their origin lays beyond the scope of this thesis and should be searched elsewhere (Potter, 1972, Whalley, 1974, Johnson, 1978, Giardino and Vitek, 1988, Barsch, 1992, Haeberli and Vonder Mühll, 1996, Berthling, 2011).

The next paragraphs introduce the current knowledge about the physics of rock glacier creep and synthesises the most important observations of rock glacier dynamics and its variability over short (seasonal) and long (decennial and beyond) temporal scales.

2.2 The physics of rock glacier creep

In early studies, the movement of rock glaciers has been thought to happen mostly near the surface and being driven by freeze-thaw cycles (Capps, 1910). Almost fifty years later, Wahrhaftig and Cox (1959) deduced solely from geomorphological observations that a large part of the deformation within a rock glacier must occur at depth. Their thesis was confirmed only in recent years, when direct observations from borehole investigations shed light on the internal structure and deformation profile of rock glaciers (Haeberli et al., 1998). Although only limited direct observations exist, the borehole data show a recurrent structure and behaviour for all the investigated landforms (Haeberli et al., 1988, Arenson et al., 2002, Krainer et al., 2015, Buchli et al., 2018, Arenson, pers. com. 2020). Based on this knowledge, rock glaciers are typically divided into three distinct structural and dynamical units, which are, from the surface to deeper ground: the active layer, the ice-rich core, and the shear horizon (See Fig. 2.2). Below these three units no or very limited movement occurs: the shear horizon delimits in a dynamic sense the thickness of the active rock glacier itself. The surface displacements of a rock glacier are the sum of the three independent contributions described below. The following sections provide a brief review of our current knowledge on

the physics of permafrost creep and rock glacier dynamics, essential for their mathematical description.

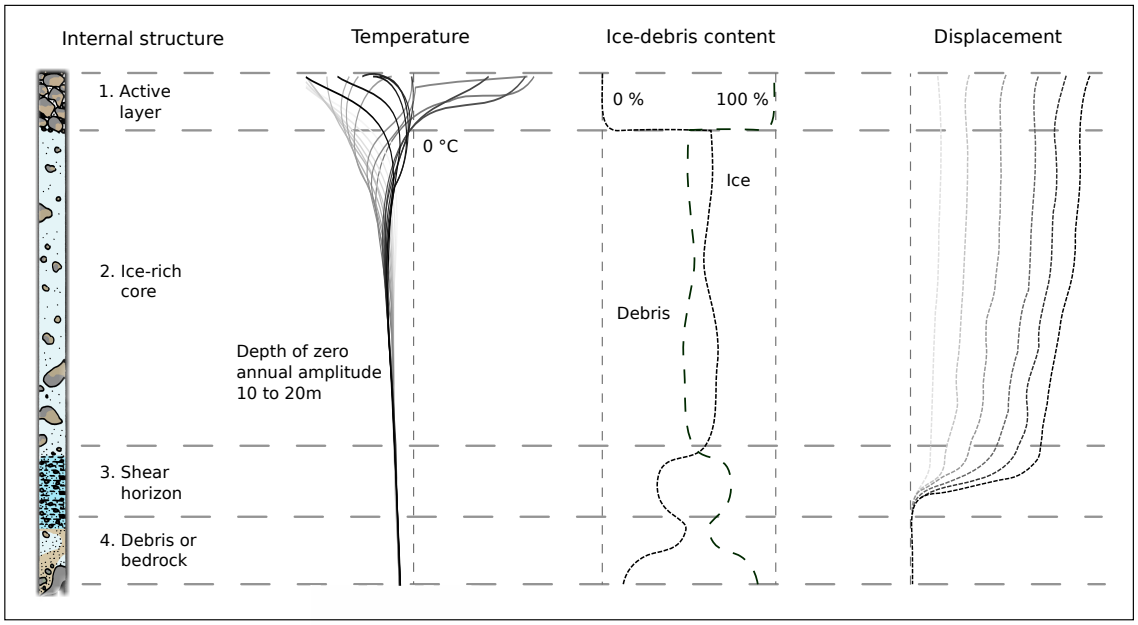

1. Active layer

Structure and composition:
unconsolidated boulders, several meters in thickness.
the composition varies seasonally due to phase changes, only frozen in winter.
Temperature:
this layer strongly insulates the underneath permafrost from external temperature forcing. It is influenced by freeze-thaw cycles and by advective heat fluxes.
Displacement:
caused by sliding, tilting or rolling of the boulders.

2. Ice-rich core

Structure and composition:
ice-rich debris constituting the main unit of the rock glacier.
The vol. ice content typically ranges from 40% to 90%.
The debris size is significantly smaller than in the a.l.
Temperature:
the thermal regime is controlled by heat diffusion.
Talik development can indicate permafrost degradation.
Displacement:
caused by temperature dependent creep of the ice.

3. Shear horizon

Structure and composition:
Frozen soil with banded ice and pressurized water.
Ice content and debris size smaller than in the ice-rich core.
A few meters in thickness.
Temperature:
the seasonal temperature signal is strongly attenuated.
Temperature variations occur at larger temporal scales.
Displacement:
accomodates up to 90% of the total displacements, the creep is influenced by pore water pressure.

4. Debris or bedrock

Structure and composition:
the lower boundary of the rock glacier, composed by sediments or bedrock. Often old material transported on top of the rock glacier and then being overridden.
Temperature:
negative and positive temperatures are possible according to the state of the permafrost.
Displacement:
the displacements are considered negligible in this region.

Figure 2.2: Graphical illustration and textual description of vertical profiles (conceptualized) of a typical rock glacier. From left to right the internal structure, the temperature variations, the composition and the displacement profiles of a typical rock glacier are shown. The concept is based on the most influencing publications on borehole investigations on rock glaciers (Arenson et al., 2002, Arenson and Springman, 2005a, Krainer et al., 2015, amongst others). The profiles are drawn on the basis of data from the Murtél borehole (Vieli et al., in preparation).

2.2.1 The active layer

At the rock glacier surface, a few meters of seasonally frozen blocky sediments represent the interface between the ice-rich permafrost and the atmosphere. The thermodynamics of the active layer are complex due to the multi-phase nature of this layer, which consists of a rock, ice, water, and air fraction, and because of the multitude of processes governing its energy balance, which include conductive, advective, and convective heat fluxes (Hanson and Hoelzle, 2004, Delaloye and Lambiel, 2005, Scherler et al., 2014, Wicky and Hauck, 2017). During the summer months, the active layer insulates the permafrost underneath it, strongly reducing the thawing process at the permafrost surface. Although melt rates at degrading rock glacier sites are usually limited to a few centimeters per year (Krainer et al., 2015), the influence of increasing air temperature can significantly (with a power law) impact the creep rates of the underlying rock glacier (Arenson and Springman, 2005a, Müller et al., 2016, Monnier and Kinnard, 2016).

The deformation of the active layer is mostly linked to tilting or sliding of the boulders on top of the permafrost table. Rare events of active layer detachments have been observed at rock glacier sites, characterized by extreme values of displacement rates due to sliding (Lugon and Stoffel, 2010, Marcer et al., 2020). In some cases, boulders can move very rapidly for a short time also in relation to tilting. In fact, when a boulder is tilting close to a terrain step, it might lose its stability and quickly roll down slope, as it often happens close to active front (Haeberli et al., 1998, Buchli et al., 2018). When measuring surface displacements, it is difficult to filter the deformation component associated with the active layer. Nevertheless, the magnitude of this component is in general orders of magnitude smaller than the total surface velocity, therefore negligible in first approximation (Wirz et al., 2016b, Cicoira et al., 2019b). An exception are extremely slow-moving rock glaciers, where the movement of the boulders on the surface can represent a relevant contribution to the total observed velocities (e.g. Murtél Rock Glacier). Based on this evidence, the dynamics of the active layer can be considered not representative of the state of the creeping permafrost underneath it and will therefore be neglected later in the thesis when mathematically describing rock glacier creep. However, it is important to remember that the active layer is essential for the surface mass and energy balance of a rock glacier and thereby has a fundamental influence on rock glacier creep.

2.2.2 The ice-rich core

The inner core of a rock glacier is composed of a mixture of ice and rocks with a typical thickness of 10 to 25 m. The ice component can be polygenetic and may include significant meteoric, superficial, and ground-water contributions (Haeberli and Vonder Mühll, 1996). Observations from boreholes at moving rock glaciers indicate values of the volumetric ice content of above 50% apart from the case of degrading permafrost, where the values can be lower (Arenson et al., 2002, Haeberli et al., 2006, Hausmann et al., 2012, Monnier and Kinnard, 2016). The rock component of rock glaciers typically originates from debris-laden

snow avalanches, episodic rock avalanches and long-lasting rockfall activities (Clark et al., 1998, Humlum, 2000, Haeberli et al., 2006). The grain size of the rock component is usually finer than in the active layer. This structural difference is the consequence of the processes that contribute to the debris supply (fall sorting and washing away) and the motion of the rock glacier itself (kinetic sieving) (Haeberli et al., 2006). As a consequence, the structure of the ice-debris matrix can be very heterogeneous within a single rock glacier and can be very diverse amongst different landforms (Clark et al., 1998, Arenson et al., 2010). The thermal regime of the inner core is mainly controlled by heat conduction (Lachenbruch et al., 1988, Haeberli et al., 2006). Therefore, the phase of the temperature signal from the surface is linearly delayed and its amplitude exponentially attenuated with depth (Carslaw and Jaeger, 1959, Cicoira et al., 2019b). The seasonal temperature signal influences the frozen ground until the depth of the zero amplitude, which is usually found at about 15 to 20 m depth. Thermal changes below this point require temperature forcing to act at longer temporal scales (decades and beyond). With regard to water flow, the ice-rich core can be considered impermeable in first approximation (Krainer and Mostler, 2002). However, water flow has the potential to affect significantly the inner core especially under conditions of permafrost degradation, when temperatures close to the melting point lead to high structural heterogeneity, preferential flow pathways and augmented interstitial water content (ibidem).

The deformation of the ice-rich core is mainly governed by the time dependent creep of its ice component (Arenson et al., 2007). Similarly to pure ice, the creep of the inner core is susceptible to temperature variations and strongly depends on the structure of the rock glacier itself. In fact, the creep behaviour of a debris-ice mixture and even its stress-strain behaviour (ductile - dilatant - brittle) can vary substantially depending on the applied strain rate, on the volumetric ice content and on the grain size of the rock component (Arenson et al., 2007). For a homogeneous matrix, the ice-rich core can be described as a creeping viscous material, as confirmed by the classical deformation profiles observed from inclinometer readings (see Fig. 2.2). However, for more heterogeneous and anisotropic structures, the debris component and the ice structure can strongly influence the deformation profile (Buchli et al., 2018). Overall, an amount of 10%-40% of the total displacement takes place within the ice-rich core and is governed by temperature variations (Arenson et al., 2002).

2.2.3 The shear horizon

The shear horizon is a shallow layer of a few meters of thickness, where the highest shear rates are observed and where most of the deformation (60%-90%) occurs (Arenson et al., 2002). It is located below the inner core, at a depth of 15 to 30 m from the surface. Despite the extreme paucity of observations, borehole investigations showed a decrease in volumetric ice content (20%-50%) and in the debris grain size within this layer (Haeberli et al., 1988, Arenson and Springman, 2005a). Moreover in this layer, the large deformation rates modify the structure and may themselves influence the properties of material itself, as suggested by the banded ice observed in the ice cores from the Lazaun Rock Glacier in Sudtirol (IT) (Krainer et al., 2015). Due to the depth of the shear horizon, the influence of surface

temperature forcing is limited and considerably delayed in time (Kääb et al., 2007, Cicoira et al., 2019a). At longer time scales, however, changes in temperature, especially in intervals close to the melting point, can cause significant variations in the mechanical properties of the rock glacier material, also at the depth of the shear horizon. While the ice-rich core can be assumed to be mostly impermeable to water flow, pressurized water has been observed during borehole perforations within the shear horizon, suggesting a strong influence of unfrozen water on the behaviour of this unit (Ikeda et al., 2008, Bast, pers. com. 2015, Buchli et al., 2018).

Debris-ice mixtures are usually more resistant to deformation at low temperatures than their pure end-member components (Moore, 2014). As a consequence, the apparent viscosity of rock glacier material is larger than for pure ice at the same temperature and stress (Monnier and Kinnard, 2016, Müller et al., 2016). However, especially close to melting conditions, the growth of unfrozen water films at the interface between ice and debris has the potential to reduce the strength of the mixture and can even lead to substantial weakening (Moore, 2014). In accordance to this consideration, the effective viscosity of the shear horizon material has been estimated to be up to seven times smaller than that of pure ice at similar conditions (Bucki and Echelmeyer, 2004, Ikeda et al., 2008).

In summary, the contribution of the shear horizon to the total surface displacement is large (60%-90%) and it also accounts for most of the inter-annual and seasonal variations in rock glacier creep (Arenson et al., 2002, Cicoira et al., 2019b). Field and theoretical studies (Ikeda et al., 2008, Buchli et al., 2018, Cicoira et al., 2019b) show that at temporal scales from months to several years, these variations are mainly controlled by pore water pressure within the shear horizon. At longer temporal scales, changes in the structure of the shear horizon, driven by the combined influence of permafrost creep and ground temperature, are still poorly understood but are expected to play an important role in determining the long-term evolution of rock glaciers and their dynamics (Kääb et al., 2007, Müller et al., 2016, Seppi et al., 2019).

2.3 Creep and dynamic models

Developing a mathematical formulation of a natural system - a model - can be used to study its properties and understand its dynamics. All models have to be constrained and validated with observations, regardless if they are based on statistical methods or on analytical formulations of physical processes. In comparison to glaciology, where copious studies have investigated the physics of ice, research on rock glaciers is characterized by a paucity of direct investigations both in the field and in the laboratory. This restrain results in a scarce understanding of the fundamental processes governing rock glacier creep and hinder the establishment of quantitative models for rock glacier dynamics.

2.3.1 Rheological models

The rheology of debris-ice mixtures, i.e. the mechanical constitutive relationship which combines the deformation of the material to its internal stresses, can be described mathematically. Having identified ice creep as the main mechanism behind the movement of rock glaciers, the first theory to consider when describing rock glacier deformation is the empirical flow law proposed by Nye (1952) and Glen (1955) for pure ice:

$$\dot{\gamma} = A\tau^n. \tag{2.1}$$

Glen's law describes thermally activated dislocation creep for an isotropic crystalline solid and is analogous to the relationships that describe deformation of metal and rock at high temperatures (Weertman, 1983). The shear rates $\dot{\gamma}$ depend only on the shear stress τ through a power law relationship, and on the constitutive properties of pure ice, which are described through two parameters: the fluidity factor A (inversely related to viscosity) and the flow exponent n. The fluidity parameter in eq. 2.1 is described by an Arrhenius relation dependent on temperature (Mellor and Testa, 1969):

$$A = A_0 exp\left(-\frac{Q}{R_* T}\right), \tag{2.2}$$

where A_0 is a parameter typical of the material, Q is the activation energy, R_* is the universal gas constant and T is the absolute temperature in Kelvin. This formulation has been proven valid for most of the glacial and periglacial conditions on Earth (Moore, 2014). When approaching the melting point, the fluidity parameter shows an additional dependence on temperature due to liquid water along grain boundaries (De La Chapelle et al., 1999, Moore, 2014). This effect can be accounted for by correcting the formulation of the fluidity parameter (Eq. 2.2) with an additional term:

$$A_w = A + \alpha W, \tag{2.3}$$

where W is the unfrozen volumetric water content and α a model parameter (Cuffey and Paterson, 2010). The flow exponent n is often considered constant and best approximated for pure ice by a value of 3, although experimental and field evidence exist that this value represents the superposition of different mechanisms (Weertman, 1983, Cuffey and Paterson, 2010).

The driving stress can be calculated as:

$$\tau = \rho g H \sin\alpha, \tag{2.4}$$

Where ρ is the density of the creeping material, g the gravitational acceleration, H the thickness of the moving rock glacier, and α the surface slope angle.

The previous theory has to be expanded when studying rock glaciers. In fact, they consist of debris-ice mixtures, whose properties depend on the volumetric fractions of their

constituents and not only on pore ice. As described above, several field observations, integrated by theoretical and experimental studies, have highlighted debris concentration and size, temperature, water content and internal stresses as the first-order variables governing the deformation of debris-ice mixtures (Moore, 2014). Arenson and Springman (2005b) have tested natural (from borehole cores at rock glacier sites in Switzerland) and synthetic soil samples in order to adapt Glen's flow law to the rheology of rock glacier material (Arenson and Springman, 2005a). The authors expressed the dependency on the volumetric ice content w_i by introducing a logarithmic term to eq. 2.2 and a linear dependency to the flow exponent:

$$A = exp\left(\frac{a}{1+T}\right) + 5 \times 10^{-11} e^{-10.2 w_i}, \tag{2.5}$$

$$n = 3 w_i. \tag{2.6}$$

In addition to the variability of material properties, also the processes governing the deformation of rock glaciers can be diverse. For debris-ice mixtures with a high volumetric content of debris, frictional effects ensue when particle to particle contact is reached. For the end-member case of unfrozen debris, the maximum strength is in first approximation described by the Terzaghi form of the Mohr-Coulomb yield criterion:

$$\tau_r = \tau_{c\theta} + \sigma_e \tan \phi_C, \tag{2.7}$$

where σ_e are the effective stresses, $\tau_{c\theta}$ is the cohesion and ϕ_C is the friction angle of the shear horizon material. Contrarily to unfrozen material, the strength of ice-rich debris is strongly strain rate and temperature dependent and preserves a viscous component due to the presence of pore ice. Ladanyi (2003) has proposed a constitutive relation that combines the frictional yield threshold with viscous flow resistance. In this mathematical formulation, the shear strain rate depends on the shear stress and the two creep factors, and additionally on the shear resistance of the deforming material. Three cases are made for describing mixtures with different volumetric debris content and the dependency of their shear resistance to temperature. For an ice-rich, cold frozen soil, where both cohesion and friction are affected by temperature and strain rate, the shear strain rate becomes:

$$\dot{\gamma} = \dot{\gamma}_C \left(\frac{\tau}{\tau_r}\right)^n, \tag{2.8}$$

where $\dot{\gamma_C}$ is the critical shear strain rate typical of the material. This formulation allows us to express the frictional behaviour of the ice-rich mixture augmented by a rate-dependent cohesive strength. Moreover, according to the definition of the shear strength, the calculation of the effective stresses σ_e allows to consider the effect of pore water pressure on the driving stress.

2.3.2 Dynamical models

Two basic laws govern the field of continuum mechanics and combined together allow the mathematical description of the motion of rivers, snow avalanches, ice glaciers and rock glaciers as well. The Navier-Stokes equation describes the conservation of momentum and embodies Newton's second law. The continuity equation states the conservation of mass expressing Lavoisier's law. Solving the coupled system allows us to explore the dynamics of a physical system. The analytical solution of the model is arduous if not impossible and even numerical computing is laborious and computationally expensive. Therefore, simplifications are required. When the ratio of inertial to viscous forces, the Reynolds number $Re = \rho UL/\mu$ is very low, the inertial terms of the Navier Stokes equation can be neglected. Another important simplification ensues when the horizontal extent of the modelled landform can be considered much larger (> 10 times) than its thickness. In this case it is justified to adopt the Shallow ice approximation Hutter (1983). Moreover when the geometry is favourable (length much larger than width), the model can be further simplified to just one dimension. This is often the case for rock glaciers, for which the Reynolds number is of the order of 10^{-12} and the length (hundred of meters) is much larger than the thickness (decameters) and often larger than the width. Under these assumptions, the longitudinal stress gradients are not considered and bi- and three dimensional effects are neglected. In summary, the surface slope and the thickness of a rock glacier are the minimum geometrical information required to design a process-based model for rock glacier creep. Here on, the formulation will be further continued based on these assumptions and will adopt the mono-dimensional shallow ice approximation.

2.4 Temporal variability in rock glacier dynamics

The movement of rock glaciers has already been observed in the first pioneering studies more than a century ago and, ever since, the very definition of rock glaciers has been inextricably intertwined with their dynamics (Spencer, 1900, Cross et al., 1905, Capps, 1910).

Investigations of the same landforms over several years allowed to detect inter-annual variability in the displacement rates already in the early stages of rock glacier research by means of geodetic surveying (Chaix, 1923, 1943, Wahrhaftig and Cox, 1959), but these findings were rarely mentioned and barely discussed from a dynamical perspective White (1976), Barsch (1992). Haeberli (1985) provided the earliest observations of seasonal velocity variations, followed almost two decades later by more consistent and detailed studies, which highlighted a significant increase in flow velocities starting in the 1990s. On the basis of glaciological studies, temperature has been suggested as the main factor controlling rock glacier creep and its variability (e.g. Arenson et al., 2002, Arenson and Springman, 2005a, Haeberli et al., 2006). Especially the introduction of modern DGPS technology allowed to improve the resolution of the measurements and extended them to more field sites with the result of substantially increasing the confidence of the scientific community in the observations (Lambiel and Delaloye, 2004, Krainer and Mostler, 2006, Perruchoud and Delaloye,

2007, Delaloye et al., 2008). Finally, the introduction of continuous differential DGPS measurements yielded unprecedented temporal resolution and allowed the detection of variations in rock glacier velocities at time scales of days to weeks at significantly increased precision and accuracy (Wirz et al., 2011, 2014).

Until the late 1990s, long time series of rock glacier surface velocities stem from the coherent work of dedicated researchers, who were personally responsible for the regular surveying of the field sites (Barsch and Zick, 1991, Francou and Reynaud, 1992, Delaloye et al., 2008) This task has been facilitated with the introduction of continuous DGPS measurements and remote sensing techniques. Analysis of aerial imagery and the introduction of repeated UAVs surveys, in combination with the use of offset tracking algorithms allow the determination of distributed maps of displacement rates at high accuracy and resolution (Kääb and Vollmer, 2000, Dall'Asta et al., 2017, Bodin et al., 2018, Vivero and Lambiel, 2019). At a decennial temporal scale, the re-analysis of historical aerial imagery allowed the reconstruction of velocity time series back in the past until the early XX century, revealing a significant increase in flow velocities starting in the 1990s (Kellerer-Pirklbauer et al., 2012, Scapozza et al., 2014, Hartl et al., 2016, Kellerer-Pirklbauer and Kaufmann, 2017, Kenner et al., 2020). Recently, advancing InSar applications have allowed the quantification of short-term displacement rates from space at high frequency and accuracy on virtually all rock glaciers on the planet Liu et al. (2013), Barboux et al. (2013), Strozzi et al. (2020). Currently, monitoring activities are regularly conducted from research institutes and from national monitoring networks, providing consistent time series of kinematic measurements and meteorological observations (see Fig. 2.3).

Overall, although only a small number of studies exist on rock glacier kinematics in comparison to ice glaciers, the available observations show a consistent flow pattern. The seasonal and inter-annual rhythm of rock glacier flow is characterized by an acceleration in early summer with flow velocity maxima occurring between summer and early winter, and a deceleration leading to a late-spring minima (e.g. Delaloye et al., 2010, Wirz et al., 2016a). The seasonal velocity signal generally shows a time lag of several months relative to air and ground surface temperatures (Wirz et al., 2016b, PERMOS, 2016, 2019). This phase lag has been interpreted as the time needed by the temperature signal to propagate into the frozen ground and thus influence rock glacier creep (e.g. Kääb et al., 2007, Haeberli et al., 2006, Delaloye et al., 2010). The observation that the spring acceleration is concurrent to the snow melt has strongly corroborated the hypothesis that unfrozen water may influence rock glacier creep (Shroder, 1978, Giardino and Steven, 1985, Krainer and Mostler, 2006, Ikeda et al., 2008, Delaloye et al., 2010, Wirz et al., 2016b, Hartl et al., 2016). The short-term velocity peaks (days to weeks) appear to be related to tilting or slip events of boulders, and therefore limited to the active layer of the rock glacier (Wirz et al., 2014). Recent studies concur to the conclusion that temperature is the main driver governing rock glacier dynamics and that water (from snow melt and liquid precipitation) can play an important role in controlling seasonal and inter-annual flow variations, but the used approaches remain speculative and lack quantitative models (Wirz et al., 2016b, Kenner et al., 2017, Kellerer-Pirklbauer et al., 2018, Buchli et al., 2018).

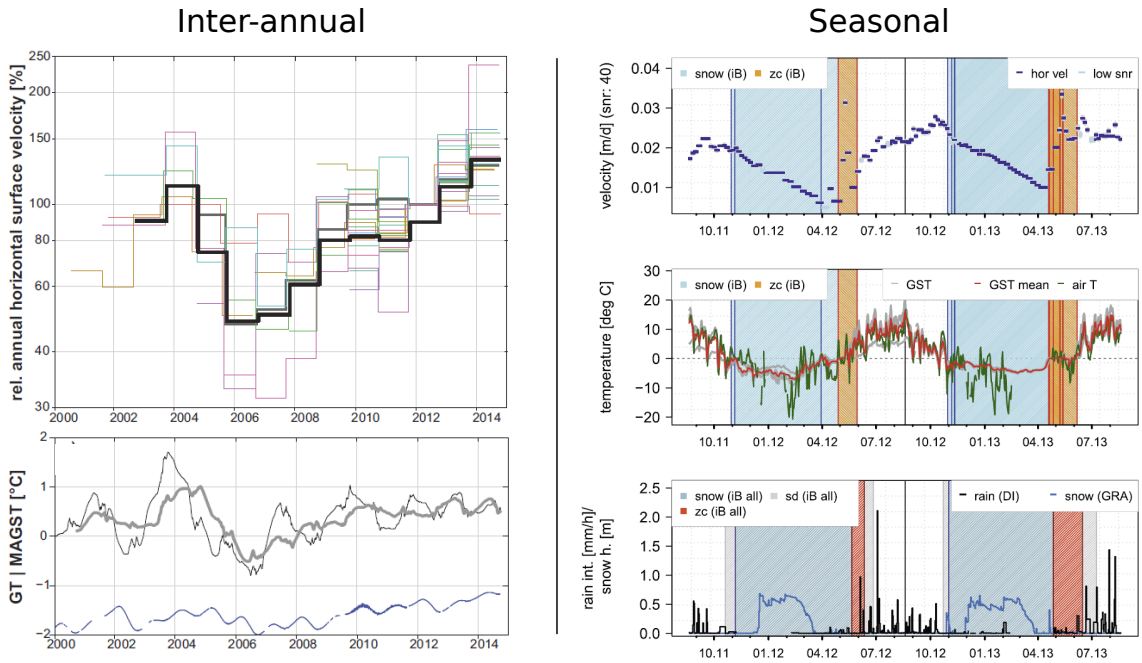

Figure 2.3: State of the art observations depicting the connection between rock glacier surface velocities and climate variables at the inter-annual (left) and seasonal (right) temporal scales. The upper panels show the horizontal velocities for 16 rock glaciers in the Swiss Alps (left - mean black line) and for the Braithorn Rock Glacier (Valais - CH). The lower panels show meteorological variables. For the inter-annual temporal scale: MAGST from six field sites and ground temperatures at 15.5 m depth for the Murtél Rock Glacier. For the seasonal temporal scale: mid, air (green) and ground surface (red) temperatures; bottom, rain intensity (black bars) and snow height (blue line). The blue and orange areas highlight the snow cover and the zero curtain periods. Modified after PERMOS (2016) and Wirz et al. (2016a).

Concomitant with the above mentioned trend in rock glacier velocities, major abrupt changes in rock glacier kinematics have been observed since the 1990s for several landforms in the European Alps and in a few more cases in other mountain ranges worldwide (Avian et al., 2005, Gärtner-Roer et al., 2008, Iribarren Anacona and Bodin, 2010, Delaloye et al., 2013, Scotti et al., 2017, Eriksen et al., 2018, Marcer et al., submitted). These unanticipated kinematic changes, commonly labeled as destabilization, can affect the entire rock glacier or a large part of it and are often anticipated by the onset of surface signs of degradation, such as cracks and scarps (Gärtner-Roer et al., 2005, Delaloye et al., 2010, Marcer et al., 2019). Topographical predisposition, given by convex topography with extensive flow and high strain rates, is a necessary but not a sufficient condition for the onset of rock glacier destabilization, which can be triggered from other causes such as thermal- and hydrological forcing, external loading, and drastic changes in the ice/debris input rates (Delaloye et al., 2013, Marcer et al., 2019). Gärtner-Roer et al. (2008) indicated the rheological properties of warming permafrost as the main controls of rock glacier destabilization, emphasizing the importance of hydrological effects of unfrozen water. It has to be noted, that the terminology "rock glacier destabilization" has a geomorphological origin and might be misleading if not correctly con-

textualized. In fact, rock glacier destabilization does not involve the onset of structural instabilities in the rock glacier body (apart from a few rare cases) and therefore it does not correspond to an instability from a geotechnical standpoint. Detailed investigations at the Furggwanghorn Rock Glacier (Turtmanntal - CH) revealed multiple superimposed shear zones indicating past failure planes, contradicted the well-established relationship between warming temperatures and surface velocities supported the hypotheses that dynamics variations may be driven by hydrological effects (Buchli et al., 2013, Merz et al., 2015a, 2016, Buchli et al., 2018).

Velocity variations at temporal scales longer than the measurements (centennial and beyond) deserve a separate discussion. Because no direct observations are possible, the creep rates can only be derived from the extrapolation of present day flow conditions and from age estimates (Frauenfelder et al., 2005, Scapozza et al., 2014, Böhlert et al., 2011, Kellerer-Pirklbauer et al., 2018). Several absolute and relative age dating techniques exist, based on different quantities such as the Schmidt-hammer rebound values, lichen cover distribution, luminescence signals, radiocarbon and cosmogenic nuclides concentrations (Haeberli et al., 2003). The results from these techniques represent minimum ages of rock glacier formation (travel time of the debris since incorporation in the rock glacier) and are accompanied by uncertainties in the order of magnitudes of centuries to millennia (Böhlert et al., 2011, Fuchs et al., 2013). The large uncertainty related to unknown changes in paleo creep rates (and possible phases of inactivity) can be limited by the combination of the above mentioned techniques and by numerical modelling, especially if (rare) age data are available at depth from borehole drillings (Krainer et al., 2015). Tree-ring dating provide indirect information about activity phases, which can be analysed in combination with long-term climatic data (precipitation and temperature) but the results are so far contradictory and a detailed discussion requires more evidence (Shroder, 1978, Sorg et al., 2015). Despite these limitations, age dating techniques provide valuable information about phases of rock glacier activity and their long-term mean displacement rates throughout the Holocene (Böhlert et al., 2011, Scapozza et al., 2014). The relevance of the results is subordinated to the quality of their discussion, which depends upon a solid knowledge of the fundamental processes governing rock glacier dynamics.

3 Methodology

In order to achieve the scope of this thesis and answer the three leading research questions, a variety of methods has been applied, including numerical modelling and data analysis supported by the compilation of previously existing datasets and the collection of novel observations from in-situ and remote sensing techniques such as drone surveying and geophysical methods. This chapter exposes the methods and the database used in this thesis.

"Pluralitas non est ponenda sine neccesitate:
frustra fit per plura quod potest fieri per pauciora."

WILLIAM OF OCKHAM

3.1 Process-based modelling of rock glacier dynamics

In almost a century of research, numerous field investigations and remote sensing observations shed light on the temporal variability of rock glacier velocities. Geophysical investigations and borehole campaigns unveiled important information about the internal structure, thermal and deformation regimes of rock glaciers. This knowledge, supported by the results of laboratory experiments on the properties of rock glacier material, allowed the development of theories on permafrost creep, and its coupling to the climate. However, the complex, transient and non-linear nature of this interaction hinders the generalization of these theories to the large-scale and long-term behaviour of rock glaciers. Therefore, the interpretation of the observations remains open to doubt and the fundamental processes controlling rock glacier dynamics still remain poorly and mostly qualitatively understood. In order to bridge the gap between the observations and a quantitative understanding of the physical processes involved, we adopted process-based numerical modelling as the main methodology. Process-based modelling, based on a theoretical understanding of physical processes, represents a useful approach to quantitatively investigate rock glacier dynamics and its coupling to the climate. It allows the explicit formulation of the theoretical assumptions and a clear physical interpretation of the results. This last essential point is embraced as a fundamental principle of the entire dissertation and as such it underlies the methods, the results and eventually their discussion. According to the heuristic principle known as Occam's razor, all the quantities that cannot be observed or interpreted are avoided as far as possible

so that the modelling is effectively designed in the simplest way needed for a physical interpretation of the results.

The modelling work conducted within this thesis can be divided into two separate parts. The first one examines the complex hydro-thermo-mechanical processes governing rock glacier dynamics and its seasonal and inter-annual variations for five well documented rock glaciers, for which abundant detailed observations are available. The second one extends the previous approach to the regional scale in order to explore the patterns and the long-term trends of rock glacier dynamics for a large database comprising more than 400 landforms.

3.1.1 Process understanding at the field site scale

In order to investigate the response of rock glacier dynamics to variations in external forcing at seasonal and inter-annual temporal scales, we design a novel conceptual and numerical modelling approach. The modelling is constrained and the results are compared against kinematic, geophysical and meteorological observations for five well documented rock glaciers in the Swiss Alps. The modelling framework consists of four coupled units describing heat transfer into the ground, the catchment hydrology, the hydro-mechanics of the rock glacier and its rheology (Fig. 3.1).

The dynamics of the rock glacier is described by two independent power-law creep relations representing deformation in the ice-rich core and in the shear horizon of the rock glacier (see Fig. 3.1). We calculate the deformation within the ice-rich core by using the temperature dependent model proposed by Arenson and Springman (2005a), whereas for capturing the influence of pore water pressure on deformation rates in the shear horizon, we use the creep-law proposed by Ladanyi (2003). According to the scope of the thesis, the modelling aims at simplicity while capturing all the essential processes needed to understand the physics behind seasonal variations in rock glacier creep. Adding more processes and variables to the modelling would increase the complexity of the study, hindering the interpretation of the results and the logic of the conclusions. Therefore, we neglect several secondary processes and assume that the properties of the rock glacier material are constant in time and homogeneous in space.

Thermodynamical model

We calculate ground temperature evolution at depth using the observed ground surface temperature time series as input. The diffusion equation for temperature is solved on the vertical direction (Carslaw and Jaeger, 1959):

$$\frac{\partial T}{\partial t} = \kappa \frac{\partial^2 T}{\partial z^2}, \tag{3.1}$$

where T [°C] is the temperature, z [m] the vertical coordinate, t [days] the time, and κ [m^2 °C^{-1} day^{-1}] the thermal diffusivity of the ground material. At the upper boundary, the ob-

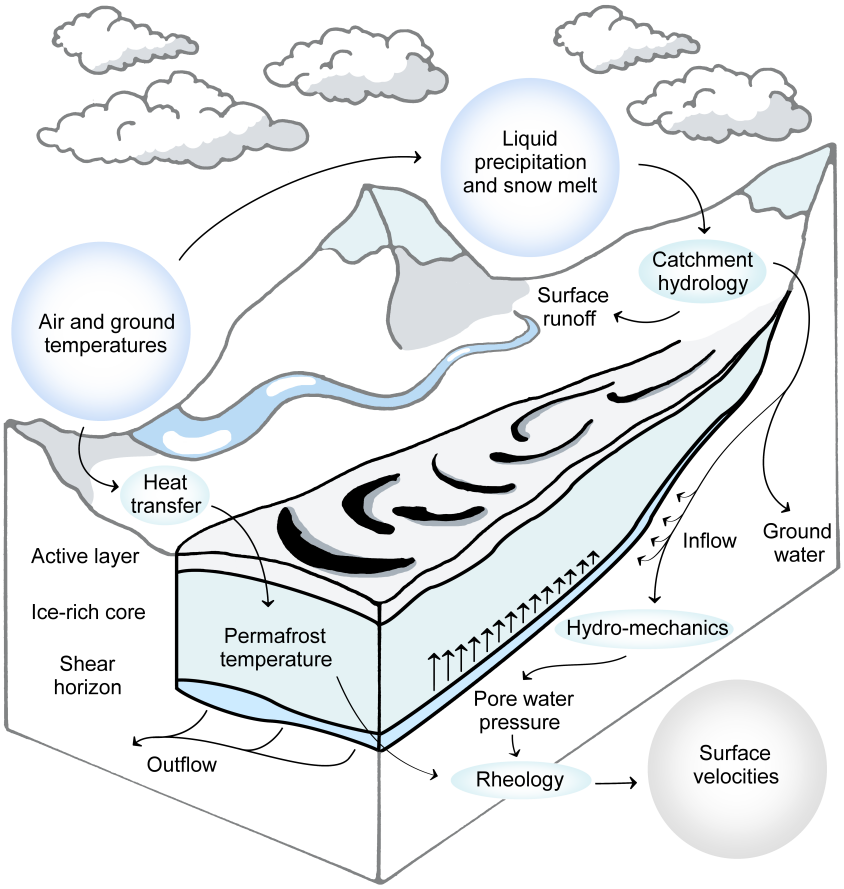

Figure 3.1: Conceptualization of the model and sketch of the moving rock glacier. Climatic forcing (dark blue), model units (light blue) and modelled surface velocities (grey) are highlighted by coloured bubbles. The interactions between the model units and the physical variables are depicted with arrows.

served ground surface temperature time series truncated at 0°C is prescribed. At the bottom of the rock glacier, just below the shear horizon, the temperature value is set to a constant value close to the melting point T_b (−0.2°C) according to observations in nearby rock glacier boreholes in Canton Valais (Zenklusen Mutter and Phillips, 2012, Buchli et al., 2018). The initial condition is prescribed as a constant vertical temperature profile with initial temperature T_0 (−1°C). In order to avoid initialization effects, we spin the model up by prescribing the data of the eight years time series prior to the model simulation starting in year 2011. The temporal resolution of the model is 1 day, its spatial resolution is 0.1 meters. Convective and advective heat fluxes, the influence of basal heating due to frictional processes, and geothermal heat flux are neglected as a first approximation.

Hydrological model

We calculate the ground-water discharge contributing to the rock glacier shear horizon on the basis of observed liquid precipitation, and near ground and air temperature time se-

ries. Liquid precipitation p_{rain} [mm day^{-1}] and air temperature T_{Air} [°C] are measured at the weather station nearby the Dirru Rock Glacier (see the description of the field site in *Publication II*), 350 m away from the GPS positions. The snow melt rate p_{snow} [mm day^{-1}] is modelled using a degree day model:

$$p_{snow} = k_d(T_{air} - T_{melt}), \tag{3.2}$$

where k_d [mm °C^{-1} day^{-1}] is the degree day factor for snow melt, and T_{melt} [°C] is the melting temperature of snow set to 0°C. Snow melt is calculated during the period when the observed ground surface temperatures show isothermal conditions at the melting point (detection of zero curtain). The model is based on the assumption that snow melt is occurring simultaneously and homogeneously in the entire contributing catchment, neglecting in first approximation the spatial variability of the process (temperature lapse rate, influence of the aspect etc.). As soon as all the snow has melted, the ground surface temperature can rise above 0°C and melt-water production from snow ceases. Note that with this approach, we directly calculate snow melt rates without the need for snow depth or solid precipitation data. Possible delays and variations in magnitude due to melt water retention within the snow pack and snow cover variability within the catchment are not considered. The total water input p_{tot} in the catchment contributing to the shear horizon is thus given by the sum of the previous two contributions multiplied by the area of the catchment A_c:

$$p_{tot}(t) = A_c\,(p_{snow} + p_{rain})\,. \tag{3.3}$$

In a next step, we calculate the amount of ground-water that flows into the rock glacier shear horizon by modelling the hydrological response of the catchment to liquid precipitation and snow melt input. We thus transform the hyetograph into an hydrograph applying a Gaussian function:

$$Q_{in}(t) = I_c \frac{p_{tot}(t)}{\sigma\sqrt{2\pi}} e^{-\frac{1}{2}\left(\frac{t-\mu}{\sigma}\right)^2}, \tag{3.4}$$

where σ and μ are two Gaussian parameters representative of the sharpness and delay of the hydrological response of the catchment. When applying this transformation the total mass of the water input is conserved. In order to calculate only the fraction of the water mass influencing the shear horizon (inflow in Fig. 3.1 and Fig. 4.3) the surface runoff and the ground water, which is not influencing the rock glacier have to be excluded. To do so, we multiply the obtained discharge by the constant inflow coefficient I_c.

Hydro-mechanical model

We calculate the effective pressures and the discharge at the rock glacier shear horizon using a 1-D hydrodynamical model forced with the water input described above. We assume the shear horizon to be an homogeneous material in saturated conditions, and the above rock glacier ice-rich core to be an impermeable confining unit. Thus, we describe the behaviour of the rock glacier shear horizon as an artesian aquifer by coupling the Darcy flow law for

water flow in porous material to the mass balance conservation equation:

$$Q_{in} - Q_{out} = \frac{\Delta(P_A A_{sh})}{\Delta t}, \tag{3.5}$$

$$Q_{out} = \frac{k}{\mu L} A\phi(P_A - P_B), \tag{3.6}$$

where Q_{in} and Q_{out} [$m^3\,day^{-1}$] are the water inflow and outflow from the shear horizon respectively, k [$m^2\,day^{-1}$] is the hydraulic conductivity of the shear horizon material, μ [Pa s] is the dynamic viscosity of water, L [m] is the length of the rock glacier from the point in which the ground-water is entering the shear horizon to the steep front, A [m^2] is the area of the average shear horizon cross section, ϕ [-] is the porosity of the shear horizon material, and P_A and P_B [Pa] are the pressure at the bottom of the rock glacier top and front respectively. The model assumes that only water from upstream of the rock glacier contributes to the shear horizon and in first approximation excludes contributions from the sides and from the rock glacier itself. The water pressure at the rock glacier front is assumed equal to the atmospheric pressure, so negligible in an hydrodynamical sense.

Prior to model the deformation profile of the rock glacier, the evaluation of mechanical properties of the shear horizon material is needed. We calculate the effective stresses σ_e [Pa] and the shear resistance τ_r [Pa] of the shear horizon material on the basis of geometrical information and the modelled water pressure. The effective stresses are calculated by applying the Terzaghi's principle:

$$\sigma_e = \rho_{rg} g H \sin\alpha - P_A, \tag{3.7}$$

where ρ_{rg} is the density of the rock glacier material, given by the averaged mean between ice density ρ_{ice} [$kg\,m^{-3}$] and rock density ρ_{rock} [$kg\,m^{-3}$] and controlled by the volumetric ice content w_i [%]:

$$\rho_{rg} = \rho_{ice} w_i + \rho_{rock}(1 - w_i). \tag{3.8}$$

After calculating the effective stresses, the shear resistance can be calculated by applying the Mohr-Coulomb criterion:

$$\tau_r = \sigma_e \tan\phi_c + \tau_{c\theta}, \tag{3.9}$$

where $\tau_{c\theta}$ [Pa] is the cohesion and ϕ_c is the friction angle of the shear horizon material.

Permafrost creep model

For modelling rock glacier creep, the rock glacier can be divided into two units: the ice-rich core and the shear horizon (Fig. 3.1). For modelling the deformation in the ice-rich core, we use the empirically derived creep relation proposed by Arenson and Springman (2005a), similarly to a previous study by Cicoira et al. (2019a). The creep relation is a modified Glen's flow law, that relates strain rate $\dot{\varepsilon}$ [day^{-1}] to the shear stress σ taking into account the volu-

metric ice content [w_i] and the temperature [T] of the rock glacier material:

$$\dot{\gamma}(z,t) = A(z,T,w_i)\sigma(z)^{n(w_i)}. \tag{3.10}$$

The flow law exponent n linearly depends on the volumetric ice content only and the creep parameter A [$\mathrm{Pa}^{-n}\,\mathrm{day}^{-1}$] depends on temperature and ice content by two independent factors as exposed in Eq. 2.5 and Eq. 2.6.

For considering the enhanced deformation taking place in the shear horizon and its dependency on pore water pressure, we apply the rheological model expressed by Eq. 2.8 and proposed by Ladanyi (2003). The shear deformation for the case of a dense ice-saturated material ($w_i > 0.6$) is thus given by:

$$\dot{\gamma}(z,t) = \dot{\gamma}_c(w_i,T)\left(\frac{\tau(z)}{\tau_{c\theta}(w_i,T) + \sigma_e(t)tan\phi_c(w_i)}\right)^{n(w_i)}, \tag{3.11}$$

where the critical shear strain rate $\dot{\gamma}_c$ and the cohesion $\tau_{c\theta}$ are two model parameters of shear deformation, and ϕ_c is the friction angle of the shear horizon material. The total creep velocity c_{tot} is the sum of the contribution of the deformation taking place in the shear horizon and in the ice-rich core

$$c_{tot}(t) = \int_{D_{sh}}^{D_{ic}} \dot{\gamma}(z,t)dz + \int_{D_{ic}}^{D_{al}} \dot{\varepsilon}(z,t)dz. \tag{3.12}$$

3.1.2 A general theory for rock glacier creep: the Bulk Creep Factor and its physical interpretation

The description of rock glacier dynamics is hampered by the high degree of heterogeneity of their physical properties in conjunction with the strenuousness to obtain accurate measurements of their internal structure, especially at a regional scale (Arenson et al., 2016). In an attempt to better understand regional patterns and tendencies, we describe rock glacier creep and dynamics with the most simple method possible, seeking a compromise between a gargantuan task and its complete omission.

Based on the current knowledge of rock glacier physics and its mathematical description presented in the previous chapter, we define the Bulk Creep Factor (here on BCF) as the ratio between observed c_{obs} and modelled c_{mod} creep rates:

$$BCF = \frac{c_{obs}}{c_{mod}}. \tag{3.13}$$

Coupling the creep model proposed by Ladanyi (2003) with a perfectly plastic model for rock glacier thickness, we calculate rock glacier creep rates by integrating Eq. 2.8 in the vertical dimension and obtain:

$$c_{mod} = \frac{\dot{\gamma}_c}{n+1}\left(\frac{\rho g \sin\alpha}{\tau_{c\theta} + \rho g H \cos\alpha \tan\phi}\right)^n H^{n+1}. \tag{3.14}$$

Combining this equation to Eq.3.13, the BCF becomes:

$$BCF = c_{obs} \frac{(n+1)}{\dot{\gamma}_C} \left(\frac{\tau_{c\theta} + \rho g H \cos\alpha \tan\phi}{\rho g \sin\alpha} \right)^n H^{-(n+1)}. \tag{3.15}$$

The BCF is a dimensionless quantity that expresses the mechanical properties of the rock glacier material. By separating the geometrical influence from the creep rates, the BCF allows to compare different rock glaciers or different areas of a single rock glacier with regard to their rheological properties. As we do not distinguish between different layers in the vertical integration of Eq. 2.8, the BCF implicitly describes the rheology of both the ice-rich core and the shear horizon. It therefore represents an averaged value over the entire rock glacier thickness. In order to overcome our limited knowledge about the internal structure of rock glaciers, we evaluate the value of the thickness H with one of the thickness models proposed in the previous section (Eq. 4.1 to Eq. 4.3). This approach has the great advantage of requiring only remote sensing data of surface creep velocities and surface slope angles of the rock glaciers. Therefore, it allows large scale applications to efficiently extend previous research efforts (Whalley and Martin, 1992, Groh and Blöthe, 2019). Here on, we set the values of the model parameters according to previous modelling and laboratory experiments (Czurda and Hohmann, 1997, Arenson and Springman, 2005b, Moore, 2014, Müller et al., 2016, Monnier and Kinnard, 2016, Cicoira et al., 2019b). While most of the parameters are well constrained and can be parametrized (e.g. as a function of the volumetric ice content), the value of $\dot{\gamma}_c$ varies between different rock glaciers and the choice of a reference value is arbitrary. We calibrate this parameter to $0.06\,\mathrm{a}^{-1}$ in order to match the velocities of the Murtél Rock Glacier, and take it here as a regional reference value for our analysis. While this reference is arbitrary and the absolute values of the BCF can change, it does not influence the relative variation between different rock glaciers.

When adopting the perfect plastic model for rock glacier thickness (discussed in *Publication III* and expressed here in Eq. 4.3, with a yield stress of 100 kPa) and assuming standard values of the material parameters ($w_i = 0.7$, $n = 2.1$, $\rho = 1500\,\mathrm{kg\,m^{-3}}$, $\phi = 25°$, $\tau_{c\theta} = 10\,\mathrm{kPa}$, and $\dot{\gamma}_c = 0.06\,\mathrm{a}^{-1}$), the formulation of the BCF simplifies to:

$$BCF = 6.6\, c_{obs} \sin\alpha \left(\frac{0.5}{\tan\alpha} + 0.1 \right)^n \tag{3.16}$$

Figure 3.2a shows the procedure and the data required for the calculation of the BCF. The interpretation of different values of the BCF are illustrated in Figure 3.2b. Here, three possible states of a rock glacier are depicted in the creep rate - surface slope angle space. One rock glacier can be described by a single point under the assumption that the spatial variability within the same landform can be represented by single values of the surface slope angles, thickness and creep rates. Point A and point C represent two rock glaciers characterized by the same rheological properties (both lay on the yellow contour line - high BCF), but show very different creep rates due to their contrasting slope angles. Point A and point B on the contrary, show rock glaciers with the same value of creep rates despite their difference in

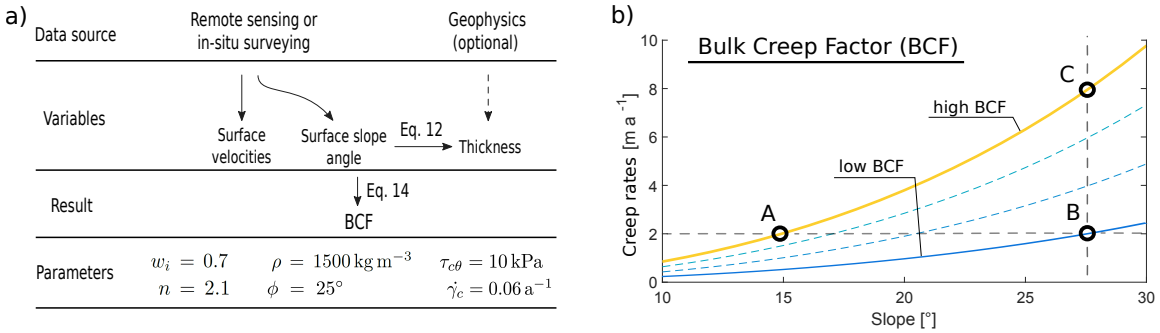

Figure 3.2: Calculation and interpretation of the BCF. (a) Procedure and data required for the calculation of the BCF and (b) interpretation of the parameter values in the creep rates - slope angle space. The coloured contour lines show constant values of the BCF. The equation number refers to the formulas in *Publication III*.

geometry (surface slope angle). This is only possible due to a reduction of the BCF. The rock glaciers visualize by point B and point C show the same value of the slope angle, but different values of creep rates due to different mechanical properties (different BCF). This illustration demonstrates the importance of accounting for geometry and material properties when comparing rock glacier dynamics. In fact, on a kinematic level, point A and point B are equivalent. However, our approach allows to illustrate the dynamic difference between those two rock glaciers: if point A had the same slope as point B, it would creep four times faster according to its rheological properties.

3.2 Study sites: field measurements and remote sensing observations

The investigation of the processes controlling rock glacier dynamics requires detailed observation of processes taking place in the ground, invisible at the surface. The collection of such a database is hampered by practical restrains. In fact, researchers have to face plentiful difficulties when surveying the periglacial environment and rock glaciers are no exception. The difficult access to the field sites, challenging and expensive logistics in the field, and not last serious safety issues obstruct monitoring activities and make the collection of data a challenging task.

Especially for the analysis at the local scale, this thesis largely benefit from already existing datasets from the PERMOS network and XSense Project database. The PERMOS network provided temperature measurements in boreholes, complemented by near-surface information on temperature and surface displacement rates from TGS (*Publication I*, for reference see the official report PERMOS (2019)). The XSense project provided meteorological, kinematical and thermal information at the surface at daily resolution, indispensable for detailed analysis (*Publication I*, and *Publication II*, for reference see Beutel et al. (2011), Wirz et al. (2016a)). To further support the process-based modelling, several other methods have been applied

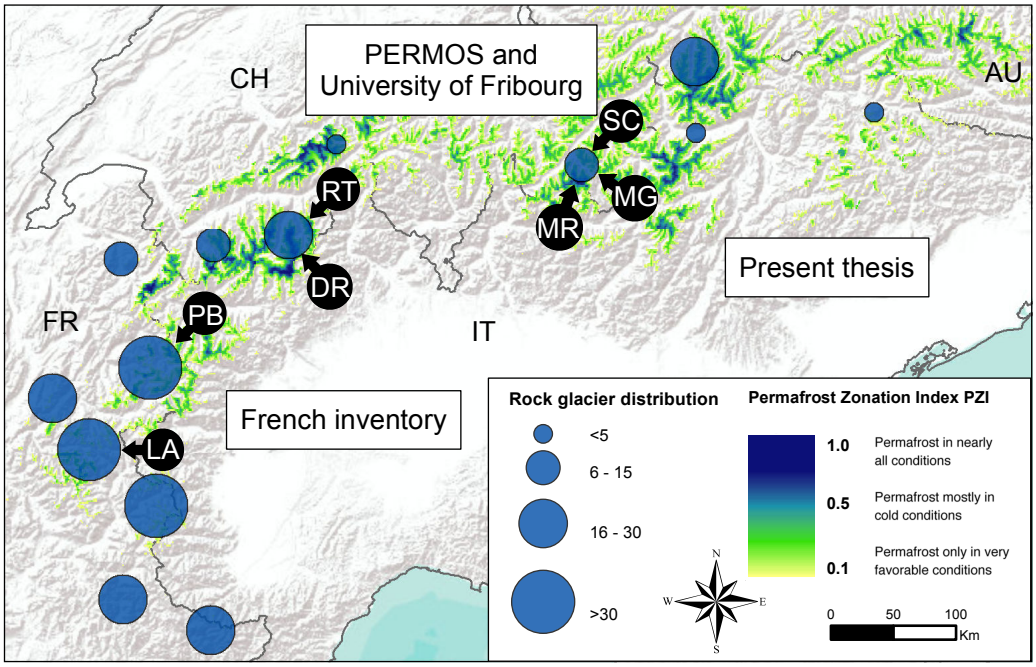

Figure 3.3: Distribution of the rock glaciers investigated in the present thesis. The diameter of the circles indicates the distribution density of the rock glaciers divided by topo-climatic regions. The black labeled circles indicate the position of the seven field sites investigated in detailed at the local scale (DR - Dirru, LA - Laurichard, MG - Muragl, MR - Murtél, PB - Pierre Brune, RT - Ritigraben, and SC - Schafberg Rock Glaciers). For a detailed description of the database refer to corresponding publications (PERMOS, 2019, Groh and Blöthe, 2019, Marcer et al., 2019, Cicoira et al., 2019a,b, submitted). The Permafrost Zonation Index PZI from (Gruber, 2012) is used to illustrate the spatial distribution of permafrost in the Alps.

for the collection and preparation of ad hoc data. Repeated drone surveys allowed, through the application of SfM techniques, the generation of multi-temporal DEMs and orthophotos at high spatial resolution and accuracy. This data sets were then used for the calculation of yearly surface displacement rates by applying offset tracking algorithms (Kääb and Vollmer, 2000, Rohner et al., 2019). The Dirru Rock Glacier was monitored for four years as part of the research activities related to this thesis, and data for the Laurichard and Pierre Brune were provided for further analysis from the University of Savoie Mont Blanc (embodied by Marco Marcer and Xavier Bodin). Additionally, in cooperation of the University of Savoie Mont Blanc, an intense field campaign to investigate the internal structure of the Pierre Brune Rock Glacier was organized and carried out in summer 2019. The Murtél (MR), Muragl (MG), Ritigraben (RT) and Schafberg (SC) Rock glaciers have been investigated in *Publication I*, the Dirru (DR) in *Publication II* and the Dirru, Laurichard, and Pierre Brune Rock Glacier in *Publication III*. The seven field sites investigated in detail at the local scale are summarized in Fig. 3.3.

For the analysis at a regional scale, mostly data from remote sensing techniques were used. The spatially heterogeneous characteristics of rock glaciers were summarized by a single value of the BCF, which represents in first approximation the entire landform (or a

significant part of it). We investigated a dataset comprising 414 rock glaciers for which surface displacement and slope angle data are available. Most of the data came from the French Alps (Marcer et al., submitted). Other data points came from the Swiss (PERMOS, 2019), Austrian (Groh and Blöthe, 2019) and Italian Alps (see Fig. 3.3). We further accounted for the permafrost conditions at each rock glacier site using as a proxy the Permafrost Zonation Index (PZI) developed by the University of Zurich (Gruber, 2012). High values (close to the unit) correspond to favourable conditions for permafrost occurrence, while values close to zero indicate unfavourable conditions. Moreover, we analyse the destabilization susceptibility of the investigated rock glaciers according to the geomorphological index proposed by (Marcer et al., 2019). For a more detailed description of the data set refer to *Publication III*.

4 Results and interpretation

Rock glaciers dynamics is highly variable and is characterized by different patterns at different temporal scales. The key factors controlling its variations are air and ground temperature, snow melt, liquid precipitation, and debris- and ice input. While the drivers and the processes governing rock glacier creep remain unchanged, their relative importance may vary according to the considered temporal scale and the relative climatic conditions. On a short temporal scale - seasonal to inter-annual - we investigated the interaction between rock glacier creep and climatic forcing by developing a novel conceptual and numerical modelling approach. The model has been constrained and the results have been compared with detailed data from five rock glaciers in the Swiss Alps, providing important insights into the processes governing rock glacier creep. However, such a detailed approach cannot be scaled due to the complexity of the processes involved and the paucity of observational evidence. In order to foster further research advances, we developed a general theory for the analysis of rock glacier creep applicable at the regional scale. This chapter summarizes the major research findings that stem from this dissertation.

"πάντα ῥεῖ"

῾Ηράκλειτος ὁ ᾽Εφέσιος

4.1 Heat conduction and thermally-activated creep

The viscosity of ice is inversely proportional to its absolute temperature, following an exponential relationship as shown by Mellor and Testa (1969). This theory is directly transferable to the periglacial environment where ice-rich debris are the main component of alpine permafrost (Kääb et al., 2007). In order to answer *Research Question I*, we test the hypothesis that the observed seasonal and inter-annual creep variations can be directly caused by changes in ground temperature. To this aim, we reproduce the observed ground temperatures as measured in boreholes on active rock glacier sites by forcing heat conduction with measured external temperature forcing. Thereafter, we couple the ground temperatures to a creep model for ice-rich frozen soil derived from laboratory experiments by Arenson and Springman (2005a). The observed surface displacements are compared with the model results, expressing the depth-integrated contribution of the driving stresses and the transient temperature regime. The modelling is constrained with an outstanding data set comprising

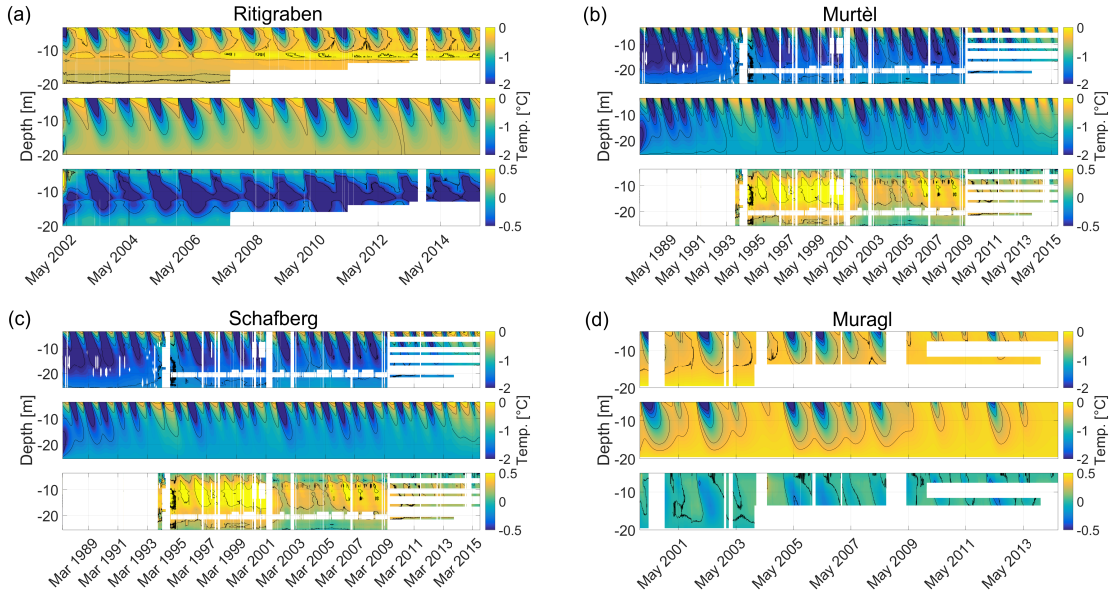

Figure 4.1: Contour plots of ground temperatures time series (colour coded) for the (a) Ritigraben, (b) Murtèl, (c) Schafberg and (d) Muragl Rock Glaciers. Each panel shows, from top to bottom, the measured temperatures, the modelled temperatures and the corresponding residuals.

measurements of surface and ground temperatures, detailed observations on the geometry and the internal structure as well as surface kinematic measurements for four active rock glaciers described in Sect.3. The methods, results and discussion related to this research - comprising a detailed sensitivity analysis - are extensively treated in *Publication I*.

4.1.1 Modelling permafrost temperatures

We calculate permafrost temperature evolution at depth by numerically solving the heat conduction equation being forced by observed near permafrost surface temperatures. The boundary condition of the model is prescribed below the active layer, allowing us to neglect the complex processes governing this layer (Delaloye and Lambiel, 2005, Wicky and Hauck, 2017) and assume heat conduction as the only process controlling the thermal regime of the underlying permafrost (Haeberli et al., 2006). In some cases, data gaps are present and linear interpolation of the data is used. The data gaps are short (below a few months) and are expected to not affect the overall modelling, but interpretation of the modelled velocities for these periods has to consider this limitation. The model results agree well with the observations as shown in Fig. 4.1, with residuals mostly lower than 0.2°C.

In general, there is a good fit between absolute values, seasonal amplitude and phase. For the case of Ritigraben Rock Glacier, the presence of a Talik at a depth of about 10 m (Luethi et al., 2017) causes substantial differences between the modelled and the measured temperatures. For all the case studies, the depth of zero annual temperature amplitude is slightly

overestimated in our calculation. Our model therefore overestimates the influence of the external temperature signal on ground temperatures. The assumption of a constant bottom temperature agrees well with the observed borehole temperatures. We assume the physical properties of the rock glacier (density, ice content and thermal diffusivity) to be constant in time and homogeneous in space, which seems justified at the considered short (seasonal to multi-annual) timescales and is supported by the good performance of the temperature evolution model.

In addition to the modelling, we produced continuous time series of ground temperatures by linearly interpolating in time the borehole observations for all data gaps shorter than one year. The interpolated time series allow us to directly use the observed ground temperatures as input for the creep model. However, due to the presence of large data gaps, the applicability of this approach shows strong limitations and it makes it better suited as validation of the modelling rather than directly useful for the interpretation of the data. Altogether, the modelled temperatures in combination with the available observations serve as a solid basis for the modelling and the analysis of rock glacier creep rates.

4.1.2 Modelling creep rates

We calculate creep rates on a vertical profile on the basis of the modelled and observed temperature time series. The constitutive relation of the rock glacier material is described using the empirical creep model proposed by Arenson and Springman (2005a). The resulting creep velocities (blue line in Fig. 4.2) can be compared against the observations (black and gray-dotted lines in the same figure). We obtain the correct order of magnitude for calibrating the volumetric ice content to a value of 70%, in accordance to the literature. Figure 4.2 shows the calibrated surface creep velocities, corrected with a calibration factor to match the mean value of the observations. The un-calibrated time series is available in *Publication I*. However, the modelled amplitude in seasonal and inter-annual velocity variations underestimate the observations by one order of magnitude the observations. Furthermore, the phase of the modelled and the observed creep velocities shows a noticeable lag. In fact, the modelled velocity maxima are only reached in late winter, while the observations reveal velocity peaks in autumn with a corresponding phase shift of 2-3 months. The calculated velocity pattern is, on the one hand, a result of the diffusion of the temperature signal and, on the other hand, a result of an integrated contribution of deformation over the entire depth. The surface velocity variations are therefore neither a direct reflection of the temperature signal at a single depth nor of the depth-averaged temperature signal. In consequence, estimating the phase lag between seasonal variations in surface temperature and surface flow from heat conduction is non-trivial and qualitative interpretation of the phase lags is potentially misleading.

In order to further improve the description of the deformation profile and of the thermal regime of the rock glacier, we perform two additional sets of simulations. Firstly, we reproduce a realistic deformation profile by increasing the flow exponent in the creep model, approximating a plastic behaviour (Arenson et al., 2002, Frehner et al., 2015). Although this approach provides a more physical description of rock glacier creep, it prompts larger dis-

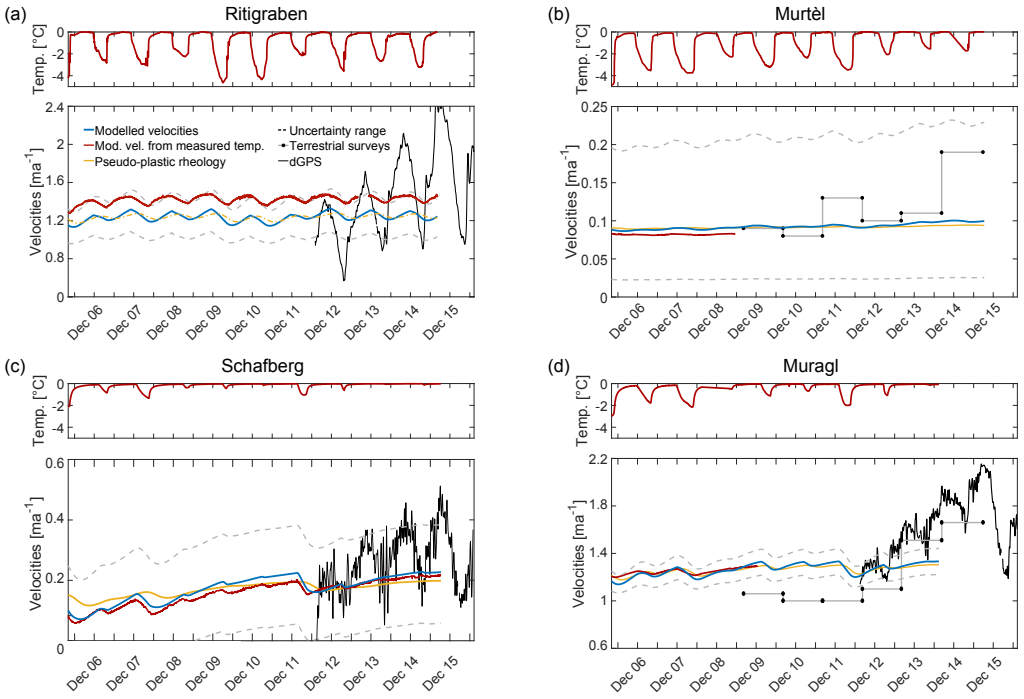

Figure 4.2: Observed and modelled creep velocities (corrected) for the (a) Ritigraben, (b) Murtèl, (c) Schafberg and (d) Muragl Rock Glaciers. The upper subpanel shows the observed subsurface temperature used as model input.

crepancies between the observed and modelled velocity variations (yellow line in Fig. 4.2). Therefore, this result confirms the overestimation of the external temperature signal in our modelling. Finally, in order to validate our results and reduce the uncertainty related to the calculation of the ground temperature, we directly force the creep model with the observed ground temperatures (red line in Fig. 4.2. The above found amplitude underestimation and phase shift do not change, with the exception of the Ritigraben Rock Glacier for which the phase of the black and the red lines match. This result is not due to an underestimation of the seasonal temperature variations, as confirmed by the results of the thermal modelling.

Regarding the multiannual variations, which are well documented and synchronous for many rock glaciers in Switzerland (PERMOS, 2019), our modelling suggests that the responsible process between the observed acceleration in flow (e.g. from 2011 to 2015) and the observed surface warming cannot be explained by heat conduction into the ground alone. It is likely an indirect effect of enhanced meltwater penetrating into the rock glacier body and thereby affecting its rheology. Phases of slowdown related to conductive cooling in cold or long winters (e.g. 2007 and 2011) are more distinct in our modelled velocities, and thus winter cooling may contribute more substantially to the longer-term slow-down of rock glacier flow. The enhanced sensitivity to winter temperatures is (in contrast to summer tempera-

tures) not surprising given that the zero curtain effect caps the summer temperature peak at 0 degrees and inhibits the propagation of the summer heat into the ground, which is well reflected in the observed temperatures below the active layer.

In summary, the strong underestimations in both amplitude in seasonal and multi-annual variations, as well as the overestimation in time lag of seasonal peaks in our modelling, suggest that heat conductive processes alone cannot explain the observed variation in flow velocity, suggesting the need for other processes, such as the interaction of rock glacier rheology with surface water advecting into the rock glacier body.

4.2 High mountain hydrology and permafrost hydro-mechanics

Borehole investigations indicate the presence of pressurized unfrozen water at the depth of the shear horizon for several rock glaciers (Arenson et al., 2002, Bast, pers. com. 2015, Buchli et al., 2018). The same layer accommodates most of the deformation (60%-90%) and accounts for most of the temporal velocity variations (Arenson et al., 2002). Having previously excluded the hypothesis that temperature can explain the observed velocity variations, we are logically directed to address *Research Question II*: how does unfrozen water influence the creep regime of a rock glacier? Can the observed seasonal and inter-annual creep variations be caused by the combined influence of temperature forcing and water input? To address these questions, we develop a novel conceptual and numerical modelling approach based on state oft the art field observations. In this framework we account for heat transfer into the ground, the catchment hydrology, the hydro-mechanics of the rock glacier and its rheology. The constitutive relation of the rock glacier material is described by two independent creep models accounting for its dependency on temperature (Arenson and Springman, 2005a) and pore water pressure (Ladanyi, 2003) respectively. The modelling is constrained and the results are compared against kinematic, geophysical and meteorological observations for the Dirru Rock Glacier (Valais - CH). For more details on the field site and on the modelling framework see Sect.3 and for a complete explaination of this research to *Publication II*.

4.2.1 Separating and quantifying external forcing

In order to quantify the influence of ground temperature on rock glacier creep, we calculate ground temperature evolution at depth using the observed ground surface temperature time series as input as explained in the previous section. The observed temperature amplitude (truncated at 0°C) at the rock glacier surface varies between 4°C and 11°C (Fig. 4.3b). At the depth of the shear horizon, about 15 m below the surface, the seasonal amplitude is reduced by one order of magnitude and the phase is shifted by approximately 5 months. In this case, no borehole temperature measurements are available and the results can only be interpreted on a conceptual level. The observed truncated mean annual ground surface temperatures range from -2.3°C to -1.2°C (Fig. 4.3d). These results confirm our previous finding and

reinforce the conclusion that temperature forcing cannot explain the seasonal phase and can only account for a limited fraction of the observed velocity variations.

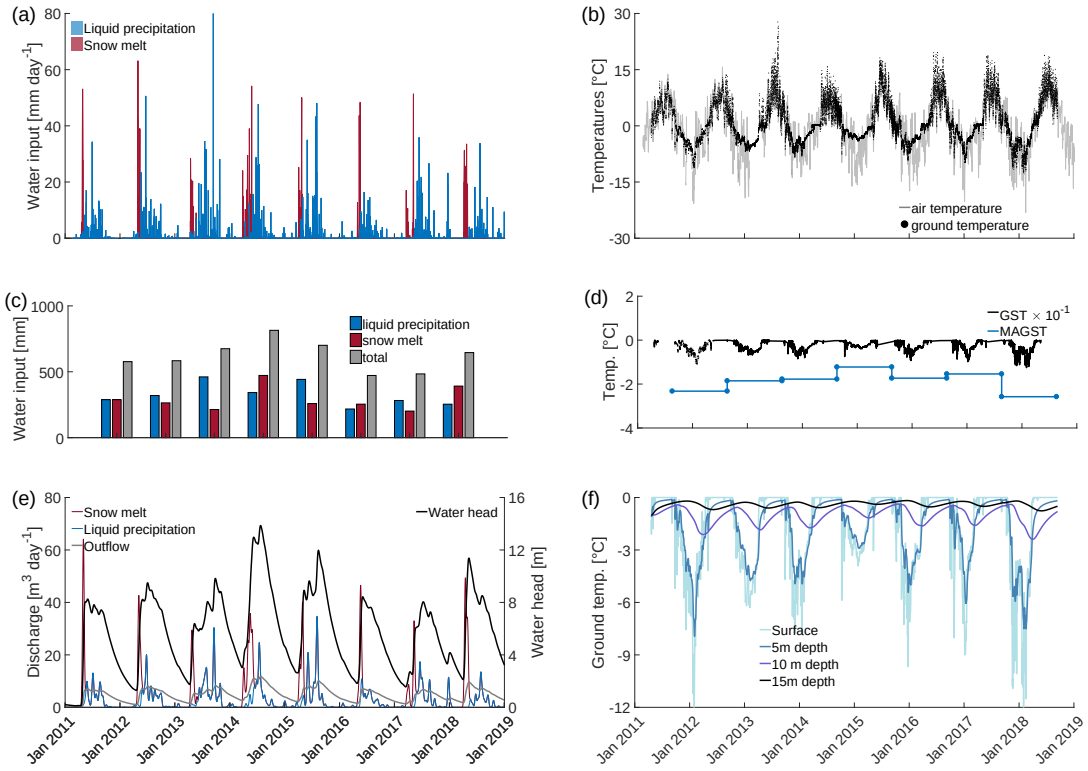

Figure 4.3: Modelling input and results. (a) Measured liquid precipitation (blue) from the weather station and modelled snow melt rates (red). (b) Observed ground surface (black dots) and air (grey line) temperatures. (c) Yearly cumulative values of liquid precipitation (blue) and snow melt (red), and total contribution (grey). (d) Ground surface temperature (black line) truncated at 0°C (scaled by a factor 10^{-1}) and its annual mean (MAGST, blue line) calculated for the hydrological year. (e) Results of the hydro-mechanical model. The output of the hydrological model is used here as input (Snow melt and Liquid precipitation components, blue and red lines). The outflow and the water head at the bottom of the rock glacier are shown with a grey and a black line respectively. (f) Results of the thermodynamic model. The modelled ground temperatures for position 17 are plotted against time at the surface (light blue, same as GST in panel d), at 5 m (dark blue), at 10 m (violet) and at 15 m (black) depth.

In a second step for describing the physical system, we include in the modelling the influence of water input on the shear horizon dynamics, which can be quantified on the basis of the water input in the contributing catchment. The estimated water input, which we assume homogeneously distributed in the rock glacier catchment is plotted in Fig.4.3a. The liquid precipitation (blue bars) is directly measured at the nearby weather station, while the snow melt (red bars) is estimated with the degree day model expressed by Eq. 3.2. The duration of the snow melt is inferred from observations of the zero curtain effect from the measured ground surface temperatures. Its magnitude is estimated for the same period by using a de-

gree day model forced with the observed air temperatures, measured at the weather station. The snow melt starts at the end of April and lasts several weeks, leading to the highest water input rates peaking at $60\,\mathrm{mm\,day^{-1}}$. Liquid precipitation events occur from the end of the snow melt period onward. Starting in late autumn the low temperatures in the catchment lead to solid precipitation, which accumulates in the catchment until the following Spring. The cumulative precipitation at the Dirru field site varies between 500 and 800 mm of water per year during the observational period. The distribution of the precipitation events as well as the source of the main contribution varies from year to year. On the basis of the water input, we can simulate the hydrological response of the catchment and by using Eq. 3.4 calculate the amount of water flowing into the rock glacier shear horizon. The modelled discharge is characterized by a multi-modal distribution throughout our entire time series, with peaks up to $40\,\mathrm{m^3\,day^{-1}}$. The highest values are always obtained in spring, due to snow melt. Further local maxima due to liquid precipitation are obtained later in the season, but never exceed $40\,\mathrm{m^3\,day^{-1}}$, corresponding to a water flow velocity of less than $1\,\mathrm{m\,day^{-1}}$. During autumn, the inflow to the shear horizon decreases to zero as a consequence of the ceased water input. The Gaussian function used for representing the catchment hydrology is described by only two parameters, which offer a clear physical interpretation. The first model parameter μ represents the delay time of the catchment response to water input. The second parameter σ describes the reactivity of the hydrological catchment. By setting both parameter values equal to 5 days, we represent a quickly reactive catchment, typical of high mountain environments (Brunner et al., 2018). In the modelling, the discharge peak is reached 5 days after the water input and 68% of the water mass is discharged from the catchment within 10 days (95% in 20 days etc.). Although the snow melt and hydrological models are simple, they are physically interpretable and have the advantage of being directly forced by in-situ observations. Uncertainties in the calibration of the two hydrological parameters have only minor effects on the velocity results (for details see the discussion in *Publication II*).

When ground-water flow reaches the shear horizon, it influences its pressure regime and its mechanical state. The water flow throughout the shear horizon, from the uppermost part of the rock glacier to its steep front, is here described using the Darcy flow law for porous materials (Eq. 3.6) under the assumption of confined conditions (Fig. 3.1). Although a direct validation is not possible, this conceptual model is confirmed by both field observations and laboratory experiments and allows us to derive indirect information about the hydro-mechanical regime of the rock glacier shear horizon. The hydraulic conductivity value used in the modelling ($1 \times 10^{-8}\,\mathrm{m\,day^{-1}}$) is consistent with literature values (Burt and Williams, 1976, Arenson and Springman, 2005b) and produces maximum water head values of up to 13 m, corresponding to 80% of the rock glacier thickness. These values of water heads are coherent with field observations and also physically acceptable, because the pressure corresponding to the water column does not exceed the weight of the rock glacier itself, which would cause unrealistic uplift forces. Moreover, the very low values of water discharge at the rock glacier front ($< 10\,\mathrm{m^3\,day^{-1}}$) are in agreement with field observations of no visible flowing water in correspondence of the shear horizon depth.

4.2.2 The rhythm of rock glacier creep

We model rock glacier creep rates using two independent creep relations for the ice-rich core (Arenson and Springman, 2005a) and the shear horizon (Ladanyi, 2003) forced by external temperature and water input respectively. The modelled creep velocities are compared against the 3D surface velocities obtained from DGPS measurements (Fig. 4.4) for the two positions on the rock glacier (see *Publication II*). Because of the chaotic nature of the high-frequency velocity peaks present in the kinematic data (Wirz et al., 2014), we filter the velocity signal by applying a two weeks running mean. Below, we first describe the results for position 17, located in the fast flowing and thin part of Dirru Rock Glacier, for which the model has been calibrated (Fig. 4.4a and b). We then use the results for the contrasting geometrical setting at position 15 (Fig. 4.4c), obtained with the same model calibration, as an independent test for our modelling approach.

The observed eight year velocity time series (black dots in Fig. 4.4a) substantially extend the data of Wirz et al. (2016b) and confirm the distinct seasonal flow rhythm of Dirru Rock Glacier. In late spring, the flow velocity exhibits a yearly minimum ranging from $2\,\mathrm{m\,a^{-1}}$ (2017) to $4\,\mathrm{m\,a^{-1}}$ (2014). The minima are directly followed by an abrupt acceleration at the onset of the snow melt period, which leads to a first annual maximum. After this early summer peak, the velocity slightly decreases for a short period of time, before accelerating again and reaching another maximum in late summer. After this phase, the velocity decreases asymptotically to the next spring minimum. The observed seasonal variations in velocity vary from $4\,\mathrm{m\,a^{-1}}$ to $15\,\mathrm{m\,a^{-1}}$ for year 2017 and 2014 respectively with a mean value of $6\,\mathrm{m\,a^{-1}}$ (Fig. 4.4a).

The modelled velocity (blue solid line in Fig. 4.4a) is the sum of the two contributions from the ice-rich core and the shear horizon velocities (dashed and dash-dotted blue line in Fig. 4.4a). The velocity component of the ice-rich core (thermally controlled) never exceeds $2\,\mathrm{m\,a^{-1}}$ and the related seasonal variations are limited to below $0.5\,\mathrm{m\,a^{-1}}$ (dashed blue line in Fig. 4.4a). In accordance with the results of Cicoira et al. (2019a), the observed velocity variations are strongly underestimated and the modelled seasonal pattern exhibits a phase lag of one to five months to the observations. The modelling improves when including the description of the shear horizon dynamics forced by water input (dash-dotted blue line in Fig. 4.4a). In fact, we obtain seasonal velocity variations in the correct order of magnitude for all years of the time series, with maximum velocity values up to $14\,\mathrm{m\,a^{-1}}$). Moreover, the modelled shear horizon velocity is in phase with the observations.

When combining the two velocity contributions (ice-rich core and shear horizon), the total modelled velocities reproduce the observed seasonal pattern well (blue solid line against black dots in Fig. 4.4a). For the eight year time series, the average modelled velocities match the observed $5.5\,\mathrm{m\,a^{-1}}$ calculated from GPS measurements. The model performs well in simulating the timing and rapid acceleration during the snow melt season as well as the delayed annual velocity maximum. Also, the inter-annual variability of the spring minima is captured by the model although in some years (e.g. 2011 and 2017) only part of the variation is reproduced. Moreover, in the modelling, the shear zone accounts for more then 70% of

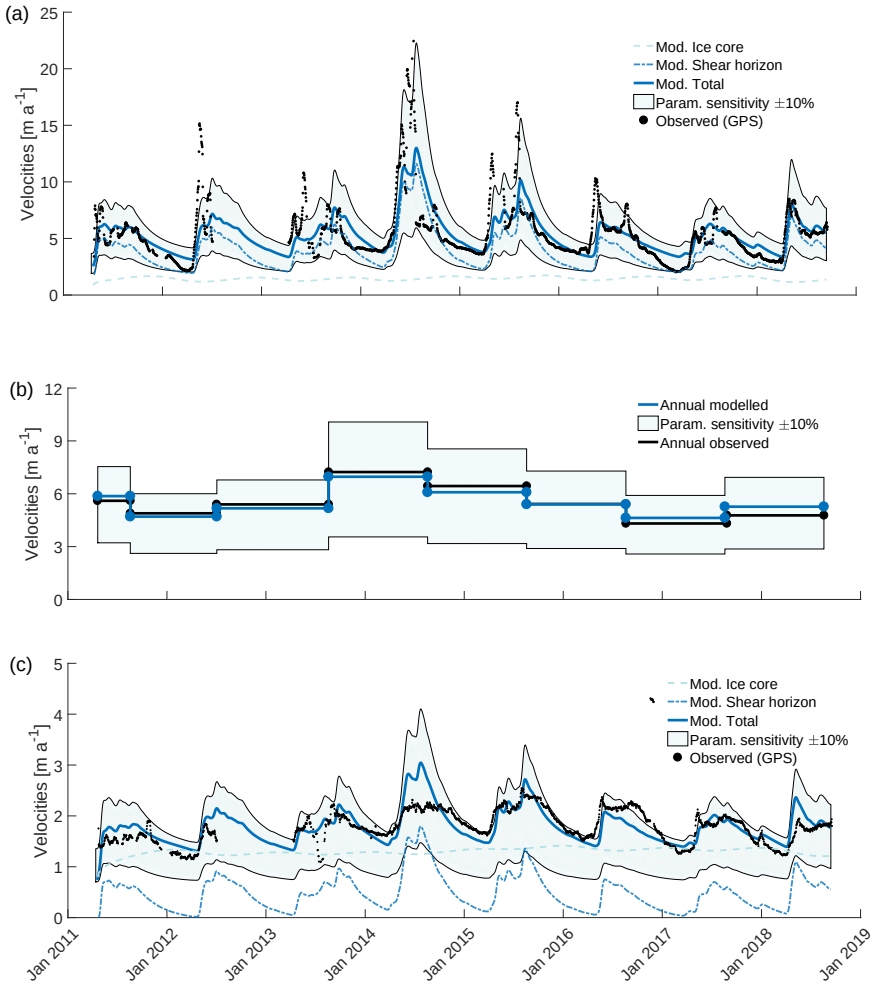

Figure 4.4: Observed (black dots) and modelled (blue lines) velocity time series for position 17 (a-b) and position 15 (c). The total modelled velocities (solid blue line in (a) and (c)) are the sum of the contributions from the ice-rich core (dashed light blue) and the shear horizon creep model (dash-dotted light blue). The light blue shaded areas encompass the modelled velocities when varying all the non-geometrical model parameters by ±10% (Param. sensitivity). (b) Mean annual velocities calculated over the hydrological year. The observed annual velocity (black line) is calculated directly from the GPS position displacements between two consecutive years (1st of September). The modelled annual velocities (blue line) are calculated by averaging the modelled velocities over the same time period.

the total deformation in the rock glacier, in good accordance with borehole observations for other sites (Arenson et al., 2002, Krainer et al., 2015, Buchli et al., 2018) Possible variations in the non-geometrical parameters (±10%) do not change the above findings and the resulting velocity range encompasses almost the entire observed velocity signal (light blue area in Fig. 4.4a).

In order to investigate inter-annual flow variations, we calculate mean annual velocities (Fig. 4.4b) as typically monitored for many rock glaciers in the Alps (PERMOS, 2019). The

observed mean annual velocities (black line) are directly calculated from the measured GPS positions at the beginning of two consecutive hydrological years (1st September). The observed and the modelled annual velocities are in very good agreement (black and blue line in Fig. 4.4a respectively), showing discrepancies lower then 10% with a multi-annual trends varying between $4.3\,\mathrm{m\,a^{-1}}$ (2017) to $7.2\,\mathrm{m\,a^{-1}}$ (2014).

In order to test the validity of our results, we repeat the flow modelling for Position 15 (Fig. 4.4c), characterized by a gentler slope (only 15°) and lower velocities (mean surface velocity equal to $1.6\,\mathrm{m\,a^{-1}}$). The model performs similarly well for this additional position when using the same model calibration as for position 17 and only adjusting the geometrical input values of rock glacier slope and thickness. For this position, the seasonal variations in velocity are lower in absolute and relative terms (values up to $1\,\mathrm{m\,a^{-1}}$) and the contribution of the shear horizon to the total deformation is lower than for the steeper position 17.

In summary, we find that water from liquid precipitation and snow melt, rather than air temperature, is the main driver of variations in rock glacier dynamics. Our results imply that the influence of water on rock glacier creep is fundamental and must be considered when investigating the historic and future evolution of rock glaciers.

4.3 Investigating the spatial patterns of rock glacier dynamics

In the past three decades, the dynamics of rock glaciers has changed substantially, rising concerns about their future behaviour and their stability. As a result, a large number of studies have investigated their dynamics and its interaction with the climate. Despite detailed studies at a field site scale have yielded valuable insights, the regional scale pattern and trends of rock glacier dynamics remain until the present day mostly unknown or only partly investigated. Advancing remote sensing techniques and the increasing availability of the observations allow analysis of rock glacier creep at the regional scale over unprecedented long time periods. Combining simple mathematical models to these unprecedented observations has a great potential for improving our understanding of rock glacier dynamics. The related theoretical and methodological questions lead to the formulation of *Research Question III*. In fact, although surface topography, slope angle, and displacement rates can be derived from remote sensing (satellite imagery and InSAR), in order to investigate rock glacier dynamics the thickness of a rock glacier has to be estimated. In order to evaluate possible solutions to this restrain, we investigate a data set of 28 rock glaciers worldwide for which information about their geometry (surface slope and thickness) and kinematics (displacement rates) are available. On the basis of this analysis and state of the art knowledge in the field of periglacial engineering, we propose a simple mathematical description of rock glacier dynamics combining simple models for the estimation of rock glacier thickness to state-of-the-art creep models for ice-rich debris mixtures. The introduction of the BCF is the main result of this analysis. We illustrate two applications of the proposed methodology at the regional and at the local scale. At the regional scale we investigate a large data set of more than 400 rock glaciers in the European Alps, for which surface slope and displacement

rates are available. At the local scale we analyse the spatial variability of the velocity field of three rock glaciers representing the spectrum of dynamic behaviour (slow quasi-steady state flow, exceptional high displacement rates, destabilization). The complete description of the theory, its interpretation, the two applications and the database used are described in *Publication III*.

4.3.1 Analysis of rock glacier thickness, slope and creep rates

While it is relatively simple to determine the surface slope and the displacement rates of rock glaciers, inferring information about their thickness remains challenging. Geophysical methods such as electrical resistivity tomography (ERT), seismic and ground penetrating radar surveys (GPR) allow the investigation of ground permafrost at depth. However, using such indirect observations to infer the thickness of the moving rock glacier remains laborious and often impossible due to practical reasons. Boreholes instrumented with slope inclinometers provide the most reliable results with this regard, but this information is only punctual and they are expensive both logistically and financially. For all of the above, the application of inverse models for the derivation of rock glacier thickness is desirable. Contrarily to ice-glaciers, where several methods have been proposed and their limitations critically reviewed and evaluated Farinotti et al. (2017), no detailed studies of such methods have been undertaken for rock glaciers. Therefore, we propose three approaches to estimate rock glacier thickness based on the analysis of a dataset of 28 rock glaciers from the Alps (23) and the Andes (5), for which detailed observations of surface creep rates, slope angle and thickness from different sources are available.

In Fig. 4.5 we analyse the thickness, driving stress, creep rates and slope angle for the investigated dataset. The distribution of thickness and driving stresses (calculated according to Eq. 2.4) for the analysed rock glaciers suggests a visco-plastic behaviour with a yield stress of about 100 kPa, similar to pure ice (Fig. 4.5a). When considering all the rock glaciers in the dataset, the average driving stress is 85 ± 21 kPa. However, a cluster of five rock glaciers in the Chilean Andes shows low values of the driving stress. These landforms are in degrading conditions (with permafrost temperatures being at 0°C) and their driving stresses might not be able any more to sustain steady state creep conditions. When excluding these five degrading rock glaciers from the analysis, the mean value of the driving stress increases up to 92 ± 13 kPa. This result confirms and extends previous observations by Wahrhaftig and Cox (1959) and Whalley and Martin (1992), which performed a similar analysis on a vast data set of rock glaciers finding that the driving stresses vary between 50 kPa and 200 kPa. Note that in these previous studies the thickness was generally estimated on the basis of expeditious field surveys subject to larger uncertainties.

The distribution of rock glacier thickness and surface slope angle is shown in Fig. 4.5b along with three model fits and their performance, which is quantified with the RMSE. The first method that we propose to estimate the thickness of a rock glacier is a constant model. This approach is supported by the fact that while most of the observed rock glaciers present a thickness of their moving part between 10 m and 30 m, only few rock glaciers have been

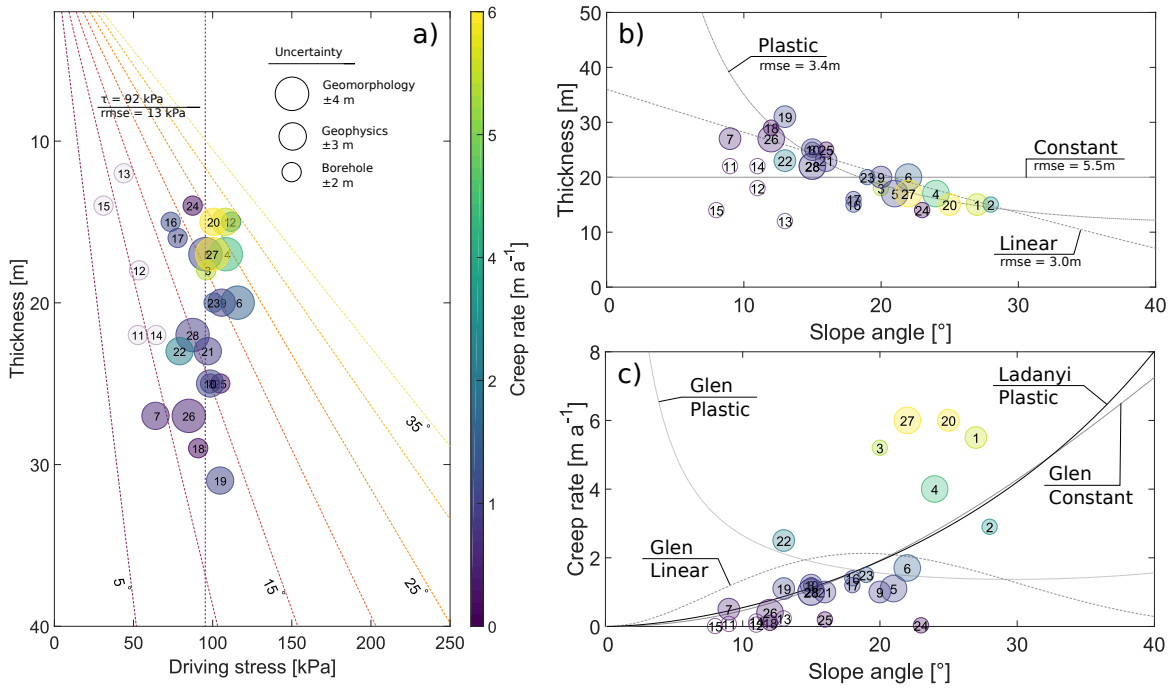

Figure 4.5: Analysis of observed rock glacier thickness, slope angle, and creep rates. Each rock glacier is depicted by a circle, whose colour represents the rock glacier creep rates [ma^{-1}] as indicated by the colour bar. For each rock glacier, the uncertainty relative to its thickness is represented by the diameter of the circles. (a) Rock glacier thickness [m] against driving stress [kPa]. The vertical dashed line shows the average value of the driving stress and the relative RMSE. The diagonal dashed lines show the slope angle, from 5° to 35°. (b) Rock glacier thickness [m] against slope angle [°]. The three models to calculate rock glacier thickness are indicated by a label along with their RMSE. (c) Rock glacier creep rates [m a^{-1}] against slope angle [°]. Four models for the calculation of rock glacier creep rates are shown. In the corresponding label, the upper and the lower lines indicate respectively the creep and the thickness models used for the calculation.

studied in such detail that the uncertainty on the estimation of the thickness is limited to less than the natural variability between different landforms. When fitting the constant model to the analysed dataset, the mean value of rock glacier thickness becomes:

$$H = 20 \pm 5.5\,\mathrm{m}. \tag{4.1}$$

The second model to estimate rock glacier thickness is a linear relationship between slope angle and thickness. From the available observations, we find a best linear fit of:

$$H = 37 - 0.9\alpha \pm 3.0\mathrm{m}. \tag{4.2}$$

The third model, also used in the field of glaciology, estimates the thickness of the rock glacier with a perfectly plastic model by solving Eq. 2.4 for H, assuming a yield stress of

$\tau = 92\,\text{kPa}$ (given the mean driving stress from the dataset):

$$H = \frac{\tau}{\rho g \sin \alpha} \pm 3.4\text{m}. \tag{4.3}$$

According to our results, the linear thickness model shows the best performance (RMSE = 3.0 m), but is only marginally better than the plastic model (RMSE = 3.4 m). Note that the suggested models should be applied with caution and only in average slope ranges roughly between 10° and 30° of slope (i.e. for the slope angle range in which they have been derived from the data).

Rock glacier creep rates can be calculated by coupling one of the thickness models (Eq. 4.1, 4.2 or 4.3) to the creep models (Eq. 2.1 or Eq. 2.8). Fig. 4.5c shows the result of this coupling and demonstrates that the choice of the thickness model has a strong influence on calculated creep rates. When coupling the linear and the plastic thickness models to Glen's flow law, the creep rates decrease for high values of the slope angle. This mathematical artefact originates from the vertical integration of Eq. 2.1. In fact, the creep rates are proportional to the thickness to the power of $n + 1$, which in turn is (in the suggested thickness models) inversely proportional to the slope angle. This artefact can be overcome by coupling the thickness models to the creep model of Ladanyi (2003). In this case (Eq. 2.8), the shear rates show a linear dependency on the thickness and a depend on the surface slope angle to the power of n, which therefore dominates the equation. A similar dependency on the slope angle is obtained when combining Glen's flow law with the constant model for rock glacier thickness, i.e. only accounting for variations in the slope angle and substantially neglecting changes in the rock glacier thickness. Although the last two mentioned combinations (constant thickness + Glen and plastic thickness + Ladanyi) provide similar results, we prefer the second approach because it represents the observed thickness dependency on slope more realistically (Fig. 4.5b).

After the above analyses, we can conclude that (i) the typical driving stress of alpine rock glaciers is $92 \pm 13\,\text{kPa}$ suggesting a plastic behaviour, (ii) the thickness of the moving part of a rock glacier can be estimated with the use of simple models on the basis of the surface slope angle, (iii) surface creep velocities can be described on the basis of surface slope observations and thickness models in combination with a creep law - preferably accounting for the frictional behaviour of rock glacier creep.

4.3.2 Analysis at the regional scale

Many efforts in the context of national and international permafrost monitoring are directed towards the assessment of rock glacier surface displacements at both local and regional scale (Kellerer-Pirklbauer et al., 2012, Jones et al., 2018, Groh and Blöthe, 2019, Marcer et al., 2019, PERMOS, 2019). In most studies where creep rates are analysed, different rock glaciers are compared on the basis of kinematic data only, despite their different geometrical properties. The introduction of the BCF allows to include information about their thickness and surface slope, thus to transpose the analysis from a kinematic to a dynamic level. Here, We investi-

gate a database comprising 414 rock glaciers for which surface displacement and slope angle data are available (for a description of the data see Chap. 3.2).

Figure 4.6 shows the results of the BCF in relation to dynamics and geometry for all rock glaciers in the database. The sub-figures visualize the relation between surface creep rates, surface slope angle, BCF and PZI in different combinations. Circular and diamond markers indicate active and destabilized rock glaciers according to the criteria from Marcer et al. (2019). Most rock glaciers show a surface slope comprised between 10° and 35°, surface creep rates lower than about 2 $m\,a^{-1}$ and exhibit a BCF lower than 5 (70% of the rock glaciers in the dataset). Almost only destabilized rock glaciers or rock glaciers with low PZI have high BCFs as shown in Fig. 4.6b-d.

As we have presented above, the calculation of the BCF expresses the rheological properties of the rock glacier material by removing the geometrical information from the velocity signal and thereby allows the comparison of the dynamical behaviour of different rock glaciers. Figure 4.6a and b confirm that the material properties (BCF) and the surface slope angle are independent (if we exclude feedback between shear rates and material structure), while the surface velocities depend with a power law on the surface slope. In the slope-velocity space in Fig. 4.6a the maximum creep rate observed increases with the slope angle: e.g. all the rock glaciers with velocities above 4 $m\,a^{-1}$ are characterized by slope values higher than 25°. Nevertheless, there are also rock glaciers with low values of creep rates regardless of their slope angle. The calculated BCFs displayed in Fig. 4.6b reveal how rock glaciers with gentle slope can exhibit material properties prone to fast deformation (high BCFs). For example the Reichenkar Rock Glacier has a similar BCF to the Pierre Brune Rock Glacier despite reaching only half of its creep rates: this discrepancy in creep velocities can be explained by the difference in surface slope. Comparing relative velocity variations is of advantage, but this approach only introduces a linear trend and remain at a kinematical level, still neglecting geometrical and mechanical properties of the rock glaciers.

Figure 4.6c depicts the relation between BCF, surface slope angle and creep rates. Given a value of the BCF, a wide range of possible velocities can be obtained, and vice-versa. The state of a rock glacier is determined when incorporating the information about the geometry, which is mostly controlled by the surface slope angle. All the points are bounded in a sector of the quadrant delimited by two lines representing the maximum and the minimum surface slope angle of the rock glaciers in our inventory (10° and 30°).

The potential influence of external factors on the BCF is analysed in Fig. 4.6d using the PZI as a proxy for permafrost conditions and temperature. We find that the maximum value of the BCF is delimited by the PZI: for favourable permafrost conditions (PZI close to 1) only small BCF are observed whereas for unfavourable conditions (PZI close to 0) the whole range of low to high BCF occurs. This pattern is consistent with the dual influence of temperature on rock glacier dynamics. Firstly, in the early stage of permafrost degradation, increasing ground temperatures and water content (corresponding to a decrease in the PZI) enhance the deformation (increasing BCF) according to Eq. 2.2 and Eq. 2.3. Secondly, in the final stage of degradation when substantial thawing occurs, the BCF decreases due to lower stresses

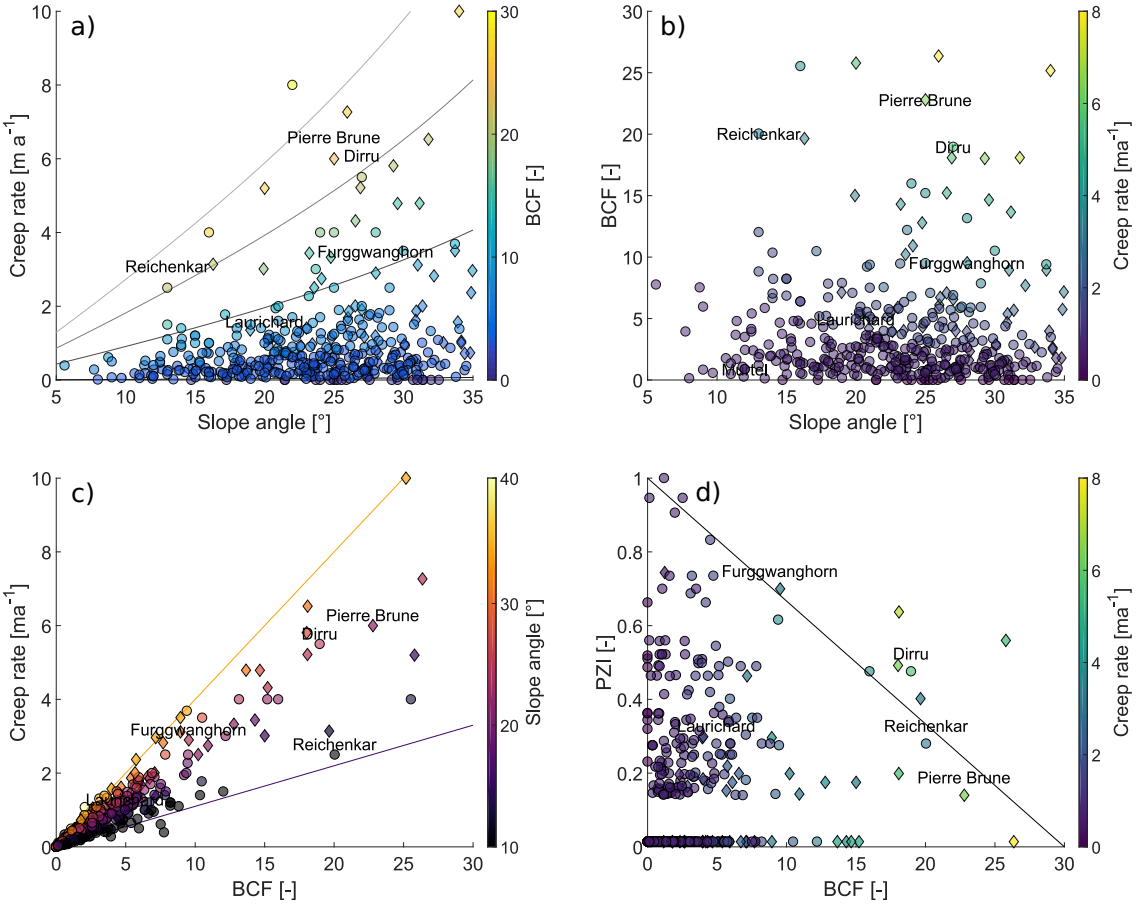

Figure 4.6: Results of the analysis at the regional scale. Each point represents a rock glacier. Destabilized landforms, according to Marcer et al. (2019), are illustrated with a diamond shape. (a) Surface creep rate against slope angle, (b) BCF against slope angle, (c)creep rate against BCF and (d) PZI against BCF. Additional information about creep rates, BCF or slope angle is provided by the corresponding colour bar.

and enhanced inter-particle friction. Rock glaciers currently experiencing a destabilization process are characterized by high values of the BCF and tend to the limiting line in Fig.4.6d. Because destabilization is an irreversible process, and degrading rock glaciers that are in the final stage of destabilization can still be classified as such, they drift towards low values of the BCF and PZI. This result implies that a classification of the dynamic state of rock glaciers might be possible on the basis of a combination of PZI, BCF and creep rates. Whereas low PZIs are in general related to unfavourable permafrost conditions, they can indicate current destabilization if occurring together with high BCFs. High values of the PZI indicate active rock glaciers in cold conditions, apparently less likely to destabilize. However, open questions remain and a classification of rock glaciers based on those parameters remains non trivial and requires additional detailed studies.

4.3.3 Analysis at the local scale

For many rock glaciers worldwide, detailed spatial information about the surface topography and their displacement field are becoming available (Dall'Asta et al., 2017, Bodin et al., 2018, Vivero and Lambiel, 2019, Strozzi et al., 2020). The BCF allows to investigate the dynamics and mechanical properties of rock glaciers for which such topographic and kinematic information are available. We investigate three rock glaciers under contrasting dynamical states: steady-state creep conditions (Laurichard, FR), exceptionally fast flow (Dirru, CH), and ongoing destabilization (Pierre Brune, FR). For all three study sites detailed digital surface models and surface velocity fields are available from different sources and at different resolutions.

The results of the analysis at the local scale are illustrated in Figure 4.7. For the Dirru and Pierre Brune Rock Glaciers, the data coverage with regard to creep velocities is almost complete. For the Laurichard Rock Glacier no velocity data is available in the area close to the rooting zone. The observed velocities show two distinctly different patterns of terrain topography and creep rates at the three field sites. For the Laurichard Rock Glacier, the highest velocities are observed in the uppermost area, whereas for the other two the largest values can be observed closer to the front. The three rock glaciers are characterized by velocity values varying between 1 $m\,a^{-1}$ and 6 $m\,a^{-1}$ and relative high values of the slope angle, with values peaking at more than 30°. The uncertainty related to the spatial variability in velocity is limited in all cases except for a limited region close to the front of the Dirru Rock Glacier. This uncertainty is caused by low performance of the feature tracking algorithm in this area as visible in the corresponding map. The observed field of surface slope angle and surface velocity are smoothed with a Gaussian filter (radius 10 m) in order to reduce undesirable effects of micro-topography on the analysis. On the basis of the values of the surface slope angle, we invert the thickness of the moving rock glacier assuming a yield stress equal to 92 kPa. Exceptionally large thickness values correspond to low slope angles due to small-scale undulations of the surface topography (e.g. furrow and ridges).

For the Laurichard Rock Glacier, the calculated BCF remains constant along the investigated profile, despite substantial variations in slope angle and creep rates. The average value of the BCF is 5 (as also visible in Fig. 4.6), confirming its validity as a reference rock glacier for the Alps.

For the Dirru Rock Glacier the analysed profile extends from the steep front up to the rooting zone. Here, despite strong variations in geometry and the possible influence of 2D effects and the acute change in slope, the BCF is almost constant along the entire profile, with the exception of the rooting zone where it decreases substantially. Similarly to the case of the Laurichard Rock Glacier, the constant value of the BCF shows that the spatial variations in creep rates can be be explained by geometry (slope and thickness). The average value of the BCF = 10, coherent with the value at the regional scale (Fig. 4.6), indicates a predisposition to high creep rates along the entire profile.

The Pierre Brune Rock Glacier on the contrary shows a distinctly different pattern in BCF. In this case, the topography cannot account for the large variations in surface creep rates

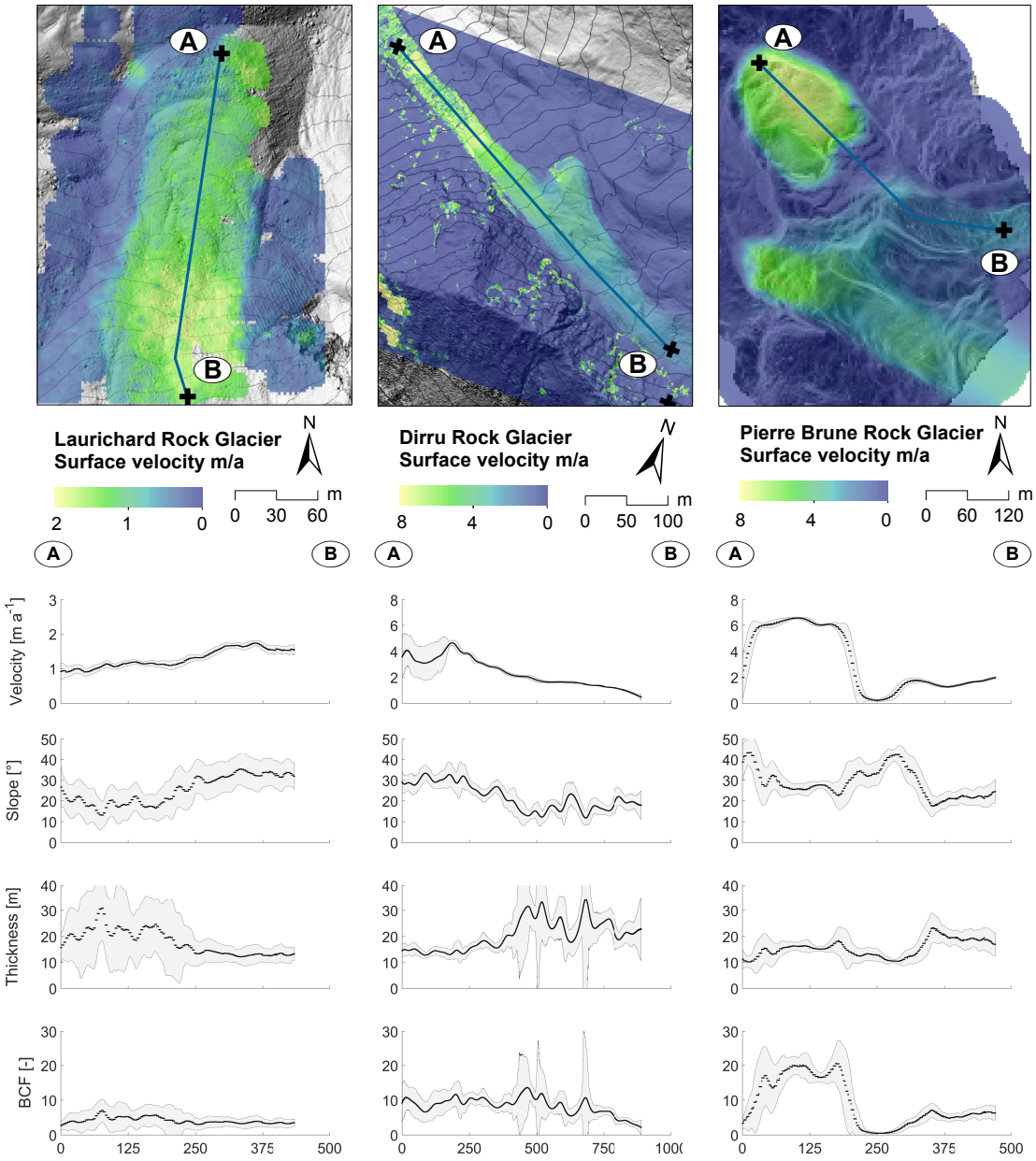

Figure 4.7: Results at local scale. From left to right, Laurichard, Dirru and Pierre Brune Rock Glaciers. The the upper panel shows the field of the surface creep velocity with the profile along which the analysis is performed: from A to B from the front to the rooting zone. Below, from the top to the bottom, the observed surface velocity and surface slope angle, and the modelled thickness and Bulk Creep Factor are plotted along the corresponding profile. The shaded gray area depicts the spatial variability of the plotted variable in an area of 25 *m* along each position and can be used as a proxy for the uncertainty of the results.

along the profile. Close to the front, where the highest rates are observed, the BCF exceeds values of 20. In the upper section, the BCF is four times smaller than close to the front.

In the center corresponding to a scarp-area (Marcer et al., 2019), the velocities are almost zero despite the large values of the slope angle. As a consequence the BCF shows very low values, confirming on the one hand the dynamic separation between the lowermost and the uppermost unit and on the other hand indicating degrading conditions in the scarp area.

According to the results of our analysis, the spatial variability in surface velocity between the upper and the lower part for the Laurichard and the Dirru Rock Glacier can be explained by the their geometry (surface slope and thickness) alone. In this sense, the two rock glaciers can be considered similar, both showing a constant value of the BCF, consistent to the analysis at the regional scale in the previous section. However, the contrasting values of the BCF between the two rock glaciers indicate rheological differences that reflect profound diversity in material properties. Further interpretation requires analysis based on detailed in-situ observations (e.g. surface or ground temperature measurements, geophysical surveying, etc.). For the Pierre Brune Rock Glacier the velocity distribution can be explained only by accounting for both the geometry and the strong spatial discontinuity in the BCF between the upper and the lower part. The discontinuity in the BCF and its exceptionally high values point towards a dynamical and rheological interpretation of the destabilization phenomenon confirming and complementing geomorphological and kinematic observations as seen in the analysis at the regional scale.

5 Synthesis

This dissertation highlights the non-linear nature of rock glacier creep and its complexity, rising questions on our previous knowledge in several research fields. Understanding the processes and the factors driving rock glacier dynamics is essential for an informed management of natural hazards in many mountain ranges over the world. It also has important implications for the interpretation of the geomorphological and paleo-climatic studies on Earth and on other planetary bodies. This chapter discusses the patterns and trends of rock glacier creep in the context of process understanding and operational monitoring activities, providing a synthesis between the state of the art in the research field and the findings of this thesis.

"If a temple is to be erected,
a temple must be destroyed."

FRIEDRICH NIETZSCHE

5.1 The result of three superimposed signals

Field surveys, geophysical investigations and borehole measurements disclosed important information about the internal structure and composition of active rock glaciers and their deformation mechanisms Wahrhaftig and Cox (1959), Haeberli et al. (1988), Vonder Mühll (1993), Arenson et al. (2002), Kääb and Reichmuth (2005), Ikeda et al. (2008), Merz et al. (2015a), Krainer et al. (2015), Buchli et al. (2018). However, despite our relatively advanced knowledge about the deformation profiles of a typical rock glacier, there are yet very few studies trying to bridge the gap between field observations and laboratory experiments on the creep of frozen ground. The few models developed so far remain mostly untested and our confidence in them limited. In light of the new insight stemming from this thesis, through monitoring activities, data analysis and numerical modelling, the surface creep velocity of rock glaciers can be described as the result of three independent superimposed signals from the active layer, the ice-rich core and the shear horizon. This approach, illustrated in Fig. 3.1, allowed us to resolve the relative contribution of each layer and its dependency on external forcing. Figure 5.1 illustrates the vertical displacement profiles as measured in the Murtél-Corvatsch Borehole along with model calculations for varying model parameters. In first approximation, the deformation within a rock glacier can be simulated as a single

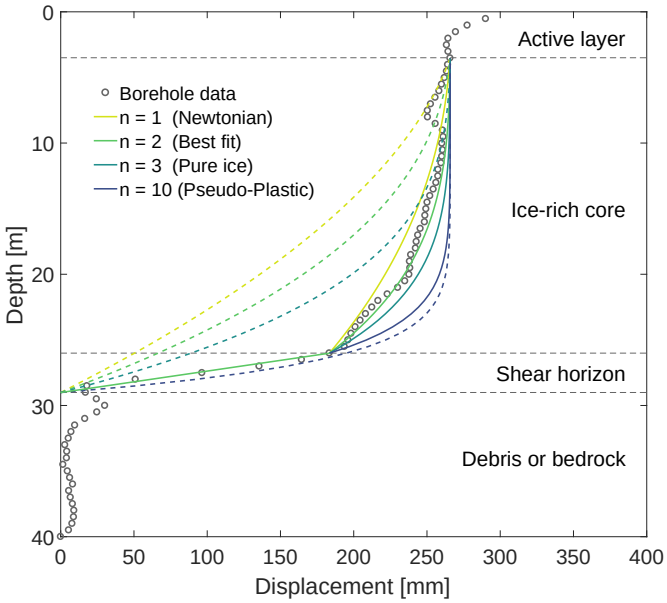

Figure 5.1: Vertical profile of cumulated displacements for the Murtél Rock Glacier. The profile is divided into four vertical layers, according to 2.2. The black dots show the measurements from inclinometer chain readings (in the period from 01/2017 to 01/2020). The coloured lines depict calculated deformation profiles with Eq. 3.10 for the entire rock glacier thickness and for the ice-rich core only (dashed and continuous lines respectively). The different colours indicate the flow exponent n. In the shear horizon, the rheology proposed by Ladanyi (2003) is used.

layer. This approach has been adopted by most of the modelling studies that have investigated rock glacier dynamics so far. The calculated displacements (dashed lines in Fig. 5.1) show the impossibility to correctly reproduce the observed profile with this approach. In fact, while a flow exponent of $n = 3$, corresponding to the rheology of pure ice, yields a satisfactory fit for the upper $\sim 10\,\text{m}$, the rest of the profile is inadequately reproduced. On the contrary, when approximating a plastic rheology with a large exponent ($n = 10$), the shear horizon is well captured by the model, but the deformation in the lower portion of the ice-rich core is considerably overestimated.

The results improve substantially when discriminating between the ice-rich core and the shear horizon. The deformation in the active layer is not treated here according to the arguments presented in Chapter 2. The discussion of *Publication I*and *Publication II* (also presented in Chapter 4.1 and 4.2) have demonstrated that the two creep models proposed by Arenson and Springman (2005a) and Ladanyi (2003) are appropriate for modelling the ice-rich core and the shear horizon respectively. In particular, differentiating between the creep models in these two layers allowed us to account for their different dependency on temperature and effective stresses (through water pressure). The displacements calculated for the ice-rich core, depicted by the continuous lines in Fig. 5.1, show a good fit with the observations. The different values of the creep model parameter n are physically interpretable as the volumetric ice content, according to Eq. 2.6. The curve with the best fit (identified for $n = 2$ for the analysed data) is in accordance with the parametrization proposed by Arenson and Springman (2005a) and the borehole investigations ($w_i = 70\%$). For rock glaciers with lower volumetric ice content it is reasonable to expect that the value of the parameter providing the best fit could change. In the shear horizon, the modelled displacement profile displays only a moderate dependency on the flow exponent and (for the sake of visualization) only

the line for $n = 2$ has been plotted in the figure. Moreover, the dual-layer approach has the advantage of allowing the use of a Newtonian rheology for the ice-rich core, which is mathematically and numerically convenient and can provide important results when correctly interpreted (see Frehner et al. (2015)).

5.2 Patterns and trends of rock glacier dynamics across scales

Recent advances in monitoring activities of the periglacial environment have unveiled the pattern and trends of rock glacier kinematics over temporal scales ranging from few days to centuries. The evolution of rock glacier creep in response to increasing air temperatures is synthesised in Figure 5.2. Panel (a) illustrates the evolution of air temperature (blue line), being the sum of a monotone long-term trend (orange line) and a short-term high-frequency signal, representing seasonal variations. In Fig. 5.2b and c, the blue and the orange lines depict the response of rock glacier creep rates to the above described long- and short-term temperature trends respectively. Panel (b) shows the response to the long-term temperature increase, according to (PERMOS, 2016, Müller et al., 2016). This curve represents not only the direct influence of increasing ground temperature on rock glacier rheology (Arenson and Springman, 2005b, Kääb et al., 2007), but is the combination of different mechanisms, with a preponderant influence of unfrozen water. Approaching the melting point, unfrozen water concentration increases with a power law, similarly to the material fluidity. This effect can strongly influence the viscosity of debris-ice mixtures, especially with high volumetric debris concentration and small particle diameters, and can reduce the shear strenght of a debris-ice mixture at the point that it becomes more fluid than pure ice at the same temperature and stress conditions. The results of *Publication I* quantified the influence of ground temperature on rock glacier rheology and showed that it cannot alone explain nor the seasonal nor the inter-annual observed variations.

Temperature also exerts an influence (direct and indirect) on the amplitude of seasonal variations as shown by field observations and consistent with the theory (Arenson et al., 2002, Arenson and Springman, 2005a, Perruchoud and Delaloye, 2007, Delaloye et al., 2010, Moore, 2014, Wirz et al., 2016a) Figure 5.2c shows the seasonal signal in creep rates relative to the long-term trend (orange line in panel (b), shown here as a constant value). The creep rates oscillate due to the short-term (seasonal) variations in temperature and their amplitude increases in time as a response to the long-term trend in air temperatures. This amplification effect is partly due to the increased sensitivity of the creep rates to warmer air temperatures, but it also includes other processes.

In the extreme case of an homogeneous temperature profile, external temperature forcing would have no influence anymore on the creep rates, being the ground temperature at 0°C (see for example the study from Ikeda et al. (2008) and Buchli et al. (2018)). Despite the paucity of data, the importance of liquid water, especially at the shear horizon depth, was demonstrated by consistent and independent observations and described by different authors (Arenson et al., 2002, Jansen and Hergarten, 2006, Ikeda et al., 2008, Buchli et al., 2018).

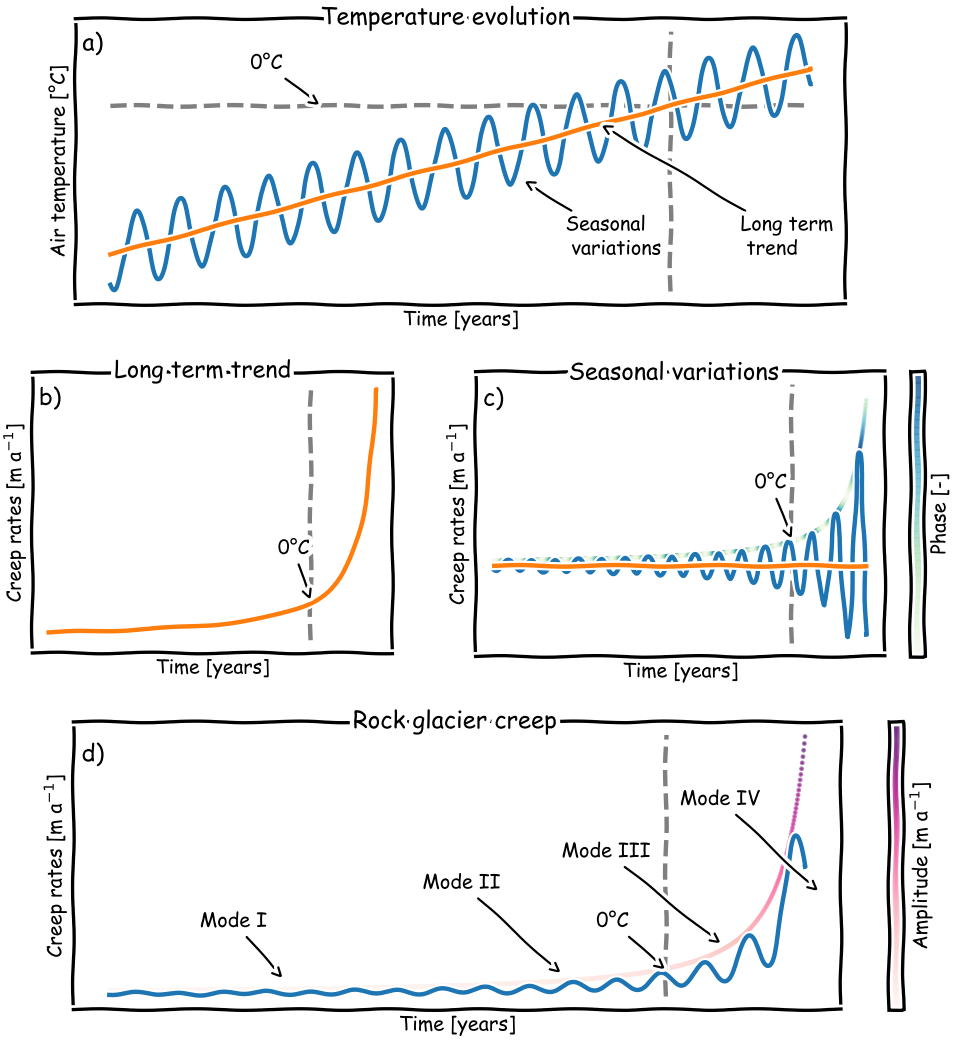

Figure 5.2: Schematic representation of (a) air temperature evolution and the consequent response of rock glacier creep rates on the (b) long term, (c) seasonal variations and (d) overall rock glacier dynamics evolution. The orange line depicts the long term trend, the blue line represents the superimposed seasonal variations. In all the four panels, a gray dashed line shows the point at which the mean annual air temperature exceeds 0°C.

Their theories were synthesised in the conceptual and modelling work presented in *Publication II* which allowed the quantification of the relative influence of pore water pressure on rock glacier creep at seasonal- and inter-annual temporal scales.

The combination of different geodetic and remote sensing techniques allowed the reconstruction of long-term time series of rock glacier velocities and in like manner the application of different methods yielded insights in rock glacier dynamics at different temporal scales. Figure 5.2d shows rock glacier creep rates and their variation in response to the long- and short-term air temperature signals (shown in panel a). Following the evolution of temper-

ature over time, four modes characterized by different combinations of air temperatures, permafrost conditions and rock glacier dynamics can be identified:

Mode I: cold air temperatures (MAAT < -1°C); favorable conditions for permafrost occurrence, thus typically cold permafrost temperatures and modest water content. Low creep rates ($c < 1\,m\,a^{-1}$) and low BCF values, with almost negligible variations at both long- and short-term temporal scales. These conditions were reported for most of the rock glaciers studied in the past century (see (Chaix, 1943, Wahrhaftig and Cox, 1959, Giardino and Steven, 1985, Haeberli, 1985, Whalley and Martin, 1992)).

Mode II: mild air temperatures (-1°C $<$ MAAT $<$ 0°C); rock glaciers creeping towards unfavourable conditions for permafrost occurrence; increasing water content and hydrological activity of the landform. Large creep rates ($c < 3\,m\,a^{-1}$) showing a strong correlation with air temperatures. Moderate values of the BCF (< 5) Displacement rates vary at decennial and seasonal scale with a distinct pattern coherent at the regional scale. These conditions were sporadically observed in the 1980's and scarce evidence exists of previous phases with similar conditions in the 1940's and 1950's, concomitant with larger air temperatures (Kellerer-Pirklbauer and Kaufmann, 2012, Delaloye et al., 2013, Hartl et al., 2016, Marcer et al., submitted). However, most of the abundant observations relative to this mode are evident since the 1990s, concurrent with large positive air anomalies and permafrost temperatures approaching the melting point (Francou and Reynaud, 1992, Lambiel and Delaloye, 2004, Krainer and Mostler, 2006, Delaloye et al., 2008).

Mode III: positive air temperatures (MAAT > 0°C); unfavourable conditions for permafrost, hence ground temperatures close to the melting point ($T \sim 0$ °C). Permafrost degradation (warming and thawing) and structural changes in the rock glacier body. The creep rates might reach very large values ($c > 3\,m\,a^{-1}$), show very high sensitivity to external forcing and an accentuated seasonal pattern, BCF values up to 20. Because of the large mass flux, the creep regime is not sustainable and the rock glacier thickness decreases. In some cases, under favorable climatic and topographic conditions, the onset of a tipping point behaviour is observed (destabilization) where the displacement rates increase dramatically, often preluded by the onset of geomorphic signs of degradation. In some extreme cases, the surface displacement rates have exceeded values of $10\,m\,a^{-1}$ (Grabengufer, Pierre Noire, Tsarmine Rock Glaciers) (Delaloye et al., 2013, Buchli et al., 2018, Eriksen et al., 2018, Cicoira et al., 2019b, Marcer et al., submitted).

Mode IV: positive air temperatures (MAAT > 0°C); very unfavourable conditions for permafrost, isotherm temperatures and widespread permafrost thaw ($T \sim 0$ °C). The combination of widespread permafrost thaw and the thinning undergone in Mode III causes the driving stresses to decrease and strengthens interlocking between the debris particles. Hence, the creep rates decrease and the rock glacier eventually transition to an inactive state (mirrored by the values of the BCF). The seasonal variations diminish together with the absolute values of the creep rates. Although only few observations are available, probably many rock glaciers (or large parts of them) are currently bearing these conditions (Val Sassa, Furggwanghorn).

The concept of the BCF, discussed in Chapter 4.3 and in *Publication III* , can be used to visualise the long-term evolution of rock glacier dynamics. Figure 5.3 illustrates the evolution of a rock glacier in a Lagrangian reference system (following a material point in space and time as it creeps down slope). In Fig. 5.3a this evolution can be followed on the basis of its surface slope angle and its velocity; in Fig. 5.3b based on its BCF and the corresponding driving stress.

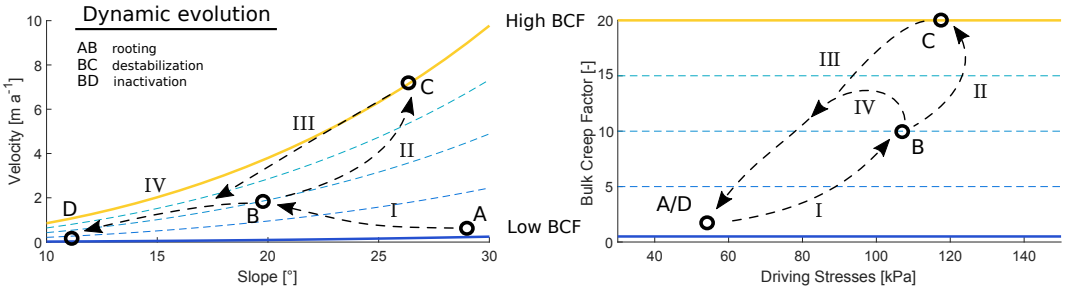

Figure 5.3: Schematic representation of possible dynamical evolution phases (indicated by the dashed arrows) of a rock glacier in the (a) velocity-slope and in the (b) BCF-driving stress space. The points represent possible combination of variables for (A) rooting , (B) secondary creep, (C) destabilization, and (D) inactivation conditions. The values are indicative of typical conditions for alpine rock glaciers.

The evolution of a rock glacier during its rooting from a talus slope is depicted by Phase I from point A to point B. Here, the slope is significantly decreasing from the steeper zone of the talus to the more gentle areas below, while the BCF is increasing due to the initiation of the creep process. The second and third Phases represent the dynamic evolution of a rock glacier experiencing destabilization. When the front of the rock glacier reaches a steeper terrain it moves faster, but maintains its physical properties for a determined period of time, therefore moving along an isoline in the figure. When destabilization occurs due to topographical predisposition and permafrost temperatures close to the melting point, the BCF drastically increases (causing a diversion of the trajectories from the isoline) until point C where the highest velocities are reached. Currently in the Alps an increasing number of rock glaciers are in Phase II, e.g. the Grabenguber, Tsarmine and the Pierre Brune Rock Glaciers (Delaloye et al., 2013, Marcer et al., submitted). From point C on (Phase III), the rock glacier continues creeping with decreasing but still relatively high velocities due to a change in surface slope or due to permafrost degradation. When permafrost thawing causes the driving stresses to decrease, the density of the rock glacier approaches the maximum packing density and interlocking becomes more and more important while the driving stresses decrease: eventually creep ceases and the dynamic evolution of the rock glacier comes to an end while it transitions from an active to an inactive state (Phase IV). Two effects independently lead to the deactivation of the rock glacier: the decrease in driving stress, which is driven by decreasing thickness and diminishing surface slope (geometrical effect), and the decrease in the BCF due to interlocking (rheological effect). Some well studied rock glaciers currently in this condition are the Furggwanghorn and Tête de Longet rock glaciers (Buchli et al., 2018, Marcer et al., submitted). Phase III and Phase IV represent the degradation process, which

can vary its trajectory depending on the different starting condition (C - destabilization or B - secondary creep). Starting from a secondary creep stage, warming permafrost can cause at first an increase in the BCF and prompt an acceleration (first part of Phase IV). However, in a more advanced stage of degradation, the onset of widespread permafrost thawing eventually yields the inactivation of the landform due to the geometrical and rheological effects. Many rock glaciers in the Alps currently find themselves in this condition with temperatures approaching the melting point, increasing velocity and onset of degradation (Delaloye et al., 2010, Groh and Blöthe, 2019, PERMOS, 2019). The positions A and D coincide in Fig. 5.3b, sharing low stresses and a low Bulk Creep Factor. The exact position of the two points in the figure depends on the rock glacier structure and on the terrain topography.

To each Phase corresponds one of the Modes defined in Fig. 5.2d. The long-term evolution of rock glacier dynamics in fact can be also described following the four Modes from the origin in the rooting zone (Mode I and II) to its transition to the inactive state (Mode IV), and under proper topographical conditions also experiencing the phenomenon of destabilization (Mode III). Whereas the Phases characterize the long-term dynamic evolution of a rock glacier, the Modes represent the corresponding conditions of creep velocities and their variability, air and ground temperatures, and permafrost conditions. The temporal scales of the different Phases and the corresponding Modes can be very different. Phase I in fact lasts for millennia, while the transition to the inactive state (Phase IV) can take place in a few centuries of even decades. The onset of rock glacier destabilization may be seen as a tipping point in the long-term evolution of a rock glacier, with an abrupt and irreversible change in its dynamical behaviour. In this sense, it reduces the inactivation time by expediting the degradation process (Phases II and III). Despite the fact that a large part of the rock glacier might be irremediably approaching inactivation, the nourishment from the rooting zone might (under favourable conditions) guarantee sufficient energy and mass fluxes in order to sustain the re-growth of the upper part of the rock glacier or to breed a new generation of the landform.

Throughout the entire evolution of rock glacier dynamics, despite the existence of very different Phases and their relative Modes, the drivers of permafrost creep and rock glacier dynamics remain the same. Their relative importance however, may vary strongly according to the changing conditions. In synthesis, air and ground temperatures appear to be the most important drivers of rock glacier dynamics at all temporal scales. In fact, they not only determine the rheological properties of the rock glacier material, but especially at longer temporal scales they also control mass and energy balance through multiple, interacting, non-linear processes. Warming permafrost temperatures yield an increase of unfrozen water content in the permafrost body and at the shear horizon depth causing substantial modifications of the material rheology. Eventually, approaching isotherm conditions at 0° C, warming temperatures, increasing water content, enhanced creep rates and the onset of degradation lead to important changes in the structure of the rock glacier itself. Hence, thermal mechanisms become less important and hydro-mechanical processes (also through the onset of rock glacier destabilization) take over the control of the short-term dynamic variations of the rock glacier and eventually govern its transition to an inactive state.

6 Conclusion and outlook

This chapter recapitulates the main research findings of this thesis. It also provides a perspective for future research in the field of rock glacier dynamics and by doing so, it concludes the first part of this dissertation.

"There are more things in heaven and earth, Horatio,
than are dreamt of in your philosophy."

HAMLET

6.1 Conclusion

Our knowledge of the patterns and trends of rock glacier dynamics and our understanding of the processes controlling them at temporal scales ranging from few days to centuries have been directed by major advances in monitoring activities of the periglacial environment. A large contribution in this field came from the project X-Sense, which granted the application of power optimized, wireless, continuous DGPS sensing systems suitable for long-term autonomous operation in harsh environments. Approximately a decade after their introduction, the results of this project represent a benchmark in operational monitoring of mass movements in permafrost environment in the Alps and beyond. This thesis is the continuation of exploratory research performed previously by Vanessa Wirz and Johann Müller (Wirz et al., 2011, 2014, 2016a, Müller et al., 2016, Wirz et al., 2016b). The previous chapters delineated the original work performed in order to continue and improve the field measurements, analyse and interpret the data, and in conclusion to explain the observations by developing a theory.

At a local scale, I investigated the dynamic response of rock glacier dynamics to variations in external temperature and water input at seasonal and inter-annual temporal scales by designing a novel conceptual and numerical modelling approach. The modelling is constrained and the results are compared against kinematic, geophysical and meteorological observations for five well documented study cases in the Swiss Alps. Using this approach, I critically discuss the hypotheses that (i) external temperature forcing through heat conduction and (ii) water input through pore water pressure at the shear horizon can explain seasonal and inter-annual variations in rock glacier dynamics. This approach, illustrated in

Fig. 3.1, allowed us to resolve the relative contribution of each layer and its dependency on external forcing (for Murtél, Muragl, Schafberg, and Ritigraben Rock Glacier) and reproduce the seasonal and inter-annual velocity patterns for Dirru Rock Glacier.

I quantitatively investigated the contribution of heat conduction to seasonal and multi-annual variations in rock glacier creep velocity on the basis of numerical modelling and a multi-year time series of observed surface velocities and borehole temperatures for Murtél, Muragl, Schafberg, and Ritigraben Rock Glacier. The numerical model couples heat conduction to an empirically derived rheology of rock glacier creep that accounts for temperature and ice-content. The thermal regime of a rock glacier (below the active layer) is mainly controlled by heat conduction and therefore relatively easy to reproduce numerically using standard parameters from the literature. However, its influence on rock glacier rheology can explain only about 25% of the observed seasonal and inter-annual variations in surface velocities. The magnitudes of variations are underestimated at least by one order of magnitude and the phase of the seasonal peaks are delayed by 2-3 months. Accounting for the observed temperatures and including a description of the shear horizon does not improve the results. Temperature changes over the whole thickness of the rock glacier can cause substantial variations in creep rates, but require changes in climate over decades or centuries. Based on the modelling results and on field observations, I conclude that non-conductive processes must dominate the short-term velocity signal. Additional sensitivity experiments underpin the robustness of these conclusions within expected parameter uncertainties. From our quantitative process modelling approach I can therefore exclude heat conduction as the governing process for seasonal to multi-annual variations in rock glacier flow. Considering the phase-lag information of the summer peak (e.g. the case of case of Ritigraben) and indications from earlier qualitative and statistical analysis of rock glacier velocities, I conclude that advection of surface water into the rock glacier and its interaction over pore water pressure with the creep rheology is required to explain short- to mid-term velocity variations of rock glacier dynamics.

In order to test this second hypothesis, I developed a process-based model accounting for heat transfer into the ground, the catchment hydrology, the hydro-mechanics of the rock glacier and its rheology. Data from the Dirru Rock Glacier (Vallis - CH) are used to constrain the modelling and to validate the results. Our model can reproduce the velocity variations both in magnitude and phase at seasonal and inter-annual time scales and can be used to derive indirect information on the hydro-mechanical regime of rock glaciers. The results corroborate the hypothesis that the rhythm of rock glacier dynamics can be explained by water and external temperature, with a preponderant influence of water at the shear horizon depth, which is also indirectly controlled by temperature. Our case study is extremely fast and it is reasonable to expect other rock glaciers characterized by different internal structure and material properties, and located in different topographic and climatic settings to have a different dynamical behaviour. The fundamental processes governing their flow, however, remain the same. Therefore, our study underlines the importance of water in determining the seasonal rhythm of rock glacier velocities and highlights the complex and non-linear nature of rock glacier dynamics.

Based on the previous conclusions, I compiled a brief review of the physics of rock glacier creep and the mathematical formulation used to describe it. The analysis of a large dataset of RGs from the Alps shows that the typical driving stress is 92 ± 13 kPa, similar to ice glaciers. Therefore, rock glacier thickness can be efficiently estimated with the inversion of simple models (e.g. perfectly plastic model), despite more detailed data is needed for further validation of this approach. Thereon, I developed a general theory of rock glacier creep and introduced the Bulk Creep Factor BCF as a measure of the rheological properties of rock glaciers. The Bulk Creep Factor (BCF) allows to disentangle the two contributions to the surface velocity of rock glaciers from (i) material properties and (ii) geometry. The proposed approach only requires data on creep velocities and slope angle, both which can be derived operationally over large areas from remote sensing data (or from detailed in-situ measurements). Additionally, I have provided two examples of possible applications of the BCF at a regional and at a local scale. At a regional scale, most alpine rock glaciers show a BCF lower than 5. Only rock glaciers currently experiencing destabilization or set in conditions unfavourable to permafrost occurrence show large values close to 20. The permafrost conditions (approximated here by the PZI) define a maximum limit for the BCF. At a local scale, I find that for dynamically stable rock glaciers the geometry can explain the spatial variability in creep rates with almost constant rheological properties (BCF) of the constitutive material. Destabilized rock glaciers are characterized by contrasting and discontinuous material properties. Thus, in addition to geomorphological observations, the definition of the dynamical state of a rock glacier should account for the material properties and the processes controlling its movement rather than solely on its kinematics.

Concluding, this thesis provides a step forward towards a better understanding of rock glacier dynamics, i.e. the coupling between rock glacier creep and the climate system, having important implications in manifold research fields.

6.2 Outlook

The research conducted within this dissertation and the dialectic process developing thereon, allowed to answer the three initial research questions and at the same time rose abundant new interrogatives on rock glaciers and their dynamics. In pursuance of a more thorough understanding of rock glacier dynamics, future studies could investigate the following research paths:

- Collect and analyse (already existing and original) detailed information with hydrological and geophysical measurements at the local scale (such as BH piezometers, active and passive tracer techniques, ERT and ambient seismic).
- Analyse multi-temporal, distributed kinematic data (such as from repeated UAVs or from remote sensing.
- Implement the conceptual models proposed so far by reviewing our knowledge of the processes controlling rock glacier dynamics at different spatio-temporal scales.
- Implement more processes in the modelling, such as complex thermodynamics in the active layer and phase change at the upper and bottom interfaces of the permafrost (and their coupling to rheological models).
- Improve the constrains of the model parameters and increase the confidence in the results through the investigation of more case studies in different geomorphological and climatic settings.
- Develop 2D and 3D models accounting for complex transient effects.
- Include analysis at longer temporal scales, accounting for geometrical changes and dynamical effects (sediment input and max fluxes).
- Extend the analysis at the regional scale and apply it to consistent inventories, not available up to date, but next to come for different regions worldwide.
- Include rheological models in the study of rock glacier ice-cores and age dating for the sake of accurate paleo-climatic and geomorphological reconstructions.
- Investigate rock glacier destabilization from a mechanical standpoint, shed light on the processes controlling it and in a second step implement the existing models to account for the tipping point behaviour in the long-term evolution of rock glaciers (paleo-destabilization).

Bibliography

Andersland, B. O. and Akili, W.: Stress Effect on Creep Rates of a Frozen Clay Soil, Geotechnique, 17, 27–39, 10.1680/geot.1967.17.1.27, 1967.

Andersland, O. B., Wiggert, D. C., and Davies, S. H.: Hydraulic Conductivity of Frozen Granular Soils, Journal of Environmental Engineering, 122, 212–216, 10.1061/(ASCE)0733-9372(1996)122:3(212), 1996.

Arenson, L. U.: pers. com. 2020.

Arenson, L. U. and Jakob, M.: Periglacial Geohazard Risks and Ground Temperature Increases, in: Engineering Geology for Society and Territory - Volume 1, 10.1007/978-3-319-09300-0_44, 2014.

Arenson, L. U. and Springman, S. M.: Mathematical descriptions for the behaviour of ice-rich frozen soils at temperatures close to 0 °C, Canadian Geotechnical Journal, 42, 431–442, 10.1139/t04-109, 2005a.

Arenson, L. U. and Springman, S. M.: Triaxial constant stress and constant strain rate tests on ice-rich permafrost samples, Canadian Geotechnical Journal, 42, 412–430, 10.1139/t04-111, 2005b.

Arenson, L. U., Hoelzle, M., and Springman, S.: Borehole deformation measurements and internal structure of some rock glaciers in Switzerland, Permafrost and Periglacial Processes, 13, 117–135, 10.1002/ppp.414, 2002.

Arenson, L. U., Johansen, M. M., and Springman, S. M.: Effects of volumetric ice content and strain rate on shear strength under triaxial conditions for frozen soil samples, Permafrost and Periglacial Processes, 15, https://doi.org/10.1002/ppp.498, 2004.

Arenson, L. U., Springman, S. M., and Sego, D.: The rheology of frozen soils, Appl. Rheol, 17, 12 147–1, 10.3933/ApplRheol-17-12147, 2007.

Arenson, L. U., Hauck, C., Hilbich, C., Seward, L., Yamamoto, Y., and Springman, S. M.: Subsurface Heterogeneities in the Murtèl. Corvatsch Rock Glacier, Switzerland, in: Proceedings of the joint 63rd Canadian Geotechnical Conference and the 6th Canadian Permafrost Conference, pp. 1494 – 1500, Canadian Geotechnical Society, the 6th Canadian Permafrost Conference; Conference Location: Calgary, Canada; Conference Date: September 12-16, 2010, 2010.

Arenson, L. U., Kääb, A., and O'Sullivan, A.: Detection and Analysis of Ground Deformation in Permafrost Environments, Permafrost and Periglacial Processes, 10.1002/ppp.1932,

2016.

Avian, M., Kaufmann, V., and Lieb, G. K.: Recent and Holocene dynamics of a rock glacier system: The example of Langtalkar (Central Alps, Austria), Norsk Geografisk Tidsskrift - Norwegian Journal of Geography, 59, 149–156, 10.1080/00291950510020637, 2005.

Baker, V. R.: Water and the martian landscape., Nature, 412, 228 – 236, 10.1038/35084172, 2001.

Barboux, C., Delaloye, R., Lambiel, C., Strozzi, T., Collet, C., and Raetzo, H.: Surveying the activity of permafrost landforms in the Valais Alps with InSAR, in: Jahrestagung der Schweizerischen Geomorphologischen Gesellschaft, 2013.

Barsch, D.: Ein Permafrostprofil aus Graubünden, Schweizer Alpen., Zeitschrift für Geomorphologie, NF 21, 79 – 86, 1977.

Barsch, D.: Permafrost creep and rockglaciers, Permafrost and Periglacial Processes, 3, 175–188, 10.1002/ppp.3430030303, 1992.

Barsch, D. and Hell, G.: Photogrammetrische Bewegungsmessungen am Blockgletscher Murtel I, Oberengadin, Schweizer Alpen., Zeitschrift für Gletscherkunde und Glazialgeologie, 11/2, 111–142, 1975.

Barsch, D. and Zick, W.: Die Bewegungen des Blockgletschers Macun 1 von 1965-1988 (Unterengadin, Graubünden, Schweiz), Zeitschrift für Geomorphologie. 35(1). Germany, 35, 1, 1991.

Bast, A.: pers. com. 2015.

Bauer, A., Paar, G., and Kaufmann, V.: Terrestrial laser scanning for rockglacier monitoring, 8th International Conference on Permafrost, pp. 55–60, 2003.

Beniston, M., Farinotti, D., Stoffel, M., Andreassen, L. M., Coppola, E., Eckert, N., Fantini, A., Giacona, F., Hauck, C., Huss, M., Huwald, H., Lehning, M., López-Moreno, J.-I., Magnusson, J., Marty, C., Morán-Tejéda, E., Morin, S., Naaim, M., Provenzale, A., Rabatel, A., Six, D., Stötter, J., Strasser, U., Terzago, S., and Vincent, C.: The European mountain cryosphere: a review of its current state, trends, and future challenges, The Cryosphere, 12, 759–794, 10.5194/tc-12-759-2018, 2018.

Berthling, I.: Beyond Confusion: Rock Glaciers as Cryo-Conditioned Landforms, Geomorphology, 131, 98–106, 10.1016/j.geomorph.2011.05.002, 2011.

Berthling, I., Etzelmüller, B., Eiken, T., and Sollid, J. L.: Rock glaciers on Prins Karls Forland, Svalbard. I: internal structure, flow velocity and morphology, Permafrost and Periglacial Processes, 9, 135–145, 10.1002/(SICI)1099-1530(199804/06)9:2<135::AID-PPP284>3.0.CO;2-R, 1998.

Bertone, A., Zucca, F., Marin, C., Notarnicola, C., Cuozzo, G., Krainer, K., Mair, V., Riccardi, P., Callegari, M., and Seppi, R.: An Unsupervised Method to Detect Rock Glacier Activity by Using Sentinel-1 SAR Interferometric Coherence: A Regional-Scale Study in the Eastern European Alps, Remote Sensing, 11, 1711, 10.3390/rs11141711, 2019.

Beutel, J., Buchli, B., Ferrari, F., Keller, M., Zimmerling, M., and Thiele, L.: X-SENSE: Sensing in extreme environments, in: Proceedings of Design, Automation and Test in Europe, DATE 2011, Grenoble, France, pp. 1460–1465, 10.1109/DATE.2011.5763236, 2011.

Biskaborn, B. K., Smith, S. L., Noetzli, J., Matthes, H., Vieira, G., Streletskiy, D. A., Schoeneich, P., Romanovsky, V. E., Lewkowicz, A. G., Abramov, A., et al.: Permafrost is warming at a global scale, Nature communications, 10, 264, 2019.

Bodin, X., Krysiecki, J.-M., Schoeneich, P., Le Roux, O., Lorier, L., Echelard, T., Peyron, M., and Walpersdorf, A.: The 2006 Collapse of the Bérard Rock Glacier (Southern French Alps), Permafrost and Periglacial Processes, 28, 209–223, 10.1002/ppp.1887, 2017.

Bodin, X., Thibert, E., Sanchez, O., Rabatel, A., and Jaillet, S.: Multi-Annual Kinematics of an Active Rock Glacier Quantified from Very High-Resolution DEMs: An Application-Case in the French Alps, Remote Sensing, 10, 547, 10.3390/rs10040547, 2018.

Boeckli, L., Brenning, A., Gruber, S., and Noetzli, J.: Permafrost distribution in the European Alps: calculation and evaluation of an index map and summary statistics, The Cryosphere, 6, 807–820, 10.5194/tc-6-807-2012, 2012.

Bolch, T., Rohrbach, N., Kutuzov, S., Robson, B., and Osmonov, A.: Occurrence, evolution and ice content of ice-debris complexes in the Ak-Shiirak, Central Tien Shan revealed by geophysical and remotely-sensed investigations, Earth Surface Processes and Landforms, 44, 129–143, 10.1002/esp.4487, 2019.

Bommer, C., Phillips, M., and Arenson, L. U.: Practical recommendations for planning, constructing and maintaining infrastructure in mountain permafrost, Permafrost and Periglacial Processes, 21, 97–104, 10.1002/ppp.679, 2010.

Brardinoni, F., Scotti, R., Sailer, R., and Mair, V.: Evaluating sources of uncertainty and variability in rock glacier inventories, Earth Surface Processes and Landforms, 44, 2450–2466, 10.1002/esp.4674, 2019.

Brunner, M., Viviroli, D., Furrer, R., Seibert, J., and Favre, A.-C.: Identification of Flood Reactivity Regions via the Functional Clustering of Hydrographs, Water Resources Research, 54, 10.1002/2017WR021650, 2018.

Bryant, B.: Movement measurements on two rock glaciers in the eastern Elk Mountains, Colorado US Geology Survey, Professional Paper, 1971.

Buchli, B., Sutton, F., and Beutel, J.: GPS-Equipped Wireless Senson Network Node for High-Accuracy Positioning Applications., Wireless Sensor Network, pp. 179–195, 2012.

Buchli, T., Merz, K., Zhou, X., Kinzelbach, W., and Springman, S.: Characterization and Monitoring of the Furggwanghorn Rock Glacier, Turtmann Valley, Switzerland: Results from 2010 to 2012, Vadose Zone Journal, 12, 0, 10.2136/vzj2012.0067, 2013.

Buchli, T., Kos, A., Limpach, P., Merz, K., Zhou, X., and Springman, S. M.: Kinematic investigations on the Furggwanghorn Rock Glacier, Switzerland, Permafrost and Periglacial Processes, 29, 3–20, 2018.

Buck, S. and Kaufmann, V.: The influence of air temperature on the creep behaviour of three rockglaciers in the Hohe Tauern, Grazer Schriften der Geographie und Raumforschung, 45, 2010.

Bucki, A. K. and Echelmeyer, K. A.: The flow of Fireweed rock glacier, Alaska, U.S.A., Journal of Glaciology, 50, 76–86, 10.3189/172756504781830213, 2004.

Burt, T. P. and Williams, P. J.: Hydraulic conductivity in frozen soils, Earth Surface Processes, 1, 349–360, 10.1002/esp.3290010404, 1976.

Böhlert, R., Compeer, M., Egli, M., Brandova, D., Maisch, M., Kubik, P., and Haeberli, W.: A combination of relative-numerical dating methods indicates two high Alpine rock glacier activity phases after the glacier advance of the Younger Dryas, The Open Geography Journal, 4, 10.5167/uzh-42941, 2011.

Capps, S. R.: Rock glaciers in alaska, Journal of Geology, 18, 359–375, 1910.

Carr, M.: Water on Mars, Nature, 326, 30–35, khttps://doi.org/10.1038/326030a0DO, 1987.

Carslaw, H. and Jaeger, J.: Conduction of heat in solids, Oxford science publications, Clarendon Press, 1959.

Chadburn, S., Burke, E., Cox, P., Friedlingstein, P., Hugelius, G., and Westermann, S.: An observation-based constraint on permafrost loss as a function of global warming, Nature Climate Change, 7, 340–344, 2017.

Chaix, A.: Les coulées de blocs du Park National suisse d'Engadine, Le Globe, 62, 1 – 35, 1923.

Chaix, A.: Les coulées de Bloc du Park National suisse. Nouvelles mesures et comparaison avec le rock-streams de la Sierra Nevada de Californie, Le Globe, 82, 1943.

Cicoira, A., Beutel, J., Gärtner-Roer, I., Faillettaz, J., and Vieli, A.: Resolving the influence of temperature forcing through heat conduction on rock glacier dynamics: a numerical modelling approach, The Cryosphere, 13, 927–942, 10.5194/tc-13-927-2019, 2019a.

Cicoira, A., Beutel, J., Faillettaz, J., and Vieli, A.: Water controls the seasonal rhythm of rock glacier flow, Earth and Planetary Science Letters, 528, 115 844, https://doi.org/10.1016/j.epsl.2019.115844, 2019b.

Cicoira, A., Marcer, M., Gärtner-Roer, I., Bodin, X., Arenson, L., and Vieli, A.: A general theory of rock glacier creep based on in-situ and remote sensing observations, Permafrost and Periglacial Processes, submitted.

Clark, D. H., Steig, E. J., Potter Jr., N., Updike, A., Fitzpatrick, J., and Clark, G. M.: Old ice in rock glaciers may provide long-term climate records, Eos, Transactions American Geophysical Union, 77, 217–222, 10.1029/96EO00149, 1996.

Clark, D. H., Steig, E. J., Potter, Jr., N., and Gillespie, A. R.: Genetic variability of rock glaciers, Geografiska Annaler: Series A, Physical Geography, 80, 175–182, 10.1111/j.0435-3676.1998.00035.x, 1998.

Corte, A.: The Hydrological Significance of Rock Glaciers, Journal of Glaciology, 17, 157–158, 10.3189/S0022143000030859, 1976.

Cremonese, E., Gruber, S., Phillips, M., Pogliotti, P., Boeckli, L., Noetzli, J., Suter, C., Bodin, X., Crepaz, A., Kellerer-Pirklbauer, A., Lang, K., Letey, S., Mair, V., Morra di Cella, U., Ravanel, L., Scapozza, C., Seppi, R., and Zischg, A.: Brief Communication: "An inventory of permafrost evidence for the European Alps", The Cryosphere, 5, 651–657, 10.5194/tc-5-651-2011, URL https://www.the-cryosphere.net/5/651/2011/, 2011.

Cross, W., Howe, E., and Ransome, F.: Description of the Silverton quadrangle, Colorado: US Geological Survey Geological Atlas, Folio, 120, 34, 1905.

Cuffey, K. and Paterson, W. S. B.: The Physics of Glaciers, Elsevier, 2010.

Czurda, K. and Hohmann, M.: Freezing effect on shear strength of clayey soils, Applied Clay Science, 12, 165 – 187, https://doi.org/10.1016/S0169-1317(97)00005-7, 1997.

Dall'Asta, E., Forlani, G., Roncella, R., Santise, M., Diotri, F., and di Cella, U. M.: Unmanned Aerial Systems and DSM matching for rock glacier monitoring, ISPRS Journal of Photogrammetry and Remote Sensing, 127, 102 – 114, https://doi.org/10.1016/j.isprsjprs.2016.10.003, 2017.

Darcy, H.: Les fontaines publiques de la ville de Dijon: exposition et application des principes a suivre et des fomules a emplyer dans les qeustions de distribution d'eau., Victor Dalmont, 1856.

De La Chapelle, S., Milsch, H., Castelnau, O., and Duval, P.: Compressive creep of ice containing a liquid intergranular phase: Rate-controlling processes in the dislocation creep regime, Geophysical Research Letters, 26, 251–254, 10.1029/1998GL900289, 1999.

Delaloye, R. and Lambiel, C.: Evidence of winter ascending air circulation throughout talus slopes and rock glaciers situated in the lower belt of alpine discontinuous permafrost (Swiss Alps), Norsk Geografisk Tidsskrift - Norwegian Journal of Geography, 59, 194–203, 10.1080/00291950510020673, 2005.

Delaloye, R., Perruchoud, E., Avian, M., Kaufmann, V., Bodin, X., Hausmann, H., Ikeda, A., Kääb, A., Kellerer-Pirklbauer, A., Krainer, K., Lambiel, C., Mihajlovic, D., Staub, B., Roer, I., and Thibert, E.: Recent interannual variations of rock glacier creep in the European Alps, in: 9th International Conference on Permafrost, pp. 343–348, 2008.

Delaloye, R., Lambiel, C., and Gärtner-Roer, I.: Overview of rock glacier kinematics research in the Swiss Alps, Geographica Helvetica, 65, 135–145, 10.5194/gh-65-135-2010, 2010.

Delaloye, R., Morard, S., Barboux, C., Abbet, D., Gruber, V., Riedo, M., and Gachet, S.: Rapidly moving rock glaciers in Mattertal, Jahrestagung Der Schweizerischen Geomorphologischen Gesellschaft, pp. 21–31, 2013.

Duval, P., Ashby, M. F., and Anderman, I.: Rate-controlling processes in the creep of polycrystalline ice, The Journal of Physical Chemistry, 87, 1983.

Duvillard, P.-A., Ravanel, L., Marcer, M., and Schoeneich, P.: Recent evolution of damage to infrastructure on permafrost in the French Alps, Regional Environmental Change, 10.1007/s10113-019-01465-z, 2019.

Elconin, R. F. and LaChapelle, E. R.: Flow and internal structure of a rock glacier, Journal of Glaciology, 43, 238–244, 10.3189/S002214300000318X, 1997.

Eriksen, H. O., Rouyet, L., Lauknes, T. R., Berthling, I., Isaksen, K., Hindberg, H., Larsen, Y., and Corner, G. D.: Recent Acceleration of a Rock Glacier Complex, Ádjet, Norway, Documented by 62 Years of Remote Sensing Observations, Geophysical Research Letters, 45, 8314–8323, 10.1029/2018GL077605, 2018.

Farbrot, H., Isaksen, K., Eiken, T., Kääb, A., and Sollid, J. L.: Composition and internal structures of a rock glacier on the strandflat of western Spitsbergen, Svalbard, Norsk Geografisk Tidsskrift - Norwegian Journal of Geography, 59, 139–148, 10.1080/00291950510020619, 2005.

Farinotti, D., Brinkerhoff, D. J., Clarke, G. K. C., Fürst, J. J., Frey, H., Gantayat, P., Gillet-Chaulet, F., Girard, C., Huss, M., Leclercq, P. W., Linsbauer, A., Machguth, H., Martin, C., Maussion, F., Morlighem, M., Mosbeux, C., Pandit, A., Portmann, A., Rabatel, A., Ramsankaran, R., Reerink, T. J., Sanchez, O., Stentoft, P. A., Singh Kumari, S., van Pelt, W. J. J., Anderson, B., Benham, T., Binder, D., Dowdeswell, J. A., Fischer, A., Helfricht, K., Kutuzov, S., Lavrentiev, I., McNabb, R., Gudmundsson, G. H., Li, H., and Andreassen, L. M.: How accurate are estimates of glacier ice thickness? Results from ITMIX, the Ice Thickness Models Intercomparison eXperiment, The Cryosphere, 11, 949–970, 10.5194/tc-11-949-2017, 2017.

Federal Office of Topography swisstopo: URL `https://map.geo.admin.ch/`, last access: 04 April 2019, 2018.

Francou, B. and Reynaud, L.: 10 year surficial velocities on a rock glacier (Laurichard, French Alps), Permafrost and Periglacial Processes, 3, 209–213, 1992.

Frauenfelder, R., Haeberli, W., Hoelzle, M., and Maisch, M.: Using relict rockglaciers in GIS-based modelling to reconstruct Younger Dryas permafrost distribution patterns in the Err-Julier area, Swiss Alp, Norsk Geografisk Tidsskrift - Norwegian Journal of Geography, 55, 195–202, 10.1080/00291950152746522, 2001.

Frauenfelder, R., Laustela, M., and Kääb, A.: Relative age dating of Alpine rockglacier surfaces, Zeitschrift fur Geomorphologie, 49, 145–166, URL `https://www.scopus.com/inward/record.uri?eid=2-s2.0-32144460152&partnerID=40&md5=59b79067379a927b04f4f7a8d2b9511d`, cited By 33, 2005.

Frehner, M., Ling, A. H. M., and Gärtner-Roer, I.: Furrow-and-Ridge Morphology on Rockglaciers Explained by Gravity-Driven Buckle Folding: A Case Study From the Murtèl Rockglacier (Switzerland), Permafrost and Periglacial Processes, 26, 57–66, 10.1002/ppp.1831, pPP-14-0032.R2, 2015.

French, H.: The development of periglacial geomorphology: 1- up to 1965, Permafrost and Periglacial Processes, 14, 29–60, 10.1002/ppp.438, 2003.

Frost, R. E. and Mintzer, O. W.: Influence of topographic position in airphoto identification of permafrost, Soil Exploration and Mapping, US Highway Research Board, Bull, 28, 100–121, 1950.

Fuchs, M. C., Böhlert, R., Krbetschek, M., Preusser, F., and Egli, M.: Exploring the potential of luminescence methods for dating Alpine rock glaciers, Quaternary Geochronology, 18, 17 – 33, https://doi.org/10.1016/j.quageo.2013.07.001, 2013.

Gärtner-Roer, I., Kääb, A., and Dikau, R.: Rockglacier acceleration in the Turtmann valley (Swiss Alps): Probable controls, Norsk Geografisk Tidsskrift - Norwegian Journal of Geography, 59, 157–163, 10.1080/00291950510020655, 2005.

Gärtner-Roer, I., Haeberli, W., Avian, M., Kaufmann, V., Delaloye, R., Lambiel, C., and Kääb, A.: Observations and considerations on destabilizing active rock glaciers in the European Alps, Ninth International Conference on Permafrost, 10.5167/uzh-6082, 2008.

Giardino, J. R. and Steven, V. G.: The Engineering Geology Hazards of Rock Glaciers, Environmental and Engineering Geoscience, 12, 201–216, 10.2113/gseegeosci.xxii.2.201, 1985.

Giardino, J. R. and Vitek, J. D.: The significance of rock glaciers in the glacial-periglacial landscape continuum, Journal of Quaternary Science, 3, 97–103, 10.1002/jqs.3390030111, 1988.

Glen, J.: The creep of polycrystalline ice, Proceedings of the Royal Society of London A: Mathematical, Physical and Engineering Sciences, 228, 519–538, 10.1098/rspa.1955.0066, 1955.

Groh, T. and Blöthe, J. H.: Rock Glacier Kinematics in the Kaunertal, Ötztal Alps, Austria, Geosciences, 9, 10.3390/geosciences9090373, 2019.

Gruber, S.: Derivation and analysis of a high-resolution estimate of global permafrost zonation, The Cryosphere, 6, 221–233, 10.5194/tc-6-221-2012, URL `https://www.the-cryosphere.net/6/221/2012/`, 2012.

Guillemot, A., Helmstetter, A., Larose, E., Baillet, L., Garambois, S., Mayoraz, R., and Delaloye, R.: Seismic monitoring in the Gugla rock glacier (Switzerland): ambient noise correlation, microseismicity and modelling, Geophysical Journal International, 221, 1719–1735, 10.1093/gji/ggaa097, 2020.

Gärtner-Roer, I.: Sediment transfer rates of two active rockglaciers in the Swiss Alps, Geomorphology, 167-168, 45 – 50, https://doi.org/10.1016/j.geomorph.2012.04.013, sedimentary fluxes and budgets in natural and anthropogenically modified landscapes – Effects of climate change and land-use change on geomorphic processes, 2012.

Haeberli, W.: Creep of mountain permafrost, Mitteilungen der Versuchsanstalt für Wasserbau. Hydrologie und Glaziologie der ETH Zürich, vol. 77, 1985.

Haeberli, W.: On the morphodynamics of ice/ debris-transport systems in cold mountain areas, Norsk Geografisk Tidsskrift-norwegian Journal of Geography - NORSK GEOGR TIDSSKR-NOR J GEO, 50, 3–9, 10.1080/00291959608552346, 2008.

Haeberli, W. and Beniston, M.: Climate Change and its Impacts on Glaciers and Permafrost in the Alps, Ambio, 27, 258–265, 1998.

Haeberli, W. and Vonder Mühll, D.: On the Characteristics and Possible Origins of Ice in Rock Glacier Permafrost, Zeitschrift fur Geomorphologie, Supplementband, 104, 43–57,

1996.

Haeberli, W., Hunder, J., Keusen, H.-R., Pika, J., and Röthlisberger, H.: Core drilling through rock-glacier permafrost, Fifth International Conference on Permafrost, Trondheim, 2, 937 – 942, 1988.

Haeberli, W., Wegmann, M., and Mühll, D.: Slope stability problems related to glacier shrinkage and permafrost degradation in the Alps, Eclogae Geologicae Helvetiae, 90, 407–414, 1997.

Haeberli, W., Hoelzle, M., Kääb, A., Keller, F., Vonder Mühll, D., and Wagner, S.: Ten years after drilling through the permafrost of the active rock glacier Murtél, Seventh International Conference on Permafrost, Yellowknife, pp. 403 – 410, 1998.

Haeberli, W., Kääb, A., Wagner, S., Mühll, D. V., Geissler, P., Haas, J. N., Glatzel-Mattheier, H., and Wagenbach, D.: Pollen analysis and 14C age of moss remains in a permafrost core recovered from the active rock glacier Murtèl-Corvatsch, Swiss Alps: geomorphological and glaciological implications, Journal of Glaciology, 45, 1–8, 10.3189/S0022143000002975, 1999.

Haeberli, W., Brandova, D., Burga, C., Egli, M., Frauenfelder, R., Kääb, A., and Maisch, M.: Methods for absolute and relative age dating of rock-glacier surfaces in alpine permafrost, Proceedings of the Eighth International Conference on Permafrost, 1, 343–348, 2003.

Haeberli, W., Hallet, B., Arenson, L. U., Elconin, R., Humlum, O., Kääb, A., Kaufmann, V., Ladanyi, B., Matsuoka, N., Springman, S., and Vonder Mühll, D.: Permafrost Creep and Rock Glacier Dynamics, Permafrost and Periglacial Processes, 17, 189 – 214, 2006.

Haeberli, W., Noetzli, J., Arenson, L., Delaloye, R., Gärtner-Roer, I., Gruber, S., Isaksen, K., Kneisel, C., Krautblatter, M., Phillips, M., and et al.: Mountain permafrost: development and challenges of a young research field, Journal of Glaciology, 56, 1043–1058, 10.3189/002214311796406121, 2010.

Hanson, S. and Hoelzle, M.: The thermal regime of the active layer at the Murtèl rock glacier based on data from 2002, Permafrost and Periglacial Processes, 15, 273–282, 2004.

Harris, C., Mühll, D. V., Isaksen, K., Haeberli, W., Sollid, J. L., King, L., Holmlund, P., Dramis, F., Guglielmin, M., and Palacios, D.: Warming permafrost in European mountains, Global and Planetary Change, 39, 215–225, 2003.

Harris, S., French, H., Heginbottom, J., Johnston, G., Ladanyi, B., Sego, D., and van Everdingen, R.: Glossary of permafrost and related ground-ice terms, Associate Committee on Geotechnical Research, National Research Council of Canada, Ottawa, 156, 1988.

Hartl, L., Fischer, A., Stocker-Waldhuber, M., and Abermann, J.: Recent speed-up of an alpine rock glacier: an updated chronology of the kinematics of Outer Hochebenkar rock glacier based on geodetic measurements, Geografiska Annaler: Series A, Physical Geography, 98, 129–141, 10.1111/geoa.12127, 2016.

Hausmann, H., Krainer, K., Brückl, E., and Mostler, W.: Internal structure and ice content of Reichenkar rock glacier (Stubai Alps, Austria) assessed by geophysical investigations, Permafrost and Periglacial Processes, 18, 351–367, 10.1002/ppp.601, URL `https:`

//onlinelibrary.wiley.com/doi/abs/10.1002/ppp.601, 2007.

Hausmann, H., Krainer, K., Brückl, E., and Ullrich, C.: Internal structure, ice content and dynamics of Ölgrube and Kaiserberg rock glaciers (Ötztal Alps, Austria) determined from geophysical surveys., Austrian Journal of Earth Sciences, pp. 12–31, 2012.

Herz, T., King, L., and Gubler, H.: Microclimate within coarse debris of talus slopes in the alpine periglacial belt and its effect on permafrost, Proceedings of the Eighth International Conference on Permafrost, pp. 383–387, 2003.

Hoelzle, M., Wagner, S., Kääb, A., and Vonder Mühll, D.: Surface movement and internal deformation of ice-rock mixtures within rock glaciers in the Upper Engadin, Switzerland, Proceedings of the 7th International Conference on Permafrost, pp. 465–471, 1998.

Huggel, C., Clague, J. J., and Korup, O.: Is climate change responsible for changing landslide activity in high mountains?, Earth Surface Processes and Landforms, 37, 77–91, 10.1002/esp.2223, 2012.

Humlum, O.: Rock Glaciers in Northern Spitsbergen: A Discussion, The Journal of Geology, 90, 214–217, 10.1086/628668, 1982.

Humlum, O.: The climatic significance of rock glaciers, Permafrost and Periglacial Processes, 9, 375–395, 10.1002/(SICI)1099-1530(199810/12)9:4<375::AID-PPP301>3.0.CO;2-0, 1998.

Humlum, O.: The geomorphic significance of rock glaciers: estimates of rock glacier debris volumes and headwall recession rates in West Greenland, Geomorphology, 35, 41 – 67, https://doi.org/10.1016/S0169-555X(00)00022-2, 2000.

Hutter, K.: Theoretical glaciology, Springer, 1983.

Ikeda, A., Matsuoka, N., and Kääb, A.: Fast deformation of perennially frozen debris in a warm rock glacier in the Swiss Alps: An effect of liquid water, Journal of Geophysical Research: Earth Surface, 113, n/a–n/a, 10.1029/2007JF000859, f01021, 2008.

Iribarren Anacona, P. and Bodin, X.: Geomorphic consequences of two large glacier and rock glacier destabilizations in the Central and Northern Chilean Andes, in: EGU General Assembly Conference Abstracts, vol. 12, p. 7162, 2010.

Jansen, F. and Hergarten, S.: Rock glacier dynamics: Stick-slip motion coupled to hydrology, Geophysical Research Letters, 33, 10.1029/2006GL026134, 2006.

Johnson, P. G.: Rock glacier types and their drainage systems, Grizzly Creek, Yukon Territory, Canadian Journal of Earth Sciences, 15, 1496–1507, 10.1139/e78-155, 1978.

Johnson, P. G.: Rock Glacier Formation by High-Magnitude Low-Frequency Slope Processes in the Southwest Yukon, Annals of the Association of American Geographers, 74, 408–419, 1984.

Jones, D., Harrison, S., Anderson, K., and Whalley, B.: Rock glaciers and mountain hydrology: A review, Earth-Science Reviews, 193, 66–90, 10.1016/j.earscirev.2019.04.001, 2019.

Jones, D. B., Harrison, S., Anderson, K., and Betts, R. A.: Mountain rock glaciers contain globally significant water stores, Scientific reports, 8, 2834–2844, 10.1038/s41598-018-21244-w, 2018.

Kääb, A. and Reichmuth, T.: Advance mechanisms of rock glaciers, Permafrost and Periglacial Processes, 16, 187–193, 10.1002/ppp.507, URL https://onlinelibrary.wiley.com/doi/abs/10.1002/ppp.507, 2005.

Kääb, A. and Vollmer, M.: Surface Geometry, Thickness Changes and Flow Fields on Creeping Mountain Permafrost: Automatic Extraction by Digital Image Analysis, Permafrost and Periglacial Processes, 11, 315–326, 10.1002/1099-1530(200012)11:4<315::AID-PPP365>3.0.CO;2-J, 2000.

Kääb, A. and Weber, M.: Development of transverse ridges on rock glaciers: Field measurements and laboratory experiments, Permafrost and Periglacial Processes, 15, 379 – 391, 10.1002/ppp.506, 2004.

Kääb, A., Haeberli, W., and Gudmundsson, G. H.: Analysing the creep of mountain permafrost using high precision aerial photogrammetry: 25 years of monitoring Gruben rock glacier, Swiss Alps, Permafrost and Periglacial Processes, 8, 409–426, 10.1002/(SICI)1099-1530(199710/12)8:4<409::AID-PPP267>3.0.CO;2-C, 1997.

Kääb, A., Gudmundsson, G., and Hoelzle, M.: Surface deformation of creeping mountain permafrost. Photogrammetric investigations on rock glacier Murtél, Swiss Alps, Proceedings of the 7th International Conference on Permafrost, 57, 531–537, 1998.

Kääb, A., Frauenfelder, R., and Roer, I.: On the response of rockglacier creep to surface temperature increase, Global and Planetary Change, 56, 172 – 187, https://doi.org/10.1016/j.gloplacha.2006.07.005, 2007.

Karjalainen, O., Aalto, J., Luoto, M., Westermann, S., Romanovsky, V., Nelson, F., Etzelmüller, B., and Hjort, J.: Circumpolar permafrost maps and geohazard indices for near-future infrastructure risk assessments, Scientific Data, 6, 190 037, 10.1038/sdata.2019.37, 2019.

Keller, F., Frauenfelder, R., JM, G., Hoelzle, M., Kneisel, C., Lugon, R., Phillips, M., Reynard, E., and Wenker, L.: Permafrost map of Switzerland, 1998.

Kellerer-Pirklbauer, A. and Kaufmann, V.: About the relationship between rock glacier velocity and climate parameters in central Austria, Austrian Journal of Earth Sciences, 105, 94–112, 2012.

Kellerer-Pirklbauer, A. and Kaufmann, V.: Deglaciation and its impact on permafrost and rock glacier evolution: New insight from two adjacent cirques in Austria, Science of The Total Environment, 621, 10.1016/j.scitotenv.2017.10.087, 2017.

Kellerer-Pirklbauer, A. and Rieckh, M.: Monitoring nourishment processes in the rooting zone of an active rock glacier in an alpine environment, Zeitschrift für Geomorphologie, 60, 99–121, 10.1127/zfg_suppl/2016/00245, 2016.

Kellerer-Pirklbauer, A., Lieb, G. K., and Kleinferchner, H.: A NEW ROCK GLACIER INVENTORY OF THE EASTERN EUROPEAN ALPS., Austrian Journal of Earth Sciences, 105, 2012.

Kellerer-Pirklbauer, A., Lieb, G., and Kaufmann, V.: The Dösen Rock Glacier in Central Austria: A key site for multidisciplinary long-term rock glacier monitoring in the Eastern Alps,

Austrian Journal of Earth Sciences, 110, 10.17738/ajes.2017.0013, 2018.

Kenner, R., Phillips, M., Beutel, J., Hiller, M., Limpach, P., Pointner, E., and Volken, M.: Factors Controlling Velocity Variations at Short-Term, Seasonal and Multiyear Time Scales, Ritigraben Rock Glacier, Western Swiss Alps, Permafrost and Periglacial Processes, 28, 675–684, 10.1002/ppp.1953, pPP-16-0044.R2, 2017.

Kenner, R., Pruessner, L., Beutel, J., Limpach, P., and Phillips, M.: How rock glacier hydrology, deformation velocities and ground temperatures interact: Examples from the Swiss Alps, Permafrost and Periglacial Processes, 31, 3–14, 10.1002/ppp.2023, 2020.

Kofler, C., Steger, S., Mair, V., Zebisch, M., Comiti, F., and Schneiderbauer, S.: An inventory-driven rock glacier status model (intact vs. relict) for South Tyrol, Eastern Italian Alps, Geomorphology, 350, 106 887, https://doi.org/10.1016/j.geomorph.2019.106887, 2020.

Krainer, K. and Mostler, W.: Hydrology of Active Rock Glaciers: Examples from the Austrian Alps, Arctic, Antarctic, and Alpine Research, 34, 142–149, 10.1080/15230430.2002.12003478, 2002.

Krainer, K. and Mostler, W.: Flow velocities of active rock glaciers in the Austrian Alps, Geografiska Annaler: Series A, Physical Geography, 88, 267–280, 10.1111/j.0435-3676.2006.00300.x, 2006.

Krainer, K. and Ribis, M.: A rock glacier inventory of the Tyrolean Alps (Austria)., Austrian Journal of Earth Sciences, 105, 2012.

Krainer, K., Bressan, D., Dietre, B., Haas, J., Hajdas, I., Lang, K., Mair, V., Nickus, U., Reidl, D., Thies, H., and Tonidandel, D.: A 10,300-year-old permafrost core from the active rock glacier Lazaun, southern Ötztal Alps (South Tyrol, northern Italy), Quaternary Research, 83, 324–335, 10.1016/j.yqres.2014.12.005, 2015.

Kummert, M. and Delaloye, R.: Mapping and quantifying sediment transfer between the front of rapidly moving rock glaciers and torrential gullies, Geomorphology, 309, 60–76, 10.1016/j.geomorph.2018.02.021, 2018.

Kummert, M., Delaloye, R., and Braillard, L.: Erosion and sediment transfer processes at the front of rapidly moving rock glaciers: Systematic observations with automatic cameras in the western Swiss Alps, Permafrost and Periglacial Processes, 10.1002/ppp.1960, 2017.

Kurz, D., Alfaro, M., and Graham, J.: Thermal conductivities of frozen and unfrozen soils at three project sites in northern Manitoba, Cold Regions Science and Technology, 140, 30 – 38, https://doi.org/10.1016/j.coldregions.2017.04.007, 2017.

Lachenbruch, A., Cladouhos, T., and Saltus, R.: Permafrost temperatures and the changing climate, in: Proceedings of the Fifth International Conference on Permafrost, vol. 3, pp. 9 – 17, 1988.

Ladanyi, B.: An Engineering Theory of Creep of Frozen Soils, Canadian Geotechnical Journal, 9, 63–80, 10.1139/t72-005, 1972.

Ladanyi, B.: Rheology of ice/rock systems and interfaces, in: Proceedings of the Eigth International Conference on Permafrost, pp. 621–625, Lisse, The Netherlands, 2003.

Lambiel, C. and Delaloye, R.: Contribution of real-time kinematic GPS in the study of creeping mountain permafrost: examples from the Western Swiss Alps, Permafrost and Periglacial Processes, 15, 229–241, 10.1002/ppp.496, 2004.

Lambiel, C., Delaloye, R., Strozzi, T., Lugon, R., and Raetzo, H.: ERS InSAR for Assessing Rock Glacier Activity, in: Proceedings of the 9th International Conference on Permafrost, 2008.

Liu, L., Millar, C. I., Westfall, R. D., and Zebker, H. A.: Surface motion of active rock glaciers in the Sierra Nevada, California, USA: inventory and a case study using InSAR, The Cryosphere, 7, 1109–1119, 10.5194/tc-7-1109-2013, URL https://www.the-cryosphere.net/7/1109/2013/, 2013.

Loewenherz, S. D., J. Lawrence, C., and L. Weaver, R.: On the Development of Transverse Ridges on Rock Glaciers, Journal of Glaciology - J GLACIOLOGY, 35, 383–391, 10.1017/S002214300000931X, 1989.

Luethi, R., Phillips, m., and Lehning, M.: Estimating Non-Conductive Heat Flow Leading to Intra-Permafrost Talik Formation at the Ritigraben Rock Glacier (Western Swiss Alps), Permafrost and Periglacial Processes, 28, 183 – 194, 10.1002/ppp.1911, 2017.

Lugon, R. and Stoffel, M.: Rock-glacier dynamics and magnitude–frequency relations of debris flows in a high-elevation watershed: Ritigraben, Swiss Alps, Global and Planetary Change, 73, 202 – 210, https://doi.org/10.1016/j.gloplacha.2010.06.004, 2010.

Marcer, M., Bodin, X., Brenning, A., Schoeneich, P., Charvet, R., and Gottardi, F.: Permafrost Favorability Index: Spatial Modeling in the French Alps Using a Rock Glacier Inventory, Frontiers in Earth Science, 5, 105, 10.3389/feart.2017.00105, 2017.

Marcer, M., Serrano, C., Brenning, A., Bodin, X., Goetz, J., and Schoeneich, P.: Evaluating the destabilization susceptibility of active rock glaciers in the French Alps, The Cryosphere, 13, 141–155, 10.5194/tc-13-141-2019, 2019.

Marcer, M., Ringsø Nielsen, S., Ribeyre, C., Kummert, M., Duvillard, P.-A., Schoeneich, P., Bodin, X., and Genuite, K.: Investigating the slope failures at the Lou rock glacier front, French Alps, Permafrost and Periglacial Processes, 31, 15–30, 10.1002/ppp.2035, 2020.

Marcer, M., Cicoira, A., Bodin, X., and Schoeneich, P.: Rock glacier destabilization due to climate change, Nature Communications, submitted.

MATLAB: version 9.1.0 (R2016b), The MathWorks Inc., Natick, Massachusetts, 2016.

Maurer, H. and Hauck, C.: Geophysical imaging of alpine rock glaciers, Journal of Glaciology, 53, 110–120, 10.3189/172756507781833893, 2007.

Mellor, M. and Testa, R.: Effect of Temperature on the Creep of Ice, Journal of Glaciology, 8, 131–145, 10.3189/S0022143000020803, 1969.

Merz, K., Green, A. G., Buchli, T., Springman, S. M., and Maurer, H.: A new 3-D thin-skinned rock glacier model based on helicopter GPR results from the Swiss Alps, Geophysical Research Letters, 42, 4464–4472, 10.1002/2015GL063951, URL https://agupubs.onlinelibrary.wiley.com/doi/abs/10.1002/2015GL063951, 2015a.

Merz, K., Maurer, H., Buchli, T., Horstmeyer, H., Green, A. G., and Springman, S. M.: Evaluation of Ground-Based and Helicopter Ground-Penetrating Radar Data Acquired Across an Alpine Rock Glacier, Permafrost and Periglacial Processes, 26, 13–27, 10.1002/ppp.1836, 2015b.

Merz, K., Maurer, H., Rabenstein, L., Buchli, T., Springman, S. M., and Zweifel, M.: Multidisciplinary geophysical investigations over an alpine rock glacier, GEOPHYSICS, 81, WA147–WA157, 10.1190/geo2015-0157.1, 2016.

Millar, C. I. and Westfall, R. D.: Geographic, hydrological, and climatic significance of rock glaciers in the Great Basin, USA, Arctic, Antarctic, and Alpine Research, 51, 232–249, 10.1080/15230430.2019.1618666, 2019.

Monnier, S. and Kinnard, C.: Interrogating the time and processes of development of the Las Liebres rock glacier, central Chilean Andes, using a numerical flow model, Earth Surface Processes and Landforms, 41, 1884–1893, 10.1002/esp.3956, 2016.

Moore, P. L.: Deformation of debris-ice mixtures, Reviews of Geophysics, 52, 435–467, 10.1002/2014RG000453, 2014.

Mourey, J., Ravanel, L., Lambiel, C., Strecker, J., and Piccardi, M.: Access routes to high mountain huts facing climate-induced environmental changes and adaptive strategies in the Western Alps since the 1990s, Norsk Geografisk Tidsskrift - Norwegian Journal of Geography, 73, 215–228, 10.1080/00291951.2019.1689163, 2019.

Müller, J., Vieli, A., and Gärtner-Roer, I.: Rock glaciers on the run – understanding rock glacier landform evolution and recent changes from numerical flow modeling, The Cryosphere, 10, 2865–2886, 10.5194/tc-10-2865-2016, 2016.

Muller, S. W.: Permafrost or permanently frozen ground and related engineering problems, 62, Army map service, US Army, 1945.

Murton, J. B. and French, H. M.: Cryostructures in permafrost, Tuktoyaktuk coastlands, western arctic Canada, Canadian Journal of Earth Sciences, 31, 737–747, 10.1139/e94-067, 1994.

Mühll, D. S. V. and Holub, P.: Borehole logging in alpine permafrost, upper Engadin, Swiss Alps, Permafrost and Periglacial Processes, 3, 125–132, 10.1002/ppp.3430030209, 1992.

Müller, J., Gärtner-Roer, I., Kenner, R., Thee, P., and Morche, D.: Sediment storage and transfer on a periglacial mountain slope (Corvatsch, Switzerland), Geomorphology, 218, 35 – 44, https://doi.org/10.1016/j.geomorph.2013.12.002, 2014a.

Müller, J., Gärtner-Roer, I., Thee, P., and Ginzler, C.: Accuracy assessment of airborne photogrammetrically derived high-resolution digital elevation models in a high mountain environment, ISPRS Journal of Photogrammetry and Remote Sensing, 98, 58 – 69, https://doi.org/10.1016/j.isprsjprs.2014.09.015, 2014b.

Nikiforoff, C.: The Perpetually Frozen Subsoil of Siberia, Soil Science, 26, 61–82, 10.1097/00010694-192807000-00005, 1928.

Nye, J. F.: The Mechanics of Glacier Flow, Journal of Glaciology, 2, 82–93, 10.3189/S0022143000033967, 1952.

Olyphant, G. A.: Computer simulation of rock-glacier development under viscous and pseudoplastic flow, GSA Bulletin, 94, 499–505, 10.1130/0016-7606(1983)94<499:CSORDU>2.0.CO;2, 1983.

Pellicciotti, F., Brock, B., Strasser, U., Burlando, P., Funk, M., and Corripio, J.: An enhanced temperature-index glacier melt model including the shortwave radiation balance: development and testing for Haut Glacier d'Arolla, Switzerland, Journal of Glaciology, 51, 573–587, 10.3189/172756505781829124, 2005.

Pepin, N., Bradley, R. S., Diaz, H., Baraër, M., Caceres, E., Forsythe, N., Fowler, H., Greenwood, G., Hashmi, M., Liu, X., et al.: Elevation-dependent warming in mountain regions of the world, Nature climate change, 5, 424–430, 2015.

PERMOS: Permafrost in Switzerland 2010/2011 to 2013/2014., Tech. rep., the Cryospheric commission of the Swiss Academy of Sciences, 85pp, 2016.

PERMOS: Permafrost in Switzerland 2014/2015 to 2017/2018. Noetzli, J., Pellet, C., and Staub, B. (eds.), Glaciological Report (Permafrost) No. 16-19, Tech. rep., the Cryospheric commission of the Swiss Academy of Sciences, 104 pp., 2019.

Perruchoud, E. and Delaloye, R.: Short-Term Changes in Surface Velocities on the Becs-de-Bosson Rock Glacier (Western Swiss Alps), Grazer Schriften der Geographie und Raumforschung, 43, 2007.

Potter, Noel, J.: Ice-Cored Rock Glacier, Galena Creek, Northern Absaroka Mountains, Wyoming, GSA Bulletin, 83, 3025–3058, 10.1130/0016-7606(1972)83[3025:IRGGCN]2.0.CO;2, 1972.

Pruessner, L., Phillips, M., Farinotti, D., Hoelzle, M., and Lehning, M.: Near-surface ventilation as a key for modeling the thermal regime of coarse blocky rock glaciers, Permafrost and Periglacial Processes, 29, 152–163, 10.1002/ppp.1978, 2018.

Ribolini, A. and Fabre, D.: Permafrost existence in rock glaciers of the Argentera Massif, Maritime Alps, Italy, Permafrost and Periglacial Processes, 17, 49–63, 10.1002/ppp.548, 2006.

Rohner, C., Small, D., Beutel, J., Henke, D., Lüthi, M. P., and Vieli, A.: Multisensor validation of tidewater glacier flow fields derived from synthetic aperture radar (SAR) intensity tracking, The Cryosphere, 13, 2953–2975, 10.5194/tc-13-2953-2019, URL `https://www.the-cryosphere.net/13/2953/2019/`, 2019.

Romanovsky, V., Burgess, M., Smith, S., Yoshikawa, K., and Brown, J.: Permafrost temperature records: Indicators of climate change, Eos, Transactions American Geophysical Union, 83, 589–594, 10.1029/2002EO000402, 2002.

Scapozza, C., Lambiel, C., Bozzini, C., Mari, S., and Conedera, M.: Assessing the rock glacier kinematics on three different timescales: a case study from the southern Swiss Alps, Earth Surface Processes and Landforms, 39, 2056–2069, 10.1002/esp.3599, 2014.

Schaffer, N., MacDonell, S., Réveillet, M., Yáñez, E., and Valois, R.: Rock glaciers as a water resource in a changing climate in the semiarid Chilean Andes, Regional Environmental Change, 10.1007/s10113-018-01459-3, 2019.

Scherler, M., Schneider, S., Hoelzle, M., and Hauck, C.: A two-sided approach to estimate heat transfer processes within the active layer of the Murtél-Corvatsch rock glacier, Earth Surface Dynamics, 2, 141–154, 10.5194/esurf-2-141-2014, 2014.

Schmidt, B. E., Hughson, K. H. G., Chilton, H. T., Scully, J. E. C., Platz, T., Nathues, A., Sizemore, H., Bland, M. T., Byrne, S., Marchi, S., O'Brien, D. P., Schorghofer, N., Hiesinger, H., Jaumann, R., Pasckert, J. H., Lawrence, J. D., Buzckowski, D., Castillo-Rogez, J. C., Sykes, M. V., Schenk, P. M., DeSanctis, M.-C., Mitri, G., Formisano, M., Li, J.-Y., Reddy, V., LeCorre, L., Russell, C. T., and Raymond, C. A.: Geomorphological evidence for ground ice on dwarf planet Ceres, Nature Geoscience, 10, 338–343, https://doi.org/10.1038/ngeo2936, 2017.

Schoeneich, P., Bodin, X., Echelard, T., Kaufmann, V., Kellerer-Pirklbauer, A., Krysiecki, J. M., and Lieb, G. K.: Velocity Changes of Rock Glaciers and Induced Hazards, in: Engineering Geology for Society and Territory - Volume 1, edited by Lollino, G., Manconi, A., Clague, J., Shan, W., and Chiarle, M., pp. 223–227, Springer International Publishing, Cham, 2015.

Schuur, E. A., McGuire, A. D., Schädel, C., Grosse, G., Harden, J., Hayes, D. J., Hugelius, G., Koven, C. D., Kuhry, P., Lawrence, D. M., et al.: Climate change and the permafrost carbon feedback, Nature, 520, 171–179, 2015.

Scotti, R., Crosta, G. B., and Villa, A.: Destabilisation of Creeping Permafrost: The Plator Rock Glacier Case Study (Central Italian Alps), Permafrost and Periglacial Processes, 28, 224–236, 10.1002/ppp.1917, 2017.

Seppi, R., Carturan, L., Carton, A., Zanoner, T., Zumiani, M., Cazorzi, F., Bertone, A., Baroni, C., and Salvatore, M. C.: Decoupled kinematics of two neighbouring permafrost creeping landforms in the Eastern Italian Alps, Earth Surface Processes and Landforms, 44, 2703–2719, 10.1002/esp.4698, 2019.

Shroder, J. F.: Dendrogeomorphological Analysis of Mass Movement on Table Cliffs Plateau, Utah, Quaternary Research, 9, 168–185, 10.1016/0033-5894(78)90065-0, 1978.

Sollid, J. L. and Sørbel, L.: Rock glaciers in Svalbard and Norway, Permafrost and Periglacial Processes, 3, 215–220, 10.1002/ppp.3430030307, 1992.

Sorg, A., Kääb, A., Roesch, A., Bigler, C., and Stoffel, M.: Contrasting responses of Central Asian rock glaciers to global warming, Scientific Reports, 5, 8228–8234, 10.1038/srep08228, 2015.

Spencer, A.: A Peculiar Form of Talus, Science, 11, 188, 1900.

Springman, S., Yamamoto, Y., Buchli, T., Hertrich, M., Maurer, H., Merz, K., Gärtner-Roer, I., and Seward, L.: Rock Glacier Degradation and Instabilities in the European Alps: A Characterisation and Monitoring Experiment in the Turtmanntal, CH, vol. 4, pp. 5–13, Springer, 10.1007/978-3-642-31337-0_1, 2013.

Sringman, S. M., ARENSON, L. U., YAMAMOTO, Y., MAURER, H., KOS, A., BUCHLI, T., and DERUNGS, G.: Multidisciplinary investigations on three rock glaciers in the Swiss Alps: legacies and perspectives, Geografiska Annaler: Series A, Physical Geography, 94, 215–243, 10.1111/j.1468-0459.2012.00464.x, 2012.

Staub, B., Lambiel, C., and Delaloye, R.: Rock glacier creep as a thermally-driven phenomenon: a decade of interannual observations from the Swiss Alps, in: Proceedings of the 11th International Conference on Permafrost, pp. 93–94, 2016.

Staub, B., Hasler, A., Noetzli, J., and Delaloye, R.: Gap-Filling Algorithm for Ground Surface Temperature Data Measured in Permafrost and Periglacial Environments, Permafrost and Periglacial Processes, 28, 275–285, 10.1002/ppp.1913, 2017.

Strozzi, T., Caduff, R., Jones, N., Barboux, C., Delaloye, R., Bodin, X., Kääb, A., Mätzler, E., and Schrott, L.: Monitoring Rock Glacier Kinematics with Satellite Synthetic Aperture Radar, Remote Sensing, 12, 10.3390/rs12030559, URL https://www.mdpi.com/2072-4292/12/3/559, 2020.

Taber, S.: The Mechanics of Frost Heaving, Journal of Geology - J GEOL, 38, 303–317, 10.1086/623720, 1930.

Vieli, A., Cicoira, A., and Noetzli, J.: A new borehole continues the longest mountain permafrost temperature record on rock glacier Murtél-Corvatsch, Swiss Alps, Nature Climate Change, 1, 1–10, 1, in preparation.

Vivero, S. and Lambiel, C.: Monitoring the crisis of a rock glacier with repeated UAV surveys, Geographica Helvetica, 74, 59–69, 10.5194/gh-74-59-2019, 2019.

Von Mises, R.: Mechanics of solid bodies in the plastically-deformable state, Nachrichten von der Gesellschaft der Wissenschaften zu Göttingen, Mathematisch-Physikalische Klasse, 1913.

Vonder Mühll, D.: Geophysikalische Untersuchungen im Permafrost des Oberengadins, Mitteilungen der Versuchsanstalt für Wasserbau, Hydrologie und Glaziologie an der Eidgenössischen Technischen Hochschule Zürich, Versuchsanstalt für Wasserbau Hydrologie und Glaziologie der Eidgenössischen Technischen Hochschule Zürich, 1993.

Vonder Mühll, D. and Schmid, W.: Geophysical and photogrammetrical investigations of rock glacier Muragl I, Engadin, Swiss Alps, in: Ed. 6th International Conference on Permafrost Proceedings, pp. 654–659, South China University Technology Press, ed. 6th International Conference on Permafrost, 1993.

Vonder Mühll, D., Arenson, L. U., and Springman, S.: Temperature conditions in two Alpine rock glaciers, Eight International Conference on Permafrost, pp. 1195 – 1200, 2003.

W. Gold, L. and H. Lachenbruch, A.: Thermal conditions in permafrost: A Review of North American literature, North American Contribution to the Second International Conference on Permafrost, pp. 3–25, 1973.

Wahrhaftig, C. and Cox, A.: Rock Glaciers in the Alaska Range, GSA Bulletin, 70, 383, 1959.

Weertman, J.: Creep deformation of ice, Annual Review of Earth and Planetary Sciences, 11, 215–240, 1983.

Whalley, B.: Rock glaciers - permafrost features or glacial relics?, in: Proceedings of the fourth International Conference on Permafrost, pp. 1396–1401, 1983.

Whalley, W. B.: Origin of rock glaciers, Journal of Glaciology, 13, 323–324, 10.3189/S0022143000023145, 1974.

Whalley, W. B. and Azizi, F.: Rock glaciers and protalus landforms: Analogous forms and ice sources on Earth and Mars, Journal of Geophysical Research: Planets, 108, 10.1029/2002JE001864, 2003.

Whalley, W. B. and Martin, H. E.: Rock glaciers : II models and mechanisms, Progress in Physical Geography: Earth and Environment, 16, 127–186, 10.1177/030913339201600201, 1992.

White, S. E.: Rock glaciers and block fields, review and new data, Quaternary Research, 6, 77 – 97, https://doi.org/10.1016/0033-5894(76)90041-7, 1976.

White, S. E.: Alpine Mass Movement Forms (Noncatastrophic): Classification, Description, and Significance, Arctic and Alpine Research, 13, 127–137, 10.1080/00040851.1981.12004236, 1981.

Wicky, J. and Hauck, C.: Numerical modelling of convective heat transport by air flow in permafrost talus slopes, The Cryosphere, 11, 1311–1325, 10.5194/tc-11-1311-2017, 2017.

Williams, P. J. and Smith, M. W.: The Frozen Earth: Fundamentals of Geocryology, Studies in Polar Research, Cambridge University Press, 10.1017/CBO9780511564437, 1989.

Winkler, S. and Lambiel, C.: Age constraints of rock glaciers in the Southern Alps/New Zealand – Exploring their palaeoclimatic potential, The Holocene, 28, 778–790, 10.1177/0959683618756802, 2018.

Wirz, V., Limpach, P., Beutel, J., Buchli, B., and Gruber, S.: Temporal characteristics of different mountain cryosphere-related debris slope movements, second World Landslide Forum; Conference Location: Rome, Italy; Conference Date: October 3-9, 2011; ., 2011.

Wirz, V., Beutel, J., Gruber, S., Gubler, S., and Purves, R. S.: Estimating velocity from noisy GPS data for investigating the temporal variability of slope movements, Natural Hazards and Earth System Sciences, 14, 2503–2520, 10.5194/nhess-14-2503-2014, 2014.

Wirz, V., Geertsema, M., Gruber, S., and Purves, R. S.: Temporal variability of diverse mountain permafrost slope movements derived from multi-year daily GPS data, Mattertal, Switzerland, Landslides, 13, 67–83, 10.1007/s10346-014-0544-3, 2016a.

Wirz, V., Gruber, S., Purves, R. S., Beutel, J., Gärtner-Roer, I., Gubler, S., and Vieli, A.: Short-term velocity variations at three rock glaciers and their relationship with meteorological conditions, Earth Surface Dynamics, 4, 103–123, 10.5194/esurf-4-103-2016, 2016b.

Yamamoto, Y. and Springman, S.: Three- and four-point bending tests on artificial frozen soil samples at temperatures close to 0°C, Cold Regions Science and Technology, 134, 10.1016/j.coldregions.2016.11.003, 2016.

Yamamoto, Y. and Springman, S. M.: Triaxial stress path tests on artificially prepared analogue alpine permafrost soil, Canadian Geotechnical Journal, 56, 1448–1460, 10.1139/cgj-2017-0737, 2019.

Yershov, E. D.: General Geocryology, Studies in Polar Research, Cambridge University Press, 10.1017/CBO9780511564505, 1998.

Zenklusen Mutter, E. and Phillips, M.: Thermal Evidence of Recent Talik Formation in Ritigraben Rock Glacier: Swiss Alps, in: Proceedings of the 10th International Conference on Permafrost, pp. 479–483, 2012.

Part II

Research publications

Publication 1

Resolving the influence of temperature forcing through heat conduction on rock glacier dynamics: a numerical modelling approach

Authors Cicoira, A., Beutel, J., Faillettaz, J., Gärtner-Roer, I., Vieli, A.

Journal The Cryosphere

Year 2019

DOI doi.org/10.5194/tc-13-927-2019

Short summary The contribution of temperature forcing to seasonal and inter-annual variations in rock glacier creep rates is investigated. Heat transfer is assumed to be completely governed by heat conduction and forced by external temperature at the permafrost surface. Rock glacier deformation is calculated using an empirical creep model derived from laboratory experiments. The model is forced and the results are compared with continuous time series of surface and ground temperatures, and displacement rates for four rock glaciers in the Swiss Alps.

Main findings The main findings of this publication are:

- Heat conduction controls the thermal regime of the ice-rich core of a rock glacier.
- The observed seasonal and inter-annual variations in rock glacier creep cannot be explained by the direct influence of temperature on rheology.
- Both the amplitude and the phase cannot be correctly reproduced.
- Accounting for the observed temperatures and including a description of the shear horizon does not improve the results.
- Temperature changes over the whole thickness of the rock glacier can cause substantial variations in creep rates, but require changes in climate over decades or centuries.
- Based on modelling results and on field observations, we conclude that non-conductive processes must dominate the short-term velocity signal.

Contributions of the PhD candidate Design of the conceptual and the numerical model with substantial contribution from Andreas Vieli. Analysis and interpretation of the data, collected in the field with Jan Beutel and Isabelle Gärtner-Roer. Preparation of the manuscript and the figures. All co-authors contributed to the interpretation of the data and the preparation of the manuscript.

Data availability Data on rock glacier kinematics and temperature are available from the PERMOS office upon request. The reference web link is http://www.permos.ch/data.html.

Journal *The Cryosphere (TC)* is a not-for-profit international scientific journal dedicated to the publication and discussion of research articles, short communications, and review papers on all aspects of frozen water and ground on Earth and on other planetary bodies. The main subject areas are ice sheets and glaciers, planetary ice bodies, permafrost, river and lake ice, seasonal snow cover, sea ice, remote sensing, numerical modelling, in situ and laboratory studies of the above and including studies of the interaction of the cryosphere with the rest of the climate system. To ensure publication precedence for authors, and to provide a lasting record of scientific discussion, TCD and TC are both ISSN-registered, permanently archived, and fully citable.
Impact Factor: **4.8**

The Cryosphere, 13, 927–942, 2019
https://doi.org/10.5194/tc-13-927-2019

The Cryosphere Open Access EGU

Resolving the influence of temperature forcing through heat conduction on rock glacier dynamics: a numerical modelling approach

Alessandro Cicoira[1], **Jan Beutel**[2], **Jérome Faillettaz**[1], **Isabelle Gärtner-Roer**[1], **and Andreas Vieli**[1]

[1]Department of Geography, University of Zurich, Zurich, Switzerland
[2]Computer Engineering and Networks Laboratory, ETH, Zurich, Switzerland

Correspondence: Alessandro Cicoira (alessandro.cicoira@geo.uzh.ch)

Received: 25 August 2018 – Discussion started: 26 September 2018
Revised: 18 January 2019 – Accepted: 13 February 2019 – Published: 18 March 2019

Abstract. In recent years, observations have highlighted seasonal and interannual variability in rock glacier flow. Temperature forcing, through heat conduction, has been proposed as one of the key processes to explain these variations in kinematics. However, this mechanism has not yet been quantitatively assessed against real-world data.

We present a 1-D numerical modelling approach that couples heat conduction to an empirically derived creep model for ice-rich frozen soils. We use this model to investigate the effect of thermal heat conduction on seasonal and interannual variability in rock glacier flow velocity. We compare the model results with borehole temperature data and surface velocity measurements from the PERMOS and PermaSense monitoring network available for the Swiss Alps. We further conduct a model sensitivity analysis in order to resolve the importance of the different model parameters. Using the prescribed empirically derived rheology and observed near-surface temperatures, we are able to model the correct order of magnitude of creep. However, both interannual and seasonal variability are underestimated by an order of magnitude, implying that heat conduction alone cannot explain the observed variations. Therefore, we conclude that non-conductive processes, likely linked to water availability, must dominate the short-term velocity signal.

1 Introduction

For several rock glaciers, and especially in Switzerland, surface displacements have been calculated over long time periods (Chaix, 1923; Wahrhaftig and Cox, 1959; Barsch and Hell, 1975; Francou and Reynaud, 1992; Berthling et al., 1998) by using position time series of landmark features (boulders). Since these early investigations, velocity variability has been detected on a multi-year scale. In the past decades, starting with some measurements on Gruben rock glacier (Haeberli, 1985), seasonal velocity variability has been observed on such creeping periglacial landforms. Even though differences exist between individual rock glaciers, velocity peak maxima are in general observed between summer and early winter and minima between spring and early summer (Delaloye et al., 2010). In the past years, advances in monitoring techniques and the introduction of continuously measuring DGPS (differential global positioning system) loggers (Buchli et al., 2012) have confirmed the previous observations on several rock glaciers and have further highlighted velocity peaks on a daily to a weekly scale, which are predominantly present during the melt season (Wirz et al., 2016a; Kenner et al., 2017; Buchli et al., 2018).

In order to explain the above introduced observations, classical concepts from related disciplines – geotechnical engineering and glaciology – have been applied to rock glacier research. Interannual velocities have been compared against climatic variables and external temperature forcing has been proposed as one of the key factors controlling the observed long-term flow variations (Roer et al., 2005; Krainer and He, 2006; PERMOS, 2016a).

Published by Copernicus Publications on behalf of the European Geosciences Union.

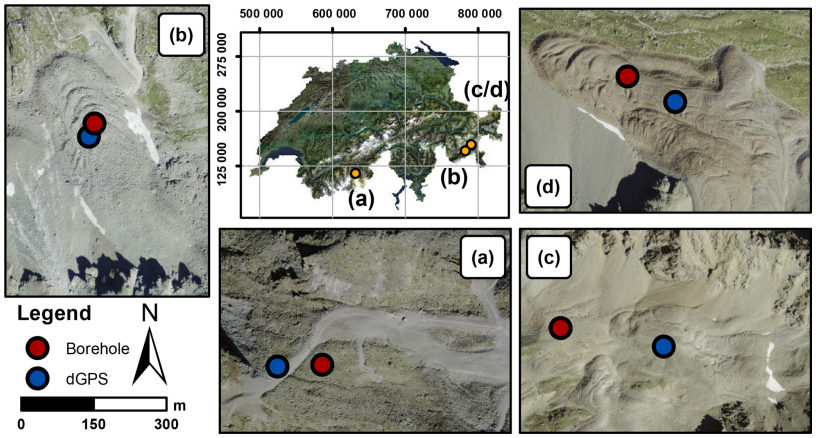

Figure 1. Overview of the four case study sites. Overview site map (middle) and aerial view of the four studied rock glaciers **(a–d)** with locations of boreholes (red dots) and DGPS (blue dots) according to PERMOS (2016a): **(a)** Ritigraben, **(b)** Murtèl, **(c)** Schafberg and **(d)** Muragl.

Similarly, temperature forcing has also been suggested as one of the most important factors controlling rock glacier flow velocity variability on a seasonal scale (Arenson et al., 2002; Kääb et al., 2007; Delaloye et al., 2010; Wirz et al., 2016b). Wirz et al. (2016b) have suggested liquid precipitation, snowmelt, air and ground temperature as the main factors controlling rock glacier flow on interannual, seasonal and shorter timescales. Previous studies (Johnson, 1978; Barsch, 1992; Krainer and He, 2006, amongst others) highlighted the influence of water on rock glacier and their dynamics. Possible positive feedback processes between rising temperature and increased deformation have also been suggested (Ikeda et al., 2008; Buchli et al., 2018).

Even though great improvements have been achieved in this field, our understanding of the processes governing rock glacier dynamics and their relation with external forcings and controlling factors remains at a qualitative level, and many questions remain unanswered. However, it is clear that, in order to understand rock glacier dynamics, the complex thermo-hydro-mechanical behaviour of the ice-rich frozen soil and its coupling with the climate have to be considered. In particular, when aiming to understand the influence of temperature forcing on permafrost creep and its relative importance on rock glacier dynamics, we have to consider two aspects. On one hand, the thermal regime of a rock glacier is mainly controlled by heat conduction, driven by external temperature forcing (Vonder Mühll et al., 2003; Haeberli et al., 2006). Nevertheless, in some cases other processes have been observed, like air and water advection through the permafrost matrix (Hanson and Hoelzle, 2004; Zenklusen Mutter and Phillips, 2012; Scherler et al., 2014; Luethi et al., 2017; Pruessner et al., 2018). On the other hand, from glaciological studies, it is well known that the rate of deformation of ice is described by a power law (Nye, 1952; Glen, 1955) and depends on ice viscosity, which in turn depends on ice temperature (Mellor and Testa, 1969; Duval et al., 1983). Therefore, heat conduction forced by external surface temperature variations is expected to influence rock glacier creep. However, investigations that quantitatively couple temperature evolution and rock glacier rheology are rare and remain very limited (Kääb et al., 2007; Müller et al., 2016). The numerical modelling study by Kääb et al. (2007) investigated this process, but has two main limitations: it used a rock glacier rheology that has been derived for pure ice, and more importantly, it applied this rheology to a purely synthetic set-up and could not directly compare the results to real-world observations.

In this study, we quantify the relative importance of the conductive thermal influence on flow and extend previous research (Kääb et al., 2007) by applying the most up-to-date rheological relation available for rock glacier material (Arenson and Springman, 2005a) to four real-world rock glaciers and constrain the modelling with observations from borehole measurements, kinematics surveys and DGPS observations available from the Swiss Permafrost Monitoring Network PERMOS (here on named PERMOS) and PermaSense monitoring networks (https://doi.org/10.13093/permos-2016-01).

2 Study sites

For constraining the numerical modelling investigations, we use observational data from four rock glaciers in the Swiss Alps, namely from the rock glaciers Ritigraben located in the Valais, and Murtèl-Corvatsch (hereafter called Murtèl), Schafberg, and Muragl all located in the Engadine (Fig. 1). These rock glaciers have been selected based on the availability of several years of data on highly time-resolved surface

Table 1. Summary of field sites. The borehole locations are given in the CH1903+ coordinate system. The values of the geometrical and physical properties of the rock glaciers are given (thickness, slope, volumetric ice content and thermal diffusivity) as discussed in Sect. 2. For the ice content an acceptable range of values is proposed according to the literature (Hoelzle et al., 1998; Arenson et al., 2002). The mean observed rock glacier bottom temperature, measured at the lower end of the shear horizon (from summer 2006 to summer 2015) and surface velocity (from summer 2009) are reported, as well as the interannual and seasonal velocity variations relative to the mean velocity (from summer 2012 to summer 2016) (PERMOS, 2016a).

Rock glacier	Borehole location	Thickness (m)	Surface slope	w_i	κ ($m^2 d^{-1}$)	Bottom temperature (°C)	Mean velocity ($m a^{-1}$)	Interannual variation	Seasonal variation
Ritigraben	1113775 N 2631755 E	18	27°	30 %–70 %	0.18	−0.5	1.5	25 %	45 %
Murtèl	1144720 N 2783160 E	27	12°	70 %–100 %	0.15	− 1.2	0.12	41 %	–
Schafberg	1152745 N 2790855 E	25	18°	30 %–100 %	0.15	−0.1	0.3	33 %	39 %
Muragl	1153688 N 2791017 E	20	20°	30 %–70 %	0.18	−0.1	1.4	25 %	14 %

displacements and subsurface temperatures from boreholes. Further, several borehole deformation profiles are available for different time steps for all rock glaciers. This type of data is rather unique and made available through the PERMOS monitoring network.

These four rock glaciers cover a wide range of geometric settings and dynamic states: thickness, slope and flow velocity from decimetres to several metres per year; for an overview see Table 1. The rock glaciers are located at elevations between 2500 to 2900 m a.s.l. and their aspect is north to north-west. Their lithology mainly consists of crystalline formations, with prevailing granodiorite and schist for Murtèl and gneiss for Muragl, Schafberg and Ritigraben. The internal structure and deformation profiles are known for all four rock glaciers from boreholes (Haeberli et al., 1998; Arenson et al., 2002; Lugon and Stoffel, 2010). Here, we define the rock glacier thickness on the basis of their deformation profiles, which are dominated by shear horizon a few metres thick at 18 to 30 m depth. Laboratory shear experiments have been undertaken on cores from boreholes for the two rock glaciers Murtèl and Muragl and were used by Arenson and Springman (2005a) to derive an empirical creep rheology (Arenson et al., 2004; Arenson and Springman, 2005b), which is also used in the flow-modelling investigations of this study (for details see Sect. 3.3).

2.1 Ritigraben

The Ritigraben rock glacier is located above the village of Grächen (VS) and originates from the northern slope of the Gabelhorn (3135 m a.s.l.). It develops a simple linear flow lobe of about 500 m length on a steep slope (27° in the proximity of the borehole, Fig. 1 and Table 1) and terminates at the upper end of the Ritigraben gully. The surface is affected by the ski slope facilities that have been built on the rock glacier. Accounting for the steep slope and the geometrical setting, the flow unit is only 20 m thick and the flow velocities are rather high relative to other rock glaciers. Continuous DGPS measurements have provided velocity data since 2012, showing a mean value of 1.4 m a^{-1} and strong seasonal and interannual variations of more then 45 % and 25 % respectively; see Table 1. Even though no ice cores have been analysed, volumetric ice content has been estimated in previous studies at 30 %–70 % (Lugon and Stoffel, 2010; Luethi et al., 2017). Borehole measurements since 2002 show warm permafrost temperatures close to the melting point and the progressive development of a talik at a depth between 10 and 12 m (Zenklusen Mutter and Phillips, 2012), which has been related to the influence of water infiltration and air circulation (Luethi et al., 2017).

2.2 Murtèl-Corvatsch

The Murtèl rock glacier originates from the north wall of Piz Murtèl (3432 m a.s.l.) and is characterised by a single lobe of 27 m thickness with well-developed surface morphology of lobate furrows and ridges (Fig. 1a) that can be attributed to compressive flow, and buckle and folding (Loewenherz et al., 1989; Kääb and Weber, 2004; Frehner et al., 2015). Consistent with a low surface slope of 12°, this rock glacier flows rather slowly at 0.14 m a^{-1} (amongst others Kääb et al., 1998; Müller et al., 2014; see Table 1). Murtèl is probably the best-studied rock glacier in the world, with continuous temperature monitoring data from boreholes available since 1987 (Haeberli et al., 1988, 1998). The drillings from 1987, 2000 and 2015 (Haeberli et al., 1988; Vonder Mühll et al., 2003) and geophysical investigations (Haeberli et al., 1998; Arenson et al., 2002, 2010) revealed relatively ice-rich material in the main rock glacier body with an estimated volumetric ice content close to 100 %.

The temperatures within the main body of the rock glacier are between −4 and −1 °C and therefore relatively cold compared to other instrumented rock glaciers in Switzerland (Vonder Mühll et al., 2003; PERMOS, 2016a). Annual velocities have been measured since 2009 by a geodetic survey of 11 surface markers around the borehole (PERMOS, 2016a). Further, several years of borehole deformation data (at time intervals of several months) are available from 1987 to 1994 (Haeberli et al., 1998; Arenson et al., 2002). The time-averaged yearly velocities show an increasing trend, coherent with observations for other rock glaciers throughout the Swiss Alps, as shown in the PERMOS Glaciological Report no. 12–15 (PERMOS, 2016a).

2.3 Schafberg

The Schafberg rock glacier originates in a cirque south of the Piz Muragl ridge, has an extent of less than 300 m and an average surface slope of 18° (Table 1, Fig. 1c). In the lower part, the rock glacier splits into two separate tongues as a result of a bedrock outcrop. This study focuses on the northwestern lobe, where in 1997 a borehole was drilled and temperatures were monitored thereafter within PERMOS. This lobe has a thickness of approximately 26 m and a flow velocity of 0.3 m a^{-1}. Investigations by Vonder Mühll (1993) show a volumetric ice content ranging from 35 % to 100 %. Hoelzle et al. (1998) investigated internal deformation profiles from borehole measurements in relation to photogrammetric analysis. Continuous daily velocities have been measured by DGPS within the PermaSense framework since 2012 approximately 200 m upstream of the borehole location and show clear seasonal variations with an amplitude of up to 39 % relative to the mean velocity and a rising interannual trend (33 % increase in the observed period).

2.4 Muragl

The Muragl rock glacier is located on the western side of the ridge of Piz Muragl (3156 m a.s.l.) and consists of several generations of overlapping flow units of variable flow velocity (Fig. 1d). The main lobe, where the borehole is located, moves at 1.5 m a^{-1}, is approximately 25 m thick and has a surface slope of 20° (Table 1). The annual surface motion has been available from terrestrial survey since 2009, whereas continuous daily velocities from DGPS measurements at the lower end of the lobe have been measured since 2012 and indicate clear interannual (25 %) and seasonal variations (14 %) (PERMOS, 2016a). Older geophysical and photogrammetrical measurements have been presented in Vonder Mühll and Schmid (1993). Volumetric ice content has been estimated from boreholes investigations at 40 %–70 % and is found to be very heterogeneous (Arenson et al., 2002). The temperatures within the rock glacier, measured since the drilling in 1999, range from −3 to 0 °C and are relatively close to the melting point (Vonder Mühll et al., 2003). As for the Murtèl rock glacier and consistent with other observations in the Alps, there is a rising trend of multi-annual velocities (PERMOS, 2016a).

3 Data and methods

We designed a suite of 1-D numerical models, based on finite differences, to simulate the response of viscous and plastic flow to external near-surface temperature forcing using the software MATLAB (2016). The modelling framework couples heat conduction, forced by external temperature, to a power-law creep relation for ice-rich frozen soils proposed by Arenson and Springman (2005a). The model inputs are the surface slope, the thickness and other physical properties (density, volumetric ice content and thermal diffusivity) of the creeping rock glacier. All the parameters are assumed to be homogeneous in time and space in first approximation. Note that geophysical investigations on several rock glaciers including the ones presented here (amongst others: Arenson et al., 2002, 2010; Maurer and Hauck, 2007; Buchli et al., 2018) showed high heterogeneity and spatial variability. The model is forced by permafrost temperature time series measured in boreholes below the active layer. At the lower boundary of the rock glacier a constant temperature value representative of the observed bottom temperature is prescribed. The model is applied to the four study cases described in Sect. 2 and the results are compared to observed borehole temperatures and surface flow velocities.

3.1 Data overview

Here, we provide a detailed description of the data used for model input and for comparison with the model results.

The surface slope values are calculated on the basis of the swisstopo digital cartography (Federal Office of Topography swisstopo, 2018) over a 200 m long profile along a flow line centred at the DGPS location and are representative of the average slope of the landform close to the DGPS positions. For all four study cases vertical profiles of borehole deformation are available at several time steps over few years (Arenson et al., 2002; Kenner et al., 2017). The rock glacier thickness is defined based on these profiles as the vertical distance from the surface to the lower end of the shear horizon. Volumetric ice content values between 30 % and 100 % have been noted in the literature and are mostly based on borehole drillings (Vonder Mühll, 1993; Arenson et al., 2002; Lugon and Stoffel, 2010). The densities of the rock glaciers are calculated as a weighted average between the density values of pure ice ρ_{ice} and solid rock ρ_{rock} from the volumetric ice content w_{i}. The thermal diffusivity κ is calculated similarly based on the thermal diffusivity values of pure ice (0.1 m^2 day^{-1}) and quartz (0.35 m^2 day^{-1}) as proposed by Williams and Smith (1989). Borehole temperature time series are available from the PERMOS database for the

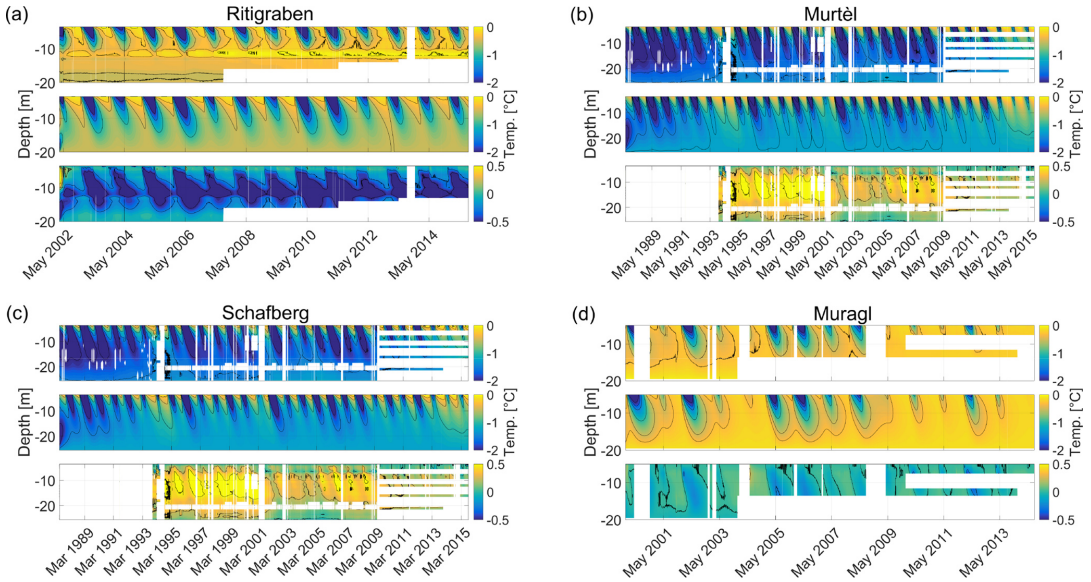

Figure 2. Contour plots of ground temperatures time series (colour coded) for rock glaciers **(a)** Ritigraben, **(b)** Murtèl, **(c)** Schafberg and **(d)** Muragl. Each panel shows, from top to bottom, measured temperatures, modelled temperatures and differences between the measured and the modelled temperatures. Note the different temperature scales of the lower sub panels with the temperature differences.

four study cases from spring 2002 to autumn 2015 with a time resolution of 6 h (the time series of Muragl terminates in autumn 2014). For our modelling, we resample these data to a daily average. For all four study cases, some data gaps occur due to sensor failure, in particular at depth. For temperatures at depth just below the active layer, which are used as forcing input for the model, the data gaps are below a few months apart from the case of Muragl, for which temperature data in the period between August 2008 and April 2009 are missing. Missing temperature data are linearly interpolated. Note that this linear interpolation does not aim to reconstruct exact real temperatures, but rather bridges the gaps in order to create a continuous temperature time series that can be used as model input. This approach is considered satisfactory due to the combination of the scarcity of data gaps in the surface temperature time series and the length of the considered seasonal to multi-annual timescales. Note that more sophisticated methods (e.g. Staub et al., 2017) could be used for interpolating the temperature time series. This means, the modelled short-term velocity variations should be analysed carefully near these gap-filled periods. Figure 2 shows the measured temperatures for all case study sites.

Several types of velocity data are available. For Murtèl and Muragl rock glacier mean annual surface velocities are available between 2009 and 2015 from terrestrial surveys with total station from the PERMOS network. For all study cases but Murtèl, daily velocities from continuous single frequency DGPS measurements are available from 2012 from the PermaSense network. For a summary of the study case sites see Table 1.

3.2 Heat conduction model

We model vertical heat conduction throughout the rock glacier unit by solving the diffusion equation for temperature evolution with depth (Williams and Smith, 1989):

$$\frac{\partial T}{\partial t} = \kappa \frac{\partial^2 T}{\partial z^2}, \tag{1}$$

where T is the permafrost temperature, z the vertical coordinate, t the time and κ the thermal diffusivity of the rock glacier material. At the upper boundary the observed temperature history just below the active layer depth is prescribed. At the bottom of the rock glacier (below the shear horizon) a constant temperature value corresponding to the time average of the observations is prescribed. The initial condition is prescribed from the measured vertical temperature profile at the first time step of the simulation. The temporal resolution of the model is 1 day, and its vertical resolution is 0.1 m. Convective and advective heat fluxes and any influence from basal heating due to frictional processes, heat dissipation from deformation and geothermal heat flux are not considered in this model.

3.3 Ice-creep model

For modelling ice creep we use the empirically derived creep relation proposed by Arenson and Springman (2005a). The

samples used to derive this relation have been cored from Murtèl and Muragl rock glacier, also investigated in this study, and are described in detail in Arenson and Springman (2005b). The creep relation is a modified Glen's flow law, which relates strain rate $\dot{\varepsilon}$ to a stress invariant σ_e as proposed by Von Mises (1913), taking into account the volumetric ice content w_i and the temperature T of rock glacier material:

$$\dot{\varepsilon} = A(T, w_\mathrm{i})\sigma_e^{n(w_\mathrm{i})}. \tag{2}$$

The flow law exponent n linearly depends on volumetric ice content only,

$$n = 3w_\mathrm{i}, \tag{3}$$

and the creep parameter A depends on temperature and volumetric ice content by

$$\log A = \frac{2}{1+T} + b(w_\mathrm{i}), \tag{4}$$

where $b(w_\mathrm{i})$ is a function of the volumetric ice content,

$$b = \log(5 \times 10^{-11} e^{-10.2 w_\mathrm{i}}). \tag{5}$$

Assuming an infinitely wide surface parallel slab, the shear stress σ_e at a depth z is given by

$$\sigma_e = \frac{1}{\sqrt{3}} \rho_\mathrm{r} g z \frac{\partial s}{\partial x}, \tag{6}$$

where ρ_r to the density of the rock glacier material, g the constant of gravity and $\frac{\partial s}{\partial x}$ the slope of the ice surface, which is assumed to be parallel to the rock glacier surface slope. Note that the density ρ_r also depends on the ice density by

$$\rho_\mathrm{r} = \rho_\mathrm{s}(1 - w_\mathrm{i}) + \rho_\mathrm{i} w_\mathrm{i}, \tag{7}$$

where ρ_i and ρ_s are the densities of ice and sediment particles respectively. As in our case the ice thickness of the rock glacier landform is fixed, any variation in volumetric ice content w_i will change the density and as consequence the shear stress σ_e (see Eq. 6).

Given the temperature field and assuming an inclined infinite parallel slab, the velocities are solved from Eq. (2) through vertical integration under the assumption of zero displacement at the lower boundary. This hypothesis is confirmed by the low deformation rates at the bottom of the borehole inclinometer profiles for all the studied rock glaciers. The physical properties of the material are considered constant in time and homogeneous in space. The temporal and the spacial model resolution are the same as for the heat conduction model. Despite its limitations, the proposed constitutive relation is one of the most up to date on rock glacier material and has the great advantage of being based on laboratory experiments.

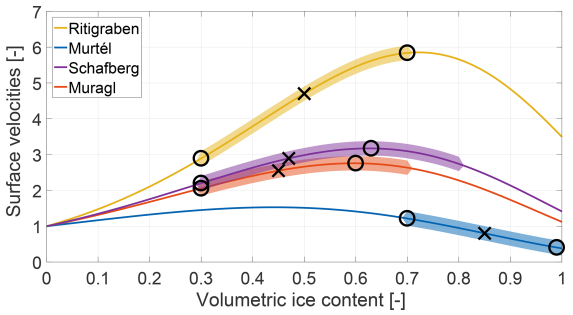

Figure 3. Normalised surface velocities for the four case studies with volumetric ice content values. For each rock glacier the velocities are normalised with the velocity value corresponding to 0 % ice content. The coloured buffer around the curve shows the range proposed by the literature (Vonder Mühll, 1993; Arenson et al., 2002; Lugon and Stoffel, 2010). The black circles show for each curve the maximum and the minimum possible velocity values within this range, also representing the uncertainty range for the modelling. The black cross shows the chosen volumetric ice content value for the modelling, i.e. the middle value of the latter range.

3.3.1 Calibration of the model

The model is calibrated to best fit the average observed surface velocities by varying the volumetric ice content parameter within the range of literature values. Because of the mathematical formulation of the applied rheology, calibrating the model by varying the volumetric ice content gives a concave curve for the mean velocities, with a maximum corresponding to around 60 % volumetric ice content (see Fig. 3). On the one hand, an increasing volumetric ice content causes the creep relation exponent to grow, resulting in higher surface velocities. On the other hand, a higher volumetric ice content implies a lower density and thus a lower shear stress and deformation. This mathematical artefact is because the thickness of the rock glacier in the modelling is fixed. In reality, for varying volumetric ice content values, the rock glacier thickness and velocity would adjust until the shear stress at the base of the rock glacier reaches a critical value.

Within the range of possible volumetric ice content values proposed in the literature (Vonder Mühll, 1993; Arenson et al., 2002; Lugon and Stoffel, 2010), we further refine the range for which the maximum and the minimum velocities are obtained (black circles in Fig. 3). We set the volumetric ice content parameter to the mean of this range and further assess the effect of the uncertainty range on the velocity results.

We consider further uncertainties in input parameters: slope $\pm 2°$, ice content (corresponding to the maximum and minimum velocity value) and thermal diffusivity $\pm 0.02\,\mathrm{m^2\,day^{-1}}$.

The creep model strongly depends on the temperature input. In order to assess uncertainties related to the heat con-

Table 2. Summary of modelling inputs and results. Values of geometrical and physical input parameters for the modelling are listed (thickness, slope, volumetric ice content and thermal diffusivity). The mean modelled surface velocity and its relative interannual and seasonal variations are reported in the last three columns.

Rock glacier	Thickness (m)	Temperature input depth (m)	Slope	w_i	κ ($\mathrm{m^2\,d^{-1}}$)	Mean surface velocity ($\mathrm{ma^{-1}}$)	Interannual variation	Seasonal variation
Ritigraben	18	3.5	$27° \pm 2°$	$50 \pm 20\,\%$	0.18 ± 0.02	0.59	2 %	8 %
Murtèl	27	3.5	$12° \pm 2°$	$85 \pm 15\,\%$	0.15 ± 0.02	0.12	5 %	2 %
Schafberg	25	5.2	$16° \pm 2°$	$48 \pm 18\,\%$	0.15 ± 0.02	0.69	4 %	5 %
Muragl	20	4.5	$20° \pm 2°$	$45 \pm 15\,\%$	0.18 ± 0.02	0.46	6 %	5 %

Table 3. Parameters and results of the sensitivity experiments. The first column indicates the scenario with a label in the form of Scnα, where α refers to the value of the multiplication factor for the investigated parameter relative to the reference values. Each column represents a set of experiments for one variable parameter, with the first number in each column referring to the input parameter value. The numbers in the bracket of each column refer to seasonal variations as a percentage of the mean value on the left side and the phase shift relative to the reference scenario on the right side (with a cycle of 2π referring to 1 year).

	Seasonal amplitude (°C)	Bottom temperature (°C)	Thickness (m)	Shear horizon depth (m)	Volumetric ice content (%)	κ ($\mathrm{m^2\,d^{-1}}$)
Scn0.2	-0.8 [3.1 % $-\frac{\pi}{14}$]	-0.2 [8.4 % $+\frac{\pi}{5}$]	4 [80.4 % $-\frac{\pi}{8}$]	4 [68.8 % $-\frac{2\pi}{3}$]	40 [11.6 % $-\frac{\pi}{8}$]	0.03 [0.8 % $-\frac{\pi}{8}$]
Scn0.4	-1.6 [4.5 % $-\frac{\pi}{17}$]	-0.4 [7.6 % $+\frac{\pi}{7}$]	8 [43.6 % $-\frac{\pi}{11}$]	8 [30.8 % $-\frac{\pi}{2}$]	48 [9.5 % $-\frac{\pi}{8}$]	0.06 [1.4 % $-\frac{\pi}{8}$]
Scn0.6	-2.4 [5.3 % $-\frac{\pi}{23}$]	-0.6 [6.9 % $+\frac{\pi}{11}$]	12 [21.0 % $-\frac{\pi}{25}$]	12 [13.2 % $-\frac{\pi}{4}$]	55 [8.0 % $-\frac{\pi}{8}$]	0.09 [2.2 % $-\frac{\pi}{12}$]
Scn0.8	-3.6 [5.7 % $-\frac{\pi}{37}$]	-0.8 [6.4 % $+\frac{\pi}{23}$]	16 [9.8 % $+\frac{\pi}{20}$]	16 [5.8 % $-\frac{\pi}{15}$]	63 [6.7 % $-\frac{\pi}{9}$]	0.12 [3.9 % $-\frac{\pi}{90}$]
Scn1.0	**−4.0** [6.1 % + 0]	**−1.0** [6.1 % + 0]	**20** [6.1 % + 0]	**20** [2.0 % + 0]	**70** [6.1 % + 0]	**0.15** [6.1 % + 0]
Scn1.2	-4.8 [6.3 % $+\frac{\pi}{37}$]	-1.2 [5.8 % $-\frac{\pi}{26}$]	24 [2.8 % + 0]	24 [0.9 % $+\frac{\pi}{4}$]	78 [5.6 % $+\frac{\pi}{9}$]	0.18 [8.5 % $-\frac{\pi}{60}$]
Scn1.4	-5.6 [6.5 % $+\frac{\pi}{17}$]	-1.4 [5.5 % $-\frac{\pi}{14}$]	28 [1.6 % $-\frac{\pi}{13}$]	28 [0.4 % $+\frac{\pi}{2}$]	85 [5.3 % $+\frac{\pi}{5}$]	0.21 [11.0 % $-\frac{\pi}{30}$]
Scn1.6	-6.4 [6.6 % $+\frac{\pi}{11}$]	-1.6 [5.4 % $-\frac{\pi}{11}$]	32 [1.2 % $-\frac{\pi}{9}$]	32 [0.2 % $+\frac{3\pi}{4}$]	93 [5.0 % $+\frac{\pi}{4}$]	0.24 [13.5 % $-\frac{\pi}{20}$]
Scn1.8	-7.2 [6.8 % $+\frac{\pi}{9}$]	-1.8 [5.2 % $-\frac{\pi}{10}$]	36 [0.9 % $-\frac{\pi}{9}$]	36 [0.1 % $+\pi$]	100 [4.8 % $+\frac{\pi}{3}$]	0.27 [15.9 % $-\frac{\pi}{15}$]

duction model and to take into account all possible heat transfer process, we perform additional numerical experiments forcing the ice-creep relation directly with the observed temperature fields with depth.

3.3.2 Consideration of shear horizon

The above described approach for creep does not consider enhanced deformation in the shear horizon, where most of the displacement takes place. In order to investigate the sensitivity of the model to such a phenomenon, we perform additional numerical experiments. We approximate the behaviour of the shear horizon with a pseudo-plastic creep relation, by increasing the flow law exponent of Eq. (2) by a factor 4 ($n_\mathrm{plastic} = 12 \cdot w_\mathrm{i}$), similarly to Frehner et al. (2015). The creep parameter A has been reduced by a factor f_A to match the time-averaged surface velocities modelled before:

$$\dot{\varepsilon}_\mathrm{plastic} = f_A(\dot{\varepsilon}) A(T, w_\mathrm{i}) \sigma_e^{n_\mathrm{plastic}(w_\mathrm{i})}. \quad (8)$$

In this way, we approximate the plastic behaviour of the lower layer to better represent the whole deformation profile of the studied rock glaciers.

3.4 Sensitivity experiments

We perform additional synthetic sensitivity experiments in order to explore the influence of the different input parameters on our model results. For these experiments we simulate seasonal temperature forcing by prescribing the temperature below the active layer as a sinusoidal function with a mean of 0 °C, which truncates positive temperatures in order to take into account the zero curtain effect. The initial vertical temperature profile is set to 0 °C. The model runs for 28 full annual cycles after which it converged to a quasi-steady-state periodic solution. We then analyse the results of the last two successive cycles. We study the sensitivity to seasonal temperature amplitude (corresponding to the minimum winter temperature), temperature at the lower boundary, rock glacier thickness, volumetric ice content and thermal diffusivity. We set up a reference scenario with typical values for rock glaciers taken as Scn1.0 in Table 3. Starting from the reference scenario, we perform 9 numerical experiments for each parameter, in which we vary the value of the parameter by a factor of 0.2 up to 1.8, with the other parameters kept constant. The numbers in the experiment name in Table 3 refer to the multiplication factor of the parameters relative to

the reference scenario. Only for the experiments on the volumetric ice content parameter the multiplications factors are different, as shown in Table 3.

Additionally, the thickness sensitivity experiments have been repeated using the pseudo-plastic rheology (Eq. 8) in order to investigate the effect of the presence of the shear horizon in our experiment. In the case of both sets of varying thickness experiments (with and without shear horizon), the bottom temperature for the scenarios with thicknesses less than the one of the reference are always prescribed at 20 m depth. For these shallow depths, prescribing a constant temperature would unrealistically constrain the temperature field. For all the values and the results of this analysis we refer to Table 3.

4 Results

4.1 Modelled temperatures

The modelled and measured temperatures are shown in Fig. 2. For Schafberg and Muragl rock glaciers (Fig. 2c and d respectively) the modelled temperatures agree very well with the measurements (temperature differences are below 0.2 °C). For the case of Murtèl rock glacier, given the prescribed temperatures below the active layer, the modelled temperature evolution with depth agrees well with regard to seasonal amplitude and phase with depth. However, between a depth of 5 and 20 m, temperatures are in particular during cold seasonal phases slightly underestimated, but the differences stay below 0.5 °C. For Ritigraben rock glacier, as shown in Fig. 2a, in a depth between 8 and 12 m and in particular in early summer, observed temperatures are substantially higher (up to 1 °C), which is related to the talik observed and discussed in Luethi et al. (2017). The depth of the zero annual temperature amplitude is according to the PERMOS (2016a) report, usually between 10 and 20 m depth. This depth is slightly overestimated by our model (see Fig. 2), with the seasonal temperature signal reaching slightly deeper in comparison to the borehole measurements (PERMOS, 2016a).

4.2 Modelled velocities

The observed and modelled surface flow velocities with time are shown in Fig. 4 for the modelled temperatures (solid blue line), for the observed temperature fields (red solid line), and for the pseudo-plastic rheology (yellow solid line) with modelled temperatures. The resulting maximum and minimum velocities accounting for uncertainties in the input parameter of volumetric ice content, slope and thermal diffusivity are shown with two black dashed lines.

For the chosen volumetric ice content values within the proposed range, we obtain the correct order of magnitude of the observed surface velocities for all four case study rock glaciers. For Ritigraben and Muragl rock glaciers the modelled velocities are smaller (by a factor 2), for Murtèl the average velocity matches the observations and for Schafberg the modelled velocities are overestimated (by a factor 3) in comparison to the observed ones.

The modelled amplitudes in seasonal and multi-annual velocity variations (values in Table 2, solid blue, yellow, and red line in Fig. 4) are in general rather low: below 10 % relative to the mean velocity. In comparison, the observed variations in flow (solid green and purple lines in Fig. 4, Table 1) are 1 order of magnitude higher. This result does not change when considering uncertainties in the input parameters (dashed black lines in the same figure).

For the three rock glaciers with continuous DGPS measurements, we are also able to compare the phase of the seasonal variations. The modelled velocity maxima occur in late winter and are substantially delayed in comparison to the observed velocity peaks in autumn. The above findings (amplitude underestimation and phase shift) do not change when the observed temperature fields are used as input for the creep model. The exception is the case of Ritigraben, where, as discussed above, substantial discrepancies between velocities obtained using modelled (blue solid line) and observed (red solid line) temperatures occur. When using the observed temperature field, the modelled and the observed seasonal velocity variations are phase synchronous (see red and green line in Fig. 4).

The discrepancies found between observed and modelled velocity variations do not improve when using the pseudo-plastic creep model for all rock glaciers. On the contrary, the seasonal velocity amplitude further reduces and the phase shift increases further (see yellow line in Fig. 4).

4.3 Sensitivity experiments

The results of the sensitivity experiments are plotted in Figs. 5 and 6 and are summarised in Table 3.

In Fig. 5, the time-averaged velocity values for the different experiments and scenarios are shown normalised to the mean values of the reference scenario. The left panel shows the results of the experiments investigating the thermal regime of the rock glacier for varying subsurface temperature-forcing amplitude, bottom and initial temperature, and thermal diffusivity. The initial condition experiment shows no differences (purple line constant at 1) and demonstrates that the model converged to a quasi-steady-state solution after the 28 annual cycles. A reduction in bottom temperature to -0.2 °C leads to an increase in the mean velocity of 50 % and a decrease in seasonal amplitude by a factor 0.2 leads to an increase in the mean velocity of 20 % (Fig. 5). Increasing the thermal diffusivity leads to only very slightly increased mean velocity values (less then 1 %). The modelled flow is more sensitive to the varying geometrical and physical parameters (thickness, slope and volumetric ice content; right panel in Fig. 5) than to the previous parameters. The velocities strongly vary with thickness and slope, in accordance with the governing equations (Eqs. 2 and 6), following

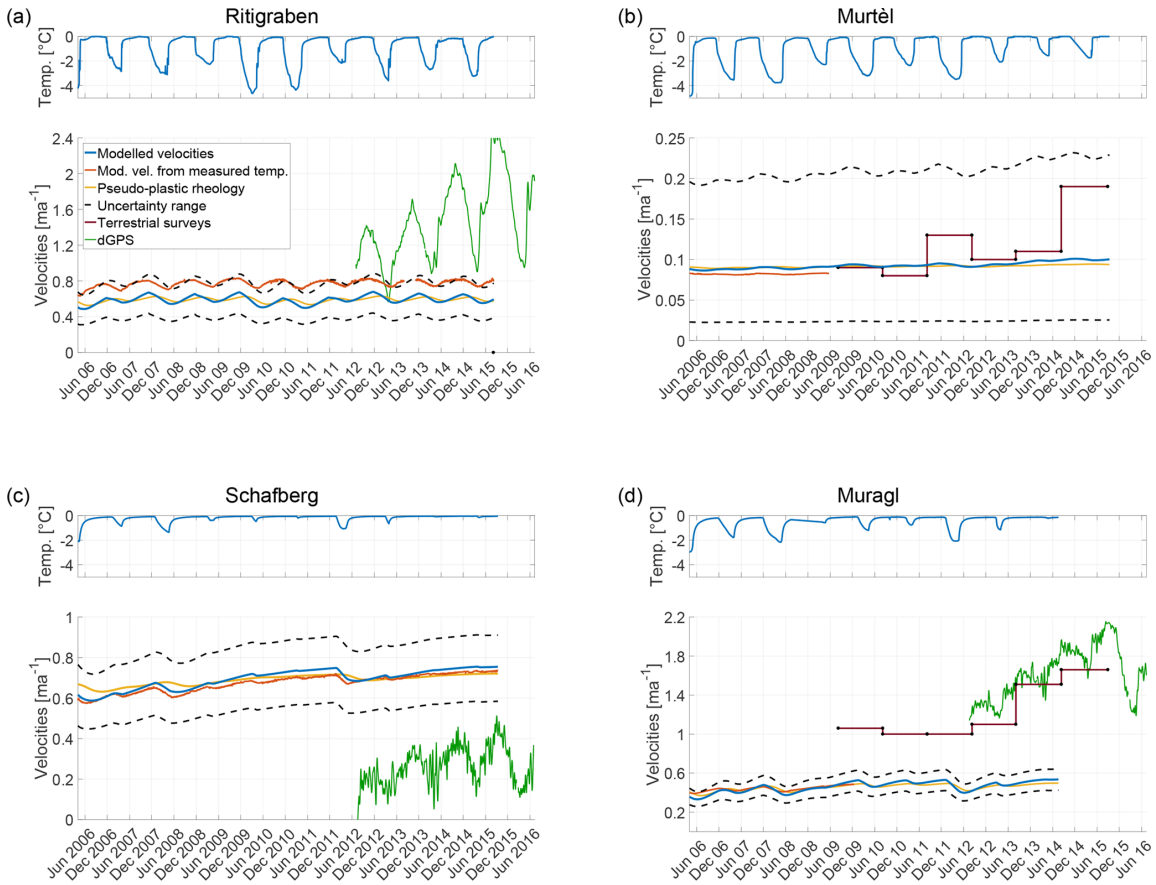

Figure 4. Observed and modelled surface flow velocities for **(a)** Ritigraben, **(b)** Murtèl, **(c)** Schafberg and **(d)** Muragl rock glaciers. The upper subpanel shows the observed subsurface temperature used as model input. The lower subpanel shows the modelled and observed velocities. The modelled velocities are shown for using the modelled temperatures (solid blue line), the observed temperature fields (red solid line), and the pseudo-plastic rheology (yellow solid line). The uncertainty range resulting from variations in slope ($\pm 2°$), volumetric ice content (within the proposed range; see Fig. 3 and Table 2) and thermal diffusivity ($\pm 0.02\,\mathrm{m^2\,day^{-1}}$) is plotted with black dashed lines. The modelled velocities are compared with the observed velocities from terrestrial surveys (dark solid red line with black dots) and with DGPS measurements (green solid line).

a power law with variations of almost 400 % and 600 % respectively. When varying volumetric ice content the mean velocities show variations of up to 70 % for the used parameter range (see Sect. 3.3).

In Fig. 6, the velocities of the different sensitivity experiments normalised with their mean are presented and a summary is given in Table 3. The seasonal velocity response to different amplitudes in surface winter temperature forcing is small and stays below 7 %, even for an 80 % increase in the temperature amplitude. The sensitivities of the velocity variations to varying bottom temperature are slightly higher, but remain below 9 % in the given range. For the thickness experiment, a velocity variation of up to 80 % is obtained when considering a 4 m thick rock glacier, representing an extreme and unrealistic scenario. For a more realistic lower bound of rock glacier thickness of 16 m, the seasonal velocity variations stay below 10 %. For thickness variations with the pseudo-plastic creep relation the sensitivity is even smaller. Variations in volumetric ice content and thermal diffusivity lead to slightly increased seasonal velocity variabilities of 12 % and 16 %, respectively. Thus in general, within a reasonable range of input parameters, the modelled seasonal variations in surface velocity remain more than 1 order of magnitude below the observed seasonal variations.

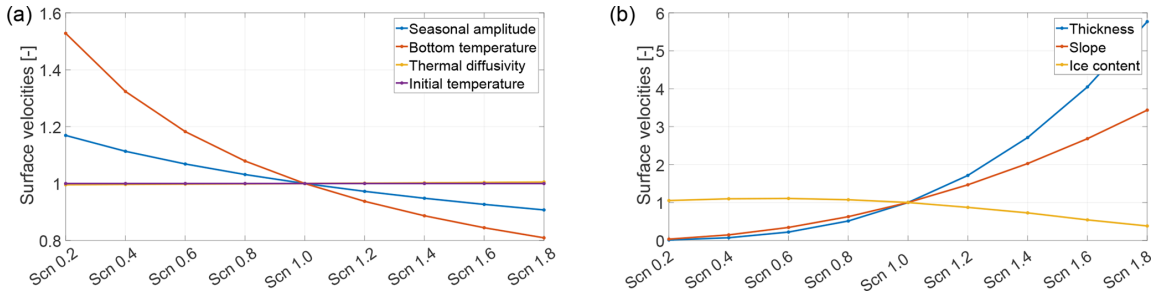

Figure 5. Plots of the time-averaged values of surface velocities for the sensitivity experiments with the different parameter scenarios. The mean velocities are normalised with the mean values of the reference scenario Scn1.0. Panel **(a)** shows the results for varying surface temperature-forcing amplitudes (blue line), bottom temperature values (red line), thermal diffusivity parameters (yellow line) and initial condition temperature values (purple line). The yellow line is hidden behind the purple line. Panel **(b)** shows the results for varying thicknesses (blue line), slope angles (red line) and volumetric ice content values (yellow line).

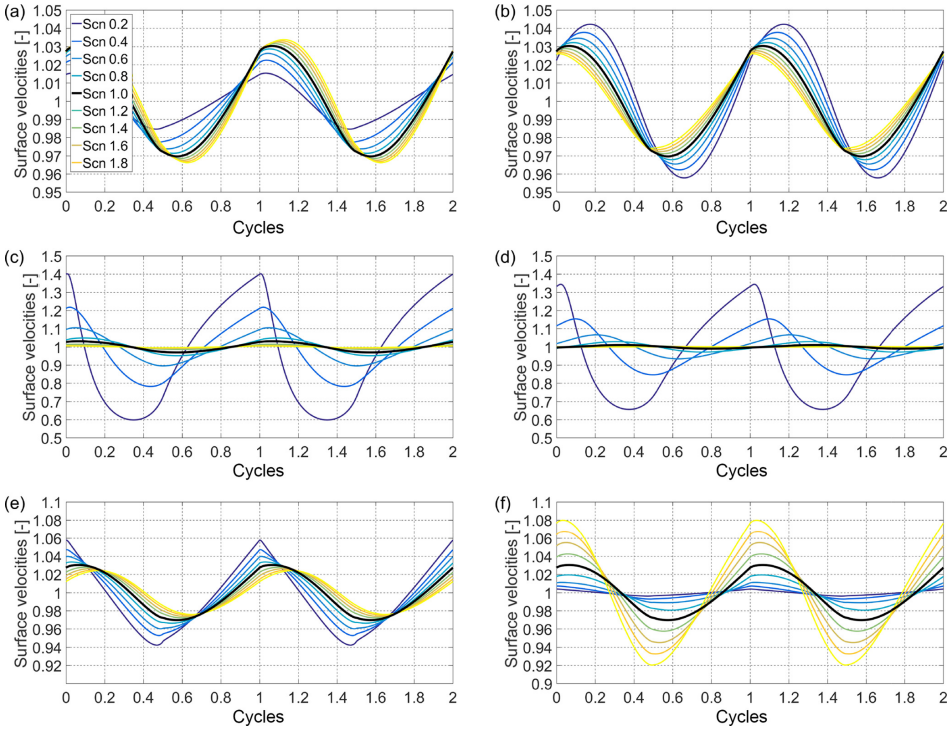

Figure 6. Results of the modelling sensitivity experiments of the model to **(a)** seasonal amplitude (winter minimum temperature), **(b)** bottom temperature, **(c)** thickness, **(d)** thickness with shear horizon, **(e)** volumetric ice content and **(f)** thermal diffusivity. The surface velocities normalised with their mean are plotted for each experiment with time, given here as the number of cycles (after the 28th cycle). One cycle corresponds to 1 year. For all experiments the different scenarios are colour coded as illustrated in the legend of panel **(a)**; the reference scenario is plotted with a thicker solid black line.

5 Discussion

In this study, we developed a simple numerical model approach to investigate the dynamical behaviour of rock glaciers with the aim of resolving the influence of external temperature forcing through heat conduction on rock glacier surface velocities. When choosing volumetric ice contents within a physical range of values proposed in the literature (see Sects. 2 and 3.3), for all the case studies the correct order of magnitude of measured mean surface velocities is

obtained. However, interannual and seasonal variations are strongly underestimated for all four cases, being at least 1 order of magnitude smaller than the observed ones.

5.1 Temperature modelling

We model rock glacier temperature evolution based on near-surface temperatures as measured below the active layer (see Sect. 3.2). In some cases, data gaps are present and linear interpolation of the data is used. The data gaps are short (below a few months) and are expected to not affect the overall modelling, but interpretation of the modelled velocities for these periods has to consider this limitation.

The assumption of constant bottom temperature agrees well with the observed borehole temperatures. This is further supported by the good agreement between the modelled velocities from prescribed observed and modelled temperatures. We assume the physical properties of the rock glacier (density, ice content and thermal diffusivity) to be constant in time and homogeneous in space, which seems justified at the considered short (seasonal to multi-annual) timescales and is supported by the good performance of the temperature evolution model.

For Schafberg (Fig. 2c) and Muragl (Fig. 2d) rock glaciers, we can reproduce the observed temperature fields very well. For Ritigraben and Murtèl (Fig. 2b and 2d) our results show some disagreement with seasonal pattern, in particular at 12–15 m depth. At Ritigraben, this disagreement can be explained by the influence of a talik caused by air and water advection (Luethi et al., 2017), which refers to processes that are not included in our modelling. For Murtèl, the cause of the discrepancy between modelled and observed temperatures is currently not clear. A possible explanation of this effect could be related to advective water fluxes or varying thermal conductivity within the rock glacier body, likely linked to the variable unfrozen water content at temperatures close to zero degree (Arenson et al., 2010). However, the results of our modelling for the four study cases, in combination with the available borehole temperature observations, allow us to confidently model and analyse rock glacier velocities.

5.2 Ice-creep modelling

Using the modelled and observed temperature fields respectively, we force the empirical creep relation for rock glacier material. Additionally, we run a separate experiment with the pseudo-plastic rheology to investigate the impact on the model from including enhanced deformation within the shear horizon.

5.2.1 Absolute velocities

When applying the creep rheology of Arenson and Springman (2005a) and using acceptable and uniform values of the model input parameters, we obtain the correct order of magnitude of the average observed surface velocities for all case studies.

For Murtèl, the mean surface velocities (averaged over the whole time series) match the observations. For Ritigraben and Muragl the modelled average velocities are between 30 % and 40 % of the observed ones. This result is consistent with the observed borehole deformation contribution from above the shear horizon, accounting for 10 % to 30 % of the total deformation (Arenson et al., 2002). This finding suggests that the rheology proposed by Arenson and Springman (2005a) may not be applicable to describe the rheology of the shear horizon of a rock glacier. On the contrary, for Schafberg the modelled velocities overestimate the observations. This mismatch can likely be explained by using an input thickness that is too high, resulting from the distance between the DGPS and borehole locations. The rock glacier thickness at the location of the observed velocities by DGPS is not known and the used thickness was taken from the borehole on the lobe further down which is less steep. The observed flow magnitude can be matched almost perfectly when using a thickness of 17 m, which was observed in a nearby borehole at the same field site (Arenson et al., 2002) and which can be expected for a steeper surface.

5.2.2 Seasonal and multi-annual variations

For all rock glaciers, we find that both seasonal and in particular interannual variations are strongly underestimated. This result is also coherent when considering relative velocity variations (see Fig. 4). In particular, the results for Murtèl and Schafberg rock glacier show very small seasonal variations of 3 % to 4 %. This result is not due to an underestimation in the seasonal temperature variations, as confirmed by the comparison between modelled and measured temperatures and further corroborated by the results of our modelling constrained with the observed temperatures. In fact, the latter forcing indirectly takes into account all non-conductive processes governing the temperature field. The lower sensitivities of rock glacier Murtèl and Schafberg compared to the other two can be explained by their greater thicknesses. For thicker rock glaciers, temperature variations at the surface reach shallower depth in relative terms and hence do not affect the near-bottom layers where most of the deformation occurs. For the thinner Muragl and Ritigraben glaciers, the modelled seasonal variations of 5% and 8% are substantially higher, but are still a factor 3 to 5 below the observations.

In general, our modelled seasonal variations for the four rock glaciers as well as for the sensitivity experiments are consistent with the obtained 3 % to 11 % by the earlier idealised modelling study of Kääb et al. (2007). The greater variations for Ritigraben and Muragl are likely a result of the higher temperature sensitivity of the rheology by Arenson and Springman (2005a) compared to the rheology based on Glen used in Kääb et al. (2007) for the case of warm permafrost (Müller et al., 2016).

Consistent with the results for similar thicknesses of Kääb et al. (2007), we also find that including a shear horizon in the modelling (by using the pseudo-plastic rheology) decreases the sensitivity of the seasonal variations in flow to temperature forcing. This result further corroborates the underestimation of seasonal and interannual variations in our modelling compared to the observations. It is unlikely that this underestimation is a result of an insufficient sensitivity of the used rheology of Arenson and Springman (2005a) to temperature. In fact, this rheology is based on laboratory deformation experiments on core material from real rock glaciers. Unfrozen water is known to have a significant influence on frozen soils creep (Arenson et al., 2006; Moore, 2014). The influence of interstitial water on creep is partially implicitly taken into account in the adopted empirical creep relation through the dependency on temperature; however, the impact on the stress regime due to pore pressure is not taken into account in the adopted rheology. Further, the discrepancy in the phase shift between modelled and observed velocity variations would not improve for a more temperature-sensitive rheology.

5.2.3 Phase shift

A phase lag of about 2–3 months between the seasonal summer peak in the observed ground surface temperatures and measured surface velocity has been detected on several rock glaciers including Ritigraben, Schafberg and Muragl (see Fig. 7) and has partly been attributed to the time it takes for the seasonal temperature signal to propagate into the rock glacier (Kääb et al., 2007; Delaloye et al., 2010; Wirz et al., 2016b). In our modelling this delay is however almost doubled, with the seasonal peak in velocity obtained in early January rather than early October. For the pseudo-plastic rheology this delay is further extended by several months.

In contrast, the seasonal winter minima in measured temperatures below the active layer (used as model input forcing) only have a lag of 2 months from the surface temperatures and seem in phase with the observed velocity minima (Fig. 7). Due to the zero curtain effect there is no clear summer peak in the observed and prescribed near-surface temperatures (Fig. 7) and the quantification of the summer peak phase shift is therefore ambiguous.

Despite the highly asymmetric seasonal temperature pattern, the resulting modelled surface flow variations are almost symmetric (Fig. 4), which is further supported by the sensitivity experiments using a capped sinusoidal forcing function pattern (Fig. 6). This transformation of the seasonal pattern is, on the one hand, a result of the diffusion of the temperature signal and, on the other hand, a result of an integrated contribution of deformation over the entire depth. The seasonal pattern in surface velocity variation is therefore neither a direct reflection of the temperature signal at a single depth nor of the depth-averaged temperature signal. In consequence, estimating the phase lag between seasonal variations in surface temperature and surface flow from heat conduction is non-trivial and interpreting phase lags is potentially misleading.

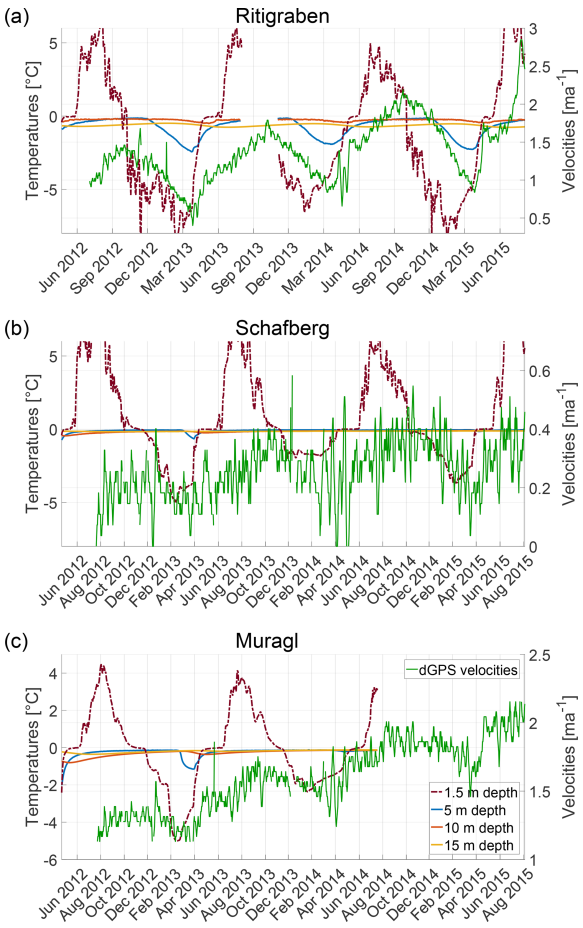

Figure 7. Temperature and velocity time series in the **(a)** Ritigraben, **(b)** Schafberg and **(c)** Muragl rock glaciers. The left y axis shows the temperatures (borehole measurements if available, model results otherwise) at 1.5 m (within the active layer), 5, 10 and 15 m depth. The right y axis with the green line shows the surface velocities from DGPS measurements.

The clear overestimation of the time lag in the modelled surface variations is a further sign that the process of heat conduction alone cannot explain the observed variations in deformation. Infiltration of surface meltwater into the permafrost in the summer season could reduce this time lag and through advection of water affect the flow in two ways. Firstly, the infiltrating water can effectively advect heat and warm up the rock glacier body at depth as observed in the case of Ritigraben, which in our modelling removed the phase lag when using the observed temperature field that includes the talik formation in summer. For the other three rock glaciers, water infiltration may also occur but it does not

seem to significantly warm the temperatures at depth, as confirmed by the good agreement between observed and modelled temperatures, and we can therefore exclude this heat advection process. Secondly, with increasing water infiltration the water content and pore-water pressure within the rock glacier material are expected to increase which in turn may reduce the shear strength and thereby enhance deformation and flow. This process has been suggested in other studies (Ikeda et al., 2008; Wirz et al., 2016b; Kenner et al., 2017; Buchli et al., 2018) and has also been proposed to explain the short-term velocity peaks with timescales of days that are related to a sudden input of water at the surface, for example during the snowmelt period (Wirz et al., 2016b; Kenner et al., 2017). To what depth such water infiltration occurs is poorly known, but this process would be most effective within the shear horizon, as deformation is highest. Further, in several boreholes, pressurised water was observed when drilling into the shear horizon (Arenson et al., 2002 and Alex Blast, personal communication, November 2015 for Murtél rock glacier, and Buchli et al., 2018 for the Furggwanghorn rock glacier).

Regarding the multi-annual variations, which are well documented and synchronous for many rock glaciers in Switzerland (PERMOS, 2016a), our modelling suggests that the responsible process between the observed acceleration in flow (e.g. from 2011 to 2015) and the observed surface warming cannot be explained by heat conduction into the ground alone. It is likely an indirect effect of enhanced meltwater penetrating into the rock glacier body and thereby affecting its rheology. Phases of slowdown related to conductive cooling in cold or long winters (e.g. 2007 and 2011) are more distinct in our modelled velocities, and thus winter cooling may contribute more substantially to the longer-term slow-down of rock glacier flow (Fig. 4). The enhanced sensitivity to winter temperatures is (in contrast to summer temperatures) not surprising given that the zero curtain effect basically caps the summer temperature peak at 0 degrees and inhibits the propagation of the summer heat into the ground, which is well reflected in the observed temperatures below the active layer (Fig. 4).

Including a shear horizon with a pseudo-plastic rheology (with the same temperature dependency as for the main rock glacier body and enforcing the same mean flow velocity) does not improve our results. On the contrary, interannual and seasonal variations are even more underestimated, because at the shear horizon depth, where the main deformation occurs, the signal of seasonal temperature variations from the surface is too small, being close to one-tenth of a degree (PERMOS, 2016a).

In summary, the strong underestimations in both amplitude in seasonal and multi-annual variations, as well as the overestimation in time lag of seasonal peaks in our modelling, suggest that heat conductive processes alone cannot explain the observed variation in flow velocity, suggesting the need for other processes, such as the interaction of rock glacier rheology with surface water advecting into the rock glacier body.

5.3 Sensitivity experiments

Sensitivity experiments were carried out to explore the influence of different input geometries and parameters on the simulated surface velocity in a systematic way. In their set-up and results, the experiments are an extension of the earlier modelling study by Kääb et al. (2007), but here we use a more realistic model set-up and rheology, and explore a more extensive parameter space.

Absolute mean velocities are strongly affected by variations in geometry due to changing stress conditions (Eq. 6). However, over the timescales considered in this study (seasonal to multi-annual), the geometry of a rock glacier is not expected to change substantially. For the other parameters, mean velocities are most sensitive to the bottom temperature of the rock glacier, which is somewhat representative of the thermal state of the entire rock glacier body. Again, the general thermal state of a rock glacier should not change over the considered timescales. Nevertheless, the considerable warming of a rock glacier would lead to faster flow, as also reflected in the observational data sets presented in Kääb et al. (2007). The insensitivity of the mean velocity to thermal diffusivity reflects the fact that the average thermal state of the rock glacier is not affected by uncertainties in this parameter. For high thermal conductivity values, which would require high water content and hence degrading permafrost conditions, relative seasonal variation of 16 % are modelled, but this remains an order of magnitude below observed seasonal velocity variations.

The model used shows a dependency of the surface velocities on the volumetric ice content value (Figs. 5 and 6). The relative seasonal variations stay below 12 %, even for a reduction to 40 % of the volumetric ice content value. For high values of ice content, the velocity peak considerably shifts in time, with a delay of 2 months ($\pi/3$ of 1-year cycle) in comparison to the reference scenario. Note that the ice content of the rock glacier material is rather static and not expected to change even over timescales of several decades.

Decreasing thicknesses lead to very different absolute mean velocities, but more interestingly, they also lead to stronger seasonal variations. Considering realistic thicknesses of 12, 20, and 28 m, we obtain seasonal velocity variations of 21.2 %, 2 % and 1.6 % respectively. We explain this sensitivity by the variable fraction of the rock glacier thickness that is affected by temperature variations. It implies that thin rock glaciers are more sensitive to the effect of heat conduction for seasonal as well as long-term temperature changes. This means that for thin rock glaciers (which are usually fast moving) heat conduction should be considered in the interpretation of short-term variations. Note that, without any borehole deformation data or detailed geophysical investigations, uncertainties in rock glacier thickness may sig-

nificantly affect modelled velocities (absolute and seasonal variations).

For all other remaining parameters, except the rock glacier thickness, the modelled seasonal velocity variations do not change much and stay again below 8 % to 12 % of their mean flow and phase shifts vary below 2 months, even for extreme and relatively unrealistic end-member parameter values.

By considering the pseudo-plastic relation, the seasonal variations are coherently decreasing for all the scenarios (even for shallow rock glaciers) and the velocity peaks are considerably shifted in time, with a delay of up to 6 months (see Table 3). Thus in summary, we conclude from our sensitivity study that our modelling results for the four rock glaciers above are, apart from thickness, insensitive to uncertainties in our input parameters, and the modelled magnitudes of seasonal variations and related conclusions are robust.

6 Conclusions

We quantitatively investigated the contribution of heat conduction to seasonal and multi-annual variations in rock glacier flow velocity on the basis of numerical modelling and a multi-year time series of observed surface velocities and borehole temperatures from four different rock glaciers. The numerical model couples heat conduction to an empirically derived rheology of rock glacier creep that accounts for temperature and ice content. We find that, using standard parameters from the literature, our modelling reproduces the correct order of magnitude of mean surface velocities for all chosen rock glaciers. However, the magnitudes of seasonal and multi annual variations are strongly underestimated by our modelling, and the phase-lags of the seasonal peaks are too long. This suggests that the effect of heat conduction on the observed variations in surface flow is very limited and cannot explain more than about 25 % of the observed variations. The exception is extremely thin rock glaciers, as shown during the sensitivity study (see Sect. 4.3), where short-term temperature variations can force heat conduction to affect the whole deforming thickness of the rock glacier, thus leading to more substantial velocity variations.

Additional sensitivity experiments underpin the robustness of these conclusions within expected parameter uncertainties, also when including a shear horizon at the bottom of the rock glacier. Our idealised sensitivity experiments further indicate that, when the temperature changes over the full depth of the rock glacier (changing bottom temperature), the mean deformation maybe affected substantially, but this requires changes in climate over periods of several decades or centuries.

From our quantitative process modelling approach we can therefore exclude heat conduction as the governing process for seasonal to multi-annual variations in rock glacier flow. Considering the phase-lag information of the summer peak (e.g. the case of case of Ritigraben) and indications from earlier qualitative and statistical analysis of rock glacier velocities (Wirz et al., 2016b), we conclude that advection of surface water into the rock glacier and its interaction over pore-water pressure with the creep rheology are required to explain short- to mid-term velocity variations of rock glacier flow. However, further investigations are required for a better understanding of the advection of water within the rock glacier material as well as of the role of water and water pressure on creep rheology.

Data availability. Data on rock glacier kinematics and temperature are available from the PERMOS office upon request. The reference web link is http://www.permos.ch/data.html (PERMOS, 2016b).

Competing interests. Andreas Vieli is an editor of *The Cryosphere*.

Acknowledgements. The work presented in this paper is part of the project X-Sense 2 funded by Nano-Tera.ch (ref. no. 530659). This work could not have been possible without the pioneering results obtained from the DGPS pilot project funded by the Swiss Federal Office for the Environment BAFU. We thank Johann Müller for the coherent fieldwork in Engadine, and Vanessa Wirz for her preliminary study on this topic. We further acknowledge the editor, Christian Hauck, and the referees, Martin Hoelzle and Lukas U. Arenson, for their constructive and thorough comments, which helped to improve the manuscript.

Edited by: Christian Hauck
Reviewed by: Lukas U. Arenson and Martin Hoelzle

References

Arenson, L., Hoelzle, M., and Springman, S.: Borehole deformation measurements and internal structure of some rock glaciers in Switzerland, Permafrost Periglac., 13, 117–135, https://doi.org/10.1002/ppp.414, 2002.

Arenson, L., Springman, S. M., and Sego, D.: The rheology of frozen soils, Appl. Rheol., 17, 12147-1, https://doi.org/10.3933/ApplRheol-17-12147, 2006.

Arenson, L. U. and Springman, S. M.: Mathematical descriptions for the behaviour of ice-rich frozen soils at temperatures close to 0 °C, Can. Geotech. J., 42, 431–442, https://doi.org/10.1139/t04-109, 2005a.

Arenson, L. U. and Springman, S. M.: Triaxial constant stress and constant strain rate tests on ice-rich permafrost samples, Can. Geotech. J., 42, 412–430, https://doi.org/10.1139/t04-111, 2005b.

Arenson, L. U., Johansen, M. M., and Springman, S. M.: Effects of volumetric ice content and strain rate on shear strength under triaxial conditions for frozen soil samples, Permafrost Periglac., 15, 261–271, https://doi.org/10.1002/ppp.498, 2004.

Arenson, L. U., Hauck, C., Hilbich, C., Seward, L., Yamamoto, Y., and Springman, S. M.: Sub-surface Heterogeneities in the

Murtèl. Corvatsch Rock Glacier, Switzerland, in: Proceedings of the joint 63rd Canadian Geotechnical Conference and the 6th Canadian Permafrost Conference, pp. 1494–1500, Canadian Geotechnical Society, the 6th Canadian Permafrost Conference, Conference Location: Calgary, Canada, Conference Date: 12–16 September 2010, 2010.

Barsch, D.: Permafrost creep and rockglaciers, Permafrost Periglac., 3, 175–188, https://doi.org/10.1002/ppp.3430030303, 1992.

Barsch, D. and Hell, G.: Photogrammetrische Bewegungsmessungen am Blockgletscher Murtel I, Oberengadin, Schweizer Alpen, Zeitschrift für Gletscherkunde und Glazialgeologie, 11, 111–142, 1975.

Berthling, I., Etzelmüller, B., Eiken, T., and Sollid, J. L.: Rock glaciers on Prins Karls Forland, Svalbard. I: internal structure, flow velocity and morphology, Permafrost Periglac., 9, 135–145, https://doi.org/10.1002/(SICI)1099-1530(199804/06)9:2<135::AID-PPP284>3.0.CO;2-R, 1998.

Buchli, B., Sutton, F., and Beutel, J.: GPS-Equipped Wireless Senson Network Node for High-Accuracy Positioning Applications, Wireless Sensor Network, 179–195, 2012.

Buchli, T., Kos, A., Limpach, P., Merz, K., Zhou, X., and Springman, S. M.: Kinematic investigations on the Furggwanghorn Rock Glacier, Switzerland, Permafrost Periglac., 29, 3–20, 2018.

Chaix, A.: Les coulées de blocs du Park National suisse d'Engadine, Le Globe, 62, 1–35, 1923.

Delaloye, R., Lambiel, C., and Gärtner-Roer, I.: Overview of rock glacier kinematics research in the Swiss Alps, Geogr. Helv., 65, 135–145, https://doi.org/10.5194/gh-65-135-2010, 2010.

Duval, P., Ashby, M. F., and Anderman, I.: Rate-controlling processes in the creep of polycrystalline ice, J. Phys. Chem., 87, 4066–4074, 1983.

Federal Office of Topography swisstopo: https://map.geo.admin.ch/, last access: 20 August 2018.

Francou, B. and Reynaud, L.: 10 year surficial velocities on a rock glacier (Laurichard, French Alps), Permafrost Periglac., 3, 209–213, 1992.

Frehner, M., Ling, A. H. M., and Gärtner-Roer, I.: Furrow-and-Ridge Morphology on Rockglaciers Explained by Gravity-Driven Buckle Folding: A Case Study From the Murtèl Rockglacier (Switzerland), Permafrost Periglac., 26, 57–66, https://doi.org/10.1002/ppp.1831, pPP-14-0032.R2, 2015.

Glen, J.: The creep of polycrystalline ice, Proceedings of the Royal Society of London A: Mathematical, Physical and Engineering Sciences, 228, 519–538, https://doi.org/10.1098/rspa.1955.0066, 1955.

Haeberli, W.: Creep of mountain permafrost, Mitteilungen der Versuchsanstalt für Wasserbau, Hydrologie und Glaziologie der ETH Zürich, vol. 77, 1985.

Haeberli, W., Hunder, J., Keusen, H.-R., Pika, J., and Röthlisberger, H.: Core drilling through rock-glacier permafrost, Fifth International Conference on Permafrost, Trondheim, 2, 937–942, 1988.

Haeberli, W., Hoelzle, M., Kääb, A., Keller, F., Vonder Mühll, D., and Wagner, S.: Ten years after drilling through the permafrost of the active rock glacier Murtél, Seventh International Conference on Permafrost, Yellowknife, 403–410, 1998.

Haeberli, W., Hallet, B., Arenson, L., Elconin, R., Humlum, O., Kääb, A., Kaufmann, V., Ladanyi, B., Matsuoka, N., Springman, S., and Vonder Mühll, D.: Permafrost Creep and Rock Glacier Dynamics, Permafrost Periglac., 17, 189–214, 2006.

Hanson, S. and Hoelzle, M.: The thermal regime of the active layer at the Murtèl rock glacier based on data from 2002, Permafrost Periglac., 15, 273–282, 2004.

Hoelzle, M., Wagner, S., Kääb, A., and Vonder Mühll, D.: Surface movement and internal deformation of ice-rock mixtures within rock glaciers in the Upper Engadin, Switzerland, Proceedings of the 7th International Conference on Permafrost, 465–471, 1998.

Ikeda, A., Matsuoka, N., and Kääb, A.: Fast deformation of perennially frozen debris in a warm rock glacier in the Swiss Alps: An effect of liquid water, J. Geophys. Res.-Earth, 113, f01021, https://doi.org/10.1029/2007JF000859, 2008.

Johnson, P. G.: Rock glacier types and their drainage systems, Grizzly Creek, Yukon Territory, Can. J. Earth Sci., 15, 1496–1507, https://doi.org/10.1139/e78-155, 1978.

Kääb, A. and Weber, M.: Development of transverse ridges on rock glaciers: Field measurements and laboratory experiments, Permafrost Periglac., 15, 379–391, https://doi.org/10.1002/ppp.506, 2004.

Kääb, A., Gudmundsson, G., and Hoelzle, M.: Surface deformation of creeping mountain permafrost. Photogrammetric investigations on rock glacier Murtél, Swiss Alps, Proceedings of the 7th International Conference on Permafrost, 57, 531–537, 1998.

Kääb, A., Frauenfelder, R., and Roer, I.: On the response of rockglacier creep to surface temperature increase, Global Planet. Change, 56, 172–187, https://doi.org/10.1016/j.gloplacha.2006.07.005, 2007.

Kenner, R., Phillips, M., Beutel, J., Hiller, M., Limpach, P., Pointner, E., and Volken, M.: Factors Controlling Velocity Variations at Short-Term, Seasonal and Multiyear Time Scales, Ritigraben Rock Glacier, Western Swiss Alps, Permafrost Periglac., 28, 675–684, https://doi.org/10.1002/ppp.1953, pPP-16-0044.R2, 2017.

Krainer, K. and He, X.: Flow velocities of active rock glaciers in the Austrian Alps, Geogr. Ann. A, 88, 267–280, https://doi.org/10.1111/j.0435-3676.2006.00300.x, 2006.

Loewenherz, S. D., Lawrence, C. J., and Weaver, R. L.: On the Development of Transverse Ridges on Rock Glaciers, J. Glaciol., 35, 383–391, https://doi.org/10.1017/S002214300000931X, 1989.

Luethi, R., Phillips, M., and Lehning, M.: Estimating Non-Conductive Heat Flow Leading to Intra-Permafrost Talik Formation at the Ritigraben Rock Glacier (Western Swiss Alps), Permafrost Periglac., 28, 183–194, https://doi.org/10.1002/ppp.1911, 2017.

Lugon, R. and Stoffel, M.: Rock-glacier dynamics and magnitude–frequency relations of debris flows in a high-elevation watershed: Ritigraben, Swiss Alps, Global Planet. Change, 73, 202–210, https://doi.org/10.1016/j.gloplacha.2010.06.004, 2010.

MATLAB: version 9.1.0 (R2016b), The MathWorks Inc., Natick, Massachusetts, 2016.

Maurer, H. and Hauck, C.: Geophysical imaging of alpine rock glaciers, J. Glaciol., 53, 110–120, https://doi.org/10.3189/172756507781833893, 2007.

Mellor, M. and Testa, R.: Effect of Temperature on the Creep of Ice, J. Glaciol., 8, 131–145, https://doi.org/10.3189/S0022143000020803, 1969.

Moore, P. L.: Deformation of debris-ice mixtures, Rev. Geophys., 52, 435–467, https://doi.org/10.1002/2014RG000453, 2014.

Müller, J., Gärtner-Roer, I., Kenner, R., Thee, P., and Morche, D.: Sediment storage and transfer on a periglacial mountain slope (Corvatsch, Switzerland), Geomorphology, 218, 35–44, https://doi.org/10.1016/j.geomorph.2013.12.002, 2014.

Müller, J., Vieli, A., and Gärtner-Roer, I.: Rock glaciers on the run – understanding rock glacier landform evolution and recent changes from numerical flow modeling, The Cryosphere, 10, 2865–2886, https://doi.org/10.5194/tc-10-2865-2016, 2016.

Nye, J. F.: The Mechanics of Glacier Flow, J. Glaciol., 2, 82–93, https://doi.org/10.3189/S0022143000033967, 1952.

PERMOS: Permafrost in Switzerland 2010/2011 to 2013/2014, edited by: Noetzli, J., Luethi, R., and Staub, B., the Cryospheric Commission of the Swiss Academy of Sciences, Glaciological Report (Permafrost) No. 12–15, 85 pp., 2016a.

PERMOS: PERMOS Database, Swiss Permafrost Monitoring Network, Fribourg, Switzerland, https://doi.org/10.13093/permos-2016-01, 2016b.

Pruessner, L., Phillips, M., Farinotti, D., Hoelzle, M., and Lehning, M.: Near-surface ventilation as a key for modeling the thermal regime of coarse blocky rock glaciers, Permafrost Periglac., 29, 152–163, https://doi.org/10.1002/ppp.1978, 2018.

Roer, I., Kääb, A., and Dikau, R.: Rockglacier acceleration in the Turtmann valley (Swiss Alps): Probable controls, Norsk Geogr. Tidsskr., 59, 157–163, https://doi.org/10.1080/00291950510020655, 2005.

Scherler, M., Schneider, S., Hoelzle, M., and Hauck, C.: A two-sided approach to estimate heat transfer processes within the active layer of the Murtèl-Corvatsch rock glacier, Earth Surf. Dynam., 2, 141–154, https://doi.org/10.5194/esurf-2-141-2014, 2014.

Staub, B., Hasler, A., Noetzli, J., and Delaloye, R.: Gap-Filling Algorithm for Ground Surface Temperature Data Measured in Permafrost and Periglacial Environments, Permafrost Periglac., 28, 275–285, https://doi.org/10.1002/ppp.1913, 2017.

Vonder Mühll, D.: Geophysikalische Untersuchungen im Permafrost des Oberengadins, Mitteilungen der Versuchsanstalt für Wasserbau, Hydrologie und Glaziologie an der Eidgenössischen Technischen Hochschule Zürich, Versuchsanstalt für Wasserbau Hydrologie und Glaziologie der Eidgenössischen Technischen Hochschule Zürich, 1993.

Vonder Mühll, D. and Schmid, W.: Geophysical and photogrammetrical investigations of rock glacier Muragl I, Engadin, Swiss Alps, in: Ed. 6th International Conference on Permafrost Proceedings, pp. 654–659, South China University Technology Press, Ed. 6th International Conference on Permafrost, 1993.

Vonder Mühll, D., Arenson, L., and Springman, S.: Temperature conditions in two Alpine rock glaciers, Eight International Conference on Permafrost, pp. 1195–1200, 2003.

Von Mises, R.: Mechanics of solid bodies in the plastically-deformable state, Nachrichten von der Gesellschaft der Wissenschaften zu Göttingen, Mathematisch-Physikalische Klasse, 1913.

Wahrhaftig, C. and Cox, A.: Rock Glaciers in the Alaska Range, GSA Bulletin, 70, 383, 1959.

Williams, P. J. and Smith, M. W.: The Frozen Earth: Fundamentals of Geocryology, Studies in Polar Research, Cambridge University Press, https://doi.org/10.1017/CBO9780511564437, 1989.

Wirz, V., Geertsema, M., Gruber, S., and Purves, R. S.: Temporal variability of diverse mountain permafrost slope movements derived from multi-year daily GPS data, Mattertal, Switzerland, Landslides, 13, 67–83, https://doi.org/10.1007/s10346-014-0544-3, 2016a.

Wirz, V., Gruber, S., Purves, R. S., Beutel, J., Gärtner-Roer, I., Gubler, S., and Vieli, A.: Short-term velocity variations at three rock glaciers and their relationship with meteorological conditions, Earth Surf. Dynam., 4, 103–123, https://doi.org/10.5194/esurf-4-103-2016, 2016b.

Zenklusen Mutter, E. and Phillips, M.: Thermal Evidence of Recent Talik Formation in Ritigraben Rock Glacier, Swiss Alps, 479–483, 2012.

Publication 2

Water controls the seasonal rhythm of rock glacier flow

Authors Cicoira, A., Beutel, J., Faillettaz, J., Vieli, A.

Journal Earth and Planetary Science Letters

Year 2019

DOI doi.org/10.1016/j.epsl.2019.115844

Short summary The processes governing rock glacier creep and its variability at seasonal and inter-annual time scales are investigated. The combination of external temperature forcing and water input through augmented pore water pressure at the shear horizon is assumed as the main driver of creep variations. A numerical model accounting for the catchment hydrology, heat conduction, hydro-mechanics and creep of the rock glacier is developed to quantitatively test this hypothesis. The model is forced and the results are compared with continuous time series of surface and ground temperatures, liquid precipitation, snow melt and displacement rates for Dirru Rock Glacier (Vallis - CH).

Main findings The main findings of this publication are:

- Seven years of continuous in-situ observations for Dirru Rock Glacier.
- Surface velocity is the combination of three superimposed signals.
- Our process based model can reproduce velocity variations both in magnitude and phase at seasonal and inter-annual time scales.
- Indirect information can be derived on the hydro-mechanical regime of rock glaciers.
- Creep variations are governed by water, rather than air and ground temperature.
- Rock glacier dynamics is complex and its coupling to climate strongly non-linear.

Contributions of the PhD candidate Autonomous design of the conceptual and the numerical model. Analysis and interpretation of the data with substantial contribution from Andreas Vieli. Collection of the data and maintenance of the measurements network, designed and managed primarily by Jan Beutel. Preparation of the manuscript and the figures with contribution from the co-authors.

Data availability The GPS data used for rock glacier kinematics and the meteorological data from the automatic weather station are available from http://data .permasense.ch. The ground temperatures data are avail-able from the authors upon request.

Journal *Earth and Planetary Science Letters (EPSL)* is a leading journal for researchers across the entire Earth and planetary sciences community. It publishes concise, exciting, high-impact articles ("Letters") of broad interest. Its focus is on physical and chemical processes, the evolution and general properties of the Earth and planets - from their deep interiors to their atmospheres.
Impact Factor: **4.6**

Earth and Planetary Science Letters 528 (2019) 115844

Contents lists available at ScienceDirect

Earth and Planetary Science Letters

www.elsevier.com/locate/epsl

Water controls the seasonal rhythm of rock glacier flow

A. Cicoira [a,*], J. Beutel [b], J. Faillettaz [a], A. Vieli [a]

[a] Department of Geography, University of Zurich, Switzerland
[b] Computer Engineering and Networks Laboratory, ETH Zurich, Switzerland

ARTICLE INFO

Article history:
Received 29 May 2019
Received in revised form 11 September 2019
Accepted 12 September 2019
Available online xxxx
Editor: A. Yin

Keywords:
rock glacier dynamics
rock glacier hydrology
permafrost creep

ABSTRACT

Rock glaciers are creeping periglacial landforms experiencing strong acceleration during recent atmospheric warming and raising concerns with regard to their future behaviour and stability. High resolution kinematic observations show strong seasonal and multi-annual variations in rock glacier creep, but the linking mechanisms to environmental forcing remain poorly understood and lack quantitative models. Here we investigate the interaction between rock glacier creep and climatic forcing - temperature and precipitation - by developing a novel conceptual and numerical modelling approach. The model is constrained and the results are compared with data from the Dirru Rock Glacier (Vallis - CH). We are able to reproduce the observed velocity variations both in magnitude and phase on seasonal and inter-annual time scales. We find that water from liquid precipitation and snow melt, rather than air temperature, is the main driver of variations in rock glacier creep. Our results imply that the influence of water on rock glacier creep is fundamental and must be considered when investigating the historic and future evolution of rock glaciers.

1. Introduction

Rock glaciers are distinctive, creeping periglacial landforms characterized by cohesive flow (Wahrhaftig and Cox, 1959). The movement of rock glaciers has already been observed in the first pioneering studies on these landforms more than a century ago (Spencer, 1900; Capps, 1910). Investigations of the same landforms over several years (Chaix, 1943; Wahrhaftig and Cox, 1959; White, 1976; Barsch and Hell, 1975) allowed to detect inter-annual flow variability already in these early stages of rock glacier research. Rock glacier flow has been linked to ice deformation (Wahrhaftig and Cox, 1959), therefore glaciological theories have been applied to these periglacial features and substantially contributed to the understanding of their dynamics. In particular, the studies by Nye (1952), followed by the contribution of Mellor and Testa (1969), identified temperature and stress conditions as important factors for ice, and thus for rock glacier creep. On the basis of these studies and further supported by field and laboratory investigations, temperature has been suggested as the main factor controlling rock glacier flow variability on inter-annual time scales (e.g. Arenson et al., 2002; Arenson and Springman, 2005a; Haeberli et al., 2006).

In the last decades of the 20th century, seasonal variations have been discovered (Haeberli, 1985; Kääb et al., 1997; Arenson et al., 2002). In the following years, investigations adopted modern differential GPS technology and were extended to other field sites (amongst others: Lambiel and Delaloye, 2004; Krainer and Mostler, 2006; Delaloye et al., 2010). Finally, the introduction of continuous differential GPS measurements yielded unprecedented temporal resolution at high accuracy and allowed the detection of variations in rock glacier surface velocities on time scales of days to weeks at significantly increased precision and accuracy (Wirz et al., 2014). The short-term velocity peaks are likely related to tilting or slip events of boulders, and therefore limited to the active layer of the rock glacier (Wirz et al., 2014). These short peaks can be interpreted as high frequency signals superimposed to a smoother velocity pattern, which better represents the movement of the entire rock glacier (or of one of its dynamical units). Although limited observation exists on rock glacier kinematics in comparison to ice glaciers, the observations show a consistent flow pattern. The seasonal rhythm of rock glacier flow is characterized by an acceleration in early summer with flow velocity maxima occurring between summer and early winter, and a deceleration leading to a late-spring minima (e.g. Delaloye et al., 2010; Wirz et al., 2016). The seasonal velocity signal generally shows a time lag of several months relative to air and ground surface temperatures. This phase lag has been interpreted as the time needed by the temperature signal to propagate into the frozen ground and thus influence rock

* Corresponding author.
E-mail address: alessandro.cicoira@geo.uzh.ch (A. Cicoira).

https://doi.org/10.1016/j.epsl.2019.115844
0012-821X/

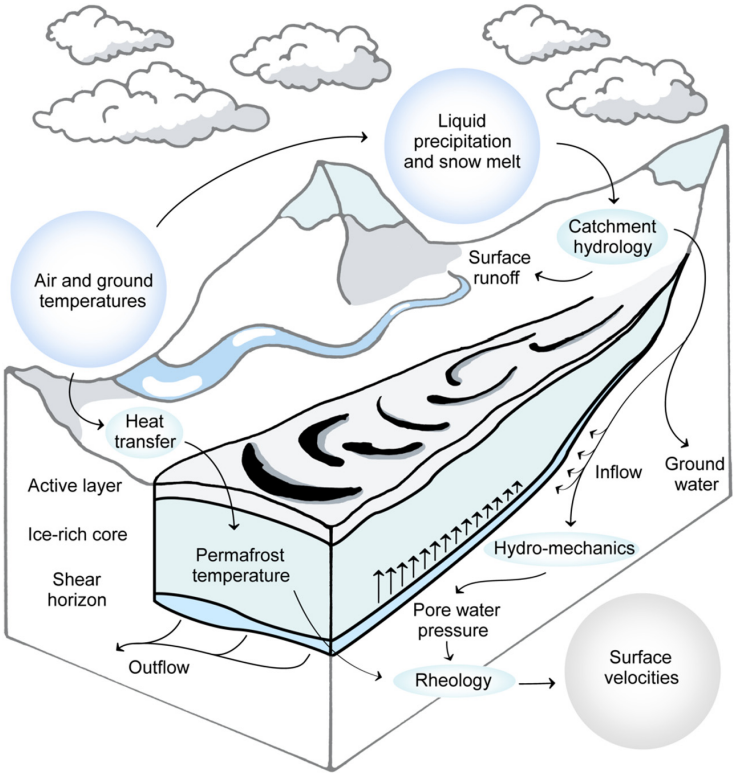

Fig. 1. Conceptualization of the model and sketch of the moving rock glacier. Climatic forcing (dark blue), model units (light blue) and modelled surface velocities (grey) are highlighted by coloured bubbles. The interactions between the model units and the physical variables are depicted with arrows.

glacier creep (e.g. Kääb et al., 2007; Haeberli et al., 2006; Delaloye et al., 2010). Overall, external temperature forcing is thought to be the most prominent factor controlling rock glacier flow variations at both inter-annual and seasonal time scales. However, a numerical modelling study by Cicoira et al. (2019) has quantitatively shown that the influence of temperature forcing through heat conduction on rock glacier rheology alone cannot explain the observed seasonal and inter-annual flow variations. Based on numerical modelling and field observations, they speculate that water must play an important role, especially at the shear horizon depth, where most of the deformation occurs (Arenson et al., 2002).

Evidence that water possibly influences rock glacier creep has already emerged earlier (amongst others: Shroder, 1978; Giardino and Steven, 1985; Krainer and Mostler, 2006; Ikeda et al., 2008; Delaloye et al., 2010; Hartl et al., 2016) and has in extreme cases also been linked to local destabilization (Gärtner-Roer et al., 2008; Delaloye et al., 2013; Buchli et al., 2018). Several geophysical investigations and laboratory experiments (e.g. Arenson et al., 2002; Arenson and Springman, 2005b) as well as theoretical studies on rock glacier rheology (Ladanyi, 2003; Arenson and Springman, 2005a; Jansen and Hergarten, 2006) confirmed the potential influence of water on creep. Recent studies (Wirz et al., 2016; Kenner et al., 2017; Buchli et al., 2018) concur to the conclusion that temperature is the main driver governing rock glacier dynamics and that water (from snow melt and liquid precipitation) can play an important role in controlling seasonal and inter-annual flow variations, but the used approaches remain qualitative.

A deeper and more quantitative understanding of rock glacier dynamics is essential to predict their future evolution and interpret their geological history. In context of continuing atmospheric warming, rock glaciers may potentially represent globally significant water sources of increasing importance especially in arid and semi-arid regions (e.g. Jones et al., 2018; Schaffer et al., 2019). In steep alpine catchments, rock glaciers can pose a considerable risk to villages and infrastructures because of their direct influence on debris flow activity (Kummert and Delaloye, 2018). Rock glaciers are also of interest in the field of planetary science for identifying ground ice (e.g. Carr, 1987). In summary, rock glaciers have attracted increasing attention in the past decades, especially because of the strong connection between their movement and rising surface temperatures (Delaloye et al., 2010; Sorg et al., 2015; PERMOS, 2019), but their relation to climate remains poorly understood and lacks quantitative models.

Here, we investigate the dynamic response of rock glacier flow to variations in external temperature and water input at seasonal and inter-annual time scales by designing a novel conceptual and numerical modelling approach. The modelling is constrained and the results are compared against kinematic, geophysical and meteorological observations for the study case of Dirru Rock Glacier in the Swiss Alps. Using this approach, we critically discuss the hypothesis that water input through pore water pressure at the shear horizon can explain seasonal and inter-annual variations in rock glacier flow and interpret the relation between climatic forcing and driving processes.

2. Mathematical description of the model

The modelling framework consists of four coupled units describing heat transfer into the ground, the catchment hydrology, the hydro-mechanics of the rock glacier and its rheology (Fig. 1). The dynamics of the rock glacier is described by two independent power-law creep relations representing deformation in the

ice-rich core and in the shear horizon of the rock glacier (see Fig. 1). Similarly to Cicoira et al. (2019), we calculate the deformation within the ice-rich core by using the temperature dependent model proposed by Arenson and Springman (2005a), whereas for capturing the influence of pore water pressure on deformation rates in the shear horizon, we use the creep-law proposed by Ladanyi (2003). According to the scope of the manuscript, the modelling aims at simplicity while capturing all the essential processes needed to understand the physics behind seasonal variations in rock glacier creep. Adding more processes and variables to the modelling would increase the complexity of the study, hindering the interpretation of the results and the logic of the conclusions. Therefore, we neglect several secondary processes and assume that the properties of the rock glacier material are constant in time and homogeneous in space.

2.1. Heat conduction model

We calculate ground temperature evolution at depth using the observed ground surface temperature time series as input. The diffusion equation for temperature is solved on the vertical direction (Carslaw and Jaeger, 1959):

$$\frac{\partial T}{\partial t} = \kappa \frac{\partial^2 T}{\partial z^2}, \tag{1}$$

where T [°C] is the temperature, z [m] the vertical coordinate, t [days] the time, and κ [$m^2\,°C^{-1}\,day^{-1}$] the thermal diffusivity of the ground material. At the upper boundary, the observed ground surface temperature time series truncated at 0 °C is prescribed. At the bottom of the rock glacier, just below the shear horizon, the temperature value is set to a constant value close to the melting point T_b (−0.2 °C) according to observations in nearby rock glacier boreholes in Canton Vallis (Zenklusen Mutter and Phillips, 2012; Buchli et al., 2018). The initial condition is prescribed as a constant vertical temperature profile with initial temperature T_0 (−1 °C). In order to avoid initialization effects, we spin the model up by prescribing the data of the eight years time series prior to the model simulation starting in year 2011. The temporal resolution of the model is 1 day, its spacial resolution is 0.1 m. Convective and advective heat fluxes, the influence of basal heating due to frictional processes, and geothermal heat flux are neglected as a first approximation.

2.2. Hydrological model

We calculate the ground-water discharge contributing to the rock glacier shear horizon on the basis of observed liquid precipitation, and near ground and air temperature time series. Liquid precipitation p_{rain} [$mm\,day^{-1}$] and air temperature T_{Air} [°C] are measured at the weather station nearby the Dirru Rock Glacier (see Fig. 2), 350 m away from the GPS positions. The snow melt rate p_{snow} [$mm\,day^{-1}$] is modelled using a degree day model:

$$p_{snow} = k_d(T_{air} - T_{melt}), \tag{2}$$

where k_d [$mm\,°C^{-1}\,day^{-1}$] is the degree day factor for snow melt, and T_{melt} [°C] is the melting temperature of snow set to 0 °C. Snow melt is calculated during the period when the observed ground surface temperatures show isothermal conditions at the melting point (detection of zero curtain). The model is based on the assumption that snow melt is occurring simultaneously and homogeneously in the entire contributing catchment, neglecting in first approximation the spatial variability of the process (temperature lapse rate, influence of the aspect etc.). As soon as all the snow has melted, the ground surface temperature can rise above 0 °C and melt-water production from snow ceases. Note that with this approach, we directly calculate snow melt rates without the need for snow depth or solid precipitation data. Possible delays and variations in magnitude due to melt water retention within the snow pack and snow cover variability within the catchment are not considered. The total water input p_{tot} in the catchment contributing to the shear horizon is thus given by the sum of the previous two contributions multiplied by the area of the catchment A_c:

$$p_{tot}(t) = A_c\,(p_{snow} + p_{rain})\,. \tag{3}$$

In a next step, we calculate the amount of ground-water that flows into the rock glacier shear horizon by modelling the hydrological response of the catchment to liquid precipitation and snow melt input. We thus transform the hyetograph into an hydrograph applying a Gaussian function:

$$Q_{in}(t) = I_c \frac{p_{tot}(t)}{\sigma\sqrt{2\pi}} e^{-\frac{1}{2}\left(\frac{t-\mu}{\sigma}\right)^2}, \tag{4}$$

where σ and μ are two Gaussian parameters representative of the sharpness and delay of the hydrological response of the catchment. When applying this transformation the total mass of the water input is conserved. In order to calculate only the fraction of the water mass influencing the shear horizon (inflow in Fig. 1 and Fig. 3) the surface runoff and the ground water which is not influencing the rock glacier have to be excluded. To do so, we multiply the obtained discharge by the constant inflow coefficient I_c.

2.3. Hydro-mechanical model

We calculate the effective pressures and the discharge at the rock glacier shear horizon using a 1-D hydrodynamical model forced with the water input described above. We assume the shear horizon to be an homogeneous material in saturated conditions, and the above rock glacier ice-rich core to be an impermeable confining unit. Thus, we describe the behaviour of the rock glacier shear horizon as an artesian aquifer by coupling the Darcy flow law for water flow in porous material to the mass balance conservation equation:

$$Q_{in} - Q_{out} = \frac{\Delta(P_A A_{sh})}{\Delta t}, \tag{5}$$

$$Q_{out} = \frac{k}{\mu L} A\phi (P_A - P_B), \tag{6}$$

where Q_{in} and Q_{out} [$m^3\,day^{-1}$] are the water inflow and outflow from the shear horizon respectively, k [$m^2\,day^{-1}$] is the hydraulic conductivity of the shear horizon material, μ [Pa s] is the dynamic viscosity of water, L [m] is the length of the rock glacier from the point in which the ground-water is entering the shear horizon to the steep front, A [m^2] is the area of the average shear horizon cross section, ϕ [–] is the porosity of the shear horizon material, and P_A and P_B [Pa] are the pressure at the bottom of the rock glacier top and front respectively. The model assumes that only water from upstream of the rock glacier contributes to the shear horizon and in first approximation excludes contributions from the sides and from the rock glacier itself. The water pressure at the rock glacier front is assumed equal to the atmospheric pressure, so negligible in an hydrodynamical sense.

Prior to model the deformation profile of the rock glacier, the evaluation of mechanical properties of the shear horizon material is needed. We calculate the effective stresses σ_e [Pa] and the shear resistance τ_r [Pa] of the shear horizon material on the basis of geometrical information and the modelled water pressure. The effective stresses are calculated by applying the Terzaghi law:

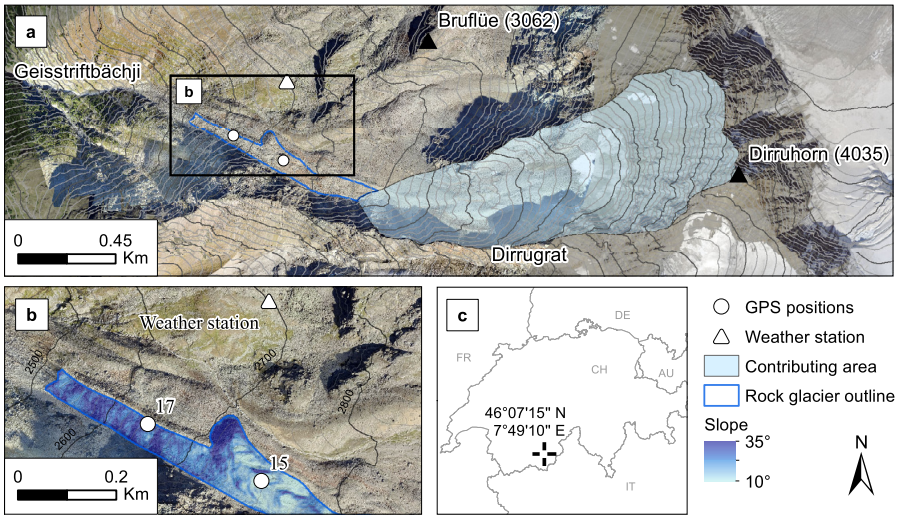

Fig. 2. Overview map of the study site. (a) Aerial view of the rock glacier (blue outline) and its contributing hydrological catchment (light blue shading). (b) Detailed view of Dirru Rock Glacier. The slope angle of the rock glacier surface is shown in blue shaded colours. For panels (a) and (b) the positions of the GPS sensors (December 2018) and the weather station are indicated by labelled markers. Panel (c) shows the geographical overview map of the study site in central Europe. The aerial imagery and elevation data have been collected in a field campaign on September 2017 by Alessandro Cicoira and Nico Mölg. The coordinates of the rock glacier are given in the WGS 84 coordinate system.

$$\sigma_e = \rho_{rg} g H \sin\alpha - P_A, \tag{7}$$

where ρ_{rg} is the density of the rock glacier material, given by the averaged mean between ice density ρ_{ice} [kg m^{-3}] and rock density ρ_{rock} [kg m^{-3}] and controlled by the volumetric ice content w_i [%]:

$$\rho_{rg} = \rho_{ice} w_i + \rho_{rock}(1 - w_i). \tag{8}$$

After calculating the effective stresses, we calculate the shear resistance by applying the Mohr-Coulomb criterion:

$$\tau_r = \sigma_e \tan\phi_c + \tau_{c\theta}, \tag{9}$$

where $\tau_{c\theta}$ [Pa] is the cohesion and ϕ_c is the friction angle of the shear horizon material.

2.4. Ice creep model

For modelling rock glacier creep we divide the rock glacier into two units: the ice-rich core and the shear horizon (Fig. 1). For modelling the deformation in the ice rich core, we use the empirically derived creep relation proposed by Arenson and Springman (2005a), similarly to a previous study by Cicoira et al. (2019). The creep relation is a modified Glen's flow law, that relates strain rate $\dot{\varepsilon}$ [day^{-1}] to the shear stress σ taking into account the volumetric ice content [w_i] and the temperature [T] of the rock glacier material:

$$\dot{\varepsilon}(z,t) = A(z,T,w_i)\sigma(z)^{n(w_i)}. \tag{10}$$

The flow law exponent n linearly depends on the volumetric ice content only:

$$n = 3w_i, \tag{11}$$

and the creep parameter A [Pa^{-n} day^{-1}] depends on temperature and ice content by two independent factors:

$$A(z,t) = e^{\frac{2}{1+T(z,t)}} + b(w_i), \tag{12}$$

where $b(w_i)$ is a function of the ice content:

$$b = 5 \times 10^{-11} e^{-10.2 w_i}. \tag{13}$$

For considering the enhanced deformation taking place in the shear horizon and its dependency on pore water pressure, we apply the rheological model proposed by Ladanyi (2003). The deformation rates in the shear horizon are considered to be independent on temperature. In fact the temporal variations in ground temperature at the shear horizon depth are negligible over the time scales considered here. The shear deformation for the case of a dense ice-saturated material ($w_i < 0.6$) is then given by:

$$\dot{\gamma}(z,t) = \dot{\gamma}_c(w_i,T)\left(\frac{\tau(z)}{\tau_{c\theta}(w_i,T) + \sigma_e(t) tan\phi_c(w_i)}\right)^{n(w_i)}, \tag{14}$$

where the critical shear strain rate $\dot{\gamma}_c$ and the cohesion $\tau_{c\theta}$ are two model parameters of shear deformation, and ϕ_c is the friction angle of the shear horizon material. The total velocity v_{tot} is the sum of the contribution of the deformation taking place in the shear horizon and in the ice rich core

$$v_{tot}(t) = \int_{D_{sh}}^{D_{ic}} \dot{\gamma}(z,t)dz + \int_{D_{ic}}^{D_{al}} \dot{\varepsilon}(z,t)dz. \tag{15}$$

3. Field site and model calibration

Dirru Rock Glacier is a steep, fast moving rock glacier located above the village of Herbriggen in Mattertal (Vallis - CH) (Fig. 2a). It originates from the north slopes of the Dirrugrat, the west ridge of Dirruhorn (4034 m a.s.l.), at an elevation ranging from 2900 to 3400 m a.s.l. The lithology mainly consist of metamorphic crystalline formations, with prevailing muscovite-biotite gneiss. The rock glacier can be divided into two main parts: an upper section, characterized by a gentle slope ($\sim$ 15°) with distinct cross cutting furrow and ridges, and a lower, narrower and steeper ($\sim$ 25°) section where the highest velocities are observed (Fig. 2b). The movement of the rock glacier has been for the past decades and

is currently extremely fast in comparison to similar landforms in the Alps. Therefore, Dirru Rock Glacier represents an end member in the spectrum of rock glacier dynamics. Information from geophysical surveying (electrical resistivity tomography, ERT) and field observations allow a rough estimate of the thicknesses of the creeping part of the rock glacier of about 15-20 m and 20-25 m for the steep and gentle units respectively (R. Delaloye, personal communication).

Air and ground surface temperature time series, along with liquid precipitation measurements are available from spring 2011 to present (Fig. 3a-b) without substantial data gaps. Ground surface temperature is measured at the two GPS sensor positions using three temperature loggers (Maxim iButton DS1922L, Fig. 2a-b). Air temperature and liquid precipitation are measured at the weather station (Vaisala WXT520, Fig. 2a-b). Stationary L1-DGPS sensor (Wirz et al., 2014) provide position measurements (thus velocity) over the same time period. GPS data are missing for almost one year from late summer 2012 to spring 2013 (Fig. A.6). For the purposes of this study, temperature and liquid precipitation data are re-sampled from hourly to daily values, whereas the velocity data is filtered with a two-weeks running mean. All the time series are available from *http://data.permasense.ch*.

3.1. Parameter calibration and model set-up

The model parameters have been calibrated within a physical range constrained by literature via an empiric approach, i.e. visually comparing the model results with the velocity observations for position 17.

The geometry of the rock glacier has been evaluated on the basis of topographical data and geophysical surveys. The slope of the rock glacier (25°) is defined as the mean slope between two points 100 m up and down slope of the GPS positions. Cartographic data at sub-meter resolution obtained in a field survey in September 2017 allow to estimate the length (600 m) and the width (50 m) of the rock glacier. Similarly, it is possible to calculate the area of the contributing catchment, which is 0.3 km^2 for the Dirru Rock Glacier. The thickness of the creeping rock glacier is calibrated to 16 m and 23 m for the lower and upper position respectively, according to the constrains given by field observations and geophysical measurements.

Due to the limited area of the hydrological catchment, its high alpine setting and the high values of the slope, we calibrate the parameters of the hydrological model in order to describe a quick reactive catchment. Therefore, we set both μ and σ equal to 5 days so that, after the water input signal, the discharge peak is reached in 5 days and 68% of the water mass is discharged by the catchment within 10 days (95% in 20 days etc.).

The degree day model was set up according to Pellicciotti et al. (2005), with $T_{melt} = 0\,°C$ and $f_s = 8$ mm day^{-1} $°C^{-1}$.

Consistent with geotechnical investigations from rock glacier boreholes (Arenson et al., 2002; Krainer et al., 2015; Buchli et al., 2018), the hydraulic conductivity of the shear horizon material has been constrained in a typical range for frozen silt and gravel (Burt and Williams, 1976). The hydraulic conductivity k has been set to 1×10^{-10} m day^{-1}. The inflow coefficient I_c has been fixed to 0.01 under the assumption that a constant fraction of 1% of the total water input reaches the shear horizon, according to literature (Krainer and Mostler, 2002; Jones et al., 2019).

In the creep relation proposed by Arenson and Springman (2005b), the volumetric ice content w_i of the rock glacier is the only calibration parameter. According to other studies for nearby rock glaciers (Cicoira et al., 2019), we set the volumetric ice content to 0.7. When modelling the dynamic behaviour of the shear horizon with the rheology proposed by Ladanyi (2003) evaluation of other mechanical properties of the ground material is needed. The friction angle for rock glacier material has been measured in laboratory experiments by Arenson and Springman (2005a) and a parametrization has been proposed based on the volumetric ice content:

$$\phi_c = 32.5(1 - w_i^{2.6}). \tag{16}$$

The value of the cohesion $\tau_{c\theta}$ is set to 20 kPa on the basis of studies on frozen soils (e.g. Czurda and Hohmann, 1997; Arenson and Springman, 2005b). The creep relation exponent n is calculated following the parametrization proposed by Arenson and Springman (2005b). The parameter $\dot{\gamma}_c$ is calibrated to 0.008 day^{-1} in order to match the mean value of the observed velocities. A test on this parameter can be performed calculating the corresponding reference strain rate $\dot{\varepsilon}_c$ at the given reference stress $\sigma_{c\theta}$ and comparing our results with laboratory experiments. In order to do so, we inverted the equation proposed by Ladanyi (2003), obtained assuming the validity of the von Mises flow rule:

$$\dot{\gamma}_c = 3^{\frac{n+1}{2}} \dot{\varepsilon}_c. \tag{17}$$

Given that $\sigma_{c\theta}$ is a value comprised between 100 kPa and 200 kPa (Wahrhaftig and Cox, 1959), the calculated reference strain rate for rock glacier material $\dot{\varepsilon}_c = 1 \times 10^{-8}$ s^{-1} results in good accordance with the laboratory experiments by Arenson and Springman (2005b) for rock glacier material at the considered temperature, volumetric ice content and stress conditions.

4. Results

4.1. Thermal regime of the rock glacier

In a first step to resolve the influence of external forcing on rock glacier dynamics, we model the evolution of ground temperatures at depth. The observed ground surface temperatures, used as input in our model, rise above zero in spring (between mid April and the beginning of May), and turn negative again in autumn (blue line in Fig. 3b). The annual minimum ground surface temperatures are generally observed in late January ranging from −11 °C to −4 °C; the maximum temperatures reach 20 °C in the warmest years. In order to take into account the zero curtain effect in the heat conduction model, the observed ground surface temperatures are truncated at 0 °C. Therefore, the minimum winter temperatures correspond to the seasonal amplitude (Fig. 3d). The observed truncated mean annual ground surface temperatures range from −2.3 °C to −1.2 °C (Fig. 3d). The modelled temperature signal (Fig. 3f), calculated from prescribing the observed truncated ground surface temperatures (Fig. 3d), is linearly delayed and its amplitude exponentially decreases with depth (Carslaw and Jaeger, 1959; Haeberli et al., 2006). At a depth of 15 m, corresponding to the shear horizon position, the modelled seasonal amplitude is reduced to 0.5 °C (one order of magnitude smaller than the external forcing amplitude) and the temperature minima show a phase lag of approximately 5 months (Fig. 3f).

4.2. Hydrological response of the catchment

In a second step to describe rock glacier dynamics, we quantify the influence of water at the rock glacier shear horizon. We calculate the water contribution from the catchment originating from liquid precipitation and snow melt (Fig. 3a). Liquid precipitation events are generally observed from the snow melt period onwards until late autumn (Fig. 3a). From year to year the distribution of the precipitation events varies. The highest value of precipitation intensity has been measured in summer 2012, slightly exceeding 50 mm day^{-1}. In summer 2014 and 2015 similar values have been observed. During the winter and spring months

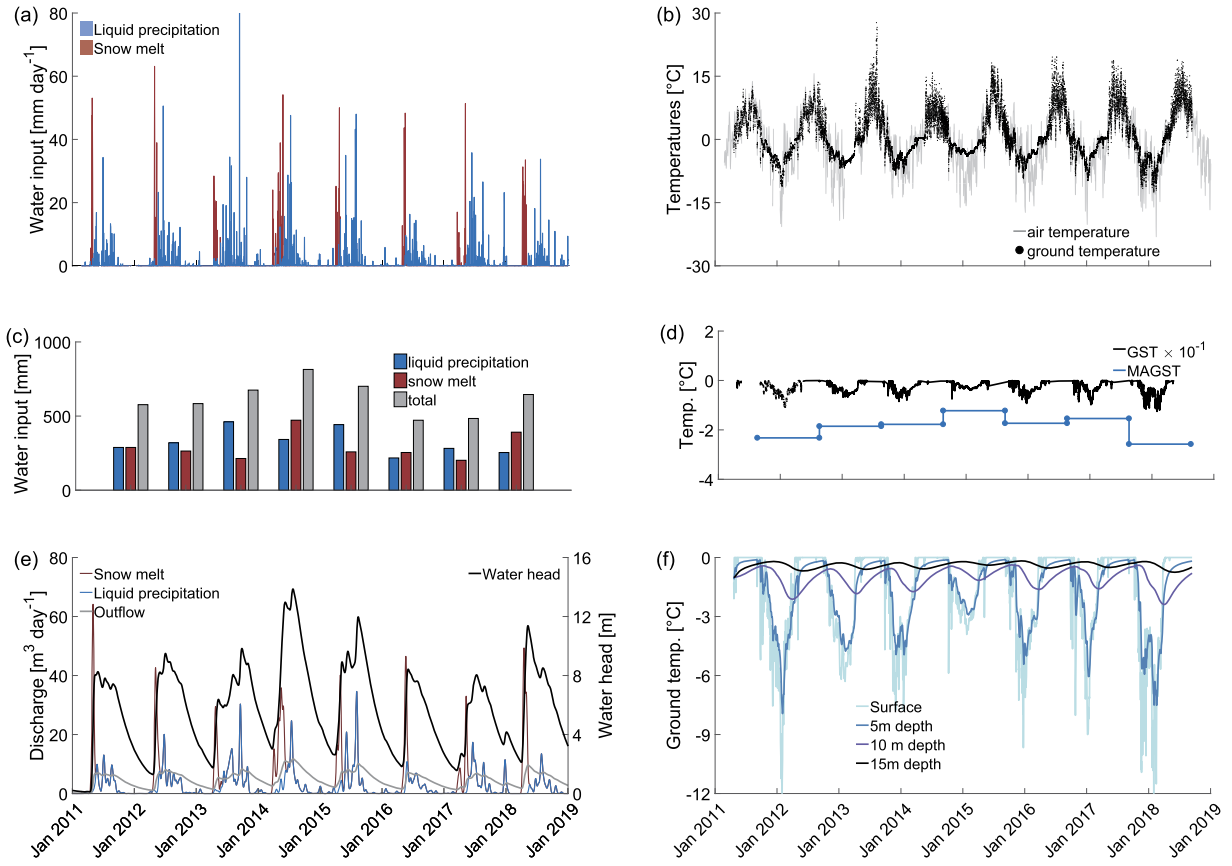

Fig. 3. Modelling input and results. (a) Measured liquid precipitation (blue) from the weather station and modelled snow melt rates (red). (b) Observed ground surface (black dots) and air (grey line) temperatures. (c) Yearly cumulative values of liquid precipitation (blue) and snow melt (red), and total contribution (grey). (d) Ground surface temperature (black line) truncated at 0 °C (scaled by a factor 10^{-1}) and its annual mean (MAGST, blue line) calculated for the hydrological year. (e) Results of the hydro-mechanical model. The output of the hydrological model is used here as input (Snow melt and Liquid precipitation components, blue and red lines). The outflow and the water head at the bottom of the rock glacier are shown with a grey and a black line respectively. (f) Results of the thermodynamic model. The modelled ground temperatures for position 17 are plotted against time at the surface (light blue, same as GST in panel d), at 5 m (dark blue), at 10 m (violet) and at 15 m (black) depth.

the solid precipitation contributes to the formation of the seasonal snow cover in the catchment. Snow melt, as inferred from the zero curtain effect, generally begins at the end of April and lasts several weeks, generating the highest water input rates, with peaks of up to 60 mm day^{-1}. The cumulative precipitation is low for an alpine setting and varies between 500 mm in 2016 and 810 mm in 2014 (Fig. 3c). On the basis of the water input, we model the hydrological response of the catchment and calculate the fraction of ground-water discharge influencing the rock glacier shear horizon (inflow in Fig. 1). The modelled discharge shows a multi-modal distribution for all years of the time series (Snow melt and Liquid precipitation in Fig. 3e). The yearly discharge maxima range from 15 to 40 m^3 day^{-1} with the highest values occurring after an abrupt increase in spring due to snow melt. Further local peaks due to liquid precipitation occur during summer but do not exceed 20 m^3 day^{-1}. During autumn, the inflow to the shear horizon decreases to zero as a consequence of the ceased water input.

4.3. Hydro-mechanical behaviour of the shear horizon

Using the Darcy flow law, we model the hydraulic behaviour of the rock glacier shear horizon (outflow and pore water pressure (water head) in Fig. 1 and Fig. 3e). The resulting seasonal flow pattern at the rock glacier front (grey line in Fig. 3e) is reduced to an almost singular summer peak showing clear variations in magnitude from year to year but never exceeding 10 m^3 day^{-1}, corresponding to water flow velocity values lower than 10^{-6} m s^{-1}. In winter, the outflow from the shear horizon asymptotically decreases but always remains above zero. The water head ranges from a minimum of 1 m to a maximum of 13 m (black line in Fig. 3e), corresponding to 10 kPa and 130 kPa of pore water pressure respectively. Although a sudden rise in pressure occurs at the onset of the snow melt period, the yearly maximum is reached later in the season as a consequence of the combined contribution from snow melt and liquid precipitation.

4.4. Rock glacier flow

We model rock glacier flow using two independent creep relations for the ice rich core (Arenson and Springman, 2005a) and the shear horizon (Ladanyi, 2003) forced by external temperature and water input respectively. The modelled flow velocities are compared against the 3D surface velocities obtained from GPS measurements (Fig. 4) for the two positions on the rock glacier (Fig. 2a-b). Because of the chaotic nature of the high-frequency velocity peaks present in the kinematic data (Wirz et al., 2014), we filter the velocity signal by applying a two weeks running mean. The complete time series of GPS positions used to calculate the velocities are shown in supplementary Fig. A.6. Below, we first describe the results for position 17, located in the fast flowing and

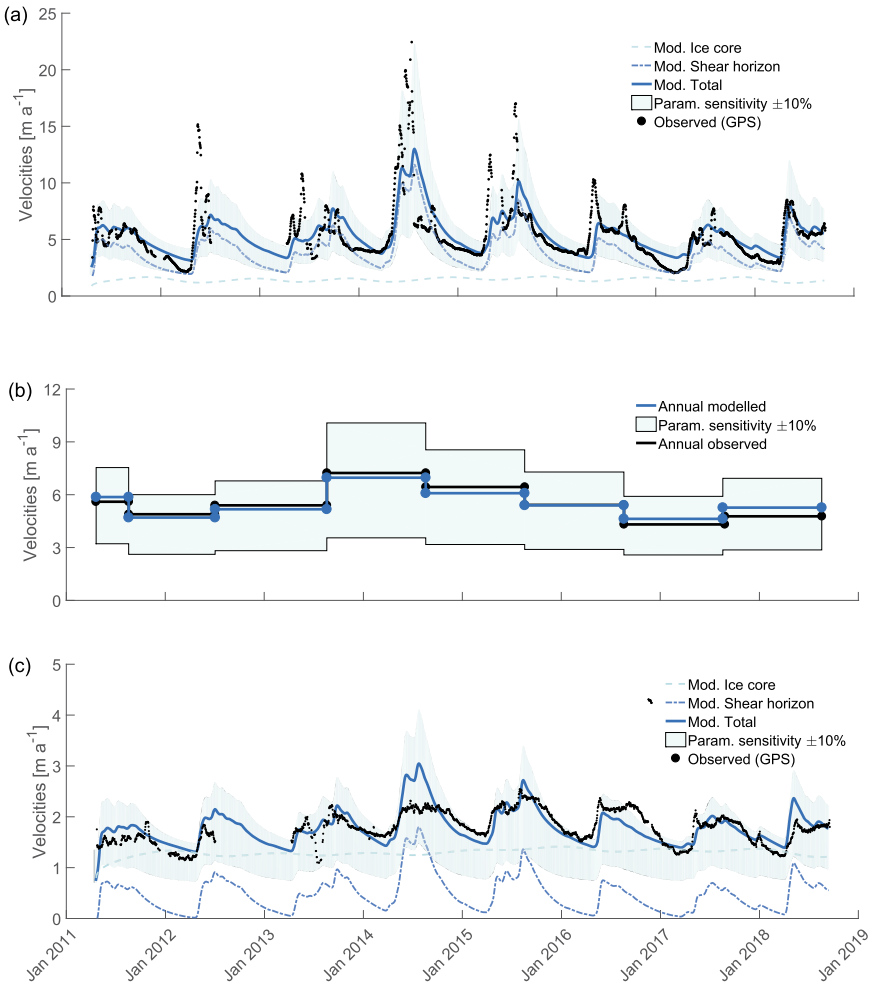

Fig. 4. Observed (black dots) and modelled (blue lines) velocity time series for position 17 (a-b) and position 15 (c). The total modelled velocities (solid blue line in (a) and (c)) are the sum of the contributions from the ice-rich core (dashed light blue) and the shear horizon creep model (dash-dotted light blue). The light blue shaded areas encompass the modelled velocities when varying all the non-geometrical model parameters by ±10% (Param. sensitivity). (b) Mean annual velocities calculated over the hydrological year. The observed annual velocity (black line) is calculated directly from the GPS position displacements between two consecutive years (1st of September). The modelled annual velocities (blue line) are calculated by averaging the modelled velocities over the same time period.

thin part of Dirru Rock Glacier, for which the model has been calibrated (Fig. 4a and b). We then use the results for the contrasting geometrical setting at position 15 (Fig. 4c), obtained with the same model calibration, as an independent test for our modelling approach.

The observed eight year velocity time series (black dots in Fig. 4a) substantially extend the data of Wirz et al. (2016) and confirm the distinct seasonal flow rhythm of Dirru Rock Glacier. In late spring, the flow velocity exhibits a yearly minimum ranging from 2 m a^{-1} (2017) to 4 m a^{-1} (2014). The minima are directly followed by an abrupt acceleration at the onset of the snow melt period, which leads to a first annual maximum. After this early summer peak, the velocity slightly decreases for a short period of time, before accelerating again and reaching another maximum in late summer. After this phase, the velocity decreases asymptotically to the next spring minimum. The observed seasonal variations in velocity vary from 4 m a^{-1} to 15 m a^{-1} for year 2017 and 2014 respectively with a mean value of 7 m a^{-1} (Fig. 4a).

The modelled velocity (blue solid line in Fig. 4a) is the sum of the two contributions from the ice-rich core and the shear horizon velocities (dashed and dash-dotted blue line in Fig. 4a). The velocity component of the ice-rich core (thermally controlled) never exceeds 2 m a^{-1} and the related seasonal variations are limited to below 0.5 m a^{-1} (dashed blue line in Fig. 4a). In accordance with the results of Cicoira et al. (2019), the observed velocity variations are strongly underestimated and the modelled seasonal pattern exhibits a phase lag of one to five months to the observations.

The modelling improves when including the description of the shear horizon dynamics forced by water input (dash-dotted blue line in Fig. 4a). In fact, we obtain seasonal velocity variations in the correct order of magnitude for all years of the time series, with maximum modelled values up to 8 m a^{-1}). Moreover, the modelled shear horizon velocity is in phase with the observations.

When combining the two velocity contributions (ice-rich core and shear horizon), the total modelled velocities reproduce the observed seasonal pattern well (blue solid line against black dots in Fig. 4a). For the eight year time series, the average modelled velocities match the observed 5.5 m a^{-1} calculated from GPS measurements. The model performs well in simulating the timing and rapid acceleration during the snow melt season as well as the de-

layed annual velocity maximum. Also, the inter-annual variability of the spring minima is captured by the model although in some years (e.g. 2011 and 2017) only part of the variation is reproduced. Moreover, in the modelling, the shear zone accounts for more than 70% of the total deformation in the rock glacier, in good accordance with borehole observations for other sites (Arenson et al., 2002; Krainer et al., 2015; Buchli et al., 2018) Possible variations in the non-geometrical parameters ($\pm$10%) do not change the above findings and the resulting velocity range encompasses almost the entire observed velocity signal (light blue area in Fig. 4a).

In order to investigate inter-annual flow variations, we calculate mean annual velocities (Fig. 4b) as typically monitored for many rock glaciers in the Alps (PERMOS, 2019). The observed mean annual velocities (black line) are directly calculated from the measured GPS positions at the beginning of two consecutive hydrological years (1st September). The observed and the modelled annual velocities are in very good agreement (black and blue line in Fig. 4a respectively), showing discrepancies lower than 10% with a multi-annual trends varying between 4.3 $\mathrm{m\,a^{-1}}$ (2017) to 7.2 $\mathrm{m\,a^{-1}}$ (2014).

In order to test the validity of our results, we repeat the flow modelling for Position 15 (Fig. 4c), characterized by a gentler slope (only 15°) and lower velocities (mean surface velocity equal to 1.6 $\mathrm{m\,a^{-1}}$). The model performs similarly well for this additional position when using the same model calibration as for position 17 and only adjusting the geometrical input values of rock glacier slope and thickness. For this position, the seasonal variations in velocity are lower in absolute and relative terms (values up to 1 $\mathrm{m\,a^{-1}}$) and the contribution of the shear horizon to the total deformation is lower than for the steeper position 17.

5. Discussion

5.1. Rock glacier thermodynamics

Temperature forcing through heat conduction has been proposed as one of the key processes to explain seasonal and inter-annual variations in rock glacier creep. In order to test this hypothesis, we model rock glacier temperature evolution at depth and its influence on rock glacier creep. Our results confirm that temperature forcing cannot explain the seasonal phase of the surface velocities and can only account for a limited fraction of the observed velocity variations. Here, we consider only heat conduction forced by ground temperature variations and thereby neglect processes like advective and turbulent fluxes (e.g.: Zenklusen Mutter and Phillips, 2012; Wicky and Hauck, 2017). Cicoira et al. (2019) showed that this approach is suited for modelling the temperature evolution at depth and its influence on rock glacier velocities. According to the results for the Ritigraben Rock Clacier, the calibration of the volumetric ice content parameter influences the absolute value of the surface velocity but has no substantial effect on the velocity amplitude. Moreover, the seasonal amplitude of the temperature is overestimated when neglecting the dampening effect of the active layer in the modelling. The obtained underestimation of the seasonal variations and phase lag in velocity are therefore robust and thereby confirm previous findings from other sites (Murtél, Muragl, Schafberg and Ritigraben Rock Glaciers, in Cicoira et al., 2019) for the fast flowing and thin Dirru Rock Glacier.

5.2. Rock glacier hydrology

In a second step for describing the physical system, we include in the modelling the influence of water input on the shear horizon dynamics. The Gaussian function used for representing the catchment hydrology is described by only two parameters, which offer a clear physical interpretation. The first model parameter μ represents the delay time of the catchment response to water input. The second parameter σ describes the reactivity of the hydrological catchment. By setting both parameter values equal to 5 days, we represent a quickly reactive catchment, typical of high mountain environments (Brunner et al., 2018). In the modelling, the discharge peak is reached 5 days after the water input and 68% of the water mass is discharged from the catchment within 10 days (95% in 20 days etc.).

Although the snow melt and hydrological models are simple, they are physically interpretable and have the advantage of being directly forced by in-situ observations. Uncertainties in the calibration of the two hydrological parameters have only minor effects on the velocity results. The value of μ has no effect on the amplitude and only a linear influence on the velocity signal phase; σ has no control on the phase and no substantial effect on the amplitude. In fact, for varying the two parameter values within one order of magnitude (from 1 to 10 days), the shift in velocity phase remains below the time scales considered in this study and therefore negligible, and the variations in velocity amplitude between the two end members do not exceed 25%.

When ground-water flow reaches the shear horizon, it influences its pressure regime and its mechanical state. The water flow throughout the shear horizon, from the uppermost part of the rock glacier to its steep front, is here described using the Darcy flow law for porous materials (Darcy, 1856) under the assumption of confined conditions (Fig. 1). This conceptual model is supported by both field observations and laboratory experiments. Firstly, in borehole drillings at several rock glaciers in the Alps, pressurized water with water head values up to the rock glacier thickness have been directly observed at the shear horizon depth (Arenson et al., 2002; Kenner et al., 2017; Buchli et al., 2018). Secondly, a distinct increase in the volumetric content of solid particles in correspondence with the shear horizon depth (and the related decrease in volumetric ice content) has been observed at the same and other borehole locations (Arenson and Springman, 2005b; Krainer et al., 2015). Hydraulic conductivity theory has been successfully applied to frozen soils with high solid particle contents (Burt and Williams, 1976) and considerable hydraulic conductivities have been found also at low temperatures (from 1×10^{-12} to 1×10^{-8} $\mathrm{m\,day^{-1}}$). The hydraulic conductivity value used in the modelling (1×10^{-8} $\mathrm{m\,day^{-1}}$) is consistent with this range and produces maximum water head values of up to 13 m, corresponding to 80% of the rock glacier thickness. These values of water heads are physically acceptable, because the pressure corresponding to the water column does not exceed the weight of the rock glacier itself, which would cause unrealistic uplift forces. Moreover, the very low values of water discharge obtained with this calibration at the rock glacier front are in agreement with field observations of no visible flowing water in correspondence of the shear horizon depth.

5.3. Rock glacier dynamics

We calculate surface flow velocities for Dirru Rock Glacier by combining the two independent creep models for the ice rich core (driven by external temperature forcing) and the shear horizon (driven by liquid precipitation and snow melt). Our model simulates the correct mean velocity value for the Dirru Rock Glacier when calibrating the parameters within a physically meaningful range according to literature (see Chapter 2). We are able to reproduce the annual velocities and their variations for the entire time series, covering a period of eight years (Fig. 4b). More specifically, the rock glacier flow model also performs well at both the seasonal and multi-annual scale and correctly reproduces the temporal pattern, amplitude, and phase in flow. This confirms that the abrupt

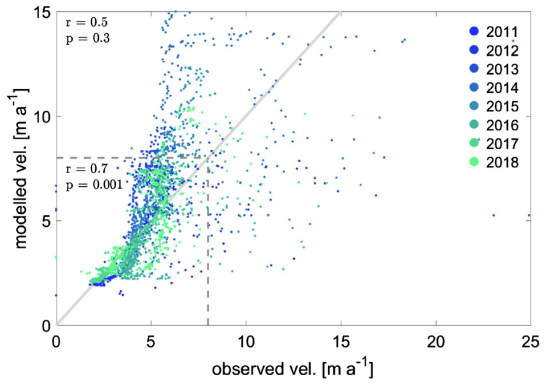

Fig. 5. Scatter plot of modelled against observed velocities. The data points are divided into different years by colour. The bisect of the first quadrant is depicted in light grey. The correlation coefficient r and the relative significance value p are reported for both the entire dataset and for velocity points below 8 m a^{-1}.

acceleration in early summer is driven by the snow melt and suggests that the subsequent velocity maxima during the summer are caused by the combined contribution of snow melt and liquid precipitation. In the modelling, the rate of deceleration during the winter is determined by the absolute values of the hydraulic conductivity and the water pressure, which asymptomatically decreases to zero as the water infiltration in the shear horizon ceases.

Two main discrepancies between the model results and the observations, which underline the limitations of the modelling, are notable in Fig. 4. Firstly, the highest velocity values, corresponding to short and sharp peaks, cannot be reproduced by the model. Earlier studies suggested that such peaks may be linked to erratic down-slope movement of boulders on the surface (onto which the GPS sensors are fixed) rather than to the dynamics of the whole rock glacier (Wirz et al., 2014). The absence of such peaks in the velocity data of the second GPS-sensor (position 15; black dots in Fig. 4c) confirms this interpretation. Secondly, the variability in the rate of the descending phase thus the evolution of the velocity minima observed in late spring cannot be reproduced (see Fig. 4a and c). These two inconsistency between the observations and the model results can be attributed to the temporal variations in mechanical and hydraulic properties of the rock glacier material, which in first approximation are neglected in our modelling approach. In fact, it is physically plausible that variations in ground temperature, hydraulic regime of the shear horizon, and displacement rates may influence the mechanical and hydraulic properties and hence the model parameters of the rock glacier material. In accordance to this logic, both discrepancies are potentially explained by our model when considering variations in the non-geometrical model parameters (Parameter sensitivity in Fig. 4a and c).

The modelling results can be further analysed in Fig. 5, where the modelled velocities are plotted against the observations for daily intervals. The distance between the points and the bisector of the first quadrant (grey line), indicate the quality of the performance of the model. For velocity values higher than 6 m a^{-1}, the point cloud is distinctly more scattered. In fact, the correlation between model results and observations for all points ($r = 0.4$ with $p = 0.03$) strongly improves when neglecting the high frequency velocity signal and only considering velocities below 8 m a^{-1} ($r = 0.7$, $p < 0.01$).

The validity of our modelling for describing rock glacier dynamics is further supported by the good agreement between our model results and the velocities observed for position 15 (Fig. 4c) obtained without adjusting the parameter calibration. The reduced contribution of the shear horizon to the total deformation for this position is caused by the reduced relative effect of pore water pressure on the effective normal stresses (due to the higher thickness value). The lower seasonal variations in velocity are a direct consequence of this result, because the velocity variations are almost completely driven by the contribution from the shear horizon.

In order to further assess the influence of the parameter uncertainty on the model results, we performed a multivariate sensitivity analysis of the hydro-mechanical and on the creep models (Fig. B.7). The ability to produce the correct seasonal amplitude with a combination of model parameter values that lay within a plausible range (spanning one order of magnitude) further supports the robustness of our modelling.

6. Conclusions

In this study we developed a process based model to investigate the essential processes controlling rock glacier dynamics at the seasonal and inter-annual time scale. Our results corroborate the hypothesis that the flow rhythm of Dirru Rock Glacier can be explained by water and external temperature, with a preponderant influence of water at the shear horizon depth, which is also indirectly controlled by temperature. This study provides a step forward towards a better understanding rock glacier dynamics, i.e. the coupling between rock glacier creep and the climate system, having manifold important implications for the interpretation of rock glacier movement.

Our case study is extremely fast and it is reasonable to expect other rock glaciers characterized by different internal structure and material properties, and located in different topographic and climatic settings to have a different dynamical behaviour. The fundamental processes governing their flow, however, remain the same. In pursuance of a more thorough understanding of rock glacier dynamics, possible future modelling studies should investigate further landforms, include other secondary water sources, describe additional mechanical processes along with their feedback mechanisms, and consider 3-dimensional effects of changes in geometry over time (Müller et al., 2016). Especially at longer time scales (decadal and beyond), thermodynamic and mechanical processes can strongly influence the properties and the internal structure of rock glaciers causing major variations in their motion, possibly leading to destabilization or degradation. In conclusion, our study underlines the importance of water in determining the seasonal rhythm of rock glacier flow and highlights the complex and non-linear nature of rock glacier dynamics.

Data availability

The GPS data used for rock glacier kinematics and the meteorological data from the automatic weather station are available from *http://data.permasense.ch*. The ground temperatures data are available from the authors upon request.

Author contributions

A.C. designed the conceptual and the numerical model, analysed and interpreted the data. A.C. prepared the figures and wrote the manuscript with substantial contribution and approval from all the authors.

Declaration of competing interest

The authors declare no competing interests.

Acknowledgements

The work presented in this paper is part of the project X-Sense 2 and was financed by nano-tera.ch (ref. no. 530659). This

work could not have been possible without the pioneering pilot project funded by the Swiss Federal Office for the Environment BAFU. The manuscript has been substantially improved through the thorough and professional revision of Lucas Arenson. Special thanks go to Marco Marcer, Nico Mölg, Reynald Delaloye and Samuel Weber for their constructive comments.

Appendix. Supplementary material

Supplementary material related to this article can be found online at https://doi.org/10.1016/j.epsl.2019.115844.

References

Arenson, L., Hoelzle, M., Springman, S., 2002. Borehole deformation measurements and internal structure of some rock glaciers in Switzerland. Permafr. Periglac. Process. 13, 117–135. https://doi.org/10.1002/ppp.414.

Arenson, L.U., Springman, S.M., 2005a. Mathematical descriptions for the behaviour of ice-rich frozen soils at temperatures close to 0 °C. Can. Geotech. J. 42, 431–442. https://doi.org/10.1139/t04-109.

Arenson, L.U., Springman, S.M., 2005b. Triaxial constant stress and constant strain rate tests on ice-rich permafrost samples. Can. Geotech. J. 42, 412–430. https://doi.org/10.1139/t04-111.

Barsch, D., Hell, G., 1975. Photogrammetrische bewegungsmessungen am blockgletscher murtel i, oberengadin, Schweizer Alpen. Z. Gletsch.kd. Glazialgeol. 11 (2), 111–142.

Brunner, M., Viviroli, D., Furrer, R., Seibert, J., Favre, A.C., 2018. Identification of flood reactivity regions via the functional clustering of hydrographs. Water Resour. Res. 54. https://doi.org/10.1002/2017WR021650.

Buchli, T., Kos, A., Limpach, P., Merz, K., Zhou, X., Springman, S.M., 2018. Kinematic investigations on the Furggwanghorn Rock Glacier, Switzerland. Permafr. Periglac. Process. 29, 3–20.

Burt, T.P., Williams, P.J., 1976. Hydraulic conductivity in frozen soils. Earth Surf. Process. 1, 349–360. https://doi.org/10.1002/esp.3290010404.

Capps, S.R., 1910. Rock glaciers in Alaska. J. Geol. 18, 359–375.

Carr, M., 1987. Water on Mars. Nature 326, 30–35. https://doi.org/10.1038/326030a0DO.

Carslaw, H., Jaeger, J., 1959. Conduction of Heat in Solids. Oxford Science Publications. Clarendon Press.

Chaix, A., 1943. Les coulées de bloc du park national suisse. Nouvelles mesures et comparaison avec le rock-streams de la Sierra Nevada de Californie. Le Globe 82.

Cicoira, A., Beutel, J., Faillettaz, J., Gärtner-Roer, I., Vieli, A., 2019. Resolving the influence of temperature forcing through heat conduction on rock glacier dynamics: a numerical modelling approach. Cryosphere 13, 927–942. https://doi.org/10.5194/tc-13-927-2019.

Czurda, K., Hohmann, M., 1997. Freezing effect on shear strength of clayey soils. Appl. Clay Sci. 12, 165–187. https://doi.org/10.1016/S0169-1317(97)00005-7.

Darcy, H., 1856. Les fontaines publiques de la ville de Dijon: exposition et application des principes a suivre et des fomules a emplyer dans les qeustions de distribution d'eau. Victor Dalmont.

Delaloye, R., Lambiel, C., Gärtner-Roer, I., 2010. Overview of rock glacier kinematics research in the Swiss Alps. Geogr. Helv. 65, 135–145. https://doi.org/10.5194/gh-65-135-2010.

Delaloye, R., Morard, S., Barboux, C., Abbet, D., Gruber, V., Riedo, M., Gachet, S., 2013. Rapidly moving rock glaciers in Mattertal. In: Jahrestagung der Schweizerischen Geomorphologischen Gesellschaft, pp. 21–31.

Gärtner-Roer, I., Haeberli, W., Avian, M., Kaufmann, V., Delaloye, R., Lambiel, C., Kääb, A., 2008. Observations and considerations on destabilizing active rock glaciers in the European Alps. In: Ninth International Conference on Permafrost.

Giardino, J.R., Steven, V.G., 1985. The engineering geology hazards of rock glaciers. Environ. Eng. Geosci. 12, 201–216. https://doi.org/10.2113/gseegeosci.xxii.2.201.

Haeberli, W., 1985. Creep of Mountain Permafrost. Mitteilungen der Versuchsanstalt für Wasserbau, Hydrologie und Glaziologie der ETH Zürich, vol. 77.

Haeberli, W., Hallet, B., Arenson, L., Elconin, R., Humlum, O., Kääb, A., Kaufmann, V., Ladanyi, B., Matsuoka, N., Springman, S., Vonder Mühll, D., 2006. Permafrost creep and rock glacier dynamics. Permafr. Periglac. Process. 17, 189–214.

Hartl, L., Fischer, A., Stocker-Waldhuber, M., Abermann, J., 2016. Recent speed-up of an alpine rock glacier: an updated chronology of the kinematics of outer hochebenkar rock glacier based on geodetic measurements. Geogr. Ann., Ser. A, Phys. Geogr. 98, 129–141. https://doi.org/10.1111/geoa.12127.

Ikeda, A., Matsuoka, N., Kääb, A., 2008. Fast deformation of perennially frozen debris in a warm rock glacier in the Swiss Alps: an effect of liquid water. J. Geophys. Res., Earth Surf. 113. https://doi.org/10.1029/2007JF000859.f01021.

Jansen, F., Hergarten, S., 2006. Rock glacier dynamics: stick-slip motion coupled to hydrology. Geophys. Res. Lett. 33. https://doi.org/10.1029/2006GL026134.

Jones, D., Harrison, S., Anderson, K., Whalley, B., 2019. Rock glaciers and mountain hydrology: a review. Earth-Sci. Rev. 193, 66–90. https://doi.org/10.1016/j.earscirev.2019.04.001.

Jones, D.B., Harrison, S., Anderson, K., Betts, R.A., 2018. Mountain rock glaciers contain globally significant water stores. Sci. Rep. 8, 2834–2844. https://doi.org/10.1038/s41598-018-21244-w.

Kääb, A., Haeberli, W., Gudmundsson, G.H., 1997. Analysing the creep of mountain permafrost using high precision aerial photogrammetry: 25 years of monitoring Gruben rock glacier, Swiss Alps. Permafr. Periglac. Process. 8, 409–426. https://doi.org/10.1002/(SICI)1099-1530(199710/12)8:4<409::AID-PPP267>3.0.CO.

Kääb, A., Frauenfelder, R., Roer, I., 2007. On the response of rockglacier creep to surface temperature increase. Glob. Planet. Change 56, 172–187. https://doi.org/10.1016/j.gloplacha.2006.07.005.

Kenner, R., Phillips, M., Beutel, J., Hiller, M., Limpach, P., Pointner, E., Volken, M., 2017. Factors controlling velocity variations at short-term, seasonal and multiyear time scales, Ritigraben rock glacier, western Swiss Alps. Permafr. Periglac. Process. 28, 675–684. https://doi.org/10.1002/ppp.1953.pPP-16-0044.R2.

Krainer, K., Mostler, W., 2002. Hydrology of active rock glaciers: examples from the Austrian Alps. Arct. Antarct. Alp. Res. 34, 142–149. https://doi.org/10.1080/15230430.2002.12003478.

Krainer, K., Mostler, W., 2006. Flow velocities of active rock glaciers in the Austrian Alps. Geogr. Ann., Ser. A, Phys. Geogr. 88, 267–280. https://doi.org/10.1111/j.0435-3676.2006.00300.x.

Krainer, K., Bressan, D., Dietre, B., Haas, J., Hajdas, I., Lang, K., Mair, V., Nickus, U., Reidl, D., Thies, H., Tonidandel, D., 2015. A 10,300-year-old permafrost core from the active rock glacier Lazaun, southern Ötztal Alps (South Tyrol, northern Italy). Quat. Res. 83, 324–335. https://doi.org/10.1016/j.yqres.2014.12.005.

Kummert, M., Delaloye, R., 2018. Mapping and quantifying sediment transfer between the front of rapidly moving rock glaciers and torrential gullies. Geomorphology 309, 60–76. https://doi.org/10.1016/j.geomorph.2018.02.021.

Ladanyi, B., 2003. Rheology of ice/rock systems and interfaces. In: Proceedings of the Eigth International Conference on Permafrost. Lisse, The Netherlands, pp. 621–625.

Lambiel, C., Delaloye, R., 2004. Contribution of real-time kinematic GPS in the study of creeping mountain permafrost: examples from the western Swiss Alps. Permafr. Periglac. Process. 15, 229–241. https://doi.org/10.1002/ppp.496.

Mellor, M., Testa, R., 1969. Effect of temperature on the creep of ice. J. Glaciol. 8, 131–145. https://doi.org/10.3189/S0022143000020803.

Müller, J., Vieli, A., Gärtner-Roer, I., 2016. Rock glaciers on the run – understanding rock glacier landform evolution and recent changes from numerical flow modeling. Cryosphere 10, 2865–2886. https://doi.org/10.5194/tc-10-2865-2016.

Nye, J.F., 1952. The mechanics of glacier flow. J. Glaciol. 2, 82–93. https://doi.org/10.3189/S0022143000033967.

Pellicciotti, F., Brock, B., Strasser, U., Burlando, P., Funk, M., Corripio, J., 2005. An enhanced temperature-index glacier melt model including the shortwave radiation balance: development and testing for Haut Glacier d'Arolla, Switzerland. J. Glaciol. 51, 573–587. https://doi.org/10.3189/172756505781829124.

PERMOS, 2019. Permafrost in Switzerland 2014/2015 to 2017/2018. Noetzli, J., Pellet, C., Staub, B. (Eds.), Glaciological Report (Permafrost) no. 16-19 of the Cryospheric Commission of the Swiss Academy of Sciences. 104 pp.

Schaffer, N., MacDonell, S., Réveillet, M., Yáñez, E., Valois, R., 2019. Rock glaciers as a water resource in a changing climate in the semiarid Chilean Andes. Reg. Environ. Change. https://doi.org/10.1007/s10113-018-01459-3.

Shroder, J.F., 1978. Dendrogeomorphological analysis of mass movement on Table Cliffs Plateau, Utah. Quat. Res. 9, 168–185. https://doi.org/10.1016/0033-5894(78)90065-0.

Sorg, A., Kääb, A., Roesch, A., Bigler, C., Stoffel, M., 2015. Contrasting responses of Central Asian rock glaciers to global warming. Sci. Rep. 5, 8228–8234. https://doi.org/10.1038/srep08228.

Spencer, A., 1900. A peculiar form of talus. Science 11, 188.

Wahrhaftig, C., Cox, A., 1959. Rock glaciers in the Alaska Range. GSA Bull. 70, 383.

White, S.E., 1976. Rock glaciers and block fields, review and new data. Quat. Res. 6, 77–97.

Wicky, J., Hauck, C., 2017. Numerical modelling of convective heat transport by air flow in permafrost talus slopes. Cryosphere 11, 1311–1325. https://doi.org/10.5194/tc-11-1311-2017.

Wirz, V., Beutel, J., Gruber, S., Gubler, S., Purves, R.S., 2014. Estimating velocity from noisy GPS data for investigating the temporal variability of slope movements. Nat. Hazards Earth Syst. Sci. 14, 2503–2520. https://doi.org/10.5194/nhess-14-2503-2014.

Wirz, V., Gruber, S., Purves, R.S., Beutel, J., Gärtner-Roer, I., Gubler, S., Vieli, A., 2016. Short-term velocity variations at three rock glaciers and their relationship with meteorological conditions. Earth Surf. Dyn. 4, 103–123. https://doi.org/10.5194/esurf-4-103-2016.

Zenklusen Mutter, E., Phillips, M., 2012. Thermal evidence of recent talik formation in Ritigraben rock glacier: Swiss Alps, pp. 479–483.

Publication 3

A general theory of rock glacier creep based on in-situ and remote sensing observations

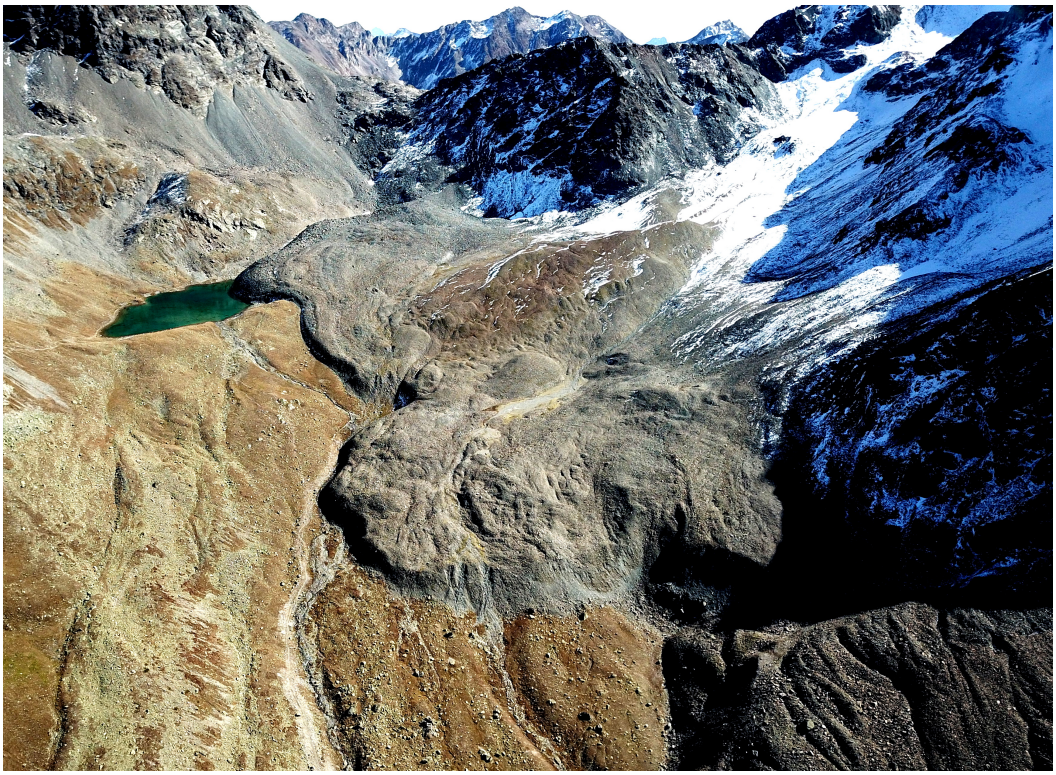

Authors Cicoira, A., Marcer, M., Gärtner-Roer, I., Bodin, X., Arenson, L., Vieli, A.

Journal Permafrost and Periglacial Processes

Year 2020 (submitted)

Short summary We derive a general theory to describe rock glacier creep and investigate its patterns and tendencies at both regional and local scale. A brief review of rock glacier physics and its mathematical formulation is compiled as foundation for further analysis. The investigation of a detailed data set comprising rock glacier thickness, creep rates, and slope angle allows the derivation of the Bulk Creep Factor, which disentangles the two contributions to surface creep rates from (i) material properties and (ii) geometry. Thereafter, the theory is applied and illustrated at a regional and at a local scale.

Main findings The main findings of this publication are:

- We derive a novel and efficient approach to asses the state of rock glacier creep and investigate its spatial patterns and temporal trends.
- We present a brief review of the physics of rock glaciers (RGs) and the mathematical models used to describe them.
- Based on a large dataset of RGs from the Alps we find that the typical driving stress is 92 ± 13 kPa, similar to ice glaciers.
- The Bulk Creep Factor (BCF) allows to disentangle the two contributions to the surface velocity of rock glaciers from (i) material properties and (ii) geometry.
- The BCF requires remote sensing data and can thus be used to efficiently asses patterns and tendencies in rock glacier dynamics at both regional and local scale and follow their dynamic evolution.

Contributions of the PhD candidate Design of the methodology; analysis of the data and interpretation of the results with contribution from the co-authors. Preparation of the database, the figures and the manuscript. The co-authors contributed to discussion and interpretation of the results and to the writing process.

Data availability The data used for the analysis of rock glacier thickness and driving stresses (Sec.3) are available according to the original references, as indicated in the manuscript. The data used for the analysis at local and regional scale are available upon request from the corresponding owners, as indicated in the manuscript. The Permafrost Zonation Index is freely available online from https://www.geo.uzh.ch/microsite/cryodata

Journal *Permafrost and Periglacial Processes (PPP)* is an international journal dedicated to the publication of scientific and technical papers concerned with earth surface cryogenic processes, landforms and sediments present in a variety of (Sub) Arctic, Antarctic and High Mountain environments. It focuses on original research based on geomorphological, hydrological, sedimentological, geotechnical and engineering aspects of these areas. The high scientific standard, interdisciplinary character and worldwide representation of PPP are maintained by regional editorial support and a rigorous refereeing system.
Impact Factor: **3.0**

A general theory of rock glacier creep based on in-situ and remote sensing observations

A. Cicoira[1], M. Marcer[2], I. Gärtner-Roer[1], X. Bodin[2], L.U. Arenson[3], A. Vieli[1]

[1]Department of Geography, University of Zurich, Switzerland
[2]Laboratoire EDYTEM, Centre National de la Recherche Scientifique, Université Savoie Mont Blanc, Le Bourget-du-Lac, France
[3]BGC Engineering Inc., Vancouver, BC, Canada

Key Points:

- We derive a novel and efficient approach to asses the state of rock glacier creep and investigate its spatial patterns and temporal trends.
- We present a brief review of the physics of rock glaciers (RGs) and the mathematical models used to describe them.
- Based on a large dataset of RGs from the Alps we find that the typical driving stress is 92 $\pm$ 13 kPa, similar to ice glaciers.
- The narrow range of driving stresses justifies a plastic approach to estimate the thickness of the deforming part of RGs on the basis of the surface slope angle.
- The definition of the Bulk Creep Factor (BCF) allows to disentangle the two contributions to the surface velocity of rock glaciers from (i) material properties and (ii) geometry.
- The calculation of the BCF requires input data from remote sensing only and can thus be used to efficiently analyse patterns and tendencies in rock glacier dynamics at both regional and local scale.

Corresponding author: Alessandro Cicoira, alessandro.cicoira@geo.uzh.ch

Abstract
The ongoing acceleration in rock glacier velocities concurrent with increasing air temperatures, and the widespread onset of rock glacier destabilization have reinforced the interest in rock glacier dynamics and in its coupling to the climate system. Despite the increasing number of studies investigating this phenomenon, our knowledge of both the fundamental mechanisms controlling rock glacier dynamics, and their long-term behaviour at the regional scale remain limited.

Here, we present a general theory to investigate rock glacier dynamics, its spatial patterns and temporal trends at both regional and local scale. To this end, we combine a model to calculate rock glacier thickness with an empirical creep model for ice-rich debris, in order to derive the Bulk Creep Factor (BCF), which allows to disentangle the two contributions to the surface velocities from (i) material properties and (ii) geometry. Thereafter, we provide two examples of possible applications of this approach. At a regional scale, we investigate the dynamic behaviour of a large dataset of rock glaciers from the Alps. We find that despite large variations in surface velocities, most of the investigated active rock glaciers show similar mechanical properties (BCF < 5), with the exception of currently destabilizing rock glaciers (BCF < 20). At a local scale, we investigate the spatial variability in surface velocities of three rock glaciers with contrasting dynamics. Our results show that the variability in the BCF can discriminate destabilized landforms and might therefore be beneficial to their definition.

1 Introduction

Rock glaciers are creeping masses of frozen debris shaping the mountain periglacial environment. The very definition of rock glaciers has been inextricably intertwined with their dynamics since the first scientific publications on these landforms (Capps, 1910). In fact, the surface appearance and the down-valley motion of rock glaciers are the visible expressions of their internal deformation, which depends on the internal stresses and on the physical properties of their constitutive material. For decades, rock glaciers were thought to creep down slope driven by gravity at a constant rate, in secondary creep stage and almost independent of any external influence (Wahrhaftig and Cox, 1959). Starting in the 1980's, kinematic observations have highlighted strong inter-annual and seasonal variability in rock glacier flow velocities, arousing renewed interest in their dynamics and in the processes that control it (Haeberli, 1985). Based on detailed kinematic data, statistical and numerical modelling have been used to link the observed temporal fluctuations in creep velocities at different time scales to climatic forcing such as air and ground temperature, snow melt, and liquid precipitation (Kääb et al., 2007; Monnier and Kinnard, 2016; Müller et al., 2016; Cicoira et al., 2019a, 2019b). Further, the onset of rock glacier destabilization, i.e. the sudden and exceptional acceleration of (a part of) the deforming rock glacier, has been related to positive air temperature anomalies under appropriate topographical conditions (Delaloye et al., 2013; Marcer et al., 2020a).

Although our knowledge of surface kinematics of rock glaciers is very detailed (Kääb and Weber, 2004; Hartl et al., 2016; Wirz et al., 2016; Bodin et al., 2018; Vivero and Lambiel, 2019) only a limited number of studies have investigated their internal structure and physical properties (Arenson et al., 2002; Ikeda et al., 2008; Buchli et al., 2018). This paucity in direct observations is caused in the first place by the extreme effort needed to investigate the complex interior of a rock glacier and the periglacial environment in general (Arenson et al., 2016). Rock glacier velocities are often directly or relatively compared (kinematic level), neglecting the influence of their material properties, geometry and stresses (dynamics level). Few more sophisticated physical and mathematical approaches have so far been proposed to describe

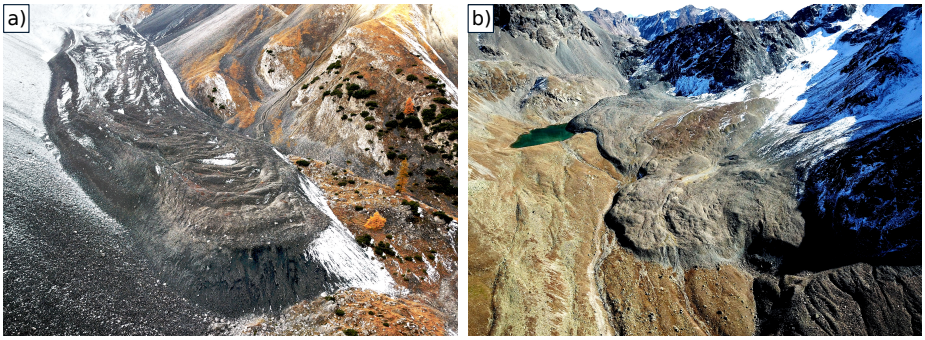

Figure 1. Rock glaciers can be simple landforms, manifesting essential geometries and flow patterns, or in the contrary they can exhibit very complex dynamics and morphology. In this figure, the Val dall'Acqua Rock Glacier located in the homonym valley (a) and the Gianda Viva rock glacier complex in the Muragl Valley (b) illustrate two extremes of this variety.

rock glacier dynamics (Olyphant, 1983; Jansen and Hergarten, 2006; Frehner et al., 2015; Müller et al., 2016; Cicoira et al., 2019b), but they are hardly re-applied in other studies. Inevitably, the above limitations inhibit interdisciplinary studies and hamper the interpretation and analysis of the climatic, geomorphological and hydrological significance of rock glaciers at all temporal and spatial scales. In addition, such limitations lead to misinterpretations and confusion amongst the scientific community and the general public.

In this paper, we propose a general conceptual and physically based model in order to overcome the above mentioned limitations and facilitate spatio-temporal investigations of rock glacier creep. First, in Section 2, we summarize the current knowledge on the internal structure of rock glaciers and on the physical processes controlling their motion, based on in-situ investigations and laboratory experiments. This brief review is tailored to the information needed to develop our conceptual and mathematical model. For a more comprehensive summary of the deformation of debris-ice mixtures the readers are referred to the two thorough reviews from Arenson et al. (2006) and Moore (2014). Section 3 is focused on the derivation and mathematical formulation of our general approach to investigate rock glacier creep. After a short review of the rheological models for rock glaciers, we analyse a comprehensive dataset of rock glacier thickness, slope and surface velocity. On this basis, we propose a mathematical formulation to describe rock glacier dynamics, which combines a perfectly plastic model to calculate rock glacier thickness with an empirical creep model for ice-rich debris (Section 3.3). The formulation leads to the definition of the Bulk Creep Factor (BCF), which represents the properties of the rock glacier material. The proposed methodology thereby allows to disentangle the geometrical and the rheological contributions to the velocity signal. It embodies a trade-off between complexity and oversimplification. After presenting a physical interpretation of the BCF, we briefly illustrate two real-world applications at regional and local scale. First, we analyse the dynamic behaviour of 414 rock glaciers from Austria, France, Italy, and Switzerland and explore the variability in the BCF. Second, we use detailed kinematic observations to investigate and compare the spatial variability in surface creep velocities of three rock glaciers which are characterized by contrasting dynamical behaviour: (slow) steady-state creep, abnormal fast creep, and destabilization. Finally, we critically discuss the limitations and further potential applications of the proposed approach.

2 A physical description of rock glacier creep

In early studies, the movement of rock glaciers has been thought to happen mostly near the surface and being driven by freeze-thaw cycles (Capps, 1910). Almost fifty years later, Wahrhaftig and Cox (1959) deduced solely from geomorphological observations that a large part of the deformation within a rock glacier must occur at depth. Their thesis was confirmed only in recent years, when direct observations from borehole investigations shed light on the internal structure and deformation profile of rock glaciers (Haeberli et al., 1998). Although only limited direct observations exist, the borehole data show a recurrent structure and behaviour for all the investigated landforms (Haeberli et al., 1988; Arenson et al., 2002; Krainer et al., 2015; Buchli et al., 2018; Arenson, pers. com. 2020). Based on this knowledge, rock glaciers are typically divided into three distinct structural and dynamical units, which are, from the surface to deeper ground: the active layer, the ice-rich core, and the shear horizon. Below these three units no or very limited movement occurs: the shear horizon delimits in a dynamic sense the thickness of the active rock glacier itself. The surface displacements of a rock glacier are the sum of the three independent contributions described below. In the following sections, we present a brief review of our current knowledge on the physics of permafrost creep and rock glacier dynamics, essential for their mathematical description.

2.1 The active layer

At the rock glacier surface, a few meters of seasonally frozen blocky sediments represent the interface between the ice-rich permafrost and the atmosphere. The thermodynamics of the active layer are complex due to the multiphase nature of this layer, which consists of a rock, ice, water, and air fraction, and because of the multitude of processes governing its energy balance, which include conductive, advective, and convective heat fluxes (Hanson and Hoelzle, 2004; Delaloye and Lambiel, 2005; Scherler et al., 2014; Wicky and Hauck, 2017). During the summer months, the active layer insulates the permafrost underneath it, preventing or strongly reducing the thawing process at the permafrost surface. Although melt rates at degrading rock glacier sites are usually limited to a few centimeters per year (Krainer et al., 2015), the influence of increasing air temperature can significantly (exponentially) impact the creep rates of the underlying rock glacier (Arenson and Springman, 2005a; Staub et al., 2016; Müller et al., 2016; Monnier and Kinnard, 2016).

The deformation of the active layer is mostly linked to tilting or sliding of the boulders on top of the permafrost table. Rare events of active layer detachments have been observed at rock glacier sites, characterized by extreme rates of displacement due to sliding (Lugon and Stoffel, 2010; Marcer et al., 2020b). In some cases, boulders can move very rapidly for a short time also in relation to tilting. In fact, when a boulder is tilting close to a terrain step, it might lose its stability and quickly roll down slope, as it often happens close to active front (Haeberli et al., 1998; Kummert et al., 2017). When measuring surface displacements, it is difficult to filter the deformation component associated to the active layer. Nevertheless, the magnitude of this component is in general orders of magnitude smaller than the total surface velocity, therefore negligible in first approximation (Wirz et al., 2016; Cicoira et al., 2019b). An exception might be slow-moving rock glaciers, where the movement of the boulders on the surface can represent a relevant contribution to the total observed velocities (e.g. Murtél Rock Glacier, unpublished data). Based on this evidence, the dynamics of the active layer can be neglected in the forthcoming mathematical description of rock glacier creep. However, it is important to remember that the active layer is essential for the surface mass and energy balance of a rock glacier and thereby has a strong influence (as we will see in the next section) on rock glacier dynamics.

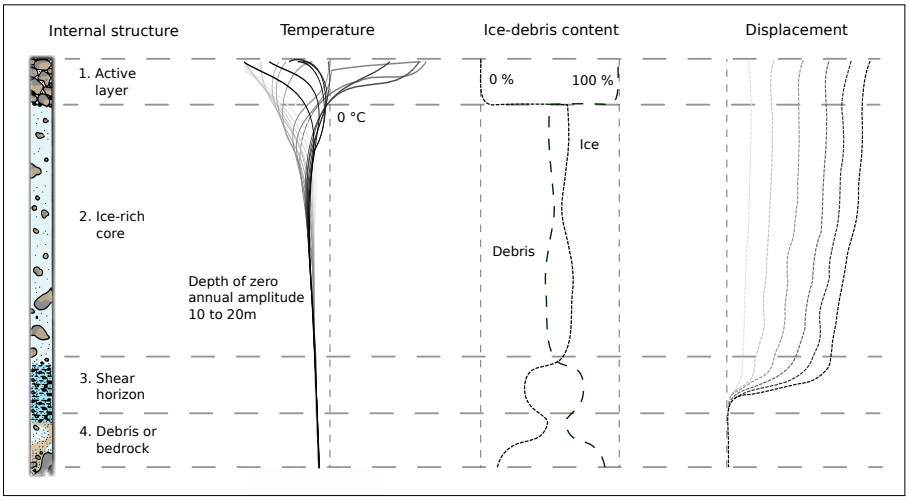

1. Active layer

Structure and composition:
unconsolidated boulders, several meters in thickness. the composition varies seasonally due to phase changes, only frozen in winter.
Temperature:
this layer strongly insulates the underneath permafrost from external temperature forcing. It is influenced by freeze-thaw cycles and by advective heat fluxes.
Displacement:
caused by sliding, tilting or rolling of the boulders.

2. Ice-rich core

Structure and composition:
ice-rich debris constituting the main unit of the rock glacier. The vol. ice content typically ranges from 40% to 90%. The debris size is significantly smaller than in the a.l.
Temperature:
the thermal regime is controlled by heat diffusion. Talik development can indicate permafrost degradation.
Displacement:
caused by temperature dependent creep of the ice.

3. Shear horizon

Structure and composition:
Frozen soil with banded ice and pressurized water. Ice content and debris size smaller than in the ice-rich core. A few meters in thickness.
Temperature:
the seasonal temperature signal is strongly attenuated. Temperature variations occur at larger temporal scales.
Displacement:
accomodates up to 90% of the total displacements, the creep is influenced by pore water pressure.

4. Debris or bedrock

Structure and composition:
the lower boundary of the rock glacier, composed by sediments or bedrock. Often old material transported on top of the rock glacier and then being overridden.
Temperature:
negative and positive temperatures are possible according to the state of the permafrost.
Displacement:
the displacements are considered negligible in this region.

Figure 2. Graphical illustration and textual description of vertical profiles (conceptualized) of a typical rock glacier. From left to right the internal structure, the ground temperature variations, the material composition and the displacement profiles of a typical rock glacier are shown. The concept is based on the most influencing publications on borehole investigations on rock glaciers (Arenson et al., 2002; Arenson and Springman, 2005a; Krainer et al., 2015, amongst others). The profiles are drawn on the basis of data from the Murtél borehole (Vieli et al., in preparation).

2.2 The ice-rich core

The inner core of a rock glacier is composed of a mixture of ice and debris with a typical thickness of 10 to 25 m. The ice component can be polygenetic and may include significant meteoric, superficial, and ground-water contributions (Haeberli and Vonder Mühll, 1996). Observations from boreholes at moving rock glaciers indicate

values of the volumetric ice content of above 50% apart the case of degrading permafrost conditions, where the values can be lower (Arenson et al., 2002; Haeberli et al., 2006; Hausmann et al., 2012; Monnier and Kinnard, 2016). The debris component of rock glaciers typically originates from debris-laden snow avalanches, episodic rock avalanches and long-lasting rockfall activities (Clark et al., 1998; Humlum, 2000; Haeberli et al., 2006). The grain size of the debris component is usually finer than in the active layer. This structural difference is the consequence of the processes that contribute to the debris supply (fall sorting and washing away) and the motion of the rock glacier itself (kinetic sieving) (Haeberli et al., 2006). As a consequence, the structure of the ice-debris matrix can be very heterogeneous within a single rock glacier and can be very diverse amongst different landforms (Clark et al., 1998; Arenson et al., 2010). The thermal regime of the inner core is mainly controlled by heat conduction. Therefore, the phase of the temperature signal from the surface is linearly delayed and its amplitude exponentially attenuated with depth (Carslaw and Jaeger, 1959; Cicoira et al., 2019b). The seasonal temperature signal influences the frozen ground down to the depth of the zero amplitude, which is usually found at about 10 to 20 m depth. Thermal changes below this depth require temperature forcing to act at longer temporal scales (decades and beyond). With regard to water flow, the ice-rich core can be considered impermeable in first approximation (Krainer and Mostler, 2002). However, water flow has the potential to affect the inner core especially under conditions of permafrost degradation, when temperatures close to the melting point lead to high structural heterogeneity, preferential flow pathways and augmented interstitial water content (ibidem).

The deformation of the ice-rich core is mainly governed by the time dependent creep of its ice component (Arenson et al., 2006). Similarly to pure ice, the creep of the inner core is susceptible to temperature variations and depends on the structure of the rock glacier itself. More specifically, the creep behaviour of a debris-ice mixture and even its stress-strain behaviour (ductile - dilatant - brittle) can vary substantially depending on the applied strain rate, on the volumetric ice content and on the grain size of the debris component (Arenson et al., 2006). For a homogeneous matrix, the ice-rich core can be described as a creeping viscous material, as confirmed by the classical deformation profiles observed from inclinometer readings (see Fig. 2). However, for more heterogeneous and anisotropic structures, the debris component and the ice structure can strongly influence the deformation profile (Buchli et al., 2018). Overall, an amount of 10%-40% of the total displacement takes place within the ice-rich core and is governed by temperature variations (Arenson et al., 2002).

2.3 The shear horizon

The shear horizon is a shallow layer of a few meters of thickness, where the highest shear rates are observed and where most of the deformation (60%-90%) occurs (Arenson et al., 2002). It is located below the inner core, at a depth of 15 to 30 m from the surface. Despite the extreme paucity of observations, borehole investigations consistently showed a decrease in volumetric ice content (20%-50%) and in the debris grain size within this layer (Haeberli et al., 1988; Arenson and Springman, 2005a). Moreover, in the shear horizon, the large deformation rates may modify the structure and influence the properties of the material itself, as suggested by the banded ice observed in the ice cores from the Lazaun Rock Glacier in Sudtirol (IT) (Krainer et al., 2015). Due to the depth of the shear horizon, the influence of surface temperature forcing is limited and considerably delayed in time (Kääb et al., 2007; Cicoira et al., 2019a). At longer time scales, however, changes in temperature, especially in intervals close to the melting point can substantially affect the mechanical properties of the rock glacier material, also at depth of the shear horizon. While the ice-rich core can be assumed to be mostly impermeable to water flow, pressurized water has been observed during borehole perforations within the shear horizon, suggesting a strong

influence from unfrozen water on the behaviour of this unit (Ikeda et al., 2008; Bast, pers. com. 2015; Buchli et al., 2018; Vieli et al., in preparation).

Debris-ice mixtures are usually more resistant to deformation at low temperatures than their pure end-member components (Moore, 2014). As a consequence, the apparent viscosity of rock glacier material is larger than for pure ice at the same temperature and stress (Monnier and Kinnard, 2016; Müller et al., 2016). However, especially close to melting conditions, the growth of unfrozen water films at the interface between ice and debris has the potential to reduce the strength of the mixture and can even lead to substantial weakening (Moore, 2014). In accordance to this consideration, the effective viscosity of the shear horizon material has been estimated to be up to seven times smaller than that of pure ice at similar thermal and stress conditions (Bucki and Echelmeyer, 2004; Ikeda et al., 2008).

In summary, the contribution of the shear horizon to the total surface displacement is large (60%-90%) and it also accounts for most of the inter-annual and seasonal variations in rock glacier creep (Arenson et al., 2002; Cicoira et al., 2019b). Field and theoretical studies (Ikeda et al., 2008; Buchli et al., 2018; Cicoira et al., 2019b) show that at temporal scales from months to several years, these variations are mainly controlled by pore water pressure within the shear horizon. At longer temporal scales, changes in the structure of the shear horizon, driven by the combined influence of permafrost creep and ground temperature, are still poorly understood but are expected to play an important role in determining the long-term evolution of rock glaciers and their dynamics (Kääb et al., 2007; Müller et al., 2016; Seppi et al., 2019).

3 The Bulk Creep Factor: a general theory for rock glacier creep

Developing a mathematical formulation of a natural system - a model - can be used to study its properties and understand its dynamics. All models have to be constrained and validated with observations, regardless if they are based on statistical methods or on analytical formulations of physical processes. In comparison to glaciology, where copious studies have investigated the physics of ice, research on rock glaciers is characterized by a paucity of direct investigations both in the field and in the laboratory. This limitation restrains our understanding of the fundamental processes governing rock glacier creep and hinders the establishment of quantitative models for investigating rock glacier dynamics. The growing interest in rock glacier dynamics, in combination with increasing data available from remote sensing techniques, attest the need for a comprehensive description of rock glacier creep. Having in mind the most important findings on the physics of rock glacier creep outlined in the previous section, we now formulate them mathematically. Thereafter, we investigate the relationship between rock glacier thickness, surface slope and creep rates for a set of 28 rock glaciers worldwide for which such data is available. On the basis of this analysis, we introduce the Bulk Creep Factor (BCF) and its physical interpretation.

3.1 Rheological models

The rheology of debris-ice mixtures, i.e. the mechanical constitutive relationship which combines the deformation of the material to its internal stresses, can be described mathematically. Having identified ice creep as the main mechanism behind the movement of rock glaciers, the first theory to consider when describing rock glacier deformation is the empirical flow law proposed by Nye (1952) and Glen (1955) for pure ice:

$$\dot{\gamma} = A\tau^n. \tag{1}$$

Glen's law describes thermally activated dislocation creep for an isotropic crystalline solid and is analogous to the relationships that describe deformation of metal

and rock at high temperatures (Weertman, 1983). The shear strain rate $\dot{\gamma}$ depends solely on the shear stress τ through a power law relationship, and on the constitutive properties of clean ice, which are described through two parameters: the fluidity factor A (inversely related to viscosity) and the flow exponent n. The fluidity parameter in eq. 1 is described by an Arrhenius relation dependent on temperature (Mellor and Testa, 1969):

$$A = A_0 exp\left(-\frac{Q}{R_* T}\right), \tag{2}$$

where A_0 is a parameter typical of the material, Q is the activation energy, R_* is the universal gas constant and T is the absolute temperature in Kelvin. This formulation has been proven valid for most glacial and periglacial conditions on earth (Moore, 2014). When approaching the melting point, the fluidity parameter shows an additional dependence on temperature due to liquid water along grain boundaries (De La Chapelle et al., 1999; Moore, 2014). This effect can be accounted for by correcting the formulation of the fluidity parameter (Eq. 2) with an additional term:

$$A' = A + \alpha w_w, \tag{3}$$

where w_w is the unfrozen volumetric water content and α a parameter (Cuffey and Paterson, 2010). The flow exponent n is often considered constant and best approximated for pure ice by a value of 3, although experimental and field evidence exist that this value represents the superposition of different mechanisms (Weertman, 1983; Cuffey and Paterson, 2010).

The previous theory has to be expanded when studying rock glaciers. In fact, they consist of debris-ice mixtures, whose properties depend on the volumetric fractions of their constituents and not only on pore ice. For a rock glacier, the driving stress can be calculated as:

$$\tau = \rho g H \sin\alpha, \tag{4}$$

where g is the gravitational acceleration, H the thickness of the moving rock glacier, α the surface slope angle and ρ is the density of the creeping material, which is given by the contribution of volumetric debris w_d and ice content w_i and the relative densities ($\rho_i = 910\,\mathrm{kg\,m^{-3}}$ and $\rho_d = 2700\,\mathrm{km\,m^{-3}}$):

$$\rho = \rho_d w_d + \rho_i w_i. \tag{5}$$

As we have seen above, several field observations, integrated by theoretical and experimental studies, have highlighted debris concentration and size, temperature, water content and internal stresses as the first-order variables governing the deformation of debris-ice mixtures (Moore, 2014). Arenson and Springman (2005b) have tested natural (from borehole cores at rock glacier sites in Switzerland) and synthetic soil samples in order to adapt Glen's flow law to the rheology of rock glacier material (Arenson and Springman, 2005a). The authors expressed the dependency on the volumetric ice content w_i by introducing a logarithmic term to eq. 2 and a linear dependency to the flow exponent:

$$A = exp\left(\frac{a}{1+T}\right) + 5 \times 10^{-11} e^{-10.2 w_i}, \tag{6}$$

$$n = 3 w_i. \tag{7}$$

In addition to the variability of material properties, also the processes governing the deformation of rock glaciers can be diverse. For debris-ice mixtures with a high volumetric content of debris, frictional effects ensue when particle to particle contact is

reached. For the end-member case of unfrozen debris, the maximum strength is in first approximation described by the Terzaghi form of the Mohr-Coulomb yield criterion:

$$\tau_r = \tau_{c\theta} + \sigma_e \tan \phi_C, \tag{8}$$

where σ_e are the effective stresses, $\tau_{c\theta}$ is the cohesion and ϕ_C is the friction angle of the shear horizon material. Contrarily to unfrozen material, the strength of ice-rich debris is strongly strain rate and temperature dependent and preserves a viscous component due to the presence of pore ice. Ladanyi (2003) has proposed a constitutive relation that combines the frictional yield threshold with viscous flow resistance. In this mathematical formulation, the shear strain rate depends on the shear stress and on two creep parameters, and additionally on the shear resistance of the deforming material. For an ice-rich, cold frozen soil, where both cohesion and friction are affected by temperature and strain rate, the shear strain rate becomes:

$$\dot{\gamma} = \dot{\gamma_C} \left(\frac{\tau}{\tau_r} \right)^n, \tag{9}$$

where $\dot{\gamma_C}$ is the critical shear strain rate typical of the material. This formulation allows to express the frictional behaviour of the ice-rich mixture augmented by a rate-dependent cohesive strength. Moreover, according to the definition of the shear strength, we are able to consider the effect of pore water pressure on the driving stress through the calculation of the effective stresses σ_e.

3.2 Rock glacier thickness and driving stress

While it is relatively simple to determine the surface slope and the displacement rates of rock glaciers, inferring information about their thickness remains challenging. Geophysical methods such as electrical resistivity tomography (ERT), seismic and ground penetrating radar surveys (GPR) allow the investigation of ground permafrost at depth. However, using such indirect observations to infer the thickness of the moving rock glacier remains laborious and often impossible due to practical reasons. Boreholes instrumented with slope inclinometers provide the most reliable results with this regard, but this information is only punctual and they are expensive both logistically and financially. For all of the above, the application of inverse models for the derivation of rock glacier thickness is desirable. Contrarily to ice-glaciers, where several methods have been proposed and their limitations critically reviewed and evaluated (Farinotti et al., 2017), no detailed studies of such methods have been undertaken for rock glaciers. Therefore, we propose three approaches to estimate rock glacier thickness based on the analysis of a dataset of 28 rock glaciers from the Alps (23) and the Andes (5), for which detailed observations of surface creep rates, slope angle and thickness from different sources are available. Detailed information about the dataset and the relative bibliography is available in Appendix A.

In Fig. 3 we analyse the thickness, driving stress, creep rates and slope angles for the investigated dataset. The distribution of thickness and driving stresses (calculated according to Eq. 4) for the analysed rock glaciers suggests a visco-plastic behaviour with a yield stress of about 100 kPa, similar to clean ice (Fig. 3a). When considering all the rock glaciers in the dataset, the average driving stress is 85 ± 21 kPa. However, a cluster of five rock glaciers in the Chilean Andes shows low values of the driving stress. These landforms are in degrading conditions (with permafrost temperatures being at 0°C) and their driving stresses might not be able to sustain steady state creep conditions any longer. When excluding these five degrading rock glaciers from the analysis, the mean value of the driving stress increases up to 92 ± 13 kPa. This result confirms and extends previous observations by Wahrhaftig and Cox (1959) and Whalley and Martin (1992), which performed a similar analysis on a vast dataset of

rock glaciers finding that the driving stresses vary between 50 kPa and 200 kPa. Note that in these previous studies the thickness was generally estimated on the basis of expeditious field surveys subject to larger uncertainties.

The distribution of rock glacier thickness and surface slope angle is shown in Fig. 3b along with three model fits and their performance, which is quantified with the RMSE. The first method that we propose to estimate the thickness of a rock glacier is a constant model. This approach is supported by the fact that while most of the observed rock glaciers present a thickness of their moving part between 10 m and 30 m, only few rock glaciers have been studied in such detail that the uncertainty on the estimation of the thickness is limited to less than the natural variability between different landforms. When fitting the constant model to the analysed dataset, the mean value of rock glacier thickness becomes:

$$H = 20 \pm 5.5\,\mathrm{m}. \tag{10}$$

The second model to estimate rock glacier thickness is a linear relationship between slope angle and thickness. From the available observations, we find a best linear fit of:

$$H = 37 - 0.9\alpha \pm 3.0\mathrm{m}. \tag{11}$$

The third model, also used in the field of glaciology, estimates the thickness of the rock glacier with a perfectly plastic model by solving Eq. 4 for H, assuming a yield stress of $\tau = 92\,\mathrm{kPa}$ (given the mean driving stress from the dataset):

$$H = \frac{\tau}{\rho g \sin\alpha} \pm 3.4\mathrm{m}. \tag{12}$$

According to our results, the linear thickness model shows the best performance (RMSE = 3.0 m), but is only marginally better than the plastic model (RMSE = 3.4 m). Note that the suggested models should be applied with caution and only in average slope ranges roughly between 10° and 30° of slope (i.e. for the slope angle range in which they have been derived from the data).

Rock glacier creep rates can be calculated by coupling one of the thickness models (Eq. 10, 11 or 12) to the creep models presented in Sec. 3 (Eq. 1 or Eq. 9). Fig. 3c shows the result of this coupling and demonstrates that the choice of the thickness model has a strong influence on calculated creep rates. When coupling the linear and the plastic thickness models to Glen's flow law, the creep rates decrease for high values of the slope angle. This mathematical artefact originates from the vertical integration of Eq. 1. In fact, the creep rates are proportional to the thickness to the power of $n+1$, which in turn is (in the suggested thickness models) inversely proportional to the slope angle. This artefact can be overcome by coupling the thickness models to the creep model of Ladanyi (2003). In this case (Eq. 9), the shear rates show a linear dependency on the thickness and a depend on the surface slope angle to the power of n, which therefore dominates the equation. A similar dependency on the slope angle is obtained when combining Glen's flow law with the constant model for rock glacier thickness, i.e. only accounting for variations in the slope angle and substantially neglecting changes in the rock glacier thickness. Although the last two mentioned combinations (constant thickness + Glen and plastic thickness + Ladanyi) provide similar results, we prefer the second approach because it represents the observed thickness dependency on slope more realistically (Fig. 3b).

After the above analyses, we can conclude that (i) the typical driving stress of alpine rock glaciers is $92 \pm 13\,\mathrm{kPa}$ suggesting a plastic behaviour, (ii) the thickness of the moving part of a rock glacier can be estimated with the use of simple models on the basis of the surface slope angle, (iii) surface creep velocities can be described on

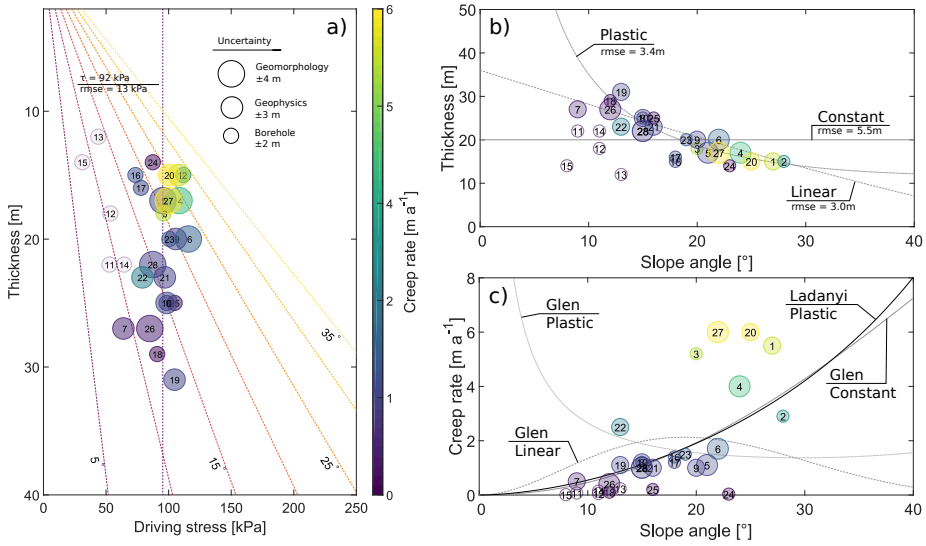

Figure 3. Analysis of observed rock glacier thickness, slope angle, and creep rates. Each rock glacier is depicted by a circle, whose colour represents the rock glacier creep rates $[ma^{-1}]$ as indicated by the colour bar. For each rock glacier, the uncertainty relative to its thickness is represented by the diameter of the circles. (a) Rock glacier thickness [m] against driving stress [kPa]. The vertical dashed line shows the average value of the driving stress and the relative RMSE. The diagonal dashed lines show constant values of the slope angle, from 5° to 35°. (b) Rock glacier thickness [m] against slope angle [°]. The three models to calculate rock glacier thickness are indicated by labelled lines along with their RMSE. (c) Rock glacier creep rates [m a^{-1}] against slope angle [°]. The four models for the calculation of rock glacier creep rates are shown. The corresponding labels indicate from top to bottom the respective creep and the thickness models used for the calculation.

the basis of surface slope observations and thickness models in combination with a creep law - preferably accounting for the frictional behaviour of rock glacier creep.

3.3 The Bulk Creep Factor BCF and its physical interpretation

A complete description of rock glacier dynamics is hampered by the high degree of heterogeneity of their physical properties in conjunction with the strenuousness to obtain accurate measurements of their internal structure, especially at a regional scale (Arenson et al., 2016). In an attempt to better understand regional patterns and tendencies, we describe rock glacier creep and dynamics with the most simple method possible, seeking a compromise between a gargantuan task and its complete omission.

Based on the brief review on rock glacier physics and its mathematical description presented in the previous sections, we define the Bulk Creep Factor (here on BCF) as the ratio between observed c_{obs} and modelled c_{mod} creep rates:

$$BCF = \frac{c_{obs}}{c_{mod}}. \tag{13}$$

Following the analysis presented in Sec. 3.2, we adopt the creep model proposed by Ladanyi (2003) and calculate rock glacier creep rates by integrating Eq. 9 in the vertical dimension and obtain:

$$c_{mod} = \frac{\dot{\gamma_c}}{n+1} \left(\frac{\rho g \sin \alpha}{\tau_{c\theta} + \rho g H \cos \alpha \tan \phi} \right)^n H^{n+1}. \tag{14}$$

Combining this equation to Eq.13, the BCF becomes:

$$BCF = c_{obs} \frac{(n+1)}{\dot{\gamma_C}} \left(\frac{\tau_{c\theta} + \rho g H \cos \alpha \tan \phi}{\rho g \sin \alpha} \right)^n H^{-(n+1)}. \tag{15}$$

The BCF is a dimensionless quantity that expresses the mechanical properties of the rock glacier material. By separating the geometrical influence from the creep rates, the BCF allows to compare different rock glaciers or different areas of a single rock glacier with regard to their rheological properties. As we did not distinguish between different layers in the vertical integration of Eq. 9, the BCF implicitly describes the rheology of both the ice-rich core and the shear horizon. It therefore represents an averaged value over the entire rock glacier thickness. In order to overcome our limited knowledge about the internal structure of rock glaciers, we evaluate the value of the thickness H with one of the thickness models proposed in the previous section (Eq. 10 to Eq. 12). This approach has the great advantage of requiring only remote sensing data of surface creep velocities and surface slope angles of the rock glaciers. Therefore, it allows large scale applications to efficiently extend previous research efforts (Whalley and Martin, 1992; Groh and Blöthe, 2019). Here on, we set the values of the model parameters according to previous modelling and laboratory experiments (Czurda and Hohmann, 1997; Arenson and Springman, 2005b; Moore, 2014; Müller et al., 2016; Monnier and Kinnard, 2016; Cicoira et al., 2019b). While most of the parameters are well constrained and can be parametrized (e.g. as a function of the volumetric ice content), the value of $\dot{\gamma_c}$ varies between different rock glaciers and the choice of a reference value is arbitrary. We calibrate this parameter to $0.06\,\mathrm{a}^{-1}$ in order to match the velocities of the Murtél Rock Glacier, and take it here as a regional reference value for our analysis. While this reference is arbitrary and the absolute values of the BCF can change, it does not influence the relative variation between different rock glaciers.

When adopting the perfect plastic model for rock glacier thickness (Eq. 12, with a yield stress of $100\,kPa$) and assuming standard values of the material parameters ($w_i = 0.7$, $n = 2.1$, $\rho = 1500\,\mathrm{kg\,m^{-3}}$, $\phi = 25°$, $\tau_{c\theta} = 10\,\mathrm{kPa}$, and $\dot{\gamma_c} = 0.06\,\mathrm{a}^{-1}$), the formulation of the BCF simplifies to:

$$BCF = 6.6\, c_{obs}\, \sin \alpha \left(\frac{0.5}{\tan \alpha} + 0.1 \right)^n \tag{16}$$

Figure 4a shows the procedure and the data required for the calculation of the BCF. The interpretation of different values of the BCF are illustrated in Figure 4b. Here, three possible states of a rock glacier are depicted in the creep rate - surface slope angle space. One rock glacier can be described by a single point under the assumption that the spatial variability within the same landform can be represented by single values of the surface slope angles, thickness and creep rates. Point A and point C represent two rock glaciers characterized by the same rheological properties (both lay on the yellow contour line - high BCF), but show very different creep rates due to their contrasting slope angles. Point A and point B on the contrary, show rock glaciers with the same value of creep rates despite their difference in geometry (surface slope angle). This is only possible due to a reduction of the BCF. The rock glaciers visualize by point B and point C show the same value of the slope angle, but different values of creep rates due to different mechanical properties (different BCF).

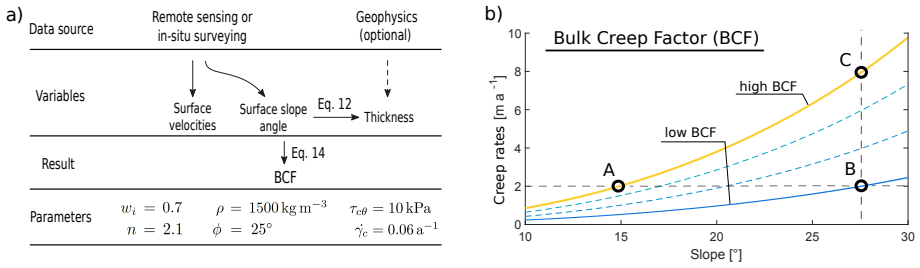

Figure 4. Calculation and interpretation of the BCF. (a) Procedure and data required for the calculation of the BCF and (b) interpretation of the parameter values in the creep rates - slope angle space. The coloured contour lines show constant values of the BCF. The interpretation is presented in the text.

This illustration demonstrates the importance of accounting for geometry and material properties when comparing rock glacier dynamics. In fact, on a kinematic level, point A and point B are equivalent. However, our approach allows to illustrate the dynamic difference between those two rock glaciers: if point A had the same slope as point B, it would creep four times faster according to its rheological properties.

4 Applications: rheological information from remote sensing data

In the following, we illustrate two possible applications of the proposed methodology for investigating rock glacier dynamics. At a regional scale, we analyse a large dataset of rock glaciers from the Alps to investigate their dynamical behaviour. At a local scale, we use detailed observations of the surface creep velocities of three rock glaciers to analyse their spatial variability.

4.1 The regional scale: a dynamic comparison of alpine rock glaciers

Many efforts in the context of national and international permafrost monitoring are directed towards the assessment of rock glacier surface displacements at both local and regional scale (Kellerer-Pirklbauer et al., 2012; Jones et al., 2018; Groh and Blöthe, 2019; Marcer et al., 2019; PERMOS, 2019). In most studies that analysed surface velocities so far, different rock glaciers are compared on the basis of kinematic data only, despite their contrasting geometrical settings. The introduction of the BCF allows to include information about their thickness and surface slope, thus to transpose the analysis from a kinematic to a dynamic level.

For our analysis at a regional scale, the spatially heterogeneous characteristics of a rock glacier are summarized by a single value of the BCF, which is in first approximation representative for the entire landform (or a substantial part of it). The proposed approach can thus be applied to analyse data on surface slope and surface displacements obtained from in-situ or remote sensing techniques. We investigate here a dataset comprising 414 rock glaciers for which surface displacement and slope angle data are available. The majority of the data come from an analysis of the French national inventory (Marcer et al., 2017). Other data points come from the Swiss (PERMOS, 2019; Delaloye, pers. com. 2020), Austrian (Groh and Blöthe, 2019) and Italian Alps. In a first step, we calculate and analyse the BCF for all rock glaciers in the dataset. In a second step, we explore the influence of permafrost conditions at each rock glacier site by using as a proxy the Permafrost Zonation Index (PZI) developed

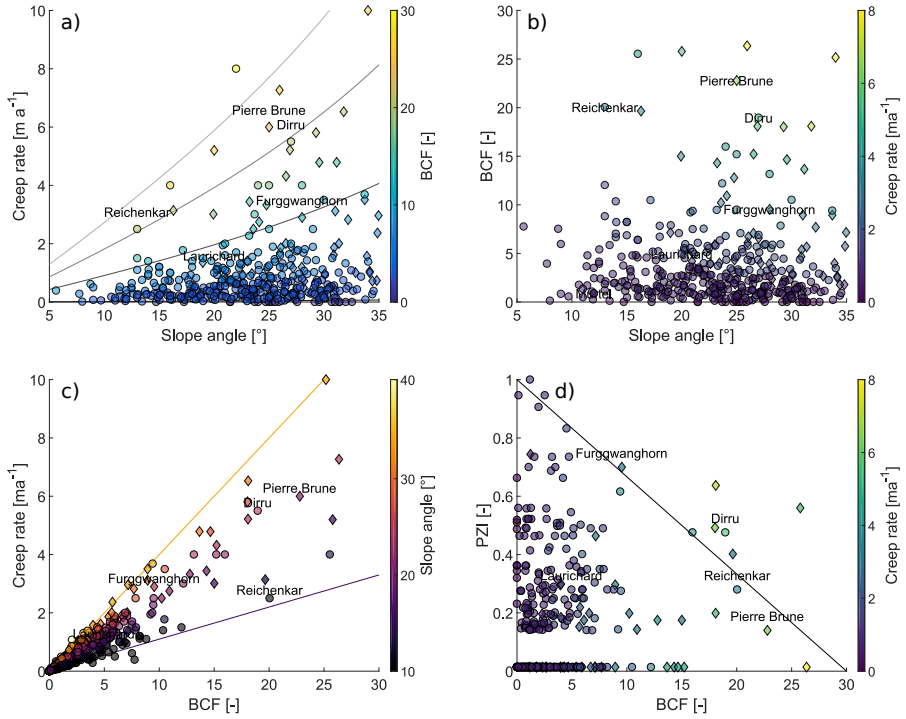

Figure 5. Results of the analysis at the regional scale. Each point represents a rock glacier. Destabilized landforms, according to Marcer et al. (2019), are illustrated with a diamond shape. (a) Surface creep rate against slope angle, (b) BCF against slope angle, (c)creep rate against BCF and (d) PZI against BCF. Additional information about creep rates, BCF or slope angle is provided by the corresponding colour bar.

by the University of Zurich (Gruber, 2012). High values (close to the unit) correspond to favourable conditions for permafrost occurrence, while values close to zero indicate unfavourable conditions. Moreover, we analyse the destabilization susceptibility of the investigated rock glaciers according to the geomorphological index proposed by (Marcer et al., 2019). For a more detailed description of the dataset we refer to the table in Appendix A.

Figure 5 shows the results of the BCF in relation to dynamics and geometry for all 414 rock glaciers in the dataset. The sub-figures visualize the relation between surface creep rates, surface slope angle, BCF and PZI in different combinations. Circular and diamond markers indicate active and destabilized rock glaciers according to the criteria from Marcer et al. (2019). Most rock glaciers show a surface slope comprised between 10° and 35°, surface creep rates lower than about $2\,m\,a^{-1}$ and exhibit a BCF lower than 5 (70% of the rock glaciers in the dataset). Almost only destabilized rock glaciers or rock glaciers with low PZI have high BCFs as shown in Fig. 5b-d.

As we have presented above, the calculation of the BCF expresses the rheological properties of the rock glacier material by removing the geometrical information from the velocity signal and thereby allows the comparison of the dynamical behaviour of different rock glaciers. Figure 5a and b confirm that the material properties (BCF)

and the surface slope angle are independent (if we exclude feedback between shear rates and material structure), while the surface velocities depend with a power law on the surface slope. In the slope-velocity space in Fig. 5a the maximum creep rate observed increases with the slope angle: e.g. all the rock glaciers with velocities above $4\,m\,a^{-1}$ are characterized by slope values higher than 25°. Nevertheless, there are also rock glaciers with low values of creep rates regardless of their slope angle. The calculated BCFs displayed in Fig. 5b reveal how rock glaciers with gentle slope can exhibit material properties prone to fast deformation (high BCFs). For example the Reichenkar Rock Glacier has a similar BCF to the Pierre Brune Rock Glacier despite reaching only half of its creep rates: this discrepancy in creep velocities can be explained by the difference in surface slope. Comparing relative velocity variations is of advantage, but this approach only introduces a linear trend and remain at a kinematical level, still neglecting geometrical and mechanical properties of the rock glaciers.

Figure 5c depicts the relation between BCF, surface slope angle and creep rates. Given a value of the BCF, a wide range of possible velocities can be found, and vice-versa. The value of the surface creep velocity of a rock glacier is fully determined when incorporating the information about the geometry, which is mostly controlled by the surface slope angle. All the rock glaciers are constrained in a sector of the quadrant bounded by two lines representing the maximum and the minimum surface slope angles of the rock glaciers in our inventory (10° and 30°).

The potential influence of external factors on the BCF is analysed in Fig. 5d using the PZI as a proxy for permafrost conditions and temperature. We find that the maximum value of the BCF is delimited by the PZI: for favourable permafrost conditions (PZI close to 1) only small BCF are observed whereas for unfavourable conditions (PZI close to 0) the whole range of low to high BCF occurs. This pattern is consistent with the dual influence of temperature on rock glacier dynamics. Firstly, in the early stage of permafrost degradation, increasing ground temperatures and water content (corresponding to a decrease in the PZI) enhance the deformation (increasing BCF) according to Eq. 2 and Eq. 3. Secondly, in the final stage of degradation when substantial thawing occurs, the BCF decreases due to lower stresses and enhanced inter-particle friction. Rock glaciers currently experiencing a destabilization process are characterized by high values of the BCF and tend to the limiting line in Fig.5d. Because destabilization is an irreversible process, and degrading rock glaciers that are in the final stage of destabilization can still be classified as such, they drift towards low values of the BCF and PZI. This result implies that a classification of the dynamic state of rock glaciers might be possible on the basis of a combination of PZI, BCF and creep rates. Whereas low PZIs are in general related to unfavourable permafrost conditions, they can indicate current destabilization if occurring together with high BCFs. High values of the PZI indicate active rock glaciers in cold conditions, apparently less likely to destabilize. However, open questions remain and a classification of rock glaciers based on those parameters remains non trivial and requires additional detailed studies.

4.2 The local scale: analysing spatial variability in rock glacier creep

For many rock glaciers worldwide, detailed spatial information about the surface topography and their displacement field are becoming available (DallAsta et al., 2017; Bodin et al., 2018; Vivero and Lambiel, 2019; Strozzi et al., 2020). The BCF allows to interpret and investigate the dynamics and mechanical properties of rock glaciers for which such topographic and kinematic information are available. We investigate three rock glaciers characterized by contrasting dynamical states: steady-state creep conditions (Laurichard, FR), exceptionally fast flow (Dirru, CH), and ongoing destabilization (Pierre Brune, FR). For all three study sites detailed digital surface models and surface velocity fields are available from different sources and at different resolutions.

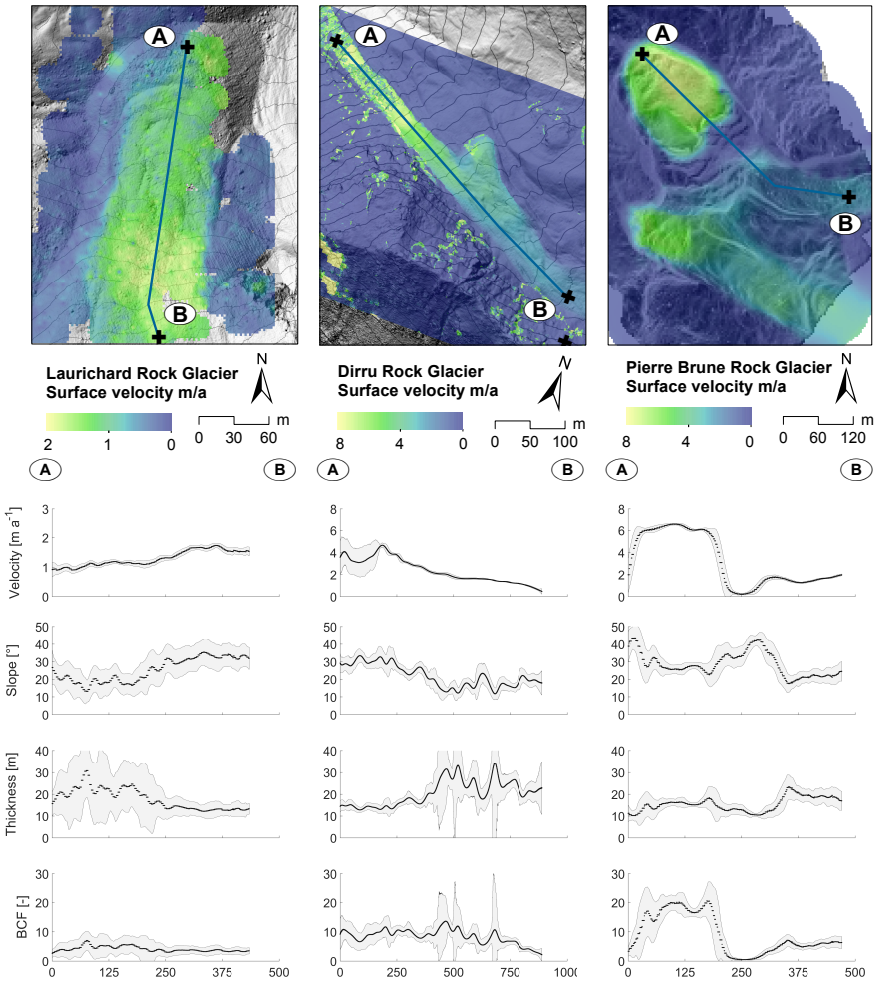

Figure 6. Results at local scale. From left to right, Laurichard, Dirru and Pierre Brune Rock Glaciers. The the upper panel shows the surface creep velocities (colour coded) together with the profile along which the analysis is performed: from A the front to B the rooting zone. Below, from the top to the bottom, the observed surface velocities, surface slope angles, modelled thickness and BCF are plotted along the corresponding profiles. The shaded gray area depicts the spatial variability of the plotted variable in an area of 25 m along each position and can be used as a proxy for the uncertainty of the results.

The results of the analysis at the local scale are illustrated in Figure 6. For the Dirru and Pierre Brune Rock Glaciers, the spatial data coverage with regard to creep velocities is almost complete. For the Laurichard Rock Glacier no velocity data is available in the area close to the rooting zone. The observed velocities show two distinctly different patterns of terrain topography and creep rates at the three field sites. For the Laurichard Rock Glacier, the highest velocities are observed in the

uppermost area, whereas for the other two the largest values can be observed closer to the front. The three rock glaciers are characterized by velocity values varying between $1\,m\,a^{-1}$ and $6\,m\,a^{-1}$ and relatively high values of the slope angle, with values peaking at more than 30°. The uncertainty related to the spatial variability in velocity is limited in all cases except for a limited area close to the front of the Dirru Rock Glacier (?, ?; Rohner et al., 2019). This uncertainty is caused by low performance of the feature tracking algorithm in this area as visible in the corresponding map. The observed field of surface slope angle and surface velocity are smoothed with a Gaussian filter (radius $10\,m$) in order to reduce undesirable effects of micro-topography on the analysis. On the basis of the values of the surface slope angle, we invert the thickness of the moving rock glacier assuming a yield stress equal to $92\,kPa$. Narrow peaks and troughs in the thickness profiles correspond to low slope angles due to small-scale undulations of the surface topography (e.g. furrow and ridges).

For the Laurichard Rock Glacier, the calculated BCF remains constant along the investigated profile, despite substantial variations in slope angle and creep rates. The average value of the BCF is 5 (as also visible in Fig. 5), confirming its validity as a reference rock glacier for the Alps.

For the Dirru Rock Glacier the analysed profile extends from the steep front up to the rooting zone. Here, despite strong variations in geometry and the possible influence of 2D effects and the acute change in slope, the BCF is almost constant along the entire profile, with the exception of the rooting zone where it decreases substantially. Similarly to the case of the Laurichard Rock Glacier, the constant value of the BCF shows that the spatial variations in creep rates can be be explained by geometry (slope and thickness). The average value of the BCF = 10, coherent with the value at the regional scale (Fig. 5), indicates a predisposition to high creep rates along the entire profile.

The Pierre Brune Rock Glacier on the contrary shows a distinctly different pattern in BCF. In this case, the topography cannot account for the large variations in surface creep rates along the profile. Close to the front, where the highest rates are observed, the BCF exceeds values of 20. In the upper section, the BCF is four times smaller than close to the front. In the center corresponding to a scarp-area (Marcer et al., 2019), the velocities are almost zero despite the large values of the slope angle. As a consequence the BCF shows very low values, confirming on the one hand the dynamic separation between the lowermost and the uppermost unit and on the other hand indicating degrading conditions in the scarp area.

According to the results of our analysis, the spatial variability in surface velocity between the upper and the lower part for the Laurichard and the Dirru Rock Glacier can be explained by the their geometry (surface slope and thickness) alone. In this sense, the two rock glaciers can be considered similar, both showing a constant value of the BCF, consistent to the analysis at the regional scale in the previous section. However, the contrasting values of the BCF between the two rock glaciers indicate rheological differences that reflect profound diversity in material properties. Further interpretation requires analysis based on detailed in-situ observations (e.g. surface or ground temperature measurements, geophysical surveying, etc.). For the Pierre Brune Rock Glacier the velocity distribution can be explained only by accounting for both the geometry and the strong spatial discontinuity in the BCF between the upper and the lower part. The discontinuity in the BCF and its exceptionally high values point towards a dynamical and rheological interpretation of the destabilization phenomenon confirming and complementing geomorphological and kinematic observations as seen in the analysis at the regional scale (Sec.4.1).

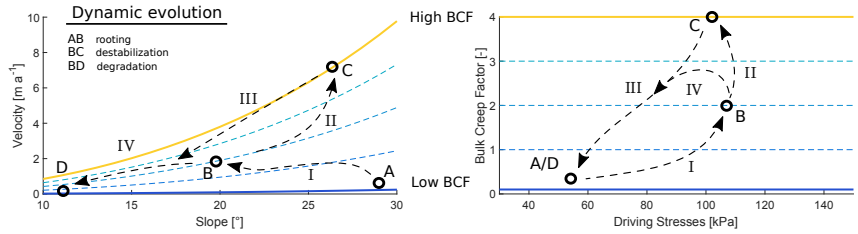

Figure 7. Schematic representation of possible dynamical evolution (indicated by the dashed arrows) of a rock glacier in the (a) velocity-slope and in the (b) BCF-driving stress space. The points represent possible combination of variables for (A) rooting , (B) secondary creep, (C) destabilization, and (D) degradation conditions. The values are indicative of typical conditions for alpine rock glaciers.

5 The long-term dynamic evolution of rock glaciers

The BCF can further be applied to interpret and investigate the evolution of rock glacier dynamics over longer time scales as illustrated in Figure 7. This figure illustrates the possible dynamical evolution of a rock glacier in a Lagrangian reference system (following an individual point in space and time as it creeps). In Fig. 7 we can follow the evolution of a material point on the surface of a rock glacier based on its surface slope and velocity; in Fig. 7b we can follow the evolution of the same point by looking at its BCF and the corresponding driving stress.

The evolution of a rock glacier during its rooting from a talus slope is depicted by line (I) moving from point A to point B. Here, the slope is significantly decreasing from the steeper zone of the talus to the more gentle areas below, while the Bulk Creep Factor is increasing due to the initiation of the creeping process (towards point B). Lines II and III show the dynamic evolution of a rock glacier experiencing destabilization. When the front of the rock glacier reaches a steeper terrain it moves faster, but maintains its physical properties for a determined period of time, therefore moving along an isoline in the two figures. When destabilization occurs due to topographical predisposition and permafrost temperatures approaching the melting point, the Bulk Creep Factor drastically increases causing a diversion of the trajectories from the isoline until point C where the highest velocities are reached. Currently in the Alps there is an increasing number of rock glaciers following this path (line II), e.g. the Tsarmine and the Pierre Brune rock glaciers (Lambiel et al., 2008; Marcer et al., 2020a). From point C onward (line III), the rock glacier continues to creep with decreasing but still relatively high velocities due to a change in surface slope or due to permafrost degradation. Permafrost thawing causes the driving stress to decrease and the density of the rock glacier approaches the maximum packing density while interlocking becomes more important. Eventually creep ceases and the dynamic evolution of the rock glacier comes to an end with its transitions from an active to an inactive state (line IV). Two mechanical effects may independently lead to the deactivation of the rock glacier: the decrease in stresses, which is driven by decreasing thickness and surface slope, and the decrease in the BCF (see (Barsch, 1992) for a geomorphological interpretation). Examples of well studied rock glaciers currently in such condition are the Furgwannghorn and Tête de Longet rock glaciers (Buchli et al., 2018; Marcer et al., 2020a). Line III and line IV represent the degradation process, which can vary its trajectory depending on the different starting condition (C - destabilization or B - secondary creep). Starting from a secondary creep phase, degradation still causes

the driving stresses to decrease but initially leads to an acceleration due to permafrost warming and therefore an increase in the BCF (line IV). Many rock glaciers in the Alps currently find themselves in this condition with temperatures approaching the melting point, increasing velocity and onset of degradation (PERMOS, 2019). The positions A and D coincide in Fig. 7b, sharing low stresses and a low BCFs. The exact position of the two points in the figure depends on the rock glacier structure and on the terrain topography.

6 Conclusions

Based on a brief review of the physics of rock glacier creep and the mathematical formulation used to describe it, we have presented a general theory of rock glacier creep and have introduced the Bulk Creep Factor as a measure of the rheological properties of rock glaciers. The proposed approach only requires data on creep velocities and slope angle, which both can be derived operationally over large areas from remote sensing data (or from detailed in-situ measurements). Therefore, the BCF has a large potential for investigating the dynamic state and rheology of large scale rock glacier datasets. Additionally, we have provided two examples of possible applications of the BCF at a regional and at a local scale. The combined analysis at both scales indicates the potential of the BCF to evaluate and compare the state of rock glacier dynamics from remotely sensed data.

With regard to limitations: the proposed theory shows two main weaknesses. On the one hand, it relies on the combination of two different rheologies for the determination of the thickness and the rheological properties of the rock glacier material. This point can be overcome by direct measurements of rock glacier thickness or by the application of dynamical models. On the other hand, the BCF neglects in first approximation the vertical structures of rock glaciers and the differences between the shear horizon and the ice-rich core. More field observations and modelling studies are still needed in order to better constrain this diversity and in order to transpose it to analyses at a regional scale.

Concluding, the main findings of this study can be summarized as follows:

- Remote sensing data in combination with mathematical formulations can be used to analyse rock glacier dynamics at a regional and at a local scale.
- The typical driving stress of alpine rock glaciers is 92 ± 13 kPa.
- Rock glacier thickness can be efficiently estimated with the inversion of simple models (e.g. perfectly plastic model), but more detailed data is needed for further validation of this approach.
- Rock glacier creep rates can be calculated by coupling a rheological model accounting for the frictional behaviour of rock glacier creep to a perfectly plastic model for rock glacier thickness.
- The introduction of the Bulk Creep Factor allows the physical interpretation of the rheological properties of the constitutive material and the processes controlling rock glacier creep by separating the geometry information from the velocity signal.
- Most alpine rock glaciers show a BCF lower than 5.
- First order variables controlling the BCF are temperature and water content. Further observational data are required to better constrain their influence.
- Only rock glaciers experiencing destabilization or set in conditions unfavourable to permafrost occurrence show large values of the BCF, with maximum values close to 20.
- The permafrost conditions (approximated here by the PZI) define a maximum limit for the BCF.

- For dynamically stable rock glaciers the geometry can explain the spatial variability in creep rates with almost constant rheological properties of the constitutive material.
- Destabilized rock glaciers are characterized by contrasting and discontinuous material properties (BCF). In addition to geomorphological observations, the definition of rock glacier destabilization should account for the rheological and dynamical state of the rock glacier rather than solely on its kinematics.

This study represents a first attempt to investigate in detail the spatial variability and the large scale patterns and trends of rock glacier dynamics. The concept of the BCF seems very promising and has the potential for further and wide spread applications. However, more research is needed and additional data must be collected in order to validate and increase the confidence in the proposed theory. In a next step the BCF should be further analysed in relation to the factors influencing it (e.g. thermal state, liquid water, internal structure...) and the modelling-approach be better constraint with more detailed observations at longer time series.

Acknowledgments
This research was part of the project X-Sense2 and was financed by nano-tera.ch (ref. no. 530659) and the University of Zurich. The authors thank the input from Reynald Delaloye for the data used in both datasets (see Appendix A and Appendix A). The authors thank the contribution of J. Beutel for its important contribution to the collection of kinematic data in the Swiss Alps, N. Mölg and C. Rohner for the support in acquiring and analysing the data for Dirru Rock Glacier. The data used for the analysis of rock glacier thickness are reported in Appendix A. The data used for the application at a regional and local scale (available from the authors upon request) are summarized in Appendix A.

Appendix A Information about the datasets.

Table A1. Dataset used for the analysis of rock glacier thickness, driving stresses and creep rates.

Num	Rock glacier	Thickness [m]	Slope angle [°]	Creep rate [m a^{-1}]	Reference
1	Dirru	15[b,c]	27	5.50	Cicoira et al. (2019b)
2	Furgwangghorn 5	15[a]	28	2.90	Buchli et al. (2018)
3	Furgwangghorn 7	17[a]	20	5.20	Buchli et al. (2018)
4	Guggla	17[c]	22	4.00	Delaloye, pers. com., (2020)
5	HuHH1	17[c]	21	1.00	Müller et al. (2016)
6	HuHH3	20[c]	22	1.70	Müller et al. (2016)
7	Kaiserberg	27[b]	9	0.50	Hausmann et al. (2012)
8	Las Liebres	25[b]	15	1.10	Monnier and Kinnard (2016)
9	Laurichard	20[b]	20	1.00	Bodin et al. (2018)
10	Lazaun	25[a]	15	1.20	Krainer et al. (2015)
11	Andes #1	22[a]	9	0.07	Arenson (pers. com. 2020)
12	Andes #2	18[a]	11	0.05	Arenson (pers. com. 2020)
13	Andes #3	12[a]	13	0.23	Arenson (pers. com. 2020)
14	Andes #4	22[a]	11	0.14	Arenson (pers. com. 2020)
15	Andes #5	14[a]	8	0.01	Arenson (pers. com. 2020)
16	Muragl 3	15[a]	18	1.40	Arenson et al. (2002)
17	Muragl 4	16[a]	18	1.20	Arenson et al. (2002)
18	Murtél	29[a]	12	0.10	Arenson et al. (2002)
19	Ölgrube	31[b]	13	1.10	Hausmann et al. (2012)
20	Pierre Brune 1	15[a,b]	25	6.00	Marcer, pers. com., (2019)
21	Pierre Brune 2	23[a,b]	16	1.00	Marcer, pers. com., (2019)
22	Reichenkar	23[b]	13	2.50	Hausmann et al. (2007)
23	Rittigraben	20[a]	20	1.50	Kenner et al. (2017)
24	Schafberg 1	14[a]	23	0.03	Arenson et al. (2002)
25	Schafberg 1	25[a]	16	0.20	Arenson et al. (2002)
26	Steintälli	27[c]	12	0.40	Cicoira, unpublished, (2018)
27	Tsarmine	17[c]	22	6.0	Delaloyle, pers. com., (2020)
28	Valdallacqua	22[c]	15	1.00	Cicoira, unpublished, (2019)

[a] From borehole investigations. Point information.

[b] From geophysical surveys. The reported value is extracted from the original dataset.

[c] From morphological analysis. Derived from the steep front and/or the lateral margins.

Table A2. Dataset used for the analysis of rock glacier creep at the regional scale comprising observations of creep rates and surface slope angle.

Count	Rock glaciers	Reference
324	French inventory[a]	Marcer et al. (2019)
30	Kaunertal inventory[a]	Groh and Blöthe (2019)
17	Permos[c]	PERMOS (2019)
15	University of Fribourg[b,c]	Delaloye, pers. com. (2020)
28	Present study[a,b,c]	Section 3.3

[a]From aerial imagery (Satellites or UAVs). Feature tracking analysis.
[b]From InSar analysis.
[c]From terrestrial surveys or in-situ GPS stations.

Table A3. Dataset used for the analysis of rock glacier creep at the local scale.

Rock glacier	Data source (velocity, thickness)	Reference and availability
Laurichard	TLS, GPR	Bodin et al. (2018)
Dirru	UAVs, ERT	Cicoira et al. (2019b); Delaloye (pers. com. 2020)
Pierre Brune	UAVs, ERT	Marcer et al. (2020a)

References

Arenson, L. U. (pers. com. 2020).

Arenson, L. U., Hauck, C., Hilbich, C., Seward, L., Yamamoto, Y., and Springman, S. M. (2010). Sub-surface heterogeneities in the murtl. corvatsch rock glacier, switzerland. In *Proceedings of the joint 63rd canadian geotechnical conference and the 6th canadian permafrost conference* (p. 1494 - 1500). Canadian Geotechnical Society. (the 6th Canadian Permafrost Conference; Conference Location: Calgary, Canada; Conference Date: September 12-16, 2010)

Arenson, L. U., Hoelzle, M., and Springman, S. (2002). Borehole deformation measurements and internal structure of some rock glaciers in switzerland. *Permafrost and Periglacial Processes*, *13*(2), 117–135. doi: 10.1002/ppp.414

Arenson, L. U., Kääb, A., and O'Sullivan, A. (2016, 11). Detection and analysis of ground deformation in permafrost environments. *Permafrost and Periglacial Processes*. doi: 10.1002/ppp.1932

Arenson, L. U., and Springman, S. M. (2005a). Mathematical descriptions for the behaviour of ice-rich frozen soils at temperatures close to 0 c. *Canadian Geotechnical Journal*, *42*(2), 431-442. doi: 10.1139/t04-109

Arenson, L. U., and Springman, S. M. (2005b). Triaxial constant stress and constant strain rate tests on ice-rich permafrost samples. *Canadian Geotechnical Journal*, *42*(2), 412-430. doi: 10.1139/t04-111

Arenson, L. U., Springman, S. M., and Sego, D. (2006, 01). The rheology of frozen soils. *Appl. Rheol*, *17*, 12147-1.

Barsch, D. (1992). Permafrost creep and rockglaciers. *Permafrost and Periglacial Processes*, *3*(3), 175–188. doi: 10.1002/ppp.3430030303

Bast, A. (pers. com. 2015).

Bodin, X., Thibert, E., Sanchez, O., Rabatel, A., and Jaillet, S. (2018, 04). Multi-annual kinematics of an active rock glacier quantified from very high-resolution dems: An application-case in the french alps. *Remote Sensing*, *10*, 547. doi: 10.3390/rs10040547

Buchli, T., Kos, A., Limpach, P., Merz, K., Zhou, X., and Springman, S. M. (2018). Kinematic investigations on the furggwanghorn rock glacier, switzerland. *Permafrost and Periglacial Processes*, *29*(1), 3–20.

Bucki, A. K., and Echelmeyer, K. A. (2004). The flow of fireweed rock glacier, alaska, u.s.a. *Journal of Glaciology*, *50*(168), 7686. doi: 10.3189/172756504781830213

Capps, S. R. (1910). Rock glaciers in alaska. *Journal of Geology*, *18*, 359-375.

Carslaw, H., and Jaeger, J. (1959). *Conduction of heat in solids*. Clarendon Press.

Cicoira, A., Beutel, J., Faillettaz, J., and Vieli, A. (2019a). Resolving the influence of temperature forcing through heat conduction on rock glacier dynamics: a numerical modelling approach. *The Cryosphere*, *13*(3), 927-942. doi: 10.5194/tc-13-927-2019

Cicoira, A., Beutel, J., Faillettaz, J., and Vieli, A. (2019b). Water controls the seasonal rhythm of rock glacier flow. *Earth and Planetary Science Letters*, *528*, 115844. doi: https://doi.org/10.1016/j.epsl.2019.115844

Clark, D. H., Steig, E. J., Potter, N., Jr., and Gillespie, A. R. (1998). Genetic variability of rock glaciers. *Geografiska Annaler: Series A, Physical Geography*, *80*(34), 175-182. doi: 10.1111/j.0435-3676.1998.00035.x

Cuffey, K., and Paterson, W. S. B. (2010). *The physics of glaciers*. Elsevier.

Czurda, K., and Hohmann, M. (1997). Freezing effect on shear strength of clayey soils. *Applied Clay Science*, *12*(1), 165 - 187. doi: https://doi.org/10.1016/S0169-1317(97)00005-7

DallAsta, E., Forlani, G., Roncella, R., Santise, M., Diotri, F., and di Cella, U. M. (2017). Unmanned aerial systems and dsm matching for rock glacier monitoring. *ISPRS Journal of Photogrammetry and Remote Sensing*, *127*, 102 - 114. doi: https://doi.org/10.1016/j.isprsjprs.2016.10.003

De La Chapelle, S., Milsch, H., Castelnau, O., and Duval, P. (1999). Compressive creep of ice containing a liquid intergranular phase: Rate-controlling processes in the dislocation creep regime. *Geophysical Research Letters*, *26*(2), 251-254. doi: 10.1029/1998GL900289

Delaloye, R. (pers. com. 2020).

Delaloye, R., and Lambiel, C. (2005). Evidence of winter ascending air circulation throughout talus slopes and rock glaciers situated in the lower belt of alpine discontinuous permafrost (swiss alps). *Norsk Geografisk Tidsskrift - Norwegian Journal of Geography*, *59*(2), 194-203. doi: 10.1080/00291950510020673

Delaloye, R., Morard, S., Barboux, C., Abbet, D., Gruber, V., Riedo, M., and Gachet, S. (2013, 01). Rapidly moving rock glaciers in mattertal. *Jahrestagung Der Schweizerischen Geomorphologischen Gesellschaft*, 21-31.

Farinotti, D., Brinkerhoff, D. J., Clarke, G. K. C., Fürst, J. J., Frey, H., Gantayat, P., ... Andreassen, L. M. (2017). How accurate are estimates of glacier ice thickness? results from itmix, the ice thickness models intercomparison experiment. *The Cryosphere*, *11*(2), 949–970. doi: 10.5194/tc-11-949-2017

Frehner, M., Ling, A. H. M., and Gärtner-Roer, I. (2015). Furrow-and-ridge morphology on rockglaciers explained by gravity-driven buckle folding: A case study from the murtl rockglacier (switzerland). *Permafrost and Periglacial Processes*, *26*(1), 57–66. (PPP-14-0032.R2) doi: 10.1002/ppp.1831

Glen, J. (1955). The creep of polycrystalline ice. *Proceedings of the Royal Society of London A: Mathematical, Physical and Engineering Sciences*, *228*(1175), 519–538. doi: 10.1098/rspa.1955.0066

Groh, T., and Blöthe, J. H. (2019). Rock glacier kinematics in the kaunertal, ötztal alps, austria. *Geosciences*, *9*(9). doi: 10.3390/geosciences9090373

Gruber, S. (2012). Derivation and analysis of a high-resolution estimate of global permafrost zonation. *The Cryosphere*, *6*(1), 221–233. Retrieved from `https://www.the-cryosphere.net/6/221/2012/` doi: 10.5194/tc-6-221-2012

Haeberli, W. (1985). Creep of mountain permafrost. *Mitteilungen der Versuchsanstalt für Wasserbau. Hydrologie und Glaziologie der ETH Zürich, vol. 77*.

Haeberli, W., Hallet, B., Arenson, L. U., Elconin, R., Humlum, O., Kääb, A., ... Vonder Mühll, D. (2006, 07). Permafrost creep and rock glacier dynamics. *Permafrost and Periglacial Processes*, *17*, 189 - 214.

Haeberli, W., Hoelzle, M., Kääb, A., Keller, F., Vonder Mühll, D., and Wagner, S. (1998). Ten years after drilling through the permafrost of the active rock glacier murtél. *Seventh International Conference on Permafrost, Yellowknife*, 403 - 410.

Haeberli, W., Hunder, J., Keusen, H.-R., Pika, J., and Röthlisberger, H. (1988). Core drilling through rock-glacier permafrost. *Fifth International Conference on Permafrost, Trondheim*, *2*, 937 - 942.

Haeberli, W., and Vonder Mühll, D. (1996, 01). On the characteristics and possible origins of ice in rock glacier permafrost. *Zeitschrift fur Geomorphologie, Supplementband*, *104*, 43-57.

Hanson, S., and Hoelzle, M. (2004). The thermal regime of the active layer at the murtl rock glacier based on data from 2002. *Permafrost and Periglacial Processes*, *15*, 273-282.

Hartl, L., Fischer, A., Stocker-Waldhuber, M., and Abermann, J. (2016, 06). Recent speed-up of an alpine rock glacier: an updated chronology of the kinematics of outer hochebenkar rock glacier based on geodetic measurements. *Geografiska Annaler: Series A, Physical Geography*, *98*, 129-141. doi: 10.1111/geoa.12127

Hausmann, H., Krainer, K., Brckl, E., and Mostler, W. (2007). Internal structure and ice content of reichenkar rock glacier (stubai alps, austria) assessed by geophysical investigations. *Permafrost and Periglacial Processes*, *18*(4), 351-367. Retrieved from `https://onlinelibrary.wiley.com/doi/abs/10.1002/`

ppp.601 doi: 10.1002/ppp.601

Hausmann, H., Krainer, K., Brückl, E., and Ullrich, C. (2012). Internal structure, ice content and dynamics of ölgrube and kaiserberg rock glaciers (ötztal alps, austria) determined from geophysical surveys. *Austrian Journal of Earth Sciences*(105), 12-31.

Humlum, O. (2000). The geomorphic significance of rock glaciers: estimates of rock glacier debris volumes and headwall recession rates in west greenland. *Geomorphology*, *35*(1), 41 - 67. doi: https://doi.org/10.1016/S0169-555X(00)00022-2

Ikeda, A., Matsuoka, N., and Kääb, A. (2008). Fast deformation of perennially frozen debris in a warm rock glacier in the swiss alps: An effect of liquid water. *Journal of Geophysical Research: Earth Surface*, *113*(F1), n/a–n/a. (F01021) doi: 10.1029/2007JF000859

Jansen, F., and Hergarten, S. (2006). Rock glacier dynamics: Stick-slip motion coupled to hydrology. *Geophysical Research Letters*, *33*(10). doi: 10.1029/2006GL026134

Jones, D. B., Harrison, S., Anderson, K., and Betts, R. A. (2018). Mountain rock glaciers contain globally significant water stores. *Scientific reports*, *8*, 2834-2844. doi: 10.1038/s41598-018-21244-w

Kääb, A., Frauenfelder, R., and Roer, I. (2007). On the response of rockglacier creep to surface temperature increase. *Global and Planetary Change*, *56*(1), 172 - 187. doi: https://doi.org/10.1016/j.gloplacha.2006.07.005

Kääb, A., and Weber, M. (2004, 10). Development of transverse ridges on rock glaciers: Field measurements and laboratory experiments. *Permafrost and Periglacial Processes*, *15*, 379 - 391. doi: 10.1002/ppp.506

Kellerer-Pirklbauer, A., Lieb, G. K., and Kleinferchner, H. (2012). A new rock glacier inventory of the eastern european alps. *Austrian Journal of Earth Sciences*, *105*(2).

Kenner, R., Phillips, M., Beutel, J., Hiller, M., Limpach, P., Pointner, E., and Volken, M. (2017). Factors controlling velocity variations at short-term, seasonal and multiyear time scales, ritigraben rock glacier, western swiss alps. *Permafrost and Periglacial Processes*, *28*(4), 675–684. (PPP-16-0044.R2) doi: 10.1002/ppp.1953

Krainer, K., Bressan, D., Dietre, B., Haas, J., Hajdas, I., Lang, K., ... Tonidandel, D. (2015, 01). A 10,300-year-old permafrost core from the active rock glacier lazaun, southern ötztal alps (south tyrol, northern italy). *Quaternary Research*, *83*, 324-335. doi: 10.1016/j.yqres.2014.12.005

Krainer, K., and Mostler, W. (2002). Hydrology of active rock glaciers: Examples from the austrian alps. *Arctic, Antarctic, and Alpine Research*, *34*(2), 142-149. doi: 10.1080/15230430.2002.12003478

Kummert, M., Delaloye, R., and Braillard, L. (2017, 10). Erosion and sediment transfer processes at the front of rapidly moving rock glaciers: Systematic observations with automatic cameras in the western swiss alps. *Permafrost and Periglacial Processes*. doi: 10.1002/ppp.1960

Ladanyi, B. (2003). Rheology of ice/rock systems and interfaces. In *Proceedings of the eigth international conference on permafrost* (p. 621-625). Lisse, The Netherlands.

Lambiel, C., Delaloye, R., Strozzi, T., Lugon, R., and Raetzo, H. (2008, 06). Ers insar for assessing rock glacier activity..

Lugon, R., and Stoffel, M. (2010). Rock-glacier dynamics and magnitude-frequency relations of debris flows in a high-elevation watershed: Ritigraben, swiss alps. *Global and Planetary Change*, *73*(3), 202 - 210. doi: https://doi.org/10.1016/j.gloplacha.2010.06.004

Marcer, M., Bodin, X., Brenning, A., Schoeneich, P., Charvet, R., and Gottardi, F. (2017). Permafrost favorability index: Spatial modeling in the french alps using a rock glacier inventory. *Frontiers in Earth Science*, *5*, 105. doi:

10.3389/feart.2017.00105

Marcer, M., Serrano, C., Brenning, A., Bodin, X., Goetz, J., and Schoeneich, P. (2019). Evaluating the destabilization susceptibility of active rock glaciers in the french alps. *The Cryosphere*, *13*(1), 141–155. doi: 10.5194/tc-13-141-2019

Marcer et al., M. (2020a). Evidence of rock glacier destabilization due to climate change. *Nature Communications*, *31*(1), 15-30.

Marcer et al., M. (2020b). Investigating the slope failures at the lou rock glacier front, french alps. *Permafrost and Periglacial Processes*, *31*(1), 15-30. doi: 10 .1002/ppp.2035

Mellor, M., and Testa, R. (1969). Effect of temperature on the creep of ice. *Journal of Glaciology*, *8*(52), 131145. doi: 10.3189/S0022143000020803

Monnier, S., and Kinnard, C. (2016). Interrogating the time and processes of development of the las liebres rock glacier, central chilean andes, using a numerical flow model. *Earth Surface Processes and Landforms*, *41*(13), 1884-1893. doi: 10.1002/esp.3956

Moore, P. L. (2014). Deformation of debris-ice mixtures. *Reviews of Geophysics*, *52*(3), 435–467. doi: 10.1002/2014RG000453

Müller, J., Vieli, A., and Gärtner-Roer, I. (2016). Rock glaciers on the run – understanding rock glacier landform evolution and recent changes from numerical flow modeling. *The Cryosphere*, *10*(6), 2865–2886. doi: 10.5194/tc-10-2865-2016

Nye, J. F. (1952). The mechanics of glacier flow. *Journal of Glaciology*, *2*(12), 8293. doi: 10.3189/S0022143000033967

Olyphant, G. A. (1983, 04). Computer simulation of rock-glacier development under viscous and pseudoplastic flow. *GSA Bulletin*, *94*(4), 499-505. doi: 10.1130/0016-7606(1983)94⟨499:CSORDU⟩2.0.CO;2

PERMOS. (2019). Permafrost in switzerland 2014/2015 to 2017/2018. noetzli, j., pellet, c., and staub, b. (eds.), glaciological report (permafrost) no. 16-19 of the cryospheric commission of the swiss academy of sciences, 104 pp.

Rohner, C., Small, D., Beutel, J., Henke, D., Lüthi, M. P., and Vieli, A. (2019). Multisensor validation of tidewater glacier flow fields derived from synthetic aperture radar (sar) intensity tracking. *The Cryosphere*, *13*(11), 2953–2975. Retrieved from `https://www.the-cryosphere.net/13/2953/2019/` doi: 10.5194/tc-13-2953-2019

Scherler, M., Schneider, S., Hoelzle, M., and Hauck, C. (2014). A two-sided approach to estimate heat transfer processes within the active layer of the murtél-corvatsch rock glacier. *Earth Surface Dynamics*, *2*(1), 141–154. doi: 10.5194/esurf-2-141-2014

Seppi, R., Carturan, L., Carton, A., Zanoner, T., Zumiani, M., Cazorzi, F., ... Salvatore, M. C. (2019, 08). Decoupled kinematics of two neighbouring permafrost creeping landforms in the eastern italian alps. *Earth Surface Processes and Landforms*, *44*, 2703-2719. doi: 10.1002/esp.4698

Staub, B., Lambiel, C., and Delaloye, R. (2016, 06). Rock glacier creep as a thermally-driven phenomenon: a decade of interannual observations from the swiss alps. In (p. 93-94).

Strozzi, T., Caduff, R., Jones, N., Barboux, C., Delaloye, R., Bodin, X., ... Schrott, L. (2020). Monitoring rock glacier kinematics with satellite synthetic aperture radar. *Remote Sensing*, *12*(3). Retrieved from `https://www.mdpi.com/2072-4292/12/3/559` doi: 10.3390/rs12030559

Vieli, A., Cicoira, A., and Noetzli, J. (in preparation). A new borehole continues the longest mountain permafrost temperature record on rock glacier murtél-corvatsch, swiss alps. *Nature Climate Change*, *1*(1), 1-10. doi: 1

Vivero, S., and Lambiel, C. (2019). Monitoring the crisis of a rock glacier with repeated uav surveys. *Geographica Helvetica*, *74*(1), 59–69. doi: 10.5194/gh-74-59-2019

Wahrhaftig, C., and Cox, A. (1959). Rock glaciers in the alaska range. *GSA Bulletin*, *70*(4), 383.

Weertman, J. (1983). Creep deformation of ice. *Annual Review of Earth and Planetary Sciences*, *11*(1), 215–240.

Whalley, W. B., and Martin, H. E. (1992). Rock glaciers : Ii models and mechanisms. *Progress in Physical Geography: Earth and Environment*, *16*(2), 127-186. doi: 10.1177/030913339201600201

Wicky, J., and Hauck, C. (2017). Numerical modelling of convective heat transport by air flow in permafrost talus slopes. *The Cryosphere*, *11*(3), 1311–1325. doi: 10.5194/tc-11-1311-2017

Wirz, V., Gruber, S., Purves, R. S., Beutel, J., Gärtner-Roer, I., Gubler, S., and Vieli, A. (2016). Short-term velocity variations at three rock glaciers and their relationship with meteorological conditions. *Earth Surface Dynamics*, *4*(1), 103–123. doi: 10.5194/esurf-4-103-2016

Part III

Appendix

A Personal bibliography

Publications being part of this thesis are marked with numbers (① – ③).

① **Cicoira, A.**, Beutel, J., Faillettaz, J., Gärtner-Roer, I., and Vieli A.: Resolving the influence of temperature forcing through heat conduction on rock glacier dynamics: a numerical modelling approach, The Cryosphere, 13, 927–942, doi.org/10.5194/tc-13-927-2019, 2019a.

② **Cicoira, A.**, Beutel, J., Faillettaz, and Vieli A.: Water controls the seasonal rhythm of rock glacier creep, Earth and Planetary Science Letters, 528, 115844, doi.org/10.1016/j.epsl.2019.115844, 2019b.

③ **Cicoira, A.**, Marcer, M., Gärtner-Roer, I., Bodin, X., Arenson, L., and Vieli, A.: A general theory of rock glacier creep based on in-situ and remote sensing observations, Permafrost and Periglacial Processes, submitted.

Marcer, M., **Cicoira, A.**, Cusicanqui, D., Bodin, X., Echelard, T., Obregon, R., Schoeneich, P.: Evidence of rock glacier destabilization due to climate change, submitted.

Vieli, A., Noetzli, J., Bolch, T., Bast, A., Gärtner-Roer, I., **Cicoira, A.**, and Hoelzle, M.: A new borehole continues the longest mountain permafrost temperature record on rock glacier Murtél-Corvatsch, Swiss Alps, in preparation.

Beutel, J., Buchli, **Cicoira, A.**, B., Da Forno, R., Geiger, A., Gruber, S., Gsell, T., Haser, A., Lim, R., Limpach, P., Meyer, M., Thiele, L., Vieli, A., Vonder Mühll, D., Weber, S., Wirz, V.: Kinematic observations of the mountain cryosphere using in-situ GNSS instruments, in preparation.